

**Agronomy and photosynthesis physiology
of hemp (*Cannabis sativa* L.)**



Kailei Tang

Propositions

1. Hemp has a great potential for the bio-economy.
(this thesis)
2. Growing hemp is easy but only if the farmer chooses the right cultivar.
(this thesis)
3. Bio-economically sustainable industrial crops coupled with advanced agronomy could help to alleviate poverty in rural China.
4. Agronomic management should aim to reduce the use of agrochemicals, especially herbicides.
5. Working long hours does not help writing a PhD thesis.
6. Advancement of society requires the orchestrated efforts of several generations.
7. Smart devices make smart man smarter while they make dumb man dumber.

Propositions belonging to the thesis of Kailei Tang, entitled:

‘Agronomy and photosynthesis physiology of hemp (*Cannabis sativa* L.)’.

Wageningen, March 23, 2018

**Agronomy and photosynthesis physiology
of hemp (*Cannabis sativa* L.)**

Kailei Tang

Thesis committee

Promotor

Prof. Dr P.C. Struik
Professor of Crop Physiology
Wageningen University & Research

Co-promotors

Dr X. Yin
Senior scientist, Centre for Crop Systems Analysis
Wageningen University & Research

Dr S. Amaducci
Associate professor, Department of Sustainable Crop Production
Università Cattolica del Sacro Cuore, Italy

Other members

Prof. Dr K.E. Giller, Wageningen University & Research
Prof. Dr S.L. Cosentino, University of Catania, Italy
Dr L.M. Trindade, Wageningen University & Research
Dr E. Heuvelink, Wageningen University & Research

This research was conducted under the auspices of the C.T. de Wit Graduate School for Production Ecology and Resource Conservation

**Agronomy and photosynthesis physiology
of hemp (*Cannabis sativa* L.)**

Kailei Tang

Thesis

submitted in fulfilment of the requirements for the degree of doctor
at Wageningen University
by the authority of the Rector Magnificus,
Prof. Dr A.P.J. Mol,
in the presence of the
Thesis Committee appointed by the Academic Board
to be defended in public
on Friday 23 March 2018
at 4 p.m. in the Aula.

Kailei Tang

Agronomy and photosynthesis physiology of hemp (*Cannabis sativa* L.),
174 pages.

PhD thesis, Wageningen University, Wageningen, the Netherlands (2018) With
references, with summary in English

ISBN: 978-94-6343-884-1

DOI: <https://doi.org/10.18174/434837>

Abstract

Kailei Tang, 2018. Agronomy and photosynthesis physiology of hemp (Cannabis sativa L.). PhD thesis, Wageningen University, Wageningen, the Netherlands, 174 pp.

Hemp (*Cannabis sativa* L.) is a sustainable high-yielding crop that delivers valuable fibres, seeds and psychoactive substances. However, there is a lack of field experimental data on the cultivation of hemp because its production was largely abandoned in the last century. Hemp is now considered as an ideal crop to produce innovative biomaterials, and in particular, the dual-purpose hemp production (fibre + seed) is now the norm in European countries, driven by the shift of a rapidly expanding market for hemp seeds coupled with lower quality fibre requirements for innovative biomaterials. This study brought new information on the agronomy and photosynthesis physiology for the resurging production of hemp, particularly for dual-purpose production in Europe.

The effects of important agronomic factors, i.e. cultivar, planting density, and nitrogen fertilization, on the performance of the hemp crop were investigated under contrasting European environments. Based on the experimental data, for dual-purpose hemp production, a planting density of 90–150 plants m⁻² is recommended for a monoecious cultivar that gives a long vegetative phase while leaving enough time for seed growth. A nitrogen fertilization rate of 60 kg N ha⁻¹ was generally sufficient in the tested environments whereas further optimization of nitrogen fertilization requires accurate and precise assessment of plant nutritional status. To facilitate assessing plant nutritional status, a critical nitrogen dilution curve was determined for hemp.

The responses of leaf photosynthesis to nitrogen content and temperature were quantified using a biochemical model of C₃ leaf photosynthesis, based on a complete set of photosynthetic measurements for hemp leaves. Then, by combining measurements and modelling, an upscaling was made from the leaf to the canopy level to analyse hemp's photosynthetic nitrogen-use efficiency (*NUE*) and water-use efficiency (*WUE*) in response to water and nitrogen supply. The effect of nitrogen supply level on hemp's *NUE* and *WUE* was largely determined by its effect on canopy size or leaf area index (*LAI*). The effect of short-term water stress on *WUE* and *NUE* was reflected in the stomatal regulation, whereas long-term water stress enhanced leaf senescence, reduced *LAI* but retained total canopy nitrogen content, and thus resulted in a further increase in *WUE*.

Findings in this thesis provided an improved understanding of the agronomy and photosynthesis physiology of hemp, particularly in relation to the dual-purpose production of hemp in Europe. Such understanding not only provides additional evidence that hemp can be grown as a sustainable crop over a wide range of climatic and agronomic conditions, but also provides essential information for parameterizing crop growth models. Prospects for further research were discussed in view of using the findings in this thesis in combination with a crop growth model to develop strategies for optimization of hemp cultivation and breeding.

Keywords: canopy; critical dilution curve; cultivar; density; fibre; hemp (*Cannabis sativa* L.); leaf; modelling; nitrogen; nitrogen use efficiency; phenology; photosynthesis; seed; stem; temperature; water; water use efficiency.

Contents

Chapter 1	General introduction	1
Chapter 2	Comparing hemp (<i>Cannabis sativa</i> L.) cultivars for dual-purpose production under contrasting environments	15
Chapter 3	A comprehensive study of planting density and nitrogen fertilization effect on dual-purpose hemp (<i>Cannabis sativa</i> L.) cultivation	47
Chapter 4	Hemp (<i>Cannabis sativa</i> L.) leaf photosynthesis in relation to nitrogen content and temperature: implications for hemp as a bio-economically sustainable crop	83
Chapter 5	Water- and nitrogen-use efficiencies of hemp (<i>Cannabis sativa</i> L.) based on whole-canopy measurements and modelling	115
Chapter 6	General discussion	149
	Summary	165
	Acknowledgements	169
	PE&RC Training and Education Statement	171
	Curriculum vitae	173
	Funding	174

Chapter 1

General introduction

Chapter 1

Abstract

This chapter first provides a brief introduction to the hemp (*Cannabis sativa* L.) plant and the state of knowledge on hemp agronomy and crop physiology. Subsequently, the aim of the thesis, the methodological framework and an overall thesis structure are outlined.

1.1 Hemp plant

Hemp (*Cannabis sativa* L.) is an annual dicotyledonous angiosperm plant belonging to the *Cannabaceae* family and the *Cannabis* genus. Hemp seedlings have two sessile seed leaves but all true leaves have a 1–3 cm petiole. The first pair of true leaves have a single narrowly elliptic blade with serrate margins. A leaf from the second pair has 3–13 cm palmately composed serrate leaflets. Each leaflet has a length of 5–15 cm and a width of 1–2 cm. In young hemp plants the number of leaflets per compound leaf increases progressively and the phyllotaxis is opposite, but as flowering begins, the number of leaf leaflets per compound leaf declines and phyllotaxis changes from opposite to alternate.

The stem of the hemp plant is hollow. Its size at maturity is very variable. At high planting densities hemp plants develop thinner stems with fewer branches whereas at low density the plants are highly branched with much thicker stems. Technically hemp stems can be separated into two components: the stem tissues outside the vascular cambium (bark) and the stem tissues inside the vascular cambium (core). The bark, accounting for 24–47% of whole stem weight (De Meijer, 1994), consists of the epidermis, the cortex and the phloem. In the phloem are sieve tubes and primary bast fibres, arising from the prodesmogen. The primary fibres have a length ranging between 3 mm and 55 mm with a mean of 20–28 mm (Amaducci *et al.*, 2005). In old hemp plants, the phloem may contain secondary bast fibres arising from the cambium. The mean length of secondary bast fibres is about 2 mm (Amaducci *et al.*, 2005). Wood core mainly consists of short fibres with length of about 5 mm (Li *et al.*, 2013).

Naturally hemp is dioecious, meaning that male and female flowers develop on separate plants. The two sexes are morphologically indistinguishable before the development of inflorescences, but in the generative phase sexual dimorphism is extremely pronounced. Male plants have a loose and branched inflorescence in the top of the plant, with few or no leaves. Each male flower has five white to yellowish-green petals about 5 mm long, and five stamens which at maturity release abundant yellow pollen for wind-pollination. The male plants die after flowering. Female plants have a compacted and leafy inflorescence in the top of the plant. Female flowers, that are surrounded by green bracts, are only recognizable after the emission of stigmas that are only a few millimetres long. In modern times, monoecious varieties, meaning that male and female flowers develop on the same plant, have been selected and cultivated (Salentijn *et al.*, 2015).

The seed of commerce is an achene with a hard shell, tightly covered by the thin wall of the

ovary. The seed is ellipsoid, slightly compressed, smooth, 2–6 mm in length and 2–4 mm in diameter. It is light brown to dark grey, in some cases mottled, containing about 28% oil and 26% crude protein (Vonapartis *et al.*, 2015).

It should be mentioned that industrial hemp generally contains a low percentage of Δ^9 -tetrahydrocannabinol (THC, the principal intoxicant cannabinoid found in marijuana). Current laws in many countries constrain cultivation of hemp cultivars bearing THC above a (low) threshold. The threshold is arbitrarily set at 0.3% in China and Canada, although a THC level of 1% is considered a minimum value to elicit an intoxicating effect (Grotenhermen & Karus, 1998). In the European Union (EU), the THC threshold is even down to 0.2% in the interest of safety. However, there is an appeal to bring the European threshold up to 0.3% (Carus *et al.*, 2017).

1.2 Growing interest for multi-purpose hemp cultivation

In recent years, the pressing need for renewable resources and sustainable materials has fuelled a renewed interest in natural plant fibres. Actual markets of natural plant fibres are dominated by cotton that, on average, accounts for over 70% of the global natural fibre production (2010–2014) (FAOSTAT, 2017). However, cotton poses particular concerns with regard to sustainability as it has one of the worst environmental footprints of any crop, with particularly high demands for irrigation and agricultural chemicals (Pfister *et al.*, 2011). An increasing concern on sustainable development of agricultural bio-economy appeals for cultivation of profitable fibre crops with positive environment effects.

Hemp has potential to produce up to 25 Mg ha⁻¹ biomass yield at relatively low inputs (Struik *et al.*, 2000) and it was said to improve soil structure, suppress weeds effectively, and to be virtually free from disease or pests (Desanlis *et al.*, 2013). Moreover, traditionally cultivated mainly for the production of textiles and ropes, hemp is now considered as an ideal crop to produce innovative biomaterials. Its stems contain high-quality cellulose (De Meijer & van der Werf, 1994); its seeds contain healthy oil (Leizer *et al.*, 2000); high added-value compounds can be recovered from the female inflorescence and from threshing residues after harvesting seeds (Calzolari *et al.*, 2017; Bertoli *et al.*, 2010). Examples of actual and potential innovative uses of hemp plant are numerous (Carus *et al.*, 2013). Hemp stem can be used as raw materials for making paper (Van der Werf *et al.*, 1994a); hemp fibre can be used as reinforcement in composites materials, to produce insulation mats (Grohe, 2004) and car interior panels (Holbery & Houston, 2006); hemp shives alone (Jarabo *et al.*, 2012) or shives together with bast fibre

(de Bruijn *et al.*, 2009) mixed with a binder (lime, clay, plaster, *etc.*) are used to form hemp concrete; hemp seeds can be used as food, feed (Callaway, 2004) and to make cosmetics (Sapino *et al.*, 2005). A summary of the many applications of hemp in Europe is presented in Figure 1.1.

Hemp is one of the oldest crops known to man that is estimated to have begun with a first harvest around 8500 years ago (Fike, 2016). As one of the most important fibre crops, hemp cultivation peaked between the 16th and the 18th century. Its cultivation declined in the last

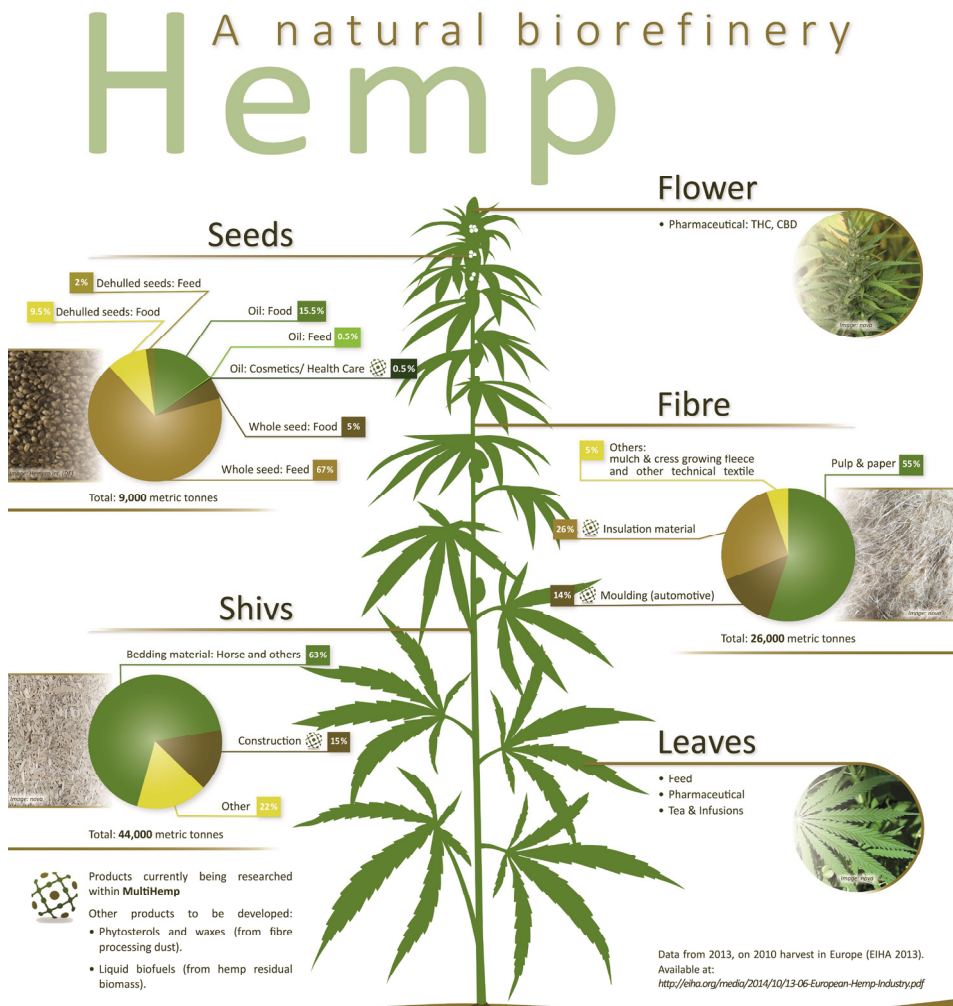


Figure 1.1 Hemp: a natural bio-refinery. Reprinted from a poster produced during EC funded Multihemp project (www.multihemp.eu).

century and was displaced largely by cotton and synthetic fibres (Allegret, 2013). This decline was hastened by concerns over the use of its illegal narcotics.

According to FAOSTAT, there was about 70,000 ha year⁻¹ of hemp cultivated worldwide (excluding the acreage in Canada) in the last decade (2004–2014). The main cultivation areas of hemp were North Korea, China, Canada and the EU. The area of hemp in North Korea was estimated at about 20,000 ha year⁻¹ mainly for the purpose of fibre production. In China, hemp was cultivated on about 18,000 ha year⁻¹, with about half of the area for the production of textile fibre in the North-eastern, Central-eastern and South-western parts while another half of the area for seed production, mainly in Northern China.

In recent years, the innovative uses of hemp materials and the increasing concern on sustainable development of the agricultural bio-economy have encouraged and sustained a development of the hemp industry that supports the cultivation, processing and use of hemp and its products, particularly in Canada and Europe (www.eiha.org). The cultivation of hemp in Canada and in the EU was reauthorized in the 1990s. Canadian hemp production has been steadily increasing since 2008 after some market adjustments during the early years. At present, licensed hemp cultivation in Canada reaches more than 20,000 ha year⁻¹, almost exclusively for the production of seeds (Cherney & Small, 2016). A fast growth of hemp cultivation was also seen in Europe, where hemp acreage increased from 8,000 ha in 2011 to more than 33,000 ha in 2016 (Carus & Sarmiento, 2016). In Europe, the main cultivation areas are in France, the Netherlands, the Baltic Countries and in Romania. However, many other European countries started or expanded their hemp cultivation, mainly for dual-purpose hemp production: for the seeds and for the fibre. The dual-purpose hemp production in Europe is driven by the shift of a fast expanding market for hemp seeds coupled with lower quality fibre requirements for innovative biomaterials (Amaducci *et al.*, 2015).

1.3 Rapidly improved hemp production

Despite the renewed interest in hemp's obvious potential as a biorefinery crop, hemp remains poorly developed (Wirtshafter, 2004), as a consequence of the declination of its production in the last century when intensive breeding and agronomic programmes have driven great improvements in major crops. Since 2012, a comprehensive 4-year study, the European project Multi hemp (<http://multi hemp.eu>), covered the levels from molecular genetics through to end product demonstration, with the aims to have significant impacts from both scientific and economic aspects by building on fundamental scientific understanding in the development of

hemp raw materials through to providing the basis for innovations in the areas of crop breeding, agronomy and harvesting, and biorefining. The ambition of Multihemp was to develop an integrated hemp-based biorefinery in which improved feedstock is subjected to efficient and modular processing steps to provide fibre, oil, construction materials, fine chemicals and biofuels using all components of the harvested biomass, and to generate new opportunities within the developing knowledge based bio-economy. This thesis reports on a major part of the research activities on the agronomy and photosynthesis physiology of hemp carried out within the Multihemp framework, paying particular attention to the effects of genotype, environment and management on dual-purpose hemp production (fibre + seed). It also investigates the physiological basis of hemp's high resource-use efficiencies (RUE). Such understanding will help to parameterize a generic crop growth model for hemp to develop strategies for optimization of cultivation and breeding in hemp.

1.3.1 Understandings of the effects of genotype, environment and management on dual-purpose hemp production

Knowledge of genotype, environment and management effects on hemp production is of paramount importance for developing strategies to optimize cultivation and breeding in hemp.

The number of registered cultivars has risen rapidly since the 1990s when hemp cultivation was progressively authorized throughout the EU. In 2016, there were more than 60 hemp cultivars registered in the common catalogue of varieties of agricultural plant species (<https://ec.europa.eu/>). These cultivars differ not only in many characters, such as stem fibre content and sex type (Höppner & Menge-Hartmann, 2007), but also in their response to the growing environment (Legros *et al.*, 2013). Cultivars bred at low latitudes show a very long vegetative phase or even fail to reach flowering when cultivated at higher latitudes, which not only results in low seed yield but also in frequent frost damage affecting the fibre quality. In contrast, cultivars bred at high latitudes have very short vegetative phases and limited biomass production when cultivated in southern environments (Amaducci *et al.*, 2015). Therefore, there is a need to characterize currently available cultivars or potential breeding lines to identify their suitability for specific environments and end-use destinations.

In the absence of water limitation, management factors that have a major influence on hemp cultivation, in terms of quality and/or quantity of products, are planting density and nitrogen fertilization. While the effects of these factors on hemp cultivation have been subjected to a number of research studies (Finnan & Burke, 2013, Westerhuis *et al.*, 2009; Amaducci *et al.*,

2002; Struik *et al.*, 2000), their effects on both stem and seed yields have not been properly addressed so far, and important agronomic information such as optimal planting and crop nitrogen demand has not been made available for growing hemp as a dual-purpose crop.

1.3.2 Understandings of hemp's resource-use efficiency

Besides a high yield potential, an important characteristic for an industrial crop, adapted to modern sustainable production systems, is the ability to use resources efficiently. The higher is the RUE of a crop, the higher is the yield for a given level of the resource and the lower is the impact on the environment.

Hemp RUE depends on growth environment and plant physiological state (Amaducci *et al.*, 2015). The most important physiological process determining RUE is photosynthesis, at both leaf and canopy levels. Leaf photosynthetic capacity is strongly related to leaf nitrogen content (Sinclair & Horie, 1989). Studies of hemp photosynthesis in response to nutritional status are generally scarce although increased hemp leaf nitrogen content (Marija *et al.*, 2011; Ivanyi & Izsaki, 2009) and biomass yield (Finnan & Burke, 2013) were reported when nitrogen was applied. Moreover, hemp RUE was widely reported to decrease after flowering (Struik *et al.*, 2000, Van der Werf *et al.*, 1994b) and this decrease was proposed to be a result of leaf senescence (Van der Werf *et al.*, 1996). In senescent leaves, chlorophyll is degraded and photosynthesis related enzymes and other proteins are broken down into amino acids (Chiba *et al.*, 2003) that are exported as a source of nitrogen transfer to seeds. Literature evidence that the photosynthetic rate of hemp decreases as a result of nitrogen loss resulting in lower RUE is lacking for hemp. On the other hand, leaf photosynthesis has been studied in detail for major crops (Sinclair & Horie, 1989; Yin *et al.*, 2009), and a biochemical leaf photosynthesis model has been developed (Farquhar *et al.*, 1980). The experimental protocols for parameterizing this model have also been standardised (Yin *et al.*, 2009; Sharkey *et al.*, 2007). Therefore, there is an excellent opportunity to fully understand hemp leaf photosynthesis and its variation in response to growth environment, developmental stage and nutritional status at leaf level.

RUE at leaf level may not represent that at canopy level (Tomás *et al.*, 2012) because the latter also depends on canopy size and the distributions of light intensity and leaf nitrogen concentration within canopy. On the basis of a thorough understanding of the underlying mechanisms of leaf and canopy photosynthesis, models have been developed to quantify the response of canopy photosynthesis to varying micro-environments under different physiological conditions (Hikosaka *et al.*, 2016). Such canopy models are capable of simulating

instantaneous canopy gas exchange measurements by micro-meteorological techniques (Wright *et al.*, 2013; Leuning *et al.*, 1998) and in canopy chambers (Müller *et al.*, 2005). In this context, the RUE of hemp at canopy level could be quantitatively assessed using a well-defined canopy model.

1.4 Objectives of the present study

The overall objective of this study is to obtain an enhanced understanding of the agronomy and photosynthesis physiology for dual-purpose production of hemp (fibre + seed) in Europe. To this end, studies are defined to assess the effects of genotype, environment and management on the functioning of hemp crops, and to elucidate the physiological basis of hemp resource-use efficiencies. The specific objectives are:

- 1) to compare hemp cultivars for dual-purpose production under contrasting environments;
- 2) to assess the effects of planting density and nitrogen fertilization on hemp production, and to quantify the optimal planting density and nitrogen demand of hemp as a dual-purpose crop;
- 3) to quantitatively analyse the photosynthetic capacities of hemp leaf under varying physiological and environmental conditions;
- 4) to upscale hemp photosynthesis from leaf level to canopy and to assess water- and nitrogen-use efficiencies of hemp crop;
- 5) to discuss potential strategies to develop cultivars and cropping practices for dual-purpose hemp production.

1.5 Structure of this thesis

This thesis consists of six chapters. Chapter 1 (this chapter) provides a brief introduction to the hemp plant and the state of knowledge on hemp agronomy and photosynthesis physiology. Knowledge gaps on the effects of genotype, environment and management on hemp production and on hemp's RUE are identified, and a list of objectives is presented. Chapter 2 evaluates the genotypic variation of hemp productivity over a wide range of environments, and potential strategies to develop cropping practices and new cultivars for dual-purpose hemp production are discussed thereof. Chapter 3 assesses the effects of planting density and nitrogen fertilization on hemp stem and seed productivities. Specific effort is dedicated to the determination of optimal planting density for dual-purpose hemp production and nitrogen demand of hemp crops during the growing season. Chapters 4 and 5 aim to understand the

physiological basis of hemp's high RUE by analysing leaf and canopy photosynthesis, respectively, of hemp grown under varying physiological and environmental conditions. Chapter 6 provides a synthesis of the main findings and discusses the potential role of hemp in sustainable development of agricultural bio-economy. Finally, the current state and prospects of hemp research are discussed.

References

- Allegret, S. (2013) The history of hemp. In: *Hemp: industrial production and uses* (eds Allegret, S., Bouloc, P. and Arnaud, L.), pp. 4–26. CPi Group (UK) Ltd, Croydon, UK.
- Amaducci, S., Errani, M. and Venturi, G. (2002) Response of hemp to plant population and nitrogen fertilisation. *Italian Journal of Agronomy*, **6**, 103–111.
- Amaducci, S., Pelatti, F. and Bonatti, P.M. (2005) Fibre development in hemp (*Cannabis sativa* L.) as affected by agrotechnique: preliminary results of a microscopic study. *Journal of Industrial Hemp*, **10**, 31–48.
- Amaducci, S., Scordia, D., Liu, F. *et al.* (2015) Key cultivation techniques for hemp in Europe and China. *Industrial Crops and Products*, **68**, 2–16.
- Bertoli, A., Tozzi, S., Pistelli, L. *et al.* (2010) Fibre hemp inflorescences: From crop-residues to essential oil production. *Industrial Crops and Products*, **32**, 329–337.
- Callaway, J.C. (2004) Hempseed as a nutritional resource: An overview. *Euphytica*, **140**, 65–72.
- Calzolari, D., Magagnini, G., Lucini, L. *et al.* (2017) High added-value compounds from Cannabis threshing residues. *Industrial Crops and Products*, **108**, 558–563.
- Carus, M., Karst, S., Kauffmann, A. *et al.* (2013) *The European hemp industry: cultivation, processing and applications for fibres, shivs and seeds*. European Industrial Hemp Association (EIHA), Hürth, Germany, European. Available at (2017, November 29): <http://eiha.org/media/2014/10/13-06-European-Hemp-Industry.pdf>
- Carus, M. and Sarmiento, L. (2016) *The European hemp industry: cultivation, processing and applications for fibres, shivs and seeds*. European Industrial Hemp Association (EIHA), Hürth, Germany, European. Available at (2017, November 29): <http://eiha.org/media/2016/05/16-05-17-European-Hemp-Industry-2013.pdf>
- Carus, M., Reinders, M., Bañas, B. *et al.* (2017) *The Cologne declaration on industrial hemp*. European Industrial Hemp Association (EIHA), Hürth, Germany, European. Available at (2017, November 29): http://eiha.org/media/2017/07/17-06-06%20EIHA%20Cologne%20Declaration_final.pdf
- Cherney, J. and Small, E. (2016) Industrial hemp in North America: production, politics and potential. *Agronomy*, **6**, 58–82.
- Chiba, A., Ishida, H., Nishizawa, N.K. *et al.* (2003) Exclusion of ribulose-1,5-bisphosphate carboxylase/oxygenase from chloroplasts by specific bodies in naturally senescing leaves of wheat. *Plant Cell Physiology*, **44**, 914–921.
- De Bruijn, P.B., Jeppsson, K-H, Sandin, K. *et al.* (2009) Mechanical properties of lime-hemp

- concrete containing shives and fibres. *Biosystems Engineering*, **103**, 474–479.
- De Meijer, E.P.M. (1994) Variation of Cannabis with reference to stem quality for paper pulp production. *Industrial Crops and Products*, **3**, 201–211.
- De Meijer, E.P.M. and Van der Werf, H.M.G. (1994) Evaluation of current methods to estimate pulp yield of hemp. *Industrial Crops and Products*, **2**, 111–120.
- Desanlis, F., Cerruti, N., Warner, P. *et al.* (2013) Hemp agronomics and cultivation. In *Hemp: industrial production and uses* (eds Allegret, S., Bouloc, P. and Arnaud, L.), pp. 98–124. CPi Group (UK) Ltd, Croydon, UK.
- Farquhar, G.D., Von Caemmerer, S. and Berry, J.A. (1980) A biochemical model of photosynthetic CO₂ assimilation in leaves of C₃ species. *Planta*, **149**, 78–90.
- Fike, J. (2016) Industrial hemp: renewed opportunities for an ancient crop. *Critical Reviews in Plant Sciences*, **35**, 406–424.
- Finnan, J. and Burke, B. (2013) Nitrogen fertilization to optimize the greenhouse gas balance of hemp crops grown for biomass. *GCB Bioenergy*, **5**, 701–712.
- Grohe, B. (2004) Heat conductivities of insulation mats based on water glass bonded non-textile hemp or flax fibres. *European Journal of Wood and Wood Products*, **62**, 352–357.
- Grotenhermen, F. and Karus, M. (1998) Industrial hemp is not marijuana: Comments on the drug potential of fiber Cannabis. *Journal of the International Hemp Association*, **5**, 96–101.
- Hikosaka, K., Kumagai, T.O. and Ito, A. (2016) Modeling canopy photosynthesis. In: *Canopy Photosynthesis: From Basics to Applications*. (eds Hikosaka, K., Niinemets, Ü. and Anten, N.P.R.), pp. 239–268. Springer, Dordrecht, Netherlands.
- Holbery, J.D. and Houston, D.Q. (2006) Natural-fiber-reinforced polymer composites in automotive applications. *JOM*, **58**, 80–86.
- Höppner, F. and Menge-Hartmann, U. (2007) Yield and quality of fibre and oil of fourteen hemp cultivars in Northern Germany at two harvest dates. *Landbauforschung Volkenrode*, **57**, 219–232.
- Ivanyi, I. and Izsaki, Z. (2009) Effect of nitrogen, phosphorus, and potassium fertilization on nutritional status of fiber hemp. *Communications in Soil Science and Plant Analysis*, **40**, 974–986.
- Jarabo, R., Fuente, E., Monte, M.C. *et al.* (2012) Use of cellulose fibers from hemp core in fiber-cement production. Effect on flocculation, retention, drainage and product properties. *Industrial Crops and Products*, **39**, 89–96.
- Legros, S., Picault, S. and Cerruti, N. (2013) Factors affecting the yield of industrial hemp - experimental results from France. In: *Hemp: industrial production and uses* (eds Allegret, S., Bouloc, P. and Arnaud, L.), pp. 72–97. CPi Group (UK) Ltd, Croydon, UK.
- Leizer, C., Ribnicky, D., Poulev, A. *et al.* (2000) The composition of hemp seed oil and its potential as an important source of nutrition. *Journal of Nutraceuticals, Functional & Medical Foods*, **2**, 35–53.
- Leuning, R., Dunin, F. and Wang, Y-P (1998) A two-leaf model for canopy conductance, photosynthesis and partitioning of available energy. II. Comparison with measurements.

- Agricultural and Forest Meteorology*, **91**, 113–125.
- Li, X., Wang, S., Du, G. *et al.* (2013) Variation in physical and mechanical properties of hemp stalk fibers along height of stem. *Industrial Crops and Products*, **42**, 344–348.
- Marija, M., Māra, V. and Veneranda, S. (2011) Changes of photosynthesis-related parameters and productivity of *Cannabis sativa* under different nitrogen supply. *Environmental and Experimental Biology*, **9**, 61–69.
- Pfister, S., Bayer, P., Koehler, A. *et al.* (2011) Environmental impacts of water use in global crop production: hotspots and trade-offs with land use. *Environmental Science & Technology*, **45**, 5761–5768.
- Salentijn, E.M.J., Zhang, Q., Amaducci, S. *et al.* (2015) New developments in fiber hemp (*Cannabis sativa* L.) breeding. *Industrial Crops and Products*, **68**, 32–41.
- Sapino, S., Carlotti, M.E., Peira, E. *et al.* (2005) Hemp-seed and olive oils: Their stability against oxidation and use in O/W emulsions. *International Journal of Cosmetic Science*, **27**, 355–355.
- Sharkey, T.D., Bernacchi, C.J., Farquhar, G.D. *et al.* (2007) Fitting photosynthetic carbon dioxide response curves for C₃ leaves. *Plant, Cell & Environment*, **30**, 1035–1040.
- Sinclair, T.R. and Horie, T. (1989) Leaf nitrogen, photosynthesis, and crop radiation use efficiency: a review. *Crop Science*, **29**, 90–98.
- Struik, P.C., Amaducci, S., Bullard, M.J. *et al.* (2000) Agronomy of fibre hemp (*Cannabis sativa* L.) in Europe. *Industrial Crops and Products*, **11**, 107–118.
- Tomás, M., Medrano, H., Pou, A. *et al.* (2012) Water-use efficiency in grapevine cultivars grown under controlled conditions: effects of water stress at the leaf and whole-plant level. *Australian Journal of Grape and Wine Research*, **18**, 164–172.
- Van der Werf, H.M.G., Harsveld Van der Veen, J.E., Bouma, A.T.M. *et al.* (1994a) Quality of hemp (*Cannabis sativa* L.) stems as a raw material for paper. *Industrial Crops and Products*, **2**, 219–227.
- Van der Werf, H.M.G., Haasken, H.J. and Wijnhuizen, M. (1994b) The effect of daylength on yield and quality of fibre hemp (*Cannabis sativa* L.). *European Journal of Agronomy*, **3**, 117–123.
- Van der Werf, H.M.G., Mathijssen, E.W.J.M. and Haverkort, A.J. (1996) The potential of hemp (*Cannabis sativa* L.) for sustainable fibre production: A crop physiological appraisal. *Annals of Applied Biology*, **129**, 109–123.
- Vonapartis, E., Aubin, M-P, Seguin, P. *et al.* (2015) Seed composition of ten industrial hemp cultivars approved for production in Canada. *Journal of Food Composition and Analysis*, **39**, 8–12.
- Westerhuis, W., Amaducci, S., Struik, P.C. *et al.* (2009) Sowing density and harvest time affect fibre content in hemp (*Cannabis sativa* L.) through their effects on stem weight. *Annals of Applied Biology*, **155**, 225–244.
- Wright, J., Williams, M., Starr, G. *et al.* (2013) Measured and modelled leaf and stand-scale productivity across a soil moisture gradient and a severe drought. *Plant, Cell & Environment*, **36**, 467–483.

Yin, X., Struik, P. C., Romero, P. *et al.* (2009) Using combined measurements of gas exchange and chlorophyll fluorescence to estimate parameters of a biochemical C₃ photosynthesis model: A critical appraisal and a new integrated approach applied to leaves in a wheat (*Triticum aestivum*) canopy. *Plant Cell & Environment*, **32**, 448–464.

Chapter 2

Comparing hemp (*Cannabis sativa* L.) cultivars for dual-purpose production under contrasting environments

K. Tang^{a,b}, P.C. Struik^a, X. Yin^a, C. Thouminot^c, M. Bjelková^d, V. Stramkale^e, S. Amaducci^b

^a Centre for Crop Systems Analysis, Department of Plant Sciences, Wageningen University & Research, Droevendaalsesteeg 1, Wageningen, The Netherlands

^b Department of Sustainable Crop Production, Università Cattolica del Sacro Cuore, via Emilia Parmense, 84, Piacenza, Italy

^c Federation Nationale des Producteurs de Chanvre, 20, rue Paul Ligneul, Le Mans, France

^d Department of Industrial Crops, AGRITEC Plant Research Ltd., Zemedělská 16, Šumperk, Czech Republic

^e Latgale Agriculture Research Centre, Kulturas Laukums 1a, Vilani, Latvia

Abstract

Interest in hemp as a multi-purpose crop is growing worldwide and for the first time in 2015 it was cultivated in Europe on more than 20,000 ha as a dual-purpose crop, for the seeds and for the fibre. In the present study, fibre and seed productivity of 14 commercial cultivars were tested in four contrasting European environments (Latvia, the Czech Republic, France, Italy). At full flowering, the stem yield ranged from 3.7 Mg ha⁻¹ to 22.7 Mg ha⁻¹, the bast fibre content ranged from 21% to 43%, and the bast fibre yield ranged from 1.3 Mg ha⁻¹ to 7.4 Mg ha⁻¹. When harvesting was postponed from full flowering until seed maturity, the stem yield of monoecious cultivars significantly increased but in dioecious cultivars it decreased at all tested sites, except for Italy. The seed yield ranged from 0.3 Mg ha⁻¹ to 2.4 Mg ha⁻¹ in Italy, France and the Czech Republic. Only the early cultivars Fedora 17 and Markant produced seed in the most northern location Latvia. The cultivar effect on stem and seed yield was mainly determined by the genetic variation in time of flowering. Stem yield at full flowering was strictly related to the duration of the vegetative phase while seed yield was lowest in the late flowering cultivar. The late cultivar CS is suitable for stem and fibre production as it had the highest stem yield at full flowering in all locations. Both Fedora 17 and Futura 75 are candidate cultivars for dual-purpose production in Italy, France and the Czech Republic, with Fedora 17 being more suitable for seed production and Futura 75 for fibre production.

The application of modelling to design production strategies for dual-purpose hemp is promising. However, accurate parameterisation is needed based on large data sets and diverse genetic background.

Key words: hemp (*Cannabis sativa* L.); cultivar; phenology; modelling; seed; fibre.

2.1 Introduction

Hemp is a high-yielding crop (Struik *et al.*, 2000) that requires little technical inputs (Amaducci *et al.*, 2015) and has a positive impact on the environment (Barth & Carus, 2015; Bouloc & Werf, 2013). Its stem contains high-quality cellulose (De Meijer, 1994), the seed contains high-quality oil (Callaway, 2004) and the inflorescence contains valuable resins (Bertoli *et al.*, 2010). From speciality pulp and paper to nutritional food, medicine and cosmetics, a wide variety of products can be derived from hemp stem, seed and inflorescence (Carus *et al.*, 2013). However, once an important non-food crop for the production of textiles and ropes, hemp cultivation progressively declined during the 20th century due to the competition from other feedstocks such as cotton and synthetic fibres (Allegret *et al.*, 2013). Recent research (Amaducci, 2005) and entrepreneurial attempt (Amaducci, 2003) to develop a hemp production chain for high quality fibre have not been successful. Consequently, hemp has not been subjected to the intensive agronomic and breeding research and development that have driven great improvements in major crops in the last 50 years (Amaducci *et al.*, 2015; Salentijn *et al.*, 2015). A renewed interest in hemp cultivation for multi-purpose production is apparent, and particularly for the combination of fibre and seeds, a profitable practice that is now the norm in European countries (Carus *et al.*, 2013). However, agronomic information to support dual-purpose hemp cultivation is scarce.

Genotype and environment have large effects on both fibre and seed production (Legros *et al.*, 2013). Since the 1990s, when hemp cultivation was progressively authorized throughout the European Union (Wirtshafter, 2004), the number of registered cultivars has risen rapidly, from 12 cultivars in 1995 to 45 in 2008 and 51 in 2013 (Salentijn *et al.*, 2015). Given the large variation in environmental conditions throughout Europe and the limited information available on hemp genotypes, it is a challenge for the farmers to choose suitable cultivars that maximize the economic returns. This study aims to assess the fibre and seed productivity of commercial hemp cultivars for dual-purpose production.

It has been reported that hemp stem yield increases proportionally with the length of vegetative phase (Faux *et al.*, 2013); thus, high stem yields are obtained with late flowering cultivars (Amaducci & Gusovius, 2010; Höppner & Menge-Hartmann, 2007). These are preferred when maximization of stem biomass is a priority, as in biomass production for bioenergy (Finnan & Styles, 2013; Prade *et al.*, 2011). In addition to high stem yield, a cultivar with high bast content is desirable because it contains high-cellulose, low-lignified long fibre

that is generally considered of higher value than the woody core. Fibre content was found stable across environments, but varied largely among genotypes, from 25% to 47% in cultivars bred during the 20th century (Amaducci & Gusovius, 2010; Westerhuis *et al.*, 2009b; De Meijer, 1994).

Late-flowering cultivars have high stem yield but low seed yield (Höppner & Menge-Hartmann, 2007) which was not a problem in traditional hemp for fibre production, for which harvesting was carried out at full flowering when bark yield reaches its maximum and fibre quality is high (Amaducci *et al.*, 2008a; Mediavilla *et al.*, 2001). Postponed harvesting time until seed maturity could increase stem yield as a consequence of continuous accumulation of secondary fibre and xylem (Amaducci *et al.*, 2005; Keller *et al.*, 2001) or decrease it due to senescence (Mediavilla *et al.*, 2001). The effect of delayed harvesting on bast fibre content and yield are modest (Höppner & Menge-Hartmann, 2007), but an increase of lignified fibre was observed (Westerhuis *et al.*, 2009a; Amaducci *et al.*, 2005), which is undesirable for applications such as textile and specialty pulp (De Meijer & van der Werf, 1994). In traditional hemp cultivation, seed production was further complicated by the use of dioecious cultivars that produced high stem yield with a large proportion of male plants that were considered of superior quality for textile applications (Berenji *et al.*, 2013). However, the male plants start their senescence soon after flowering which results in biomass loss and an increase in fibre heterogeneity. The shift of modern hemp cultivation to lower quality fibre coupled to seed production has led hemp breeding to focus on the development of monoecious cultivars that are considered suitable for producing stem and seed simultaneously (Salentijn *et al.*, 2015; Berenji *et al.*, 2013).

The large influence of flowering time on biomass production and seed set has stimulated numerous studies on the influence of genotype by environment interactions on hemp flowering (Hall *et al.*, 2012). Hemp is a quantitative short-day plant with temperature and photoperiod having strong effects on hemp development. The development rate increases with increasing temperature between a base and a cut-off temperature and with decreasing day-length during the photoperiod-sensitive phase (Amaducci *et al.*, 2008b; Lisson *et al.*, 2000a). Few studies are aimed at predicting hemp flowering as affected by temperature and photoperiod (Cosentino *et al.*, 2012; Amaducci *et al.*, 2008b; Lisson *et al.*, 2000a). Amaducci *et al.* (2008b, 2012) successfully modelled the flowering time of several cultivars across diverse environments in Europe on the basis of temperature and photoperiod. Such model could facilitate developing strategies for dual-purpose hemp production in different environments by simulating hemp

flowering time and hemp flowering duration, that in particular conditions can be longer than 2 months (Amaducci *et al.*, 2008c).

Relatively few studies have compared the stem and seed yield potential of a large selection of commercial hemp cultivars (Faux *et al.*, 2013; Höppner & Menge-Hartmann, 2007) and no information is available on the productivity of hemp cultivars in a wide range of European environments. In this study, stem and seed productivity of diverse commercial cultivars were compared in contrasting European environments, with the aim of providing novel information to support dual-purpose cultivation of hemp in Europe. In particular, we aim: 1) to investigate the effects of genotype and environment on hemp stem and seed productions; and 2) to discuss potential strategies to develop cultivars and cropping practices for dual-purpose hemp production.

2.2 Materials and methods

2.2.1 Environmental conditions, plant materials and trial arrangement

Field trials were carried out in four contrasting locations (Latvia, the Czech Republic, France, Italy) in 2013, to compare 14 commercial hemp cultivars (Tables 2.1, 2.2). The southern location (Italy; IT) had a hot and dry summer while the other three environments were cool and humid. The average temperature between May and October (during the hemp season) ranged from 16.0 °C (the Czech Republic; CZ) to 21.6 °C (IT), the total precipitation ranged from 227 mm (IT) to 419 mm (Latvia; LV). The latitude difference between the most northern (LV) and most southern (IT) location is 12° which corresponds to 2 h of maximum day-length (Figure 2.1).

Ten monoecious and four dioecious commercial cultivars were sown in a randomized complete block design with four replicates. Single plot size was 40 m². Sowing was carried out between the end of April and the middle of May according to local conditions. In IT, sowing was delayed until the middle of May due to unfavourable weather conditions. A total of 240 germinable seeds m⁻² were drilled at 3-4 cm depth using experimental-plot sowing machines. The distance between rows varied between 15 cm and 25 cm, depending on the sowing machine used at each location. Nitrogen fertilization was carried out at sowing (Table 2.2), with the exception of IT where fertilisation was carried out after emergence. Irrigation was only applied in IT (120 mm in total), due to the late sowing and an exceptionally dry summer. Herbicide

(Afalon, active ingredient: 37.6% w/w linuron) was only applied in CZ to control dicotyledonous weeds after sowing.

Table 2.1 List of origin and sexual type of tested cultivars.

Cultivar	Abbreviation	Origin	Sexual type
Beniko	BEN	Poland	Monoecious
Bialobrzeskie	BIA	Poland	Monoecious
Epsilon 68	EPS	France	Monoecious
Fedora 17	FED	France	Monoecious
Felina 32	FEL	France	Monoecious
Férimon	FER	France	Monoecious
Futura 75	FUT	France	Monoecious
Markant	MAR	Netherlands	Monoecious
Monoica	MON	Hungary	Monoecious
Tygra	TYG	Poland	Monoecious
CS	CS	Italy	Dioecious
KC Dora	KC	Hungary	Dioecious
Tiborszallasi	TIB	Hungary	Dioecious
Tisza	TIS	Hungary	Dioecious

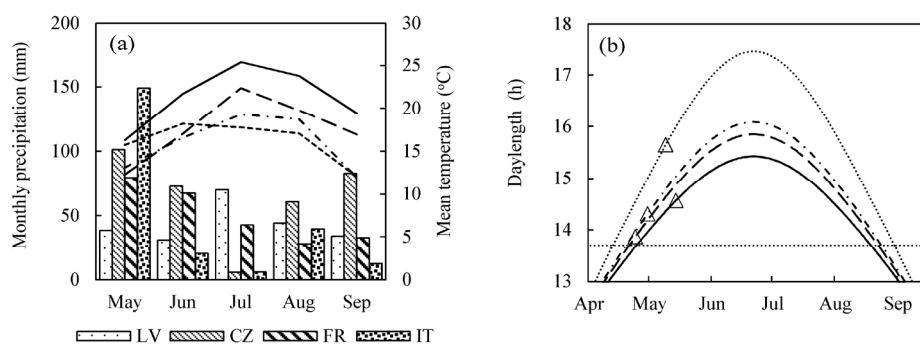


Figure 2.1 The meteorological parameters during the growing season of hemp. Panel a: the time course of mean temperature (line) and precipitation (bar); Panel b: the time course of photoperiod, the critical photoperiod for hemp (13.7 h) reported by Amaducci *et al.* (2012) is presented with a horizontal dashed line. Sowing dates are presented with an open triangle. The locations name are abbreviated as: LV (Latvia); CZ (the Czech Republic); FR (France); IT (Italy).

Table 2.2 Details of the experimental sites.

Country	Partner	Geographical coordinates	Altitude (m asl)	Soil total N (%)	Soil organic matter (g kg ⁻¹)	Mean temperature ^a (°C)	Precipitation ^a (mm)	Maximum daylength (h)	Sowing date	Fertilization (kg N ha ⁻¹)
Latvia	LARC	57N;27E	64	NA ^b	11.0	16.3	216.5	17.5	9 May	48
the Czech Republic	Agritec	50N;17E	319	0.14	NA	16.0	260.4	16.1	30 Apr	100
France	FNPC	48N;0E	67	0.07	10.9	17.7	330.6	15.9	24 Apr	46
Italy	UCSC	45N;10E	60	0.2	2.0	21.6	131.4	15.4	14 May	50

NA: Not available.

^a: Average from May to October

^b: The nitrate-N content in the soil was determined in Latvija (68 mg l⁻¹) instead of total N content.

2.2.2 Determination of development and yield

The number of emerged plants in each plot was counted in one row on a length of 1 m or in two rows on a length of 50 cm, every two days from the appearance of the first plant until full emergence. The emergence date for each cultivar was set as the date when 50% of seedlings had appeared. On 10 representative plants that were selected and marked before flowering, flowering state (i.e. onset of flowering, full flowering and end of flowering) was recorded weekly. To capture the full flowering date precisely, the observation was conducted twice a week when the full flowering stage was approaching. For each cultivar it was considered that a specific phenological stage was reached when 50% of the observed plants had reached that stage.

Harvesting was carried out in each plot twice: at full flowering (H1) and seed maturity (H2) (see Supplementary Material Table S2.1). The first harvest was carried out within 10 d from full flowering in IT, CZ and LV, while in France (FR) it was carried out with a certain delay (from 11 d to 25 d to full flowering depending on cultivars). The second harvesting was conducted for both stem and seed production at 46 d (from 40 d to 52 d), 37 d (from 26 d to 52 d), 38 d (from 26 d to 51 d) and 27 d (from 18 d to 35 d) after full flowering in IT, FR, CZ and LV, respectively. With the exception of the two early-flowering cultivars, Fedora 17 (FED) and Markant (MAR), the second harvesting in LV was conducted at the beginning of October after a killing frost. At that time, seeds were still immature, therefore, seed yield in LV was only determined for FED and MAR.

At each harvesting time, all plants in a 4-m² area were cut above soil surface and fresh weight was immediately measured. Ten representative plants were then subsampled, and their fresh weight was measured. Subsequently, their dry weight was measured after oven drying at 105 °C until constant weight. Dry matter content was calculated as the ratio of dry weight: fresh weight. The proportion of stem, leaf and seed (H2) in the total biomass was determined from another subsample of ten representative plants after oven drying. Plant density at harvesting was calculated by counting all the plants in the first harvested 1 m². Stem diameter at 10 cm from the stem base and whole stem length were measured on 25 representative plants in each plot.

After harvesting stems were air-dried in a ventilated place. Bast content in the stem was then determined on ten representative stems by mechanically separating bark and woody core. The dried stems were pressed to break by passing them through a laboratory decorticator and,

subsequently, remaining shives were removed manually from the bast. The decorticator in IT and LV had four pairs of rollers while in FR it had six pairs of rollers. Decortication was conducted with a UTR-scutching machine in CZ. The entire stem was decorticated in FR while in IT, LV and CZ the base 20 cm containing coarse fibre was removed and the next 1 m of stem was decorticated. The bast content of the selected stem section was considered representative for the whole stem (Van der Werf *et al.*, 1994). Stems harvested at full flowering were decorticated at all four locations while stems harvested at seed maturity were only processed in IT and CZ. Bast yield (in Mg ha⁻¹) was estimated by multiplying stem yield (in Mg ha⁻¹) by bast content in the stem (in percentage).

2.2.3 Calculating parameters of a phenological model

To characterise the phenology of the tested cultivars, flowering data was used to calibrate the phenological model developed by Amaducci *et al.* (2008b). The model divides post-emergence hemp phenology into three phases: the basic vegetative phase (BVP), the photoperiod induction phase (PIP), and the flower development phase (FDP). The latter ends when 50% of plants in a stand have visible flowers. Among the 13 parameters of the model, the days needed to complete BVP under the optimal condition (DI) and the steepness of the photoperiod response curve during PIP (n) were considered to depend on genotype while the other ones were considered constant (Amaducci *et al.*, 2012). Therefore, only DI and n were estimated in the present study by minimizing the difference between observed and predicted flowering time. The other parameters calculated by Amaducci *et al.* (2012) were used as default value in our calculations. Evaluation of fitting was performed via the performance indices relative root mean square error ($RRMSE$, %) and modelling efficiency (EF):

$$RRMSE = \frac{100}{\bar{O}} \sqrt{\frac{\sum_{i=1}^N (E_i - O_i)^2}{N}} \quad (2.1)$$

$$EF = 1 - \frac{\sum_{i=1}^N (E_i - O_i)^2}{\sum_{i=1}^N (O_i - \bar{O})^2} \quad (2.2)$$

where E is the estimated value, O the observed value, \bar{O} the mean of the observed values, i the i th E/O pair, and N is the number of E/O pairs. $RRMSE$ varies from 0 (best) to positive infinity. EF can give either positive or negative values, 1 being the upper limited, while negative infinity is the theoretical lower boundary. Negative values of EF indicate that the model introduces more ambiguity than that introduced by simply using the mean value of the observations as an estimator.

2.2.4 Statistical analysis

Statistical analyses were performed to assess the effects of cultivar and location on phenophases, biometric traits and yield components using SPSS statistics 22.0 (SPSS, Chicago, IL, USA). Data was subjected to a two-way ANOVA to assess the effect of cultivar \times location. The “block” was considered to be discrete and random. The effect of harvest on biometric traits and yield components were analysed in each sexual type, i.e. dioecious and monoecious. The duration of the phenophases was expressed in days and degree-days when the rate of development was correlated to the temperature. The degree-days was calculated as the time integral of $T_{ave} - T_b$, with T_{ave} being the daily average temperature and $T_b = 1\text{ }^{\circ}\text{C}$, the base temperature for hemp development (Lisson *et al.*, 2000b; Van der Werf *et al.*, 1995).

2.3 Results

2.3.1 Development

Of the seedlings, 50% appeared between 6 to 12 days after sowing, depending on locations and cultivars (Tables 2.3, 2.4). A significant effect of genotype on emergence was observed in IT, FR and LV, where MAR emerged significantly earlier than Tisza (TIS). The degree-days

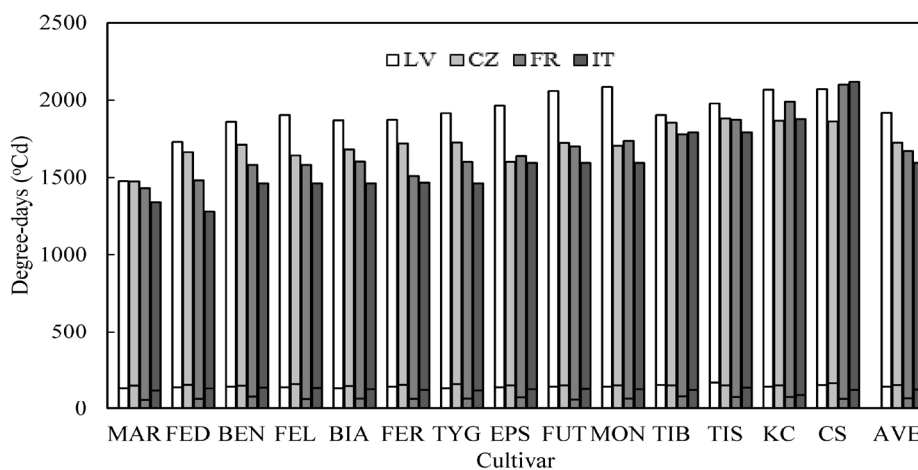


Figure 2.2 Degree-days required to complete phenological stages of tested varieties in different locations. The line in the bar indicates emergence time. The average of 14 varieties at each location is indicated as AVE. The LSD (0.05) for the emergence and vegetative growth periods were 17.3 °Cd and 54.1 °Cd, respectively. The locations name are abbreviated as: LV (Latvia); CZ (the Czech Republic); FR (France); IT (Italy). The cultivars name are abbreviated as: BEN (Beniko); BIA (Bialobrzeskie); EPS (Epsilon 68); FED (Fedora 17); FEL (Felina 32); FER (Férimon); FUT (Futura 75); MAR (Markant); MON (Monoica); TYG (Tygra); CS (CS); KC (KC Dora); TIB (Tiborszallasi); TIS (Tisza).

Table 2.3 F-statistics of fixed effects (cultivar and location) for the phenology, plant density, biometric traits and yield components.

Factor	Full flowering				Seed maturity							
	Cultivar		Location		Cultivar × Location		Cultivar		Location		Cultivar × Location	
	d.f.	F value	d.f.	F value	d.f.	F value	d.f.	F	d.f.	F value	d.f.	F value
Sowing to emergence	13	4.2**	3	688.0**	39	2.5**						
Emergence to full flowering	13	2.9**	3	550.7**	39	2.0**						
Plant density	13	203.8**	3	2866.5**	39	17.0**						
Plant height	13	249.8**	3	563.7**	39	23.2**						
Stem diameter	13	22.7**	3	131.8**	39	6.6**	13	18.4**	3	222.1**	39	5.5**
Stem yield	13	43.0**	3	662.2**	39	3.7**	13	15.7**	1	553.8**	13	6.6**
Leaf yield	13	10.9**	3	542.6**	39	1.4	13	9.7**	1	39.7**	13	1.6
Seed yield ^b	13	48.2**	3	1780.4**	39	13.0**	13	46.0**	3	1892.8**	39	17.6**
Bast content	13	33.2**	3	2714.9**	39	14.5**	13	42.4**	3	2441.0**	39	24.0**
Bast yield	13	76.6**	3	1811.1**	39	32.3**	13	46.4**	2	538.1**	26	10.3**
	13	43.0**	3	262.9**	39	3.5**	13	20.9**	1	210.0**	13	2.0
	13	76.6**	3	1811.1**	39	32.3**	13	44.3**	1	845.9**	13	41.6**

* Denotes significant difference at $P = 0.05$; ** denotes significant difference at $P = 0.01$.^a: The degree days was calculated with base temperature 1 °C.^b: Data from Lativa was not included.

Table 2.4 Duration of phenophases of tested cultivars in different locations.

Cultivar	Sowing to emergence (d)				Emergence to full flowering (d)				Average	
	CZ	FR	IT	LV	Average	CZ	FR	IT		LV
BEN	11.0	7.8a	8.7ab	8.3ab	8.9	96.1b	91.2gh	63.3f	103.4d	88.5
BIA	10.6	6.7abcd	8.1ab	8.0b	8.3	94.2bc	93.3fg	63.9ef	104.5cd	89.0
EPS	11.1	7.3abc	8.2ab	8.1b	8.7	89.2e	94.5efg	68.8d	111.9bc	91.1
FED	11.3	6.5bcd	8.4ab	8.1b	8.6	92.4cd	88.0gh	56.1g	94.4e	82.7
FEL	11.3	6.3cd	8.5ab	8.1b	8.5	91.2de	93.0fg	63.5ef	107.2cd	88.7
FER	11.2	6.5bcd	8.0ab	8.2ab	8.5	96.3b	89.2gh	64.3def	104.5cd	90.2
FUT	11.2	6.2cd	8.5ab	8.4ab	8.6	96.6b	98.8def	68.5de	119.1ab	95.8
MAR	10.8	6.0d	7.3b	8.0b	8.0	84.2f	86.0h	59.7fg	80.0f	77.3
MON	11.0	6.7abcd	8.2ab	8.3ab	8.5	95.5b	100.3de	68.8d	121.2a	96.5
TYG	11.4	6.7abcd	7.5ab	8.0b	8.4	96.6b	93.3fg	64.5def	108cd	90.6
CS	11.9	6.5bcd	7.8ab	8.6ab	8.7	104.6a	120.5a	91.2a	119.9ab	109.0
KC	10.8	7.7ab	7.9ab	8.4ab	8.7	105.9a	113.3b	82.3b	119.9ab	104.2
TIB	10.8	7.7ab	7.8ab	8.7ab	8.7	105.2a	101.6cd	76.7c	106.6cd	97.2
TIS	11.0	7.5ab	8.9a	9.0a	9.1	106.8a	107.1bc	75.6c	112.2bc	100.0
Average	11.1	6.9	8.1	8.3	8.6	96.8	97.0	69.2	108.6	92.8

Numbers followed by different letters in the same row are statistically different for $P = 0.05$ (Tukey test).

The cultivars name are abbreviated as: BEN (Beniko); BIA (Bialobrzeskie); EPS (Epsilon 68); FED (Fedora 17); FEL (Felina 32); FER (Férimon); FUT (Futura 75); MAR (Markant); MON (Monoica); TYG (Tygra); CS (CS); KC (KC Dora); TIB (Tiborszallasi); TIS (Tisza).

The locations name are abbreviated as: LV (Latvia); CZ (the Czech Republic); FR (France); IT (Italy).

required for emergence varied significantly among locations, with 69 °Cd, 125 °Cd, 144 °Cd, and 154 °Cd required in FR, IT, LV and CZ, respectively (Figure 2.2).

Flowering was observed from the beginning of July until the end of September. The duration of the vegetative phase, from emergence until full flowering, ranged from a minimum of 56 d (FED in IT) to a maximum of 121 d (Monoica and MON in LV) (Table 2.4). The vegetative phase, which was generally shorter in IT and was longer at higher latitudes, varied significantly among cultivars. As an example, the vegetative phase of MAR was 26 d shorter in IT than in LV while that of MON was 52 d shorter in IT than in LV. The variation among locations was smaller when expressed in degree-days than when expressed in days (Table 2.3). The degree-days required to complete the vegetative phase was positively correlated with the latitude for the cultivars Beniko (BEN), Bialobrzekie (BIA), Felina 32 (FEL), Ferimon (FER), Tygra (TYG), Futura 75 (FUT) and Tiborszallasi (TIB) ($P < 0.05$) while the trend was not significant for the other cultivars ($P > 0.05$) (Table 2.5).

The duration of the vegetative phase was significantly different among cultivars (Table 2.4). On average the dioecious cultivars reached flowering later than the monoecious ones, with the exception of the dioecious cultivar TIB which was significantly earlier (107 d) in LV than the monoecious cultivars MON (121 d) and FUT (119 d). CS was the latest among all the cultivars while FUT was the latest among the 8 monoecious cultivars. Cultivars MAR and FED were the earliest ones in IT (60 d and 56 d), FR (86 d and 83 d) and LV (80 d and 94 d), whereas the flowering time of Epsilon 68 (EPS; 89 d) was significantly earlier than that of FED (92 d, $P < 0.05$) in CZ.

Table 2.5 The correlation between degree-days from emergence to full flowering and latitude.

Cultivar	<i>r</i>	<i>P</i>	Cultivar	<i>r</i>	<i>P</i>
BEN	0.97	0.033	MAR	0.54	0.456
BIA	0.93	0.038	MON	0.92	0.077
EPS	0.87	0.128	TYG	0.98	0.020
FED	0.87	0.133	CS	-0.27	0.728
FEL	0.97	0.032	KC	0.45	0.553
FER	0.99	0.014	TIB	0.99	0.004
FUT	0.95	0.048	TIS	0.73	0.265
			Average	0.94	0.057

Numbers in bold are significant at $P = 0.05$ (2-tailed).

The cultivars name are abbreviated as: BEN (Beniko); BIA (Bialobrzekie); EPS (Epsilon 68); FED (Fedora 17); FEL (Felina 32); FER (Férimon); FUT (Futura 75); MAR (Markant); MON (Monoica); TYG (Tygra); CS (CS); KC (KC Dora); TIB (Tiborszallasi); TIS (Tisza).

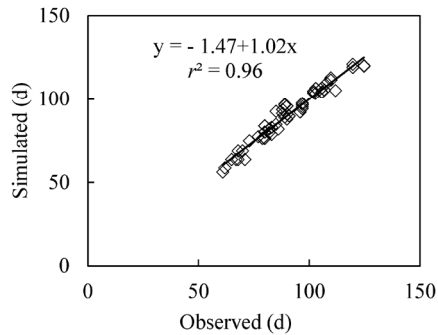


Figure 2.3 Predicted and observed duration between emergence and full flowering. Observed phenological data was fitted to the phenological model developed by Amaducci *et al.* (2008b).

The flowering time was simulated using the model developed by Amaducci *et al.* (2008b) on the basis of daily average temperature and photoperiod (Figure 2.3). The maximum difference between observed and simulated flowering time was 8 days. The relative root mean square error (*RRMSE*) was between 1.2% and 5.8%, model efficiency (*EF*) was between 0.85 and 1.0 (Table 2.6). Comparing with the parameters calculated by Amaducci *et al.* (2012) and Amaducci *et al.* (2008b) for the three cultivars that are common to our study (FEL, FUT and TIB), the values calculated with our observations were higher for *DI* (the days needed to complete basic vegetative phase under optimal conditions) but lower for *n* (the steepness parameter of the photo-inductive phase). The parameter values reported in Amaducci *et al.* (2012) enabled a relatively accurate estimation of flowering time for FEL and FUT but the *EF* of TIB was low (0.19). The parameter values reported in Amaducci *et al.* (2008b) provided an acceptable estimation of flowering time for FUT, but the *EF* of FEL and TIB was low.

2.3.2 Biomass yield

The average plant density at full flowering was 106 plants m^{-2} in CZ, 134 plants m^{-2} in both IT and FR, and 169 plants m^{-2} in LV (see Supplementary Material Table S2.2), at seed maturity plant density remained constant in FR and LV, while it decreased significantly in IT and CZ for both monoecious and dioecious cultivars (Table 2.7).

Stem dry matter yield at full flowering ranged from 3.7 $Mg\ ha^{-1}$ to 9.5 $Mg\ ha^{-1}$ in IT, from 3.8 $Mg\ ha^{-1}$ to 10.2 $Mg\ ha^{-1}$ in FR, from 10.2 $Mg\ ha^{-1}$ to 17.9 $Mg\ ha^{-1}$ in CZ and from 8.8 $Mg\ ha^{-1}$ to 22.7 $Mg\ ha^{-1}$ in LV (Table 2.8). The average plant height and stem diameter ranged respectively from 122 cm (BEN in IT) to 309 cm (CS in CZ) and from 3.8 mm (BEN in IT) to 10.4 mm (CS at CZ) (see Supplementary Material Table S2.2). The effects of genotype on stem

Table 2.6 The calculated parameter values for the phenological model developed by Amaducci *et al.* (2008b) when the difference between observed and predicted flowering date were minimized. *DI*: the days needed to complete the basic vegetative phase (BVP) under optimal conditions; *n*: steepness parameter of the photo-inductive phase. The other model parameters were set according to Amaducci *et al.* (2012); *RRMSE*: relative root mean square error; *EF*: modelling efficiency.

Cultivar	<i>DI</i>	<i>n</i>	<i>RRMSE</i>	<i>EF</i>
BEN	50.2	21.7	5.8	0.89
BIA	43.7	23.9	3.9	0.95
EPS	43.9	25.8	1.3	0.99
FED	37.2	21.4	5.8	0.91
FEL	39.1	25.2	2.2	0.98
FEL (2012) ^a	11.1	33.4	9.3	0.74
FEL (2008) ^a	13.2	47.0	13.0	-0.29
FER	44.8	24.3	5.6	0.91
FUT	25.1	33.6	1.2	1.00
FUT (2012) ^a	14.7	39.6	5.6	0.92
FUT (2008) ^a	19.7	52.1	2.2	0.99
MAR	41.9	12.6	3.9	0.91
MON	26.8	34.0	1.4	1.00
TYG	42.0	25.5	5.0	0.93
CS	51.6	77.4	3.9	0.85
KC	32.5	50.9	2.6	0.97
TIB	60.9	14.1	2.9	0.95
TIB (2012) ^a	20.6	38.6	10.6	0.19
TIB (2008) ^a	18.5	66.7	13.3	0.50
TIS	61.5	15.6	3.1	0.95

^a: 2008 indicates value of parameters reported by Amaducci *et al.* (2008b); 2012 indicates value parameters reported by Amaducci *et al.* (2012)

The cultivars name are abbreviated as: BEN (Beniko); BIA (Bialobrzeskie); EPS (Epsilon 68); FED (Fedora 17); FEL (Felina 32); FER (Férimon); FUT (Futura 75); MAR (Markant); MON (Monoica); TYG (Tygra); CS (CS); KC (KC Dora); TIB (Tiborszallasi); TIS (Tisza).

yield, plant height and stem diameter were significant in all locations (Table 2.3). With the exception of FR, higher stem yields from taller and thicker stems were obtained from late-flowering cultivars (Figure 2.4). As a consequence of its long vegetative phase, the late-flowering cultivar CS produced the highest biomass yield across all experimental sites; among monoecious cultivars, FUT had the highest stem yield. Stem yield of monoecious cultivars increased significantly from full flowering to seed maturity in IT and CZ while, with the exception of IT, the stem yield of dioecious cultivars decreased significantly (Table 2.7).

Bast fibre content ranged from 21% to 43% at full flowering, depending on cultivar (Table 2.8). The ranking of the 14 cultivars according to bast fibre content was rather similar in the different experimental sites (Figure 2.5). Cultivars BEN and BIA had the highest bast fibre content while the lowest contents were found in TIB, KC and FED. The bast fibre content decreased significantly from full flowering to seed maturity in CZ in both monoecious and dioecious cultivars while only in monoecious cultivars in IT (Table 2.7).

Bast fibre yield depended on both stem yield and bast fibre content in the stem. Cultivar CS had the highest stem yield and a medium bast fibre content at full flowering; consequently,

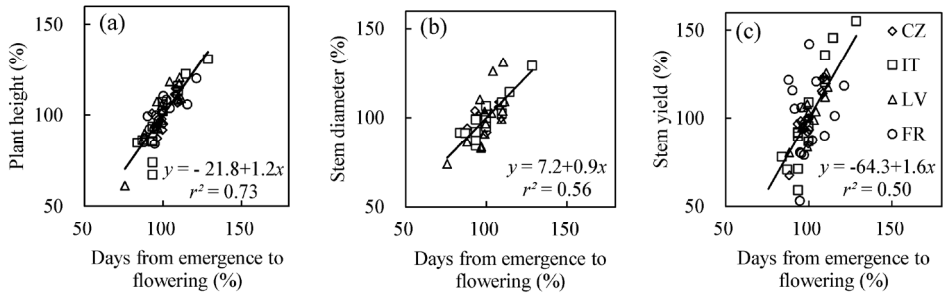


Figure 2.4 Plant height (panel a), stem diameter (panel b) and stem yield (panel c) against days from emergence to full flowering. Data are presented as percentage of the average at each location. The locations name are abbreviated as: LV (Latvia); CZ (the Czech Republic); FR (France); IT (Italy).

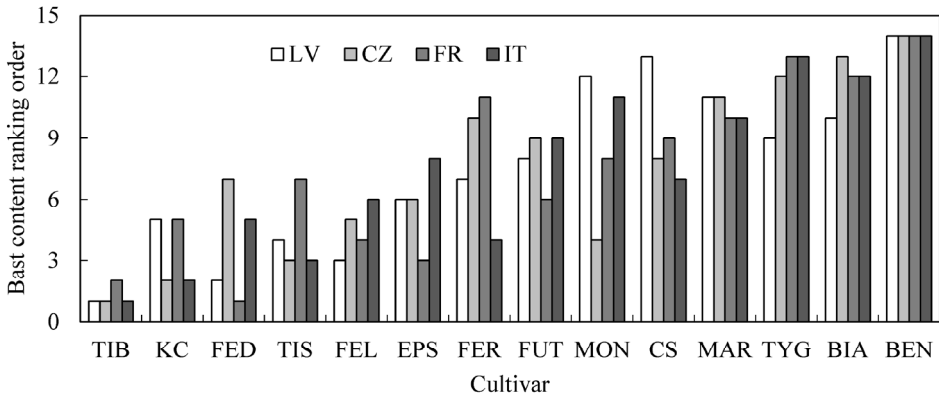


Figure 2.5 Bast content ranking order of the tested varieties in different locations at full flowering. The locations name are abbreviated as: LV (Latvia); CZ (the Czech Republic); FR (France); IT (Italy). The cultivars name are abbreviated as: BEN (Beniko); BIA (Bialobrzeskie); EPS (Epsilon 68); FED (Fedora 17); FEL (Felina 32); FER (Férimon); FUT (Futura 75); MAR (Markant); MON (Monoica); TYG (Tygra); CS (CS); KC (KC Dora); TIB (Tiborszallasi); TIS (Tisza).

Table 2.7 The effect of delayed harvesting from flowering to seed maturity on yield components.

Location	Cultivar type	Harvest time	Density (plants m ⁻²)	Plant height (cm)	Stem diameter (mm)	Stem yield (Mg ha ⁻¹)	Leaf yield (Mg ha ⁻¹)	Bark content (%)	Bast yield (Mg ha ⁻¹)
CZ	Monoecious	Full flowering	98	258	9.4	14.2	2.6	30	4.3
		Seed maturity	88*			16.1**	1.9**	25**	4.1
	Dioecious	Full flowering	111	299	10.1	17.9	2.4	25	4.6
		Seed maturity	81**			14.3**	1.3**	19**	3.0**
FR	Monoecious	Full flowering	129	161	5.2	7.1	1.4	37	2.5
		Seed maturity	131	169	5.4	6.5	0.6**		
	Dioecious	Full flowering	146	191	6.1	7.8	1.0	36	2.8
		Seed maturity	147	184	6.1	6.3**	0.3**		
IT	Monoecious	Full flowering	129	152	4.3	5.2	2.5	34	1.7
		Seed maturity	116*			6.0**	2.3	32**	1.9*
	Dioecious	Full flowering	146	199	5.3	8.6	2.2	29	2.5
		Seed maturity	118**			9.7*	2.4	27	2.7
LV	Monoecious	Full flowering	178	220	5.4	17.0	4.4	27	4.7
		Seed maturity	178	240	6.1**	17.3	3.2**		
	Dioecious	Full flowering	151	254	6.6	20.8	4.3	25	5.2
		Seed maturity	146	290**	7.7**	18.5**	2.7		

The locations name are abbreviated as: LV (Latvia); CZ (the Czech Republic); FR (France); IT (Italy).

* Denotes significant difference between full flowering and seed maturity at $P = 0.05$; ** denotes significant difference at $P = 0.01$.

Table 2.8 Yield components of different cultivars at full flowering (1st harvesting).

Cultivar	Inflorescence yield (Mg ha ⁻¹)				Stem yield (Mg ha ⁻¹)				Bast yield (Mg ha ⁻¹)			
	CZ	FR	IT	LV	CZ	FR	IT	LV	CZ	FR	IT	LV
BEN	2.1efg	0.9f	1.9d	3.5h	13.5de	3.8f	3.7f	17.2g	4.6ab	1.9c	1.3e	6.2abc
BIA	2.6abcd	1.0ef	2.2cd	4.5de	13.9de	5.8ef	4.4ef	19.2de	4.6ab	2.5abc	1.8cde	5.7bcd
EPS	3.0a	1.4bcde	2.2cd	4.0f	14.4cde	5.7ef	5.3de	17.9fg	3.9bc	1.8c	1.8cde	4.7cde
FED	2.5abcde	1.9a	3.0ab	5.1ab	14.3cde	8.3abcd	4.8ef	14.5h	4.1abc	2.5abc	1.5de	3.4ef
FEL	2.6abcd	1.2cdef	2.6bcd	4.0fg	14.3cde	5.8ef	5.5de	15.1h	3.9bc	1.9c	1.7cde	3.5ef
FER	2.3cdefg	1.7ab	3.4a	4.7cd	12.2ef	7.5bcde	5.7de	17.4g	4.1bc	2.6abc	1.8cde	4.1def
FUT	2.7abc	1.7ab	2.3bcd	4.7cde	15.2abcd	10.2a	6.7cd	20.3cd	4.6ab	3.7a	2.1bcd	5.4bcd
MAR	1.9f	1.5bcd	2.4bcd	4.1f	10.2f	8.8ab	4.4ef	8.8i	3.2c	3.3ab	1.5de	2.7f
MON	2.7abc	1.6abc	2.0d	4.8cd	14.8abcde	6.3de	5.9cde	21.2bc	4.2bc	2.3bc	2.0bcde	6.4ab
TYG	2.5abcde	1.1def	2.7bc	4.4e	14.4cde	7.6acde	5.6de	18.6ef	4.5abc	2.9abc	2.0bcd	4.8bcde
CS	2.2defg	1.2cdef	2.1cd	4.9bc	17.6ab	8.5abcd	9.5a	22.7a	5.5a	3.1abc	3.1a	7.4a
KC	2.1efg	0.8f	2.5bcd	3.7gh	16.9abc	7.3bcde	8.9ab	22.1ab	4.1bc	2.4abc	2.5ab	5.0bcde
TIB	2.8ab	1.0ef	2.0d	3.5h	17.0abc	8.7abc	8.3ab	19.5de	3.8bc	3.1abc	2.2bc	4.1def
TIS	2.4bcdef	1.0ef	2.2cd	5.2a	17.9a	6.5cde	7.4bc	18.8ef	4.5ab	2.5abc	2.3bc	4.4de
Average	2.5	1.3	2.4	4.4	14.9	7.3	6.1	18.1	4.3	2.6	2.0	4.8

Numbers followed by different letters in the same column are statistically different for $P = 0.05$ (Tukey test).

The cultivars name are abbreviated as: BEN (Beniko); BIA (Bialobrzieszkie); EPS (Epsilon 68); FED (Fedora 17); FEL (Felina 32); FER (Férimon); FUT (Futura 75); MAR (Markant); MON (Monoica); TYG (Tygra); CS (CS); KC (KC Dora); TIB (Tiborszállasi); TIS (Tisza).

The locations name are abbreviated as: LV (Latvia); CZ (the Czech Republic); FR (France); IT (Italy).

it had the highest bast fibre yield in CZ, IT and LV (Table 2.8). Similarly, FUT had the highest bast fibre yield among the monoecious cultivars in IT and FR. It is interesting to note that cultivars having a modest stem yield could still have a high bast yield, due to a high bast fibre content in the stem. As an example, the stem yield of BEN in CZ was significantly lower than that of the cultivars TIB and KC whereas its bast yield was significantly higher due to the high bast fibre content. At full flowering, bast fibre yield ranged from 1.3 Mg ha⁻¹ to 3.1 Mg ha⁻¹ in IT, from 1.6 Mg ha⁻¹ to 3.6 Mg ha⁻¹ in FR, from 3.2 Mg ha⁻¹ to 5.2 Mg ha⁻¹ in CZ and from 2.6 Mg ha⁻¹ to 7.4 Mg ha⁻¹ in LV. At seed maturity, the bast fibre yield of monoecious cultivars increased significantly in IT, whereas the bast fibre yield of dioecious cultivars decreased significantly in CZ (Table 2.7).

Seed yield ranged from 1.1 Mg ha⁻¹ to 2.4 Mg ha⁻¹ in IT, from 0.7 Mg ha⁻¹ to 2.3 Mg ha⁻¹ in CZ and from 0.3 Mg ha⁻¹ to 1.0 Mg ha⁻¹ in FR (Table 2.9). Only FED (1.5 Mg ha⁻¹) and MAR (1.4 Mg ha⁻¹) produced seeds in LV; the other cultivars flowered too late. In contrast to stem yield, the highest seed yield and seed harvest index were found in earlier cultivars (Figure 2.6). The early-flowering cultivar FED had the highest seed harvest index and the highest seed yield in all locations, while the seed yield of late-flowering dioecious cultivars was the lowest. Only

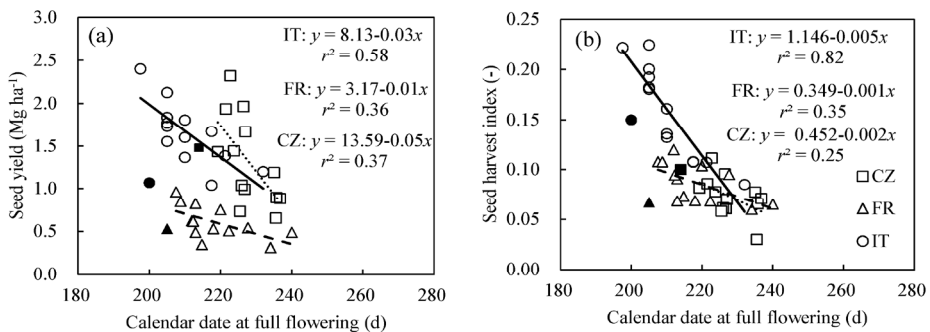


Figure 2.6 The seed yield (panel a) and seed harvest index (panel b) against calendar date at full flowering. Early-flowering varieties had high seed yield and seed harvest index, except for Markant (solid marker, excluded from regression) which flowered early while it had a low seed yield and a low harvest index. The locations name are abbreviated as: CZ (the Czech Republic); FR (France); IT (Italy). Regression lines are indicated as solid line (IT); dash line (FR); dot line (CZ).

Table 2.9 Yield components of different cultivars at seed maturity (2nd harvesting).

Location	Inflorescence yield (Mg ha ⁻¹)			Seed yield (Mg ha ⁻¹)			Stem yield (Mg ha ⁻¹)			Bast yield (Mg ha ⁻¹)				
	CZ	FR	IT	LV	CZ	FR	IT	LV	CZ	FR	IT	LV	CZ	IT
BEN	1.6defg	0.5cde	1.8cd	2.6ef	1.0ef	0.6bcd	1.6bcde	14.0def	4.1d	4.7e	4.7e	19.8ab	4.6a	1.92abcd
BIA	2.1abc	0.4de	2.1bcd	3.0d	1.4cd	0.8ab	1.8bc	14.9bcde	7.9ab	4.9e	4.9e	20.3a	4.83a	1.60bcd
EPS	1.8bcde	0.8b	2.5ab	3.8ab	1.4cd	0.3e	1.6bcde	14.2cdef	5.5cd	7.6c	7.6c	17.5d	3.13bc	2.28abc
FED	2.3a	1.0a	2.9a	3.2d	2.3a	1.0a	2.4a	16.3abcde	7.1abc	5.5de	5.5de	15.0f	3.87abc	1.63bcd
FEL	2.2ab	0.7b	2.8a	3.1d	1.9b	0.6bcd	2.1ab	18.8ab	5.4cd	6.7cd	6.7cd	17.6d	4.85a	2.09abcd
FER	1.7bcdef	0.4de	1.8cd	2.6ef	2.0ab	0.8ab	1.7bcd	16.0abcd	6.6abc	4.3e	4.3e	16.3e	3.86abc	1.55bcd
FUT	1.7bcdef	0.6bc	1.7d	3.7abc	1.0efg	0.5cde	1.4cde	19.2a	8.4a	7.3c	7.3c	19.0bc	4.86a	2.36ab
MAR	2.1abcd	0.3e	1.7d	3.9a	1.5cd	0.5cde	1.1e	10.9f	7.0abc	4.4e	4.4e	9.8g	2.78cd	1.47cd
MON	1.5efg	0.6bcd	2.1bcd	3.5bc	0.7fg	0.8abc	1.8bc	17.1abc	5.8bcd	7.3c	7.3c	19.6ab	3.99abc	2.21abc
TYG	2.0abcd	0.5cde	2.3abc	2.5ef	1.7bc	0.5de	1.8bc	20.0a	6.3abcd	6.0cde	6.0cde	17.5d	3.85a	2.06abcd
CS	1.5efg	0.3e	2.2bcd	2.2g	0.7fg	0.5de	1.2de	18.6abc	6.6abc	11.4a	11.4a	20.4a	4.58ab	2.49a
KC	1.4efg	0.1f	2.4ab	2.4fg	0.9efg	0.3e	1.4cde	12.7ef	5.9bcd	9.5b	9.5b	17.6d	1.91d	1.74abcd
TIB	1.3gf	0.6bcd	2.0bcd	3.5bc	1.2de	0.5cde	1.2de	13.1def	7.2abc	7.4c	7.4c	18.1cd	2.47cd	1.26d
TIS	1.2g	0.3e	2.8a	2.7e	0.9efg	0.5cde	1.5cde	12.6ef	5.6bcd	10.1ab	10.1ab	18.1cd	2.46cd	1.91abcd
Average	1.7	0.5	2.3	3.0	1.3	0.6	1.6	15.4	6.4	7.1	7.1	17.6	3.07	1.90

Numbers followed by different letters in the same column are statistically different for $P = 0.05$ (Tukey test).

The cultivars name are abbreviated as: BEN (Beniko); BIA (Bialobrzskie); EPS (Epsilon 68); FED (Fedora 17); FEL (Felina 32); FER (Férimon); FUT (Futura 75); MAR (Markant); MON (Monoica); TYG (Tygra); CS (CS); KC (KC Dora); TIB (Tiborszallasi); TIS (Tisza).
The locations name are abbreviated as: LV (Latvia); CZ (the Czech Republic); FR (France); IT (Italy).

MAR deviated significantly from this behaviour, showing low seed yield and harvest index while being a relatively early cultivar in FR and IT (Figure 2.6).

2.4 Discussion

Hemp has a great potential as a high yielding multi-purpose crop (Amaducci *et al.*, 2015; Salentijn *et al.*, 2015) but so far it has been bred mainly for stem yield and bast fibre content (Salentijn *et al.*, 2015) or for seed yield (Callaway & Laakkonen, 1996). Since the value of hemp seed is being gradually recognized, the production of seed is gaining attention (Carus *et al.*, 2013) but very limited information on yield potential from dual-purpose crops (fibre + seed) is available in the literature. In this paper we present and discuss the results from 14 commercial hemp cultivars tested in four contrasting environments, with the aim of providing novel information to support dual-purpose cultivation of hemp in Europe.

2.4.1 The effect of genotype and environment on dual-purpose production

Average hemp stem yield in Europe was 7.3 Mg ha⁻¹ in 2010 (Carus *et al.*, 2013), so considering the maximum stem yield measured in our trial (22.7 Mg ha⁻¹ in LV) (Table 2.8), which was slightly higher than the maximum stem yield reported in a previous work that compared hemp yield potential across Europe (Struik *et al.*, 2000), a large potential to improve actual hemp stem yield can be expected.

The significant effect of genotype on stem yield has been widely reported (Cosentino *et al.*, 2013; Pahkala *et al.*, 2008; Höppner & Menge-Hartmann, 2007; Struik *et al.*, 2000). In spite of the large variation in stem yields observed among locations, our results (Figure 2.4) confirm that stem yield at full flowering is proportional to the duration of the vegetative phase (Faux *et al.*, 2013). Hemp tolerates low temperatures during early and late stages of growth, 0–2.5 °C in early stages (Amaducci *et al.*, 2012; Lisson *et al.*, 2000a; Van der Werf *et al.*, 1995) and even light frost (-2 °C) in late stages (Pahkala *et al.*, 2008). In Northern Italy, it is often recommended to sow at the end of March or at the beginning of April (personal observation). In our experiment, the length of vegetative phase and stem yield in IT were limited by a combination of late sowing and early flowering (Tables 2.2, 2.4). Given the relation between stem yield and the duration of the vegetative phase, large increases in stem yield can be achieved by prolonging the vegetative growth phase, particularly in southern environments.

High bast fibre content is desirable because fibre has a higher economic value than the woody core (Carus *et al.*, 2013). Our results show that the ranking of the tested cultivars based

on bast fibre content was relatively stable among locations (Figure 2.5), which is in agreement with previous studies (Amaducci *et al.*, 2008a; Sankari, 2000) and indicates that fibre content is under strong genetic control (Hennink, 1994). Westerhuis *et al.* (2009b) reported that stem fibre content (retted) can be considered as a genotypic parameter because the difference of fibre content among genotypes was not influenced by environmental conditions and harvesting times. Thus, high bast fibre yield can be pursued by choosing late cultivars that in a given environment have the highest stem yield, and by selecting cultivars with a high bast fibre content, considering that a high variability for this trait was found in our experiment (Table 2.8).

Although stem yield was high in late-flowering cultivars, their seed yield was low (Figures 2.4, 2.6). Similarly, Höppner & Menge-Hartmann (2007) reported that late-maturing cultivars produced consistently lower seed yield than early cultivars. This is most likely a consequence of the lower temperatures, shorter day-length and lower light intensities that are experienced during seed development of late-flowering cultivars. As an example, in IT the mean temperature between full flowering and seed harvesting of FED was 23.2 °C, while it was 17.7 °C for the late cultivar CS; day-length at full flowering was 15.0 h and 13.5 h for FED and CS, respectively; average daily global radiation between full flowering and seed harvesting was 21.2 MJ m⁻² d⁻¹ and 13.7 MJ m⁻² d⁻¹ for FED and CS, respectively. The effects of such differences in temperature, day-length and light intensities during the reproductive period on hemp seed production are unknown. However, cold temperature could induce flower abortion, pollen and ovule infertility, causes reduced fertility and poor seed set (Thakur *et al.*, 2010). Examples were widely reported on crops such as rice (*Oryza sativa* L.; Gunawardena *et al.*, 2003), maize (*Zea mays* L.; Lafitte & Edmeades, 1997) and soybean [*Glycine max* (L.) Merr; Ohnishi *et al.*, 2010]. Faux *et al.* (2013) assumed that the temperature during seed-fill duration may affect seed yield in hemp. Short day-length was reported to promote leaf senescence in soybean (Han *et al.*, 2006). As an evidence in hemp, the leaf yield of early-flowering cultivar FED was significantly higher than that of the late-flowering cultivar CS in all locations at seed maturity, in contrast to the low stem yield (Table 2.9). The fast senescence of leaf in association with low light intensities during the reproductive period of late-flowering cultivars suggests low availability of photosynthates for seed production. It was reported that decreasing total resource availability during reproductive period results in low seed number in soybean cultivars (Kantolic *et al.*, 2013; Jiang *et al.*, 2011; Kantolic & Slafer, 2007, 2001).

Considering that long vegetative growth results in high stem yield while early flowering favours seed yield, it can be concluded that genotype affects the production of stem and seed

mainly through its effect on flowering time. In our experiment, no cultivar produced both the highest stem and seed yields. Dioecious cultivar CS had the highest stem and bast fibre yield (Table 2.8) but low seed yield and it is therefore preferable for fibre production. Moreover, the stem yield of dioecious cultivars decreased significantly from flowering to seed maturity in FR and CZ (Table 2.7), which is an additional reason for discarding dioecious cultivars (i.e., CS, TIB, KC and TIS in our experiment) for dual-purpose production. FED had the highest seed yield in all locations due to early flowering (Figure 2.7), thus it can be considered as a good option for seed production. FED can also be cultivated for dual-purpose production in FR and CZ as it had a higher stem yield than average among the tested cultivars at seed maturity (Table 2.9). However, the low bast fibre content in the stem limits its bast fibre yield. Special attention should be paid when choosing MAR for seed production because its seed yield was low despite its early flowering (Figure 2.6). Such low seed yield was probably due to the high percentage of male flowers, which is under genetic as well as environmental control (Faux & Bertin, 2014; Faux *et al.*, 2013). The bast fibre yield of FUT was constantly the highest among the monoecious cultivars tested in IT, CZ and FR, as a consequence of late flowering and high bast fibre content, while its seed yield was close to the average yield in our experiment (Figure 2.7). Thus, FUT can be chosen for dual-purpose production when high fibre yield is desirable.

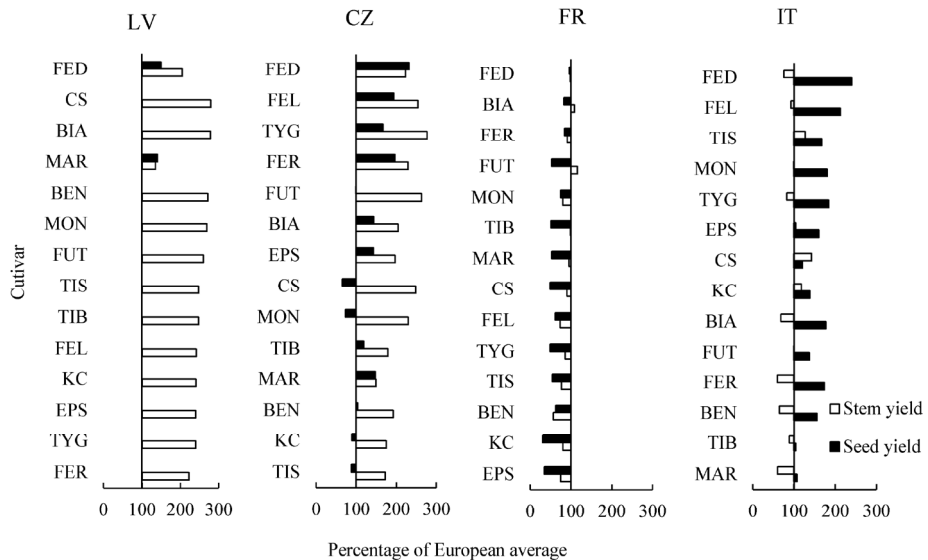


Figure 2.7 The stem and seed yields compared with the average in Europe. The average of stem yield was 7.3 Mg ha^{-1} , given by Carus *et al.* (2013). The average of seed yield was 1.0 Mg ha^{-1} , average between 0.9 Mg ha^{-1} and 1.1 Mg ha^{-1} given by Desanlis *et al.* (2013). The locations name are abbreviated as: CZ (the Czech Republic); FR (France); IT (Italy).

Among the tested locations, IT, FR and CZ had both seed and stem yield close to the average yield in Europe (Figure 2.7). Hemp cultivation for dual-purpose production is therefore foreseeable in these three locations by cultivating FED or FUT. High seed yield can also be expected in LV with cultivar FED. However, considering that FED was harvested in LV in the middle of September, which was very close to the first frost, it seems advisable to choose an earlier cultivar for dual-purpose production in LV, for example, Finola which flowered in the beginning of September in LV in 2014 (unpublished data) and had high seed yield at high latitude, 1.7 Mg ha⁻¹ seed yield was produced in Finland (Callaway, 2002).

2.4.2 The effect of genotype and environment on hemp development

Days from sowing to emergence measured in our study is in agreement with values reported from other European experiments (Cosentino *et al.*, 2013; Van der Werf *et al.*, 1995). The large variation of degree-days until emergence among locations was probably a consequence of soil structure and moisture at sowing (Hyatt *et al.*, 2007; Nasr & Selles, 1995), and sowing depth. Even though it was relatively small (*CV* 8%), a significant variation in emergence time among cultivars was observed in our experiments (Table 2.4). Different germination rates among cultivars were also observed during germinability tests (unpublished data). The difference of germination rates among cultivars could be attributed to the variation of seed quality (i.e. maturation degree and storage duration) but also genetic differences as noted in other crops, such as soybean (Hopper *et al.*, 1979) and wheat (*Triticum aestivum* L.) (Lafond & Baker, 1986). In view of the importance to have a uniform and simultaneous emergence in hemp crop (Struik *et al.*, 2000), further study is needed to investigate the effect of genotype on seed vigour and rate of emergence.

As discussed above, flowering is the main developmental event that affects the production of stem and seed in hemp genotypes. An accurate prediction of flowering time would facilitate agronomic activities. Hemp is a quantitative short-day crop that requires shorter thermal time to reach flowering at low latitude (Figure 2.2). The good fitness between observed and simulated flowering time, using the phenological model developed by Amaducci *et al.* (2008b) indicates that hemp flowering time can be modelled on the basis of temperature and photoperiod (Figure 2.3). However, it should be noted that the parameterisation found in our study is different from the one previously published Amaducci *et al.* (2012) and Amaducci *et al.* (2008b) for the common cultivars (i.e., FUT, FEL and TIB) (Table 2.6). Although the reason for this discrepancy is not clear, it might be partly due to the limited number of observations in our

trials. The parameters reported in Amaducci *et al.* (2012) were derived from a wide range of environmental conditions, sites ranged from Sicily to Finland and sowing time ranged from March to August. The relatively accurate estimation of flowering time of FEL and FUT using the parameter values reported in Amaducci *et al.* (2012) indicates that these parameter values enable the prediction of flowering time of FEL and FUT across a wide range of environmental conditions in Europe.

2.4.3 Strategies to develop dual-purpose cultivars — crop growth modelling approach

Dual-purpose hemp production requires a long vegetative phase that leaves enough time for seed growth. Using the phenological model developed by Amaducci *et al.* (2008b) and parameter values reported in Amaducci *et al.* (2012), we explored the effect of emergence time on flowering date of FEL and FUT in IT. The results show that procrastinating emergence date from May to August in IT gradually decreases the length of vegetative phase of FEL and FUT while the flowering date is slightly delayed (Figure 2.8). Similar results were reported by Faux *et al.* (2013) in central Europe where early sowing resulted in a long vegetative growth period while flowering date was advanced. It would therefore be possible to prolong the vegetative phase of FEL and FUT while still having a relatively early flowering by sowing early in IT so that high yield of stem and seed can be obtained from the same crop. Unfortunately, early sowing of early cultivars at low latitudes results in very early flowering, which is documented as “pre-flowering” in sites like Southern Italy where hemp was once traditionally grown (Barbieri, 1952, cited by Amaducci *et al.*, 2008). This behaviour is adequately simulated by the hemp phenological model (Figure 2.8, FEL, Amaducci *et al.*, 2008b) and it is suggested not to

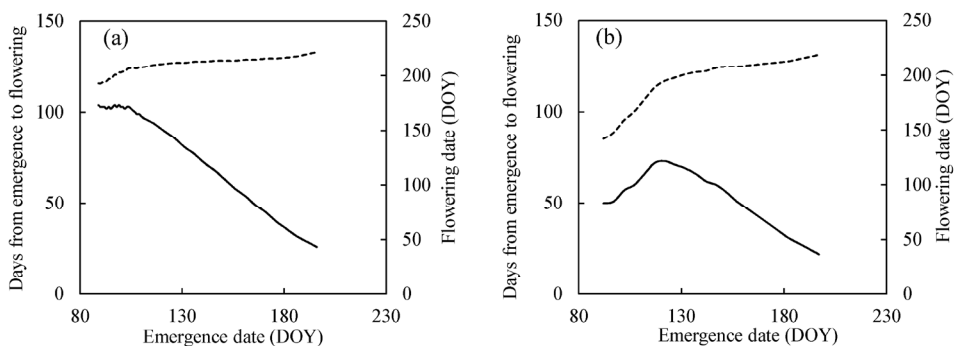


Figure 2.8 Simulated flowering time of Futura 75 (panel a) and Felina 32 (panel b) in response to emergence date in Italy by using the phenological model developed by Amaducci *et al.* (2008b) and parameters provided by Amaducci *et al.* (2012). Solid line: days from emergence to flowering; dashed line: flowering date.

plant FEL before May in IT.

The abovementioned application of modelling to develop strategies for dual-purpose hemp production is promising. However, the model parameterisation is time consuming and multi-location trials are required to accurately parameterise the model for all the available commercial cultivars. Considering that flowering is under genetic control (Table 2.6), the development of a gene-based phenological model, as done for rice (Nakagawa *et al.*, 2005) and barley (Yin *et al.*, 2005), would provide a powerful tool to plan hemp cultivation and to aid breeders in the development of hemp cultivars suitable for dual-purpose production in various environments.

Under the framework of the MultiHemp project (<http://multihemp.eu/>) a genome-wide association mapping is being carried out and a hemp crop growth model is being developed. These unique works will provide an excellent opportunity to use the combined modelling and genetic mapping approach for unravelling the complexity of hemp growth and production.

2.5 Conclusions

The stem and seed productivity of 14 commercial hemp cultivars were compared in four contrasting environmental conditions in Europe. The variation of stem and seed yield among genotypes was mainly determined by the difference in flowering time, which is under control of temperature and photoperiod. In late cultivars stem yield was high and seed yield was low. When harvesting was postponed from full flowering to seed maturity, the stem yield of monoecious cultivars significantly increased but that of the dioecious cultivars decreased, with the exception of Italy. Among the tested cultivars, not one combined the highest stem with the highest seed yield. The late cultivar CS is suitable for stem production as it had the highest stem yield. Both FED and FUT are suitable for dual-purpose production in IT, FR and CZ, with FED producing the highest seed yield and FUT the highest stem yield.

The application of modelling to develop strategies for dual-purpose hemp production is promising. However, accurate estimation of modelling parameters from field observations or based on genetic information is needed.

Acknowledgements

The research leading to these results has received funding from the European Union's Seventh Framework Programme for research, technological development and demonstration under grant agreement n° 311849. The authors gratefully acknowledge Birgit Uhrlaub

(Hochschule Bremen) for fibre extraction and all the staff members and students involved in field trials.

References

- Allegret, S., Bouloc, P. and Arnaud, L. (2013) The history of hemp. In: *Hemp: industrial production and uses* (eds Bouloc, P., Allegret, S. and Arnaud, L.), pp. 4–26. CPi Group Ltd, Croydon, UK.
- Amaducci, S. (2003) HEMP-SYS. *Journal of Industrial Hemp*, **8**, 79–83.
- Amaducci, S. (2005) Hemp production in Italy. *Journal of Industrial Hemp*, **10**, 109–115.
- Amaducci, S., Colauzzi, M., Bellocchi, G. *et al.* (2012) Evaluation of a phenological model for strategic decisions for hemp (*Cannabis Sativa* L.) biomass production across European sites. *Industrial Crops and Products*, **37**, 100–110.
- Amaducci, S., Zatta, A., Pelatti, F. *et al.* (2008a) Influence of agronomic factors on yield and quality of hemp (*Cannabis sativa* L.) fibre and implication for an innovative production system. *Field Crops Research*, **107**, 161–169.
- Amaducci, S., Colauzzi, M., Bellocchi, G. *et al.* (2008b) Modelling post-emergent hemp phenology (*Cannabis sativa* L.): Theory and evaluation. *European Journal of Agronomy*, **28**, 90–102.
- Amaducci, S., Colauzzi, M., Zatta, A., G. *et al.* (2008c) Flowering dynamics in monoecious and dioecious hemp genotypes. *Journal of Industrial Hemp*, **13**, 5–19.
- Amaducci, S. and Gusovius, H.J. (2010) Hemp — cultivation, extraction and processing. In: *Industrial Applications of Natural Fibres: Structure, Properties and Technical Applications* (ed Müssig, J.), pp. 109–134. John Wiley & Sons Ltd, West Sussex, UK.
- Amaducci, S., Pelatti, F. and Bonatti, P.M. (2005) Fibre development in hemp (*Cannabis sativa* L.) as affected by agrotechnique: preliminary results of a microscopic study. *Journal of Industrial Hemp*, **10**, 31–48.
- Amaducci, S., Scordia, D., Liu, F. *et al.* (2015) Key cultivation techniques for hemp in Europe and China. *Industrial Crops and Products*, **68**, 2–16.
- Barbieri, P. (1952) La prefioritura della canapa in Campania nell'annata. *Agric. Napoletana*, 7–9.
- Barth, M. and Carus, M. (2015) *Carbon footprint and sustainability of different natural fibres for biocomposites and insulation material*. nova-Institute, Hürth, Germany. Available at (2017, February 29): http://multihemp.eu/media/2015/05/15-04-20_PR_Carbon-Footprint-of-Natural-Fibres_nova.pdf
- Berenji, J., Sikora, V., Fournier, G. *et al.* (2013) Genetics and selection of hemp. In: *Hemp: industrial production and uses* (eds Bouloc, P., Allegret, S. and Arnaud, L.), pp. 48–71. CPi Group Ltd, Croydon, UK.
- Bertoli, A., Tozzi, S., Pistelli, L. *et al.* (2010) Fibre hemp inflorescences: From crop-residues to essential oil production. *Industrial Crops and Products*, **32**, 329–337.
- Bouloc, P. and Van der Werf, H.M.G. (2013) The role of hemp in sustainable development. In:

- Hemp: industrial production and uses* (eds Bouloc, P., Allegret, S. and Arnaud, L.), pp. 278–289. CPi Group Ltd, Croydon, UK.
- Callaway, J. and Laakkonen, T. (1996) Cultivation of Cannabis oil seed varieties in Finland. *Journal of the International Hemp Association*, **3**, 32–34.
- Callaway, J.C. (2002) Hemp as food at high latitudes. *Journal of Industrial Hemp*, **7**, 105–117.
- Callaway, J.C. (2004) Hempseed as a nutritional resource: An overview. *Euphytica*, **140**, 65–72.
- Carus, M., Karst, S., Kauffmann, A. *et al.* (2013) *The European hemp industry: Cultivation, processing and applications for fibres, shivs and seeds*. European hemp Industry Association. Available at (2017, February 29): <http://eiha.org/media/2014/10/13-06-European-Hemp-Industry.pdf>
- Castaldini, M., Fabiani, A. and Santomassimo, F. (2001) Effects of hemp retting water on the composition of soil bacterial community and on wheat yield. *Italian Journal of Agronomy*, **5**, 21–27.
- Cosentino, S.L., Riggi, E., Testa, G. *et al.* (2013) Evaluation of European developed fibre hemp genotypes (*Cannabis sativa* L.) in semi-arid Mediterranean environment. *Industrial Crops and Products*, **50**, 312–324.
- Cosentino, S.L., Testa, G., Scordia, D. *et al.* (2012) Sowing time and prediction of flowering of different hemp (*Cannabis sativa* L.) genotypes in southern Europe. *Industrial Crops and Products*, **37**, 20–33.
- De Meijer, E.P.M. (1994) Variation of Cannabis with reference to stem quality for paper pulp production. *Industrial Crops and Products*, **3**, 201–211.
- De Meijer, E.P.M. and Van der Werf, H.M.G. (1994). Evaluation of current methods to estimate pulp yield of hemp. *Industrial Crops and Products*, **2**, 111–120.
- Faux, A.M. and Bertin, P. (2014) Modelling approach for the quantitative variation of sex expression in monoecious hemp (*Cannabis sativa* L.). *Plant Breeding*, **133**, 782–787.
- Faux, A.M., Draye, X., Lambert, R. *et al.* (2013) The relationship of stem and seed yields to flowering phenology and sex expression in monoecious hemp (*Cannabis sativa* L.). *European Journal of Agronomy*, **47**, 11–22.
- Finnan, J. and Styles, D. (2013) Hemp: A more sustainable annual energy crop for climate and energy policy. *Energy Policy*, **58**, 152–162.
- Gunawardena, T., Fukai, S. and Blamey, F. (2003) Low temperature induced spikelet sterility in rice. I. Nitrogen fertilisation and sensitive reproductive period. *Crop & Pasture Science*, **54**, 937–946.
- Hall, J., Bhattarai, S.P. and Midmore, D.J. (2012) Review of flowering control in industrial hemp. *Journal of Natural Fibers*, **9**, 23–36.
- Han, T., Wu, C., Tong, Z. *et al.* (2006) Postflowering photoperiod regulates vegetative growth and reproductive development of soybean. *Environmental and Experimental Botany*, **55**, 120–129.
- Hennink, S. (1994) Optimisation of breeding for agronomic traits in fibre hemp (*Cannabis sativa* L.) by study of parent-offspring relationships. *Euphytica*, **78**, 69–76.

- Hopper, N.W., Overhot, J.R. and Martin, J.R. (1979) Effect of cultivar, temperature and seed size on the germination and emergence of soybeans [*Glycine max* (L.) Merr.]. *Annals of Botany*, **44**, 301–308.
- Höppner, F. and Menge-Hartmann, U. (2007) Yield and quality of fibre and oil of fourteen hemp cultivars in Northern Germany at two harvest dates. *Landbauforsch Volk*, **57**, 219–232.
- Hyatt, J., Wendroth, O., Egli, D.B. *et al.* (2007) Soil compaction and soybean seedling emergence. *Crop Science*, **47**, 2495–2503
- Jiang, Y., Wu, C., Zhang, L. *et al.* (2011) Long-day effects on the terminal inflorescence development of a photoperiod-sensitive soybean [*Glycine max* (L.) Merr.] variety. *Plant Science*, **180**, 504–510.
- Kantolic, A.G., Peralta, G.E. and Slafer, G.A. (2013) Seed number responses to extended photoperiod and shading during reproductive stages in indeterminate soybean. *European Journal of Agronomy*, **51**, 91–100.
- Kantolic, A.G. and Slafer, G.A. (2001) Photoperiod sensitivity after flowering and seed number determination in indeterminate soybean cultivars. *Field Crops Research*, **72**, 109–118.
- Kantolic, A.G. and Slafer, G.A. (2007) Development and seed number in indeterminate soybean as affected by timing and duration of exposure to long photoperiods after flowering. *Annals of Botany*, **99**, 925–933.
- Keller, A., Leupin, M., Mediavilla, V. *et al.* (2001) Influence of the growth stage of industrial hemp on chemical and physical properties of the fibres. *Industrial Crops and Products*, **13**, 35–48.
- Lafitte, H.R. and Edmeades, G.O. (1997) Temperature effects on radiation use and biomass partitioning in diverse tropical maize cultivars. *Field Crops Research*, **49**, 231–247.
- Lafond, G.P. and Baker, R.J. (1986) Effects of genotype and seed size on speed of emergence and seedling vigor in nine spring wheat cultivars. *Crop Science*, **26**, 341–346.
- Legros, S., Picault, S. and Cerruti, N. (2013) Factors affecting the yield of industrial hemp - experimental results from France. In *Hemp: industrial production and uses* (eds Bouloc, P., Allegret, S. and Arnaud, L.), pp. 72-97. CPi Group Ltd, Croydon, UK.
- Lisson, S.N., Mendham, N.J. and Carberry, P.S. (2000a) Development of a hemp (*Cannabis sativa* L.) simulation model 1. General introduction and the effect of temperature on the pre-emergent development of hemp. *Australian Journal of Experimental Agriculture*, **40**, 405–411.
- Lisson, S.N., Mendham, N.J. and Carberry, P.S. (2000b) Development of a hemp (*Cannabis sativa* L.) simulation model 2. The flowering response of two hemp cultivars to photoperiod. *Australian Journal of Experimental Agriculture*, **40**, 413–417.
- Mediavilla, V., Leupin, M. and Keller, A. (2001) Influence of the growth stage of industrial hemp on the yield formation in relation to certain fibre quality traits. *Industrial Crops and Products*, **13**, 49–56.
- Nakagawa, H., Yamagishi, J., Miyamoto, N. *et al.* (2005) Flowering response of rice to photoperiod and temperature: a QTL analysis using a phenological model. *Theoretical and Applied Genetics*, **110**, 778–786.

- Nasr, H.M. and Selles, F. (1995) Seedling emergence as influenced by aggregate size, bulk density, and penetration resistance of the seedbed. *Soil & Tillage Research*, **34**, 61–76.
- Ohnishi, S., Miyoshi, T. and Shirai, S. (2010) Low temperature stress at different flower developmental stages affects pollen development, pollination, and pod set in soybean. *Environmental and Experimental Botany*, **69**, 56–62.
- Pahkala, K., Pahkala, E. and Syrjala, H. (2008) Northern limits to fiber hemp production in Europe. *Journal of Industrial Hemp*, **13**, 104–116.
- Prade, T., Svensson, S.E., Andersson, A. *et al.* (2011) Biomass and energy yield of industrial hemp grown for biogas and solid fuel. *Biomass Bioenergy*, **35**, 3040–3049.
- Salentijn, E.M.J., Zhang, Q., Amaducci, S. *et al.* (2015) New developments in fiber hemp (*Cannabis sativa* L.) breeding. *Industrial Crops and Products*, **68**, 32–41.
- Sankari, H.S. (2000) Comparison of bast fibre yield and mechanical fibre properties of hemp (*Cannabis sativa* L.) cultivars. *Industrial Crops and Products*, **11**, 73–84.
- Struik, P.C., Amaducci, S., Bullard, M.J. *et al.* (2000) Agronomy of fibre hemp (*Cannabis sativa* L.) in Europe. *Industrial Crops and Products*, **11**, 107–118.
- Thakur, P., Kumar, S., Malik, J.A. *et al.* (2010) Cold stress effects on reproductive development in grain crops: An overview. *Environmental and Experimental Botany*, **67**, 429–443.
- Van der Werf, H.M.G., Brouwer, K., Wijnhuizen, M. *et al.* (1995) The effect of temperature on leaf appearance and canopy establishment in fibre hemp (*Cannabis sativa* L.). *Annals of Applied Biology*, **126**, 551–561.
- Van der Werf, H.M.G., Harsveld van der Veen, J.E., Bouma, A.T.M. *et al.* (1994) Quality of hemp (*Cannabis sativa* L.) stems as a raw material for paper. *Industrial Crops and Products*, **2**, 219–227.
- Westerhuis, W., Amaducci, S., Struik, P.C. *et al.* (2009a) Sowing density and harvest time affect fibre content in hemp (*Cannabis sativa* L.) through their effects on stem weight. *Annals of Applied Biology*, **155**, 225–244.
- Westerhuis, W., Pakhala, K., Struik, P.C. *et al.* (2009b) Site does not affect the fibre content ranking order among fibre hemp varieties. *Pflanzenbauwissenschaften*, **13**, 60–71.
- Wirtshafter, D.E. (2004) Ten years of a modern hemp industry. *Journal of Industrial Hemp*, **9**, 9–14.
- Yin, X., Struik, P.C., Tang, J. *et al.* (2005) Model analysis of flowering phenology in recombinant inbred lines of barley. *Journal of Experimental Botany*, **6**, 959–965.

Supplementary Materials in Chapter 2

Table S2.1 Harvesting date from sowing. Differences between flowering and harvesting date were presented in brackets with negative value indicating that harvesting was conducted before full flowering.

Cultivar	First harvest			Second harvest			Average			
	CZ	FR	IT	LV	Average	CZ		FR	IT	LV
BEN	94(-2)	97(6)	68(5)	109(5)	92	122(26)	130(39)	103(40)	139(35)	124
BIA	96(2)	98(5)	69(5)	109(5)	93	122(28)	131(38)	105(41)	139(35)	124
EPS	90(1)	112(17)	72(3)	109(-3)	96	140(51)	131(36)	118(49)	138(26)	132
FED	86(-7)	98(11)	65(9)	95(1)	86	131(38)	126(39)	104(48)	122(28)	121
FEL	88(-4)	99(6)	69(5)	105(-2)	90	139(48)	127(34)	105(41)	138(31)	127
FER	87(-10)	98(9)	69(5)	109(4)	91	131(35)	126(37)	104(40)	138(33)	125
FUT	90(-7)	113(14)	72(3)	122(3)	99	140(43)	139(40)	118(49)	138(19)	133
MAR	85(1)	99(13)	66(6)	85(5)	84	122(38)	132(46)	105(45)	111(31)	117
MON	95(-1)	98(-2)	72(3)	122(1)	97	142(47)	126(26)	118(49)	139(18)	131
TYG	97(0)	118(25)	70(5)	109(1)	98	130(33)	145(52)	106(41)	138(30)	130
CS	103(-2)	135(15)	93(2)	121(2)	113	141(37)	148(28)	142(51)	137(18)	142
KC	106(0)	124(11)	83(3)	122(2)	109	143(37)	144(31)	128(48)	139(19)	139
TIB	103(-2)	117(16)	83(7)	108(2)	103	143(38)	137(36)	128(52)	138(32)	137
TIS	102(-5)	117(10)	82(7)	121(9)	106	144(37)	144(37)	127(52)	138(26)	138
Average	94	109	74	110	97	135	135	115	135	130

The cultivars name are abbreviated as: BEN (Beniko); BIA (Bialobrzесьkie); EPS (Epsilon 68); FED (Fedora 17); FEL (Felina 32); FER (Férimon); FUT (Futura 75); MAR (Markant); MON (Monoica); TYG (Tygra); CS (CS); KC (KC Dora); TIB (Tiborszállasi); TIS (Tisza).
The locations name are abbreviated as: LV (Latvia); CZ (the Czech Republic); FR (France); IT (Italy).

Table S2.2 Plant density and biometric parameters of different cultivars at full flowering (1st harvesting).

Cultivar	Density (plants m ⁻²)				Plant height (cm)				Diameter (mm)			
	CZ	FR	IT	LV	CZ	FR	IT	LV	CZ	FR	IT	LV
BEN	69	46c	83b	113hi	264def	156bcde	122g	238bcd	9.7	5.7abc	3.8c	6.0bc
BIA	103	140abc	129ab	254a	265def	150cde	142fg	212de	9.3	4.5bc	3.9bc	4.4e
EPS	90	111cd	127ab	172def	273cde	160bcde	169cdef	250abc	9.9	5.7abc	4.5abc	6.2abc
FED	118	127bcd	149a	193bcd	236g	165bcde	140fg	209e	8.8	5.3abc	4.2bc	5.2cde
FEL	104	135abc	123ab	179cde	253efg	134e	155fe	218de	9.7	4.5bc	4.2bc	5.1cde
FER	89	137abc	135a	200bc	248fg	150cde	141fg	209e	9.0	4.6bc	4.5abc	5.0cde
FUT	95	145abc	128ab	161ef	275cd	197ab	169cdef	248abc	9.6	6.4a	4.3bc	5.9bcd
MAR	115	158ab	143a	145fg	237g	142de	143fg	145f	9.0	4.4c	4.1bc	4.7de
MON	103	149abc	142a	173cdef	273cde	187abc	177bcde	235cde	9.7	5.8abc	4.8abc	5.6cde
TYG	92	147abc	129ab	190bcd	257def	171abcde	159def	234cde	9.4	4.9abc	4.5abc	5.7bcd
CS	115	93d	132a	90i	309a	215a	216a	275a	10.4	7.3a	5.8a	7.7a
KC	107	157ab	142a	172cdef	300ab	184abcd	202ab	245bc	10.1	5.4abc	5.2ab	5.9bcd
TIB	111	164ab	168a	217b	300ab	182abcd	187abcd	232cde	10.1	5.7abc	4.6abc	5.6cde
TIS	109	171	142a	126gh	288bc	185abcd	192abc	265ab	9.5a	6.0ab	4.9abc	7.3ab
Average	102	134	134	170	269	170	165	230	9.6	5.4	4.5	5.7

Numbers followed by different letters in the same column are statistically different for $P = 0.05$ (Tukey test)

The cultivars name are abbreviated as: BEN (Beniko); BIA (Bialobrzieszkie); EPS (Epsilon 68); FED (Fedora 17); FEL (Felina 32); FER (Férimon); FUT (Futura 75); MAR (Markant); MON (Monoica); TYG (Tygra); CS (CS); KC (KC Dora); TIB (Tiborszallasi); TIS (Tisza).

The locations name are abbreviated as: LV (Latvia); CZ (the Czech Republic); FR (France); IT (Italy).

Chapter 3

A comprehensive study of planting density and nitrogen fertilization effect on dual-purpose hemp (*Cannabis sativa* L.) cultivation

K. Tang^{a,b}, P.C. Struik^a, X. Yin^a, D. Calzolari^b, S. Musio^b, C. Thouminot^c, M. Bjelková^d, V. Stramkale^e, G. Magagnini^f, S. Amaducci^b

^a *Centre for Crop Systems Analysis, Department of Plant Sciences, Wageningen University & Research, Droevendaalsesteeg 1, Wageningen, The Netherlands*

^b *Department of Sustainable Crop Production, Università Cattolica del Sacro Cuore, via Emilia Parmense, 84, Piacenza, Italy*

^c *Federation Nationale des Producteurs de Chanvre, 20, rue Paul Ligneul, Le Mans, France*

^d *Department of Industrial Crops, AGRITEC Plant Research Ltd., Zemědělská 16, Šumperk, Czech Republic*

^e *Latgale Agriculture Research Centre, Kulturas Laukums 1a, Vilani, Latvia*

^f *Council for Research and Experimentation in Agriculture - Research Centre for Industrial Crops (CRA-CIN), Viale G. Amendola 82, Rovigo, Italy*

Abstract

Harvesting hemp (*Cannabis sativa* L.) for both stems and seeds is now a common practice in Europe while crop management strategies for dual-purpose hemp cultivation have not been properly addressed so far. In the present study, the effects of planting density and nitrogen fertilization on hemp stem and seed yields were tested with the cultivars Futura 75 and/or Bialobrzeskie in eight contrasting environments (Italy in 2013; Italy and Latvia in 2014; Italy (two sites), Latvia, the Czech Republic, and France in 2015). Stem yield ranged between 1.3 Mg ha⁻¹ and 22.3 Mg ha⁻¹. The effects of planting density and nitrogen fertilization on stem yield did not interact significantly with each other, or with cultivar and harvest time. Increasing planting density from 30 plants m⁻² to 120 plants m⁻² and increasing nitrogen fertilization rate from 0 to 60 kg N ha⁻¹ increased stem yield by 29% and 32%, respectively. Further increase in planting density and nitrogen fertilization did not result in a significant increase in stem yield. Seed yield ranged from 0.3 Mg ha⁻¹ to 2.1 Mg ha⁻¹. The seed yield was not affected significantly by planting density between 30 plants m⁻² and 240 plants m⁻². Although the seed yield showed an increasing trend with increasing nitrogen fertilization, the effects of nitrogen fertilization on seed yield were not statistically significant.

To grow hemp as a dual-purpose crop it is recommended to plant 90–150 plants m⁻² across all tested environments. Nitrogen fertilization rate at 60 kg N ha⁻¹ was generally sufficient in the tested environments whereas further optimization of nitrogen fertilization requires accurate assessment of plant nitrogen status. To facilitate assessing plant nutritional status, a critical nitrogen dilution curve was determined for hemp and a practical method to determine nitrogen nutritional status was discussed.

Key words: hemp (*Cannabis sativa* L.); density; nitrogen; critical dilution curve; stem; seed.

3.1 Introduction

Hemp (*Cannabis sativa* L.) is resurging as an ideal multipurpose crop worldwide (Aubin *et al.*, 2016; Amaducci *et al.*, 2015; Faux *et al.*, 2013; Bertoli *et al.*, 2010). For the first time, it was cultivated in Europe on more than 33,000 ha in 2016 mainly as a dual-purpose crop where stems and seeds were harvested simultaneously (Carus *et al.*, 2017). However, hemp was traditionally a fibre crop and most past research focused on this purpose (Westerhuis *et al.*, 2009; Amaducci *et al.*, 2008a, 2002a; Struik *et al.*, 2000; Van der Werf *et al.*, 1996). Very limited information is available on growing dual-purpose hemp (Amaducci *et al.*, 2015). In the frame of the EC funded project Multihemp (www.multihemp.eu), extensive experiments have been carried with the aim of providing novel information to support dual-purpose hemp cultivation in Europe. Aspects related to cultivar choice for dual-purpose hemp cultivation have been presented in Chapter 2. The present study focuses on the effect of the two main agronomic practices affecting the performance of dual-purpose hemp: planting density and nitrogen fertilization.

The effects of planting density and nitrogen fertilization on both stem and seed yields have not been properly addressed so far. Previous researches indicate that planting density has little effect on stem yield, but plants grown at high density are shorter and thinner than those grown at low density (Amaducci *et al.*, 2002b; Struik *et al.*, 2000). Slender stems are desirable for fibre hemp production because they produce more long fibre (Westerhuis *et al.*, 2009) and require less energy for their mechanical processing (Khan *et al.*, 2010). Thus, a high planting density is generally used, ranging from 90 plants m⁻² to 350 plants m⁻² (Martinov *et al.*, 1996; Starcevic, 1996), to achieve required fibre quantity and quality. On the other hand, a low planting density, ranging from 30 plants m⁻² to 75 plants m⁻², is recommended for producing hemp seeds (Amaducci & Gusovius, 2010 and references therein). Optimal planting density has not been researched for growing hemp as a dual-purpose crop.

The effect of nitrogen fertilization on stem yield varies in literature. For relatively low fertility conditions, Amaducci *et al.* (2002b) reported that stem yield increased by 20 kg kg⁻¹ N. Finnan & Burke (2013) reported a very high stem yield increase with increasing fertilization from 0 up to 120 kg N ha⁻¹ (as high as 60 kg kg⁻¹ N). In contrast, the yield response of hemp to nitrogen fertilization was found negligible when soil fertility was high (Prade *et al.*, 2011; Struik *et al.*, 2000). Few studies have been conducted considering the response of seed yield to nitrogen fertilization. Aubin *et al.* (2015) and Marija *et al.* (2011) reported that both stem

and seed yields were positively related to nitrogen fertilization. Vera *et al.* (2010, 2004) reported that hemp seed yield increased progressively with increasing nitrogen availability until a high fertilization rate, ranging from 99 kg N ha⁻¹ to 198 kg N ha⁻¹ depending on growing conditions. Given the wide range of the results regarding stem and seed yields in response to nitrogen fertilization and the large variation of soil nitrogen availability, it is a challenge for farmers to optimize fertilization rate and to maximize economic return.

Nitrogen fertilization affects crop yield mainly through its effect on plant nitrogen status (Sadras & Lemaire, 2014). When nitrogen supply is deficient, aboveground biomass yield (W) increases with increasing nitrogen uptake until a critical nitrogen concentration (N_{critical}) has been reached; further increasing nitrogen uptake has little impact on increasing W (Lemaire & Meynard, 1997). In general, the N_{critical} decreases exponentially with increasing W during plant growth, which is called the N_{critical} dilution curve (Greenwood *et al.*, 1991, 1990). Although the N_{critical} dilution curve varies among species, it remains fairly consistent at different environmental growth conditions (Lemaire & Gastal, 2009). Therefore, the N_{critical} dilution curve has been used to determine the nitrogen status for many crops, including rice (*Oryza sativa* L.; Ata-Ul-Karim *et al.*, 2013; Sheehy *et al.*, 1998), maize (*Zea mays* L.; Ziadi *et al.*, 2010), oilseed rape (*Brassica napus* L.; Colnenne *et al.*, 1998) and linseed (*Linum usitatissimum* L.; Flénet *et al.*, 2006). Estimating a N_{critical} dilution curve for hemp would be useful to optimize its nitrogen fertilization.

The objective of this study was to assess the effects of planting density and nitrogen fertilization across a wide range of environments to support dual-purpose hemp cultivation in Europe. First, the effects of planting density and nitrogen fertilization on hemp stem and seed yields were investigated. Second, the characteristics of hemp's nitrogen demand were analysed, and a critical nitrogen dilution curve was assessed for hemp.

3.2 Materials and methods

3.2.1 Experimental locations and field layout

Field experiments were carried out at five locations in Europe: Piacenza-IT (Piacenza, Italy), Budrio-IT (Budrio, Italy), FR (La Trugalle, France), CZ (Sumperk, the Czech Republic) and LV (Vilani, Latvia) from 2013 to 2015 (Table 3.1). Latitude difference between the most northern (LV) and the most southern (Budrio-IT) location was 12°, which corresponds to 2 h of maximum day-length. Average temperature between May and October (during the hemp

Table 3.1 List of locations, soil characteristics and field managements.

Year	Location ^a	Geographical coordinates	Altitude (m asl)	Soil texture ²	Soil total N (%) ^b	Soil organic matter content (%) ^b	Cultivars	Management combination ^c	Harvesting/sampling
2013	Piacenza-IT	45N;10E	60	Silty clay loam	0.18	2.8	Futura 75	D30; N(0-50-100) D60; N(0-50-100) D120; N(0-50-100) D240; N(0-50-100)	Full flowering and seed maturity
2014	Piacenza-IT	45N;10E	60	Silty clay loam	0.14	2.2	Futura 75 Bialobrzeskie	D60; N60 D120; N60 D240; N(0-30-60-120)	Full flowering Growth analysis
	LV	57N;27E	64	Sandy clay	NA	11.0	Futura 75 Bialobrzeskie	D60; N60 D120; N60 D240; N(0-30-60-120)	Full flowering
2015	Piacenza-IT	45N;10E	60	Silty clay loam	0.14	2.6	Futura 75	D30; N60 D60; N60 D120; N(0-30-60-120)	Full flowering and seed maturity Growth analysis
	Budrio-IT	45N;12E	26	Silty clay loam	0.09	3.4	Futura 75	D240; N60 D30; N60 D60; N60	Seed filling rate Full flowering and seed maturity Growth analysis
	FR	48N;0E	67	Sandy loam	0.11	1.8	Futura 75	D120; N(0-30-60-120) D240; N60 D30; N60 D60; N60	Full flowering and seed maturity Seed filling rate
	CZ	50N;17E	319	Loam	0.14	NA	Futura 75	D120; N(0-30-60-120) D240; N60 D30; N60 D60; N60	Full flowering and seed maturity
	LV	57N;27E	64	Sandy clay	0.12	6.5	Futura 75	D120; N(0-30-60-120) D240; N60 D30; N60 D60; N60 D120; N(0-30-60-120) D240; N60	Full flowering

^a The location names are abbreviated as: Piacenza-IT (Piacenza, Italy); Budrio-IT (Budrio, Italy); FR (La Trugalle, France); CZ (Sumperk, the Czech Republic) and LV (Vilani, Latvia).

^b Soil sampling depth was 0–40 cm at Piacenza-IT, Budrio-IT and CZ; 0–30 cm at FR and 0–35 cm at LV.

^c D and N stands for planting density (plants m⁻²) and nitrogen fertilization (kg N ha⁻¹) factors, respectively. NA: data not available.

growing season) ranged from 14.9 °C (LV) to 21.8 °C (Piacenza-IT); total precipitation ranged from 212 mm (CZ) to 297 mm (FR). The most southern locations, Piacenza-IT and Budrio-IT, were hot and dry in the summer while the other three locations were cool and humid (Supplementary Material Figure S3.1).

Planting density was varied from 30 plants m⁻² to 240 plants m⁻²; nitrogen fertilization range was from 0 to 120 kg N ha⁻¹. The planting density × nitrogen fertilization interaction was tested with the cultivar Futura 75 in Piacenza-IT in 2013. The planting density × cultivar and nitrogen fertilization × cultivar interactions were tested with the cultivars Futura 75 and Bialobrzeskie in Piacenza-IT and LV in 2014. As the effects of planting density and nitrogen fertilization on stem and seed yields did not interact with each other in 2013 and did not interact with cultivar in 2014 (see Results section), the effects of planting density and nitrogen fertilization were tested separately in 2015 for the cultivar Futura 75 at all five locations (Piacenza-IT, Budrio-IT, FR, CZ and LV).

The main factors (i.e., planting density, nitrogen fertilization and cultivar) were tested in a randomized complete block design with four replicates. Single plot size was 42 m² when only two harvests were scheduled, or 60 m² when multiple harvests were scheduled for a detailed growth analysis. Sowings were carried out as soon as the soil was accessible and average daily temperature rose above 8–10 °C. Sowing dates spanned from the earliest on 7 April 2014 in Piacenza-IT to the latest on 14 May 2015 in Budrio-IT (Supplementary Material Table S3.1). Seeds were drilled at 3–4 cm depth using experimental-plot sowing machines. The distance between rows varied between 15 cm and 25 cm, depending on the sowing machine used at each location. Seed rates were calculated based on the target density considering weight of 1000 seeds and results of seed germination tests. In Piacenza-IT and Budrio-IT, densities of 30 plants m⁻² and 60 plants m⁻² were obtained by sowing seeds in excess (90 plants m⁻²) and hand-thinning to target density after emergence. Hand-thinning was conducted carefully so that any impact (e.g. increase of soil compaction due to worker's footprint) on plant growth would be minimized. Nitrogen fertilizer was distributed at sowing or immediately after emergence. Irrigation was only applied in Piacenza-IT; in total 120 mm, 60 mm and 155 mm of water was provided with a travelling sprinkler in 2013, 2014 and 2015, respectively.

3.2.2 Assessing crop development and yields

Seedling emergence was monitored in the plots with 120 plants m⁻² by counting the emerged plants in one row over a length of 1 m or in two rows over a length of 50 cm, every two days

from the appearance of the first plant until full emergence. Date of emergence was set when 50% of final seedlings had emerged. Flowering was monitored on 20 representative plants that were selected and labelled before flowering. A single plant was considered at the full flowering stage when its top appeared as a compact (i.e., with very short internodes) inflorescence with visible stigmata. The full flowering stage of a plot was set when 50% of the monitored plants had reached full flowering.

In each plot, harvest was carried out at least twice: at full flowering (H1) and at seed maturity (H2). At each harvest, all plants in an area of 4 m² were cut just above the soil level. Fresh weight of all harvested plants was assessed immediately and the number of plants in the first harvested 1 m² was counted. Among the plants of this first 1 m², 20 representative plants were sampled. A subsample of 10 plants was dried at 75 °C until constant weight to assess dry matter content. On the remaining 10 plants, stem diameter (at 10 cm from stem base), plant height and proportion of stem, leaf and seed (H2) in the above ground biomass (after oven drying) were assessed. W (aboveground biomass yield) was calculated as the product of fresh weight and dry matter content. The yields of stem (W_{stem}), leaf (W_{leaf}) and seed (W_{seed}) were estimated as the product of W and the corresponding proportions.

In addition to H1 and H2, periodic samplings were carried out on 1 m² area in Piacenza-IT (2014 and 2015) and in Burdío-IT (2015), in total 4–5 times. At each sampling date, all plants in an area of 1 m² were cut just above the soil level using pruning scissors. Plant number, plant height, stem diameter, W , W_{stem} , W_{leaf} and W_{seed} (when present) were assessed following the same procedure described for H1 and H2. Total nitrogen concentration in stem (N_{stem}), leaf (N_{leaf}) and seed (N_{seed} , if present) was analysed for each nitrogen treatment plot using a CN analyser (Vario Max CN Analyzer; Elementar Americas, Inc., Hanau, Germany). In Piacenza-IT (2014 and 2015), the interception of photosynthetically active radiation (PAR) by the canopy was measured before each sampling with a ceptometer (Decagon Devices, Inc., Pullman, Washington, USA); leaf area index (LAI) was calculated as the product of W_{leaf} and specific leaf area (SLA). The SLA was determined as the ratio of leaf area and dry weight of all leaves of two representative plants per plot. The leaf area was determined from scanned pictures using ImageJ (version 1.49; <https://imagej.nih.gov/>). In Piacenza-IT in 2015, $SPAD$ ($SPAD-502$, Minolta, Japan) measurements were taken at each harvesting time on 3 marked representative plants per plot.

3.2.3 Nitrogen demand analysis

When plant nitrogen is limiting, W generally increases with increasing nitrogen concentration (N) until a N_{critical} (critical nitrogen concentration) has been reached; above the N_{critical} , W is little dependent of N indicating that nitrogen is in excess. The N_{critical} (%) decreases with increasing W (Mg ha^{-1}) during the vegetative growth period. This relationship can be described by a negative power function (Lemaire *et al.*, 2008a; Greenwood *et al.*, 1991, 1990):

$$N_{\text{critical}} = \begin{cases} aW^{-b} & W \geq W_{\text{threshold}} \\ N_{\text{constant}} & W < W_{\text{threshold}} \end{cases} \quad (3.1)$$

Where a represents the value of N_{critical} for $W = 1 \text{ Mg ha}^{-1}$; b represents the ratio between the relative decline in N_{critical} and the relative crop growth rate. $W_{\text{threshold}}$ (Mg ha^{-1}) represents the minimum W for which the relationship between N_{critical} and W can be described using Eqn. (3.1); N_{constant} (%) means the N when $W < W_{\text{threshold}}$. Multiplying Eqn. (3.1) by W (Mg ha^{-1}) gives the critical curve for above ground nitrogen uptake ($N_{\text{uptake,cri}}$; kg N ha^{-1}):

$$N_{\text{uptake,cri}} = \begin{cases} 10aW^{1-b} & W \geq W_{\text{threshold}} \\ 10N_{\text{constant}}W & W < W_{\text{threshold}} \end{cases} \quad (3.2)$$

The ratio of N : N_{critical} or N_{uptake} : $N_{\text{uptake,cri}}$, called nitrogen nutrition index (NNI), can be used to diagnose plant nitrogen status. $NNI < 1$ indicates nitrogen is limiting while $NNI \geq 1$ indicates nitrogen is sufficient.

To determine a N_{critical} dilution curve for hemp, the relationship between W and N_{uptake} in Piacenza-IT (2014 and 2015) and in Budrio-IT (2015) was assessed for solving the coefficients a , b , $W_{\text{threshold}}$ and N_{constant} in Eqn. (3.1) and Eqn. (3.2). The methodology proposed by Justes *et al.* (1994) was adopted. Specifically, for each sampling date when both nitrogen limiting and non-limiting treatments occurred, a value of $N_{\text{uptake,cri}}$ was identified at the intersection of an oblique line (positive linear regression between N_{uptake} and W) and a vertical line (relative to the average value of W in non-limiting nitrogen conditions) in the plot of N_{uptake} against W (see Figure 3.7a in Results section), using the GAUSS method in PROC NLIN of SAS (SAS Institute Inc., Cary, North Carolina, USA). The nitrogen limiting and non-limiting treatments were identified by analysis of variance (SPSS statistics 22.0, SPSS, Chicago, Illinois, USA). A condition of nitrogen limitation occurs whenever W increased significantly ($P < 0.05$) with an increase in N_{uptake} . A condition of non-limiting nitrogen condition occurs whenever W remained unchanged with an increase in N_{uptake} . All identified $N_{\text{uptake,cri}}$ - W points were fitted to Eqn. (3.2) for the value of a , b , $W_{\text{threshold}}$ and N_{constant} .

Under changing nitrogen supply in the field, rather than instant nitrogen status, the plant biomass production is the result of the nitrogen nutrition status during the whole growth season. Therefore, nitrogen deficiency duration and intensity were integrated into an index of crop nitrogen status, NNI_{int} (Jeuffroy & Bouchard, 1999). The NNI_{int} was calculated as: $1/n \sum n_i NNI_i$, where n means the growth duration, expressed in degree-days ($^{\circ}\text{Cd}$) in this study; n_i means the representing duration of i th sampling; NNI_i means the NNI at i th sampling. The degree-days was calculated as the time integral of $T_{ave} - T_b$, with T_{ave} being the daily average temperature and $T_b = 1\text{ }^{\circ}\text{C}$ (Lisson *et al.*, 2000; Van der Werf *et al.*, 1995a).

3.2.4 Statistical analysis

Mixed models were used to assess the effects of planting density (D) and nitrogen fertilization (N) on biomass production and biometric traits using SPSS statistics 22.0 (SPSS, Chicago, Illinois, USA). Harvests at different times were conducted in the same plot; therefore, harvesting time (H) was considered as a repeated factor. Location, year and block were considered as random factors (Blouin *et al.*, 2011). If the effect of one factor on a dependent variable was significant, multiple comparison was performed using the Bonferroni method. The data collected in 2013 was analysed to assess the $D \times N$ effect. The data collected in 2014 was analysed to assess the D and N effects in association with cultivar (G). The overall D and N effects were analysed by pooling the data collected in 2014 and 2015 at different locations.

3.3 Results

Seedling emergence was attained at 75–112 $^{\circ}\text{Cd}$ after sowing and full flowering at 1150–1982 $^{\circ}\text{Cd}$, depending on growing location and cultivar (Supplementary Material Table S3.1). Harvest was carried out on average at 94 $^{\circ}\text{Cd}$ and 878 $^{\circ}\text{Cd}$ after full flowering for H1 (full flowering) and H2 (seed maturity), respectively.

3.3.1 The effects of planting density and nitrogen fertilization on stem and seed yields

W_{stem} (stem yield) ranged from 1.3 Mg ha^{-1} until 10.6 Mg ha^{-1} , from 7.8 Mg ha^{-1} until 9.6 Mg ha^{-1} , from 2.8 Mg ha^{-1} until 5.2 Mg ha^{-1} , from 8.1 Mg ha^{-1} until 18.8 Mg ha^{-1} and from 13.7 Mg ha^{-1} until 22.3 Mg ha^{-1} in Piacenza-IT (2013, 2014 and 2015), Budrio-IT, FR, CZ and LV (2014 and 2015), respectively. The effect of planting density and nitrogen fertilization on W_{stem} did not interact significantly with each other (Supplementary Material Table S3.2), or with the effects of cultivar (Supplementary Material Table S3.3) and harvest time (Table 3.2). The W_{stem} was increased significantly with increasing planting density and nitrogen fertilization rate

Table 3.2 The effect of planting density and nitrogen application on the biomass yields and plant biometrics. Data collected in 2014 and 2015 were pooled in the analysis using mixed models with location and year as random effects.

	Plant number (plants m ⁻²)	Height (cm)	Diameter (mm)	Biomass yield (Mg ha ⁻¹)	Stem yield (Mg ha ⁻¹)	Leaf yield (Mg ha ⁻¹)	Seed yield (Mg ha ⁻¹)
Density (D)^a							
D30	33 d ^d	217.2 c	9.4 a	10.0 c	7.7 c	1.6 a	0.8 a
D60	55 c	200.1 b	7.9 b	11.2 bc	9.0 b	1.7 a	0.7 a
D120	93 b	194.2 ab	7.1 c	12.3 ab	9.9 ab	1.8 a	0.7 a
D240	170 a	183.7 a	6.0 d	13.2 a	10.9 a	1.9 a	0.8 a
Nitrogen (N)^b							
N0	88 a	177.3 c	6.8 c	9.4 c	7.5 c	1.4 d	0.6 a
N30	89 a	193.6 b	7.5 bc	11.4 b	9.2 b	1.6 c	0.8 a
N60	91 a	208.3 ab	7.9 ab	12.4 b	9.9 ab	1.9 b	0.8 a
N120	84 a	215.9 a	8.2 a	13.6 a	10.9 a	2.2 a	0.7 a
Harvest (H)^c							
H1	88 a	192.9 a	7.5 a	11.2 a	8.9 b	2.0 a	NA
H2	88 a	204.7 a	7.7 a	12.2 a	10.0 a	1.5 b	0.7
Statistics (P values)							
D	0.000	0.000	0.000	0.000	0.000	0.035	0.670
N	0.430	0.000	0.000	0.000	0.000	0.000	0.227
H	0.914	0.078	0.439	0.098	0.049	0.000	NA
D × H	0.016	0.860	0.982	0.379	0.565	0.024	NA
N × H	0.035	0.545	0.643	0.147	0.335	0.000	NA

^a D30, D60, D120 and D240 stand for planting density 30 plants m⁻², 60 plants m⁻², 120 plants m⁻² and 240 plants m⁻², respectively.

^b N0, N30, N60 and N120 stand for nitrogen application rate 0 kg N ha⁻¹, 30 kg N ha⁻¹, 60 kg N ha⁻¹ and 120 kg N ha⁻¹, respectively.

^c H1 and H2 stand for harvesting at full flowering and seed maturity, respectively.

^d Numbers followed by different letters under the same category are statistically different for $P = 0.05$ (Bonferroni test).

NA: Not available.

(Table 3.2). Increasing planting density from 30 plants m⁻² to 120 plants m⁻² resulted in an overall increase in W_{stem} by 29% while the difference in W_{stem} was not significant between 120 plants m⁻² and 240 plants m⁻² (Table 3.2). Increasing nitrogen fertilization rate from 0 to 60 kg N ha⁻¹ resulted in an overall increase in W_{stem} by 32% while the difference in W_{stem} was not significant between 60 kg N ha⁻¹ and 120 kg N ha⁻¹. The effect of planting density and nitrogen fertilization on W_{stem} varied at specific environments. The variation was larger among nitrogen treatments than among planting densities (Figure 3.1).

Plant height ranged from 55 cm (Piacenza-IT, 2014) to 312 cm (LV, 2015); stem diameter ranged from 2.6 mm (Piacenza-IT, 2014) to 11.4 mm (CZ, 2015). Increasing planting density from 30 plants m⁻² to 240 plants m⁻² resulted in overall decreases in plant height and stem diameter by 15% and 37%, respectively (Table 3.2). Increasing nitrogen fertilization rate from 0 to 120 kg N ha⁻¹ resulted in overall increases in plant height and stem diameter by 22% and 20%, respectively.

W_{seed} (seed yield) range was 0.75–2.14 Mg ha⁻¹, 0.26–0.37 Mg ha⁻¹, 0.56–0.75 Mg ha⁻¹ and 0.88–1.09 Mg ha⁻¹ in Piacenza-IT (2013 and 2015), Budrio-IT, FR and CZ, respectively. W_{seed}

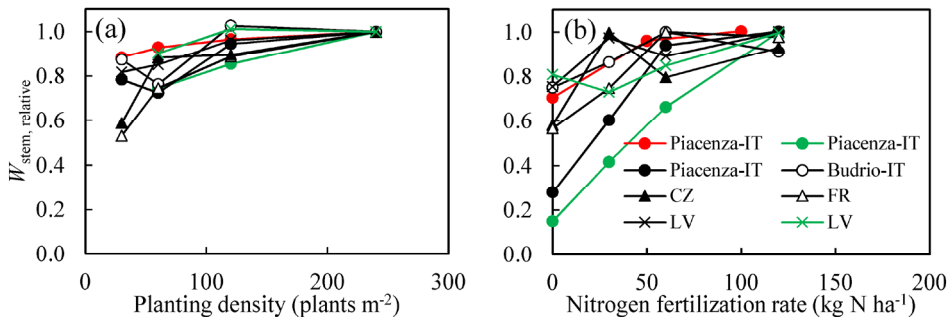


Figure 3.1 The effect of planting density (panel a) and nitrogen fertilization (panel b) on relative stem yield ($W_{\text{stem,relative}}$) in different environments. The data presented was collected at full flowering in 2013 (red), 2014 (green) and 2015 (black). The location names are abbreviated as: Piacenza-IT (Piacenza, Italy); Budrio-IT (Budrio, Italy); FR (La Trugalle, France); CZ (Sumperk, the Czech Republic) and LV (Vilani, Latvia). The $W_{\text{stem,relative}}$ was calculated as the ratio of actual stem yield and the maximum stem yield at each location. In 2013, the maximum stem yield in Piacenza-IT was 8.2 Mg ha⁻¹ and 8.7 Mg ha⁻¹ across density and nitrogen treatments, respectively. In 2014, the maximum stem yield across density treatments in Piacenza-IT and LV was 5.6 Mg ha⁻¹ and 19.2 Mg ha⁻¹, respectively; across nitrogen treatments, it was 8.5 Mg ha⁻¹ and 22.3 Mg ha⁻¹, respectively. In 2015, the maximum stem yield across density treatments in Piacenza-IT, Budrio-IT, FR, CZ and LV was 7.9 Mg ha⁻¹, 9.5 Mg ha⁻¹, 5.6 Mg ha⁻¹, 15.2 Mg ha⁻¹ and 16.8 Mg ha⁻¹, respectively; across nitrogen treatments, it was 7.9 Mg ha⁻¹, 9.5 Mg ha⁻¹, 5.0 Mg ha⁻¹, 15.9 Mg ha⁻¹ and 18.1 Mg ha⁻¹, respectively.

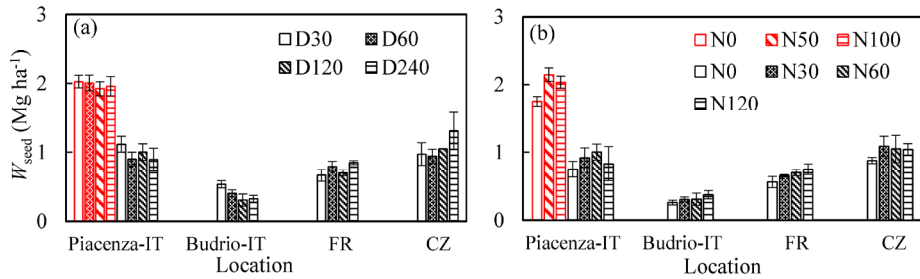


Figure 3.2 The effect of planting density (panel a) and nitrogen fertilization (panel b) on seed yield (W_{seed}) in 2013 (red bars) and 2015 (black and white bars). The location names are abbreviated as: Piacenza-IT (Piacenza, Italy); Budrio-IT (Budrio, Italy); FR (La Trugalle, France) and CZ (Sumperk, the Czech Republic). Vertical bars indicate standard error. D30, D60, D120 and D240 stand for planting density 30 plants m^{-2} , 60 plants m^{-2} , 120 plants m^{-2} and 240 plants m^{-2} , respectively. N0, N30, N50, N60, N100 and N120 stand for nitrogen application rate 0 $kg\ N\ ha^{-1}$, 30 $kg\ N\ ha^{-1}$, 50 $kg\ N\ ha^{-1}$, 60 $kg\ N\ ha^{-1}$, 100 $kg\ N\ ha^{-1}$ and 120 $kg\ N\ ha^{-1}$, respectively.

was not determined in 2014 in both locations (i.e., Piacenza-IT and LV) nor in 2015 in LV. W_{seed} showed an increasing trend with an increase in nitrogen fertilization whereas the overall effects of both planting density and nitrogen fertilization on W_{seed} were not statistically significant (Table 3.2, Figure 3.2).

3.3.2 The effects of planting density and nitrogen fertilization on plant growth

Canopy closure was reached fast at high planting density and high nitrogen fertilisation. In Piacenza-IT in 2015, light interception with 240 plants m^{-2} reached 90% at 732 °Cd after emergence that was significantly earlier than with 30 plants m^{-2} (1065 °Cd; Figure 3.3a); 90% of light interception with 120 $kg\ N\ ha^{-1}$ was reached at 700 °Cd after emergence that was 402 °Cd and 1072 °Cd earlier than with 30 $kg\ N\ ha^{-1}$ and the unfertilised control treatment, respectively (Figure 3.4a). The overall light extinction coefficient was 0.96. The earlier canopy closure was mainly a consequence of a significantly higher leaf area index (LAI) that was proportional to the level of planting density and nitrogen fertilization (Figures 3.3b, 3.4b). After canopy closure, the LAI continued to increase until full flowering while light interception remained constant, slightly above 90%. The difference of LAI among planting density treatments progressively reduced after canopy closure while it remained significant among nitrogen fertilization treatments. In Piacenza-IT in 2015, no significant difference of LAI among planting densities was observed at full flowering while the LAI with the highest nitrogen fertilization level ($6.4\ m^2\ m^{-2}$) was about three times higher than that of the control treatment ($2.3\ m^2\ m^{-2}$). W (aboveground biomass yield) increased in accordance with LAI

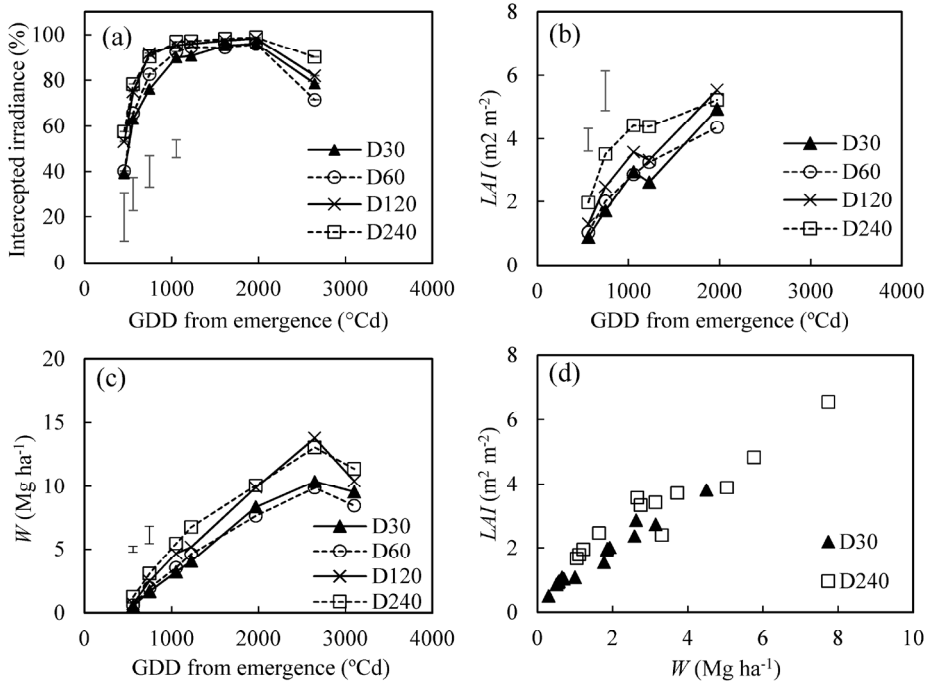


Figure 3.3 The effect of planting density on growth. Panels a, b and c indicate the time course of light interception, leaf area index (LAI) and biomass yield (W), respectively. Panel d is the plot of LAI against W before flowering. Data presented was collected in the field in Piacenza, Italy in 2015. D30, D60, D120 and D240 stand for planting density 30 plants m^{-2} , 60 plants m^{-2} , 120 plants m^{-2} and 240 plants m^{-2} , respectively. Vertical bars in Panels a, b, c indicate the Bonferroni LSD for which the effect of planting density was significant at $P = 0.05$.

(Figures 3.3b, 3.4b). The relationship between LAI and W was not affected by planting density or nitrogen fertilization (Figure 3.3d, 3.4d).

Plant height and stem diameter increased exponentially with increasing W_{stem} ($R^2 > 0.76$; Figure 3.5). This relationship was affected by planting density but it was independent from nitrogen fertilization. Considering the same stem yield level, plants cultivated at low planting densities were tallest and thickest.

3.3.3 Dynamics of nitrogen uptake and nitrogen concentration

N_{uptake} (above ground nitrogen uptake) and N (above ground nitrogen concentration) were proportional to the level of nitrogen fertilisation. At the first sampling date in Piacenza-IT in 2015, N_{uptake} and N of the unfertilised control treatment were 34.8 kg N ha^{-1} and 4.3%, respectively. Nitrogen fertilization with 120 kg N ha^{-1} resulted in increases in N_{uptake} and N by

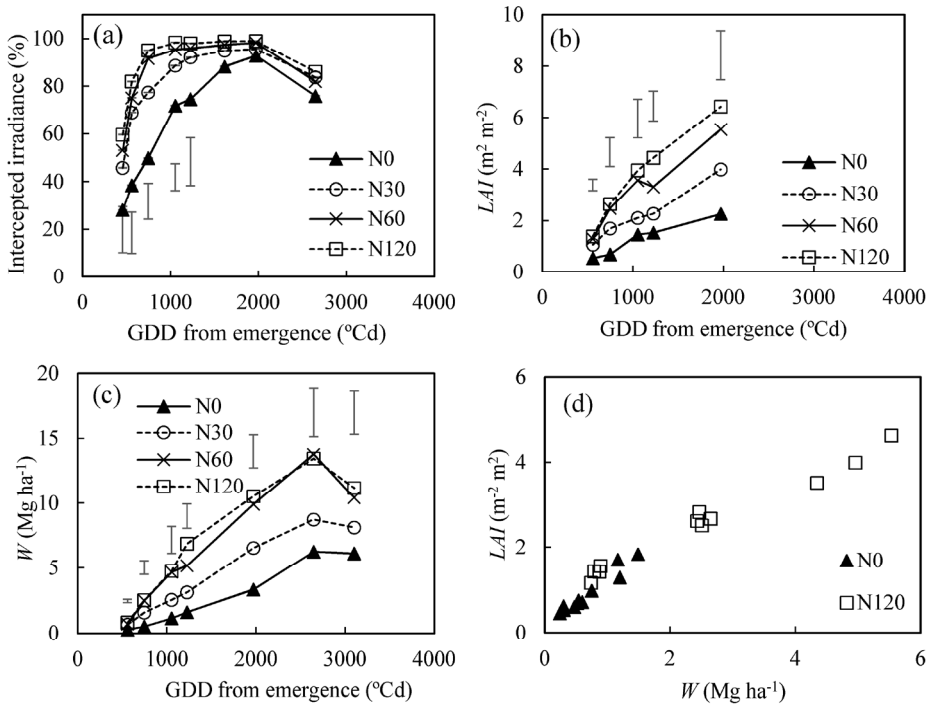


Figure 3.4 The effect of nitrogen fertilization on growth. Panels a, b and c indicate the time course of light interception, leaf area index (LAI) and biomass yield (W), respectively. Panel d is the plot of LAI against W before flowering. Data presented was collected in the field in Piacenza, Italy in 2015. N0, N30, N60 and N240 stand for nitrogen fertilization rate 0 kg N ha⁻¹, 30 kg N ha⁻¹, 60 kg N ha⁻¹ and 120 kg N ha⁻¹, respectively. Vertical bars in Panels a, b and c indicate the Bonferroni LSD for which the effect of nitrogen fertilization was significant at $P = 0.05$.

5.3 times and 1.9 times, respectively (Figure 3.6a, b). During the growing season, N_{uptake} increased uniformly in the unfertilised control treatment until the end of flowering while the increase at increasing fertilisation levels was more intense before canopy closure. The $N_{\text{uptake}}:LAI$ ratio was higher with additional fertilization than with no fertilization (Figure 3.6c). From the end of flowering to seed maturity, N_{uptake} was consistent in the unfertilised control treatment while it decreased slightly in the fertilized plots. N decreased moderately in the unfertilised control treatment and progressively more intense at increasing fertilisation levels. In Piacenza-IT in 2015, significant differences in N among nitrogen treatments were present until full flowering (1970 °Cd). After full flowering, the N was identical among nitrogen treatments.

Considering the analysis of samples collected at seed maturity in Piacenza-IT in 2013–2015, N_{leaf} , N_{stem} and N_{seed} ranges were 1.5–2.6%, 0.5–0.7%, and 2.7–4.0%, respectively (Table 3.3). Without fertilization N_{uptake} at seed maturity was 150.5 kg N ha⁻¹, 23.0 kg N ha⁻¹, and

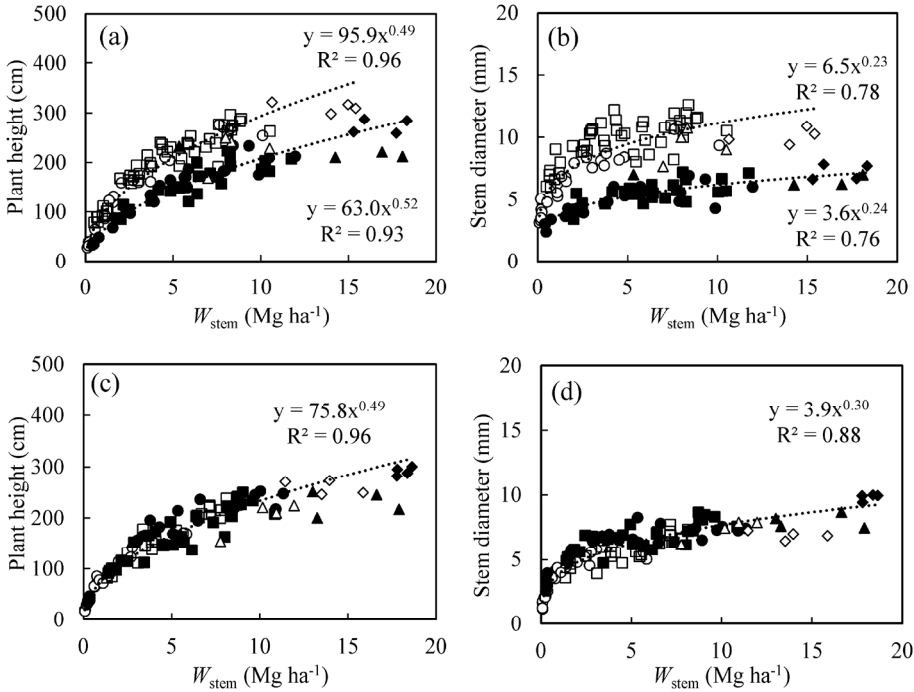


Figure 3.5 The relationship between stem yield (W_{stem}) and plant height (panels a, c), and between (W_{stem}) and stem diameter (panels b, d). Panels a and b: the open symbols denote planting density at 30 plants m^{-2} while the closed symbols indicate planting density at 240 plants m^{-2} . Panels c and d: the open symbols indicate no fertilization was applied while the closed symbols indicate fertilization rate at 120 kg N ha^{-1} . Data presented was collected in 2015 in Budrio, Italy (\blacksquare , \square), Piacenza, Italy (\bullet , \circ), the Czech Republic (\blacklozenge , \diamond) and Latvia (\blacktriangle , \triangle).

74.2 kg N ha^{-1} in 2013, 2014, and 2015, respectively (Table 3.3). With respect to the unfertilised control treatment the N_{uptake} at the highest fertilisation treatment (120 kg N ha^{-1}) increased by 57.7 kg N ha^{-1} , 94.3 kg N ha^{-1} , and 53.5 kg N ha^{-1} in 2013, 2014, and 2015, respectively. Nitrogen utilization efficiency at seed maturity ranged from 75.8 kg DM kg N^{-1} to 108.8 kg DM kg N^{-1} , independently of nitrogen treatments and growing years (Table 3.3).

3.3.4 The plant nitrogen nutrition status

None of the sampling dates in Piacenza-IT in 2014 includes both nitrogen limiting and non-limiting treatments. Among the sampling dates in Piacenza-IT and Budrio-IT in 2015, 10 sampling dates were identified for which both nitrogen limiting and non-limiting treatments were included. By assessing $N_{\text{uptake,cri}}-W$ points for each of the 10 sampling dates and fitting the $N_{\text{uptake,cri}}-W$ points to Eqn. (3.2), the coefficients a , b , $W_{\text{threshold}}$ and N_{constant} were obtained.

Table 3.3 Nitrogen content and uptake among organs at seed maturity (H2). Data was obtained in 2013–2015 in Piacenza, Italy. In 2013, nitrogen analysis was only conducted for the samples collected in the plots with planting density 240 plants m⁻². Analysis of variance was conducted with nitrogen × year as independent factor.

	2013				2014				2015						
	N0 ^a	N50	N100	N0	N30	N60	N120	N0	N30	N60	N120	N0	N30	N60	N120
Nitrogen content (%)															
Stem	0.5 a ^b	0.6 a	0.7 a	0.5 a	0.5 a	0.5 a	0.5 a	0.6 a	0.5 a	0.5 a	0.6 a	0.6 a	0.5 a	0.5 a	0.6 a
Leaf	1.8 ab	2.3 ab	2.3 ab	1.6 ab	1.5 b	1.6 ab	2.4 ab	2.0 ab	1.9 ab	2.0 ab	2.4 ab	2.0 ab	1.9 ab	2.0 ab	2.6 a
Seed	3.7 ab	3.7 ab	4.0 a	2.7 c	2.8 c	2.9 bc	3.0 bc	3.3 abc	3.1 abc	2.9 bc	3.0 bc	3.3 abc	3.1 abc	2.9 bc	3.4 abc
Nitrogen uptake (kg ha ⁻¹)															
Stem	42.9 abcd	67.6 ab	74.1 a	7.3 e	17.5 de	32.1 cde	49.8 abc	22.2 cde	28.6 cde	40.1 bcd	49.8 abc	22.2 cde	28.6 cde	40.1 bcd	50.9 abc
Leaf	42.6 abcd	60.1 a	54.9 ab	9.2 e	16.2 de	24.2 cde	40.4 abcd	27.6 bcde	29.1 bcde	35.8 abcde	49.1 abc	27.6 bcde	29.1 bcde	35.8 abcde	49.1 abc
Seed	65.0 a	73.6 a	79.2 a	6.4 b	12.0 b	26.9 b	27.1 b	24.4 b	29 b	28.3 b	27.8 b	24.4 b	29 b	28.3 b	27.8 b
Total	150.5 bc	201.3 ab	208.2 a	23.0 f	45.6 ef	83.2 de	117.2 cd	74.2 def	86.7 de	104.3 cd	127.7 cd	74.2 def	86.7 de	104.3 cd	127.7 cd
Nitrogen utilization efficiency (kg DM kg ⁻¹ N)															
N0	86.9 a	75.8 a	76.0 a	98.5 a	108.8 a	105.0 a	107.8 a	82.7 a	97.6 a	104.0 a	89.3 a	82.7 a	97.6 a	104.0 a	89.3 a

^a N0, N30, N60 and N120 stand for nitrogen application rate 0 kg N ha⁻¹, 30 kg N ha⁻¹, 60 kg N ha⁻¹ and 120 kg N ha⁻¹, respectively.

^b Numbers followed by the same letter in the same row were not significantly different at $P = 0.05$ (Bonferroni test).

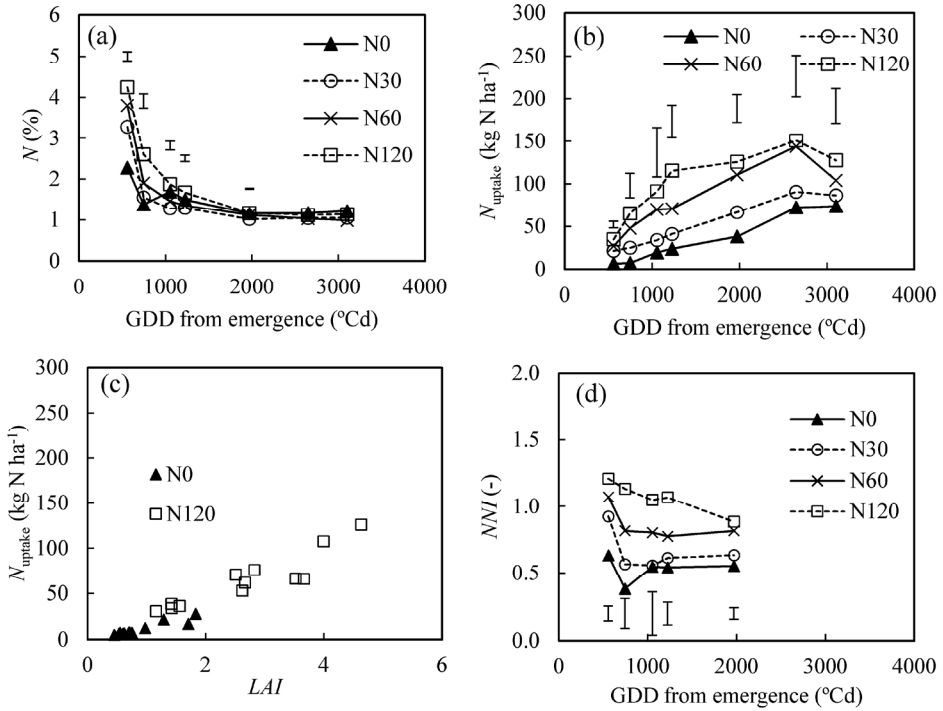


Figure 3.6 The effect of nitrogen fertilization on plant nitrogen dynamics. Panels a, b and d indicate the time course of shoot nitrogen concentration (N), nitrogen uptake (N_{uptake}) and nitrogen nutrition index (NNI), respectively. Panel c is the plot of N_{uptake} against LAI before flowering. Data presented was collected in the field in Piacenza, Italy in 2015. N0, N30, N60 and N240 stand for nitrogen fertilization rate 0 kg N ha^{-1} , 30 kg N ha^{-1} , 60 kg N ha^{-1} and 120 kg N ha^{-1} , respectively. Vertical bars in Panels a, b, d indicate the Bonferroni LSD for which the effect of nitrogen fertilization was significant at $P = 0.05$.

The $N_{\text{uptake,cri}} \text{ (kg N ha}^{-1}\text{)}-W \text{ (Mg ha}^{-1}\text{)}$ curve is represented in Figure 3.7 and its mathematical expression is as follows:

$$N_{\text{uptake,cri}} = \begin{cases} 32.6W^{0.62} & W \geq 0.78 \text{ Mg ha}^{-1} \\ 36.0W & W < 0.78 \text{ Mg ha}^{-1} \end{cases} \quad (3.3)$$

Therefore, the $N_{\text{critical}} \text{ (%)}$ dilution curve can be expressed as:

$$N_{\text{critical}} = \begin{cases} 3.26W^{-0.38} & W \geq 0.78 \text{ Mg ha}^{-1} \\ 3.60 & W < 0.78 \text{ Mg ha}^{-1} \end{cases} \quad (3.4)$$

The $N_{\text{uptake,cri}}-W$ curve separated accurately the nitrogen status of hemp crops in Piacenza-IT (2014 and 2015) and Budrio-IT (2015) (Figure 3.7b). Nitrogen nutrition index (NNI), calculated as the ratio of $N:N_{\text{critical}}$, for each nitrogen treatment and sampling date in Piacenza-IT in 2015 is presented in Figure 3.6d. The NNI of the unfertilised control treatment remained

constant throughout the whole growing season at about 0.5. Nitrogen fertilization increased NNI at all sampling dates. During plant growth, the NNI with additional fertilization decreased gradually. At 30 kg N ha^{-1} and 60 kg N ha^{-1} the decrease of the NNI was limited to the period between the first and the second samplings whereas it decreased steadily throughout the whole growing season with 120 kg N ha^{-1} . Consequently, at flowering the difference of NNI among nitrogen treatments was reduced. NNI_{int} , calculated on the basis of nitrogen deficiency duration and intensity, positively correlated with relative W (W_{relative} : calculated as the ratio of actual W and maximum W at the same sampling date) when the NNI_{int} was lower than 1. The relationship between W_{relative} and NNI_{int} was independent of growth environments (Figure 3.8).

3.4 Discussion

Growing hemp as a multi-purpose crop is gaining attention, particularly for producing both stems and seeds (Aubin *et al.*, 2016; Faux *et al.*, 2013). While numerous studies have been carried out to improve hemp cultivation for fibre production (e.g., Westerhuis *et al.*, 2009; Amaducci *et al.*, 2008a, 2002a; Struik *et al.*, 2000; De Meijer *et al.*, 1995), very limited information is available on the agronomy of dual-purpose (i.e., stems and seeds) hemp crops (Amaducci *et al.*, 2015). In this paper, data obtained in eight environments (combinations of year and location) at five contrasting locations throughout Europe were analysed to study the effect on stem and seed yields of the main agronomic factors affecting hemp production:

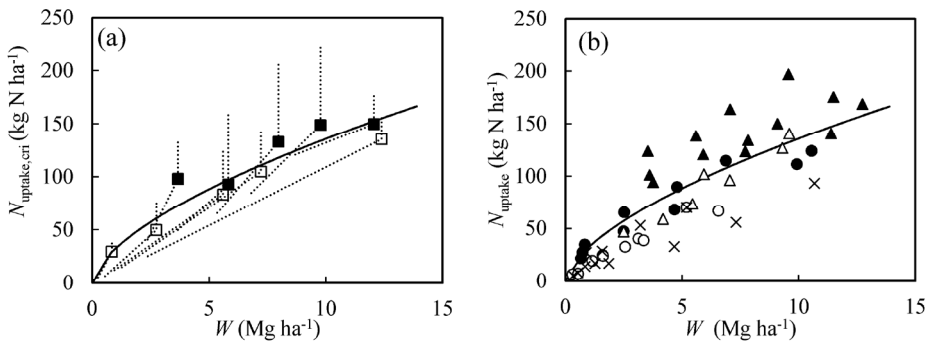


Figure 3.7 Panel a: Determination of critical nitrogen uptake ($N_{\text{uptake,cri}}$) curve. Dotted lines represent broken stick model for relationship between nitrogen uptake (N_{uptake}) and above ground biomass yield (W); Squares denote $N_{\text{uptake,cri}}-W$ points obtained in Budrio (■) and Piacenza (□), in Italy in 2015. The solid line represents the $N_{\text{uptake,cri}}$ as a function of W (see Eqn. 3.2). Panel b: The $N_{\text{uptake,cri}}$ curve in relation to field measurements of N_{uptake} . The solid line represents the $N_{\text{uptake,cri}}$ curve. × denotes data collected in Piacenza-IT, Italy in 2014. Δ and ○ denote nitrogen limiting treatment in Budrio and Piacenza, Italy, respectively, in 2015. ▲ and ● denote nitrogen non-limiting treatment in Budrio and Piacenza, Italy, respectively, in 2015. Note the data collected in 2015 were used to estimate the critical N_{uptake} curve.

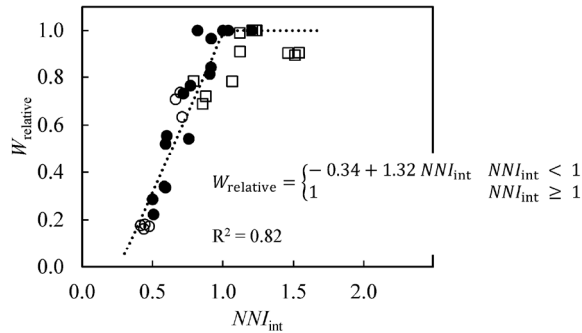


Figure 3.8 The relationship between integrated nitrogen nutrition index (NNI_{int}) and relative biomass yield ($W_{relative}$; calculated as the ratio of actual and maximum biomass at the same sampling date) at H1 (full flowering). \circ and \bullet denote samplings in Piacenza, Italy in 2014 and 2015, respectively; \square denotes samplings in Budrio, Italy in 2015.

planting density and nitrogen fertilization. Considering that the effect of these two factors on hemp stem and seed yields did not interact with each other in 2013 in Piacenza-IT (Supplementary Material Table S3.2) and did not interact with cultivar in 2014 in Piacenza-IT and LV (Supplementary Material Table S3.3), which confirms results of previous research (Amaducci *et al.*, 2008a, 2002a; Struik *et al.*, 2000), results of planting density and nitrogen fertilization will be discussed separately.

3.4.1 The effects of planting density on stem and seed yields

In line with previous studies (Amaducci *et al.*, 2008a, 2002a; Struik *et al.*, 2000), increasing planting density from 30 plants m^{-2} to 240 plants m^{-2} had limited effect on W_{stem} (stem yield) (Table 3.2). The lack of response of W_{stem} across a wide density range is mainly a consequence of the high incidence of self-thinning at high planting density (Van der Werf *et al.*, 1995b; Willey & Heath, 1969) and of the plastic behaviour that hemp generally shows for above ground and below ground development (Amaducci *et al.*, 2008b). Until canopy closure, LAI increases fast at high planting density which goes hand-in-hand with a high W accumulation rate and is accompanied by a density independent ratio $LAI: W$ (Figure 3.3). Therefore, canopy closure is reached fast at high planting density. Hemp canopies have a light extinction coefficient (k) close to 1 (Amaducci & Stutterheim, 1999; De Meijer *et al.*, 1995). The initially high LAI at high planting density results in severe light competition and reduction in plant number after canopy closure (unshown data and Van der Werf, 1997). As a result, the yield advantage in the first growth phases is lost at high planting density (Figure 3.3c). When planting density is extremely low, however, the canopy closure is significantly delayed and W

is reduced due to the reduction of intercepted radiation during the growing cycle. Consequently, the W_{stem} at 60 plants m^{-2} and 30 plants m^{-2} was the lowest among planting density treatments (Figure 3.1a). It should be noted that planting at extremely low density could result in weed competition, which could result in further significant yield reduction (Hall *et al.*, 2014 and authors' experience).

Even when the effect of planting density on W_{stem} is limited, there are very large effects on plant biometrics (Struik *et al.*, 2000). Plants grown at high densities are usually shorter and thinner than those grown at low planting densities (Figure 3.5a, b). The results in this study suggest that the effect of planting density on stem diameter is higher than on plant height. For example, when yield was 5 Mg ha^{-1} , at 240 plants m^{-2} stems were 31% shorter and 45% thinner than at 30 plants m^{-2} (Figure 3.5a, b). This effect indicates an increase in stem slenderness at high planting density (Westerhuis *et al.*, 2009; De Meijer *et al.*, 1995).

The W_{seed} (seed yield) were not significantly affected by planting density between 30 plants m^{-2} and 240 plants m^{-2} (Table 3.2, Figure 3.2). This result confirms the observation of Legros *et al.* (2013) that W_{seed} was independent of planting density until a seeding rate of 40 kg ha^{-1} (corresponding to 200 plants m^{-2}). A constant W_{seed} across a wide range of planting densities is a consequence of the increase in seed yield per single plant with decreasing planting density, which is a result of the increase in inflorescence length (data not shown) and number of branches bearing seeds (Desanlis *et al.*, 2013).

The optimal planting density for dual-purpose production should be chosen to optimise both stem and seed yields and also considering that planting density, affecting stem biometrics, interacts with long bast fibre production (Westerhuis *et al.*, 2009; Amaducci *et al.*, 2002b) and with mechanisation of harvest and post-harvest processing (Amaducci & Gusovius, 2010; Amaducci *et al.*, 2008a). It has been recommended to sow at a lower density for hemp seed production (30–75 plants m^{-2}) than for fibre production (90–200 plants m^{-2}) (Amaducci *et al.*, 2015 and references therein). Seed yield in the present study was not significantly affected by plant population across a wide range of plant densities (Table 3.2, Figure 3.2a); it is therefore recommended to aim at plant populations exceeding 90 plants m^{-2} as lower densities reduce stem fineness, increase the cost of weeding and render mechanical harvesting more difficult due to increased plant height, stem diameter and spike length. On the other hand, although the stems are more slender at higher planting density, densities above 150 plants m^{-2} are not recommended because they do not only increase seed input but also the risk of lodging due to

very fine stems (Legros *et al.*, 2013), particularly when soil fertility and/or nitrogen fertilization are high. Considering that stems are more slender at high density and W_{stem} reaches plateaus at a planting density above 120 plants m^{-2} in all environments in the present study (Tables 3.2, Figure 3.2), the optimum planting density for dual-purpose hemp cultivation could be set at 90–150 plants m^{-2} . It should be noted that the optimal planting density should also consider the effects on fibre quality in terms of post-harvesting processing and final products, which requires further researches.

3.4.2 The effect of nitrogen fertilization on stem and seed yields

The effect of nitrogen fertilization on W_{stem} interacted with the environment (Figure 3.1b), confirming the wide range of responses found in literature (Finnan & Burke, 2013; Prade *et al.*, 2011; Amaducci *et al.*, 2002b; Struik *et al.*, 2000). The results of this study suggest that the effect of nitrogen fertilization on hemp W_{stem} is a consequence of the duration and the intensity of nitrogen deficiency (Figure 3.8). Crops respond to nitrogen deficiency through a reduction in resource capture and/or resource use efficiency (Lemaire *et al.*, 2008b). In this study, the ratio $LAI: W$, which is an approximate measure of radiation capture efficiency, was not affected by nitrogen fertilisation, while the $N_{\text{uptake}}: LAI$ ratio, which is an approximate measure of radiation use efficiency, decreased when nitrogen was deficient (Figures 3.4d, 3.6c). The response of hemp to nitrogen deficiency is similar to that reported in maize and in tall fescue (*Festuca arundinacea*) while it is different to that of wheat (*Triticum aestivum* L.) and oilseed rape, which respond to nitrogen deficiency keeping $N_{\text{uptake}}: LAI$ constant while decreasing $LAI: W$ (Lemaire *et al.*, 2008b). The reduction of $N_{\text{uptake}}: LAI$ in hemp under nitrogen deficient condition results in a low biomass accumulation rate (Figure 3.4c). Consequently, canopy development is restricted and canopy closure is delayed (Figure 3.4b). After canopy closure, self-shading occurs and as consequence nitrogen use efficiency of fertilized plots was reduced. Thus, the differences in biomass accumulation rate among nitrogen treatments decreased after canopy closure despite the level of nitrogen deficiency was still high (Figure 3.6d).

It has been commonly observed that additional nitrogen fertilization increases hemp plant height and stem diameter (Finnan & Burke, 2013; Amaducci *et al.*, 2008a; Forrest & Young, 2006). The results of the present study suggest that plant height and stem diameter are strongly correlated with W_{stem} (Figure 3.5c, d). Given that W_{stem} is generally modelled in process based models (e.g. GECROS: Yin & van Laar, 2005), the relationships presented in Figure 3.5 are useful to model plant biometrics under different nitrogen regimes.

The positive effect of nitrogen fertilisation on W_{seed} (Table 3.2, Figure 3.2b) confirms the results of previous experiments (Aubin *et al.*, 2015; Marija *et al.*, 2011; Vera *et al.*, 2010; Vera *et al.*, 2004). W_{seed} is the product of seed number and seed mass (i.e., 1000 seed weight). It has been reported that nitrogen availability has little effect on hemp seed mass (Marija *et al.*, 2011; Vera *et al.*, 2004). Therefore, we hypothesise that the increase of W_{seed} achieved with additional nitrogen fertilization is a consequence of the positive effect of nitrogen on seed number, as reported for crops such as oilseed rape (Asare & Scarisbrick, 1995; Allen & Morgan, 1972). The reason for the lack of significant effect of nitrogen fertilisation on W_{seed} in our study is not clear (Table 3.2). In 2015 in Piacenza-IT and Budrio-IT, this is probably a consequence of unfavourable weather during the seed filling period. From the beginning of August to September, the crops suffered from limited and unevenly distributed rainfall and high temperature (Supplementary Material Figure S3.1). Drought during the seed filling period results in a reduction in seed dry matter accumulation rate, seed mass and W_{seed} (Plaut *et al.*, 2004). Indeed, in Piacenza-IT in 2015, the seed mass at seed maturity was 37% lower than that measured for the seed used for sowing and the average W_{seed} was 43% lower than that obtained in 2013. Further study is needed to investigate the effect of the interaction between nitrogen fertilization and drought on hemp W_{seed} , which has been reported for crops such as wheat (Ercoli *et al.*, 2008). Ercoli *et al.* (2008) reported that wheat grain yield reduction by severe post-anthesis water stress was high when combined with additional nitrogen application and was associated with a decrease in kernel weight.

It should be pointed out that determination of W_{seed} at plot level in hemp is very challenging due to the large heterogeneity in the crop (Van der Werf *et al.*, 1995b) and bird predation. Bird predation can only partially be prevented at high cost using nets or bird scarers. Heterogeneity is determined by the contemporary presence of plants of different height, with short plants having short inflorescences with few seeds, and it is aggravated by the duration of hemp seed ripening (from the first seed ripening to the last) which can last for weeks depending on genotype and environmental conditions (Amaducci *et al.*, 2008c) and can cause significant reduction of seed yield by seed shattering or bird predation. The large degree of heterogeneity in our experiments is demonstrated by the high coefficients of variation for W_{seed} ranging from 19% to 36%. These high values might also partly explain the lack of nitrogen fertilization effect on W_{seed} .

While W_{stem} and W_{seed} are restricted by nitrogen deficiency, excess nitrogen supply is not desirable for hemp production. When nitrogen fertilisation is excess, stems stay green for

longer and this can lead to difficulties in harvesting, longer drying times and difficulties with fibre processing (Legros *et al.*, 2013). Moreover, not only does it increase production cost, excess nitrogen supply has also been widely criticized for its negative environmental effects such as eutrophication of surface water (London & Häusser, 2005) and gaseous emissions of oxides and ammonia into the atmosphere (Stulen *et al.*, 1998). Therefore, sustainable hemp production requires a supply of nitrogen considering the critical demand.

3.4.3 Nitrogen demand of hemp

To illustrate hemp nitrogen requirement, a comparison of $N_{critical}$ (critical nitrogen concentration in W) dilution curves between hemp and other crops is presented in Figure 3.9a and Supplementary Material Table S3.4. In hemp the relationship between W and $N_{critical}$ became exponential at $W > 0.78 \text{ Mg ha}^{-1}$, a value lower than that found for wheat (Justes *et al.*, 1994) and rice (ssp. japonica, Ata-Ul-Karim *et al.*, 2013) but close to that of oilseed rape (Colnenne *et al.*, 1998) and sunflower (*Helianthus annuus* L.; Debaeke *et al.*, 2012). Generally the decrease of $N_{critical}$ at increasing W is a consequence of self-shading and of the decreasing ratio $LAI: W$ (Lemaire *et al.*, 2008a). Considering that the $LAI: W$ ratio in hemp remained relatively stable until a high $W (> 5 \text{ Mg ha}^{-1})$ was reached, the low threshold $W (0.78 \text{ Mg ha}^{-1})$ is a sign that self-shading occurred before canopy closure (the incident radiation reached 90% at $W \approx 2 \text{ Mg ha}^{-1}$) (Figure 3.4a, c). This is probably a consequence of the horizontal leaves and the high planting density that has triggered intra-row light competition shortly after emergence.

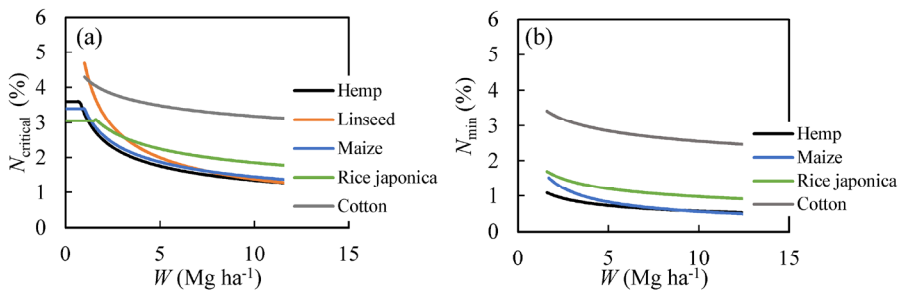


Figure 3.9 Illustration of hemp critical nitrogen ($N_{critical}$) dilution curve (panel a) and minimum nitrogen (N_{min}) dilution curve (panel b) in comparison with linseed (only in panel a), maize, rice (ssp. japonica) and cotton. W denotes above ground biomass yield. See Supplementary Material Table S3.4 for parameters and references of $N_{critical}$ dilution curve. The N_{min} dilution curve presented for hemp is determined using data collected from the unfertilised treatment.

The position of hemp N_{critical} dilution curve is at the low range of C_3 crops (Figure 3.9a, Supplementary Material Table S3.4): consistently lower than that of rice (ssp. japonica; Ata-Ul-Karim *et al.*, 2013) and cotton (Xiaoping *et al.*, 2007) and similar to that of the C_4 crop maize (Plénet & Lemaire, 1999). The N_{critical} is comparable for hemp and linseed (Flénet *et al.*, 2006) when W is higher than 5 Mg ha^{-1} whereas it is lower for hemp than linseed when W is lower than 5 Mg ha^{-1} . The low position of the hemp N_{critical} dilution curve indicates a relatively high nitrogen use efficiency (Table 3.3). For example, under non-limiting nitrogen conditions, the minimum nitrogen requirement to produce 10 Mg ha^{-1} of W for hemp is 3%, 7%, 15%, 47% and 58% less than that for linseed, maize, sorghum, oilseed rape and cotton, respectively. The high nitrogen use efficiency of hemp confirms the widely reported low fertilization requirement of this crop (Finnan & Burke, 2013; Prade *et al.*, 2011; Struik *et al.*, 2000).

Although the mechanisms underlying high nitrogen use efficiency for hemp are not clear, we speculate that this is probably the consequence of two reasons. First, hemp contains low structural nitrogen, which is confirmed by the low minimum nitrogen content in W (N_{min}) that is consistently lower than that of cotton (Xiaoping *et al.*, 2007) and rice (ssp. japonica; Ata-Ul-Karim *et al.*, 2013) (Figure 3.9b). The low N_{min} of hemp could be explained by the high proportion of stem, on above ground biomass, having very low nitrogen content. Second, hemp has high leaf photosynthetic nitrogen use efficiency at low nitrogen level. In Chapter 4, we found that the light saturated net leaf photosynthesis rate of hemp was higher than that of cotton when leaf nitrogen content is lower than 2 g N m^{-2} .

3.4.4 Determination of nitrogen nutrition status

Direct determination of NNI (nitrogen nutrition index) requires very time consuming procedures and these procedures are beyond the expertise and labour availability of farmers (Lemaire *et al.*, 2008a). Thus, a practical estimation is desirable for optimizing hemp fertilization. Several indirect methods to estimate NNI have been summarized by Lemaire *et al.* (2008a). Since estimation of N_{leaf} (leaf nitrogen concentration) is relatively easy, it has been proposed to correlate it with NNI directly (Ziadi *et al.*, 2009). However, such a direct estimating does not seem correct for hemp because N_{leaf} and N_{stem} (stem nitrogen concentration) are not linearly correlated (Supplementary Material Figure S3.2a). As the relationship between N_{leaf} and N_{stem} is consistent, though, N_{stem} can be approximated using N_{leaf} . Having N_{leaf} and W and an estimate of N_{stem} , the NNI can in turn be estimated. This empirical method resulted in a better

estimation of NNI than by the correlation between N_{leaf} and NNI (Supplementary Material Figure S3.3).

In agronomic practice, a fast and indirect estimation of N_{leaf} is required. *SPAD*, an indicator of the leaf chlorophyll concentration, could be a useful index for quantifying N_{leaf} as a good correlation between N_{leaf} and *SPAD* was observed (Supplementary Material Figure S3.2b). However, despite the fact that many authors found a good correlation between *SPAD* and N_{leaf} (Lin *et al.*, 2010; Matsunaka *et al.*, 1997), one should be aware that this relationship is highly variable from one study to another due to differences in environmental conditions and genotypes. In an attempt to eliminate the effect of environmental conditions and genotypes on the diagnosis of plant nitrogen status through *SPAD*, several *SPAD* based indexes have been proposed such as: normalized *SPAD* index (Yuan *et al.*, 2016) and positional differences chlorophyll measurements index (Zhao *et al.*, 2016). Further study is necessary to evaluate the performance of these *SPAD* based indexes on hemp nitrogen status diagnosis before a nitrogen nutrition status based decision on nitrogen management can be attempted.

3.5 Conclusions

The effects of planting density and nitrogen fertilization on hemp stem and seed productions were assessed in eight environments (combinations of year and location) at five contrasting locations throughout Europe. The effects of these two factors on hemp stem and seed yields neither interacted with each other nor with cultivar. Changing planting density over a wide range had limited effect on both stem and seed yields while plant height and stem diameter decreased with increasing population. The optimum planting density for dual-purpose hemp cultivation could be set at 90–150 plants m^{-2} . Nitrogen deficiency reduced stem yield and seed yield. The effect of nitrogen deficiency on plant height and stem diameter was in accordance with its effect on stem yield. Hemp has a high nitrogen use efficiency and 60 kg N ha^{-1} was generally sufficient in the tested environments for dual-purpose hemp cultivation. However, optimization of nitrogen fertilization requires assessment of plant nitrogen status. Direct determination of nitrogen status for hemp are too complex while *SPAD* based diagnosis techniques requires further investigations.

Acknowledgements

The research leading to these results has received funding from the European Union's Seventh Framework Programme for research, technological development and demonstration under

Grant agreement n° 311849. The authors gratefully acknowledge Sudati Rebecca for conducting nitrogen analysis, Tjeerd-Jan Stomph for his helpful comments on an earlier version of the manuscript and all the staff members and students involved in the field trials.

References

- Allen, E.J. and Morgan, D.G. (1972) A quantitative analysis of the effects of nitrogen on the growth, development and yield of oilseed rape. *Journal of Agricultural Science*, **78**, 315–324.
- Amaducci, S. and Stutterheim, N.C. (1999) The effect of light use on hemp (*Cannabis Sativa* L.) growth. In: *Alternative crops for sustainable agriculture*, pp. 205–214. Workshop held at Biocity, Turku, Finland.
- Amaducci, S., Errani, M. and Venturi, G. (2002a). Response of hemp to plant population and nitrogen fertilisation. *Italian Journal of Agronomy*, **6**, 103–111.
- Amaducci, S., Errani, M. and Venturi, G. (2002b) Plant population effects on fibre hemp morphology and production. *Journal of Industrial Hemp*, **7**, 33–60.
- Amaducci, S., Zatta, A., Pelatti, F. *et al.* (2008a). Influence of agronomic factors on yield and quality of hemp (*Cannabis sativa* L.) fibre and implication for an innovative production system. *Field Crops Research*, **107**, 161–169.
- Amaducci, S., Zatta, A. and Raffanini, M. (2008b) Characterisation of hemp (*Cannabis sativa* L.) roots under different growing conditions. *Plant Soil*, **313**, 227–235.
- Amaducci, S., Colauzzi, M., Zatta, A. *et al.* (2008c). Flowering dynamics in monoecious and dioecious hemp genotypes. *Journal of Industrial Hemp*, **13**, 5–19.
- Amaducci, S. and Gusovius, H.J. (2010) Hemp — cultivation, extraction and processing. In: *Industrial Applications of Natural Fibres: Structure, Properties and Technical Applications* (ed Müssig, J.), pp. 109–134. John Wiley & Sons Ltd, West Sussex, UK.
- Amaducci, S., Scordia, D., Liu, F.H. *et al.* (2015) Key cultivation techniques for hemp in Europe and China. *Industrial Crops and Products*, **68**, 2–16.
- Asare, E. and Scarisbrick, D.H. (1995) Rate of nitrogen and sulphur fertilizers on yield, yield components and seed quality of oilseed rape (*Brassica napus* L.). *Field Crops Research*, **44**, 41–46.
- Ata-Ul-Karim, S.T., Yao, X., Liu, X. *et al.* (2013) Development of critical nitrogen dilution curve of Japonica rice in Yangtze River Reaches. *Field Crops Research*, **149**, 149–158.
- Aubin, M.P., Seguin, P., Vanasse, A. *et al.* (2015) Industrial hemp response to nitrogen, phosphorus, and potassium fertilization. *Crop, Forage & Turfgrass Management*, **1**, 1–10.
- Aubin, M.P., Seguin, P. and Vanasse, A. (2016) Evaluation of eleven industrial hemp cultivars grown in Eastern Canada. *Agronomy Journal*, **108**, 1972–1980.
- Bertoli, A., Tozzi, S., Pistelli, L. *et al.* (2010) Fibre hemp inflorescences: From crop-residues to essential oil production. *Industrial Crops and Products*, **32**, 329–337.
- Blouin D.C., Webster E.P. and Bond J.A. (2011) On the analysis of combined experiments.

- Weed Technology*, **25**, 165–169.
- Carus, M. (2017) *Record cultivation of industrial hemp in Europe in 2016*. European Industrial Hemp Association (EIHA), Hürth, Germany. Available at (2017, November 29): <http://www.eiha-conference.org/media/files/2017/leaflet/EIHA-2017.pdf>
- Colnenne, C., Meynard, J.M. and Reau, R. (1998). Determination of a critical nitrogen dilution curve for winter oilseed rape. *Annals of Botany*, **81**, 311–317.
- De Meijer, W.J.M., Van der Werf, H.M.G., Mathijssen, E.W.J.M. *et al.* (1995) Constraints to dry matter production in fibre hemp (*Cannabis sativa* L.). *European Journal of Agronomy*, **4**, 109–117.
- Debaeke, P., Van Oosterom, E.J. and Justes, E. (2012) A species-specific critical nitrogen dilution curve for sunflower (*Helianthus annuus* L.). *Field Crops Research*, **136**, 76–84.
- Desanlis, F., Cerruti, N., Warner, P. *et al.* (2013) Hemp agronomics and cultivation. In *Hemp: industrial production and uses* (eds Allegret, S., Bouloc, P. and Arnaud, L.), pp. 98–124. CPi Group Ltd, Croydon, UK.
- Ercoli, L., Lulli, L., Mariotti, M. *et al.* (2008) Post-anthesis dry matter and nitrogen dynamics in durum wheat as affected by nitrogen supply and soil water availability. *European Journal of Agronomy*, **28**, 138–147.
- Faux, A.M., Draye, X., Lambert, R. *et al.* (2013) The relationship of stem and seed yields to flowering phenology and sex expression in monoecious hemp (*Cannabis sativa* L.). *European Journal of Agronomy*, **47**, 11–22.
- Finnan, J. and Burke, B. (2013) Nitrogen fertilization to optimize the greenhouse gas balance of hemp crops grown for biomass. *GCB Bioenergy*, **5**, 701–712.
- Flénet, F., Guérif, M., Boiffin, J. *et al.* (2006) The critical N dilution curve for linseed (*Linum usitatissimum* L.) is different from other C₃ species. *European Journal of Agronomy*, **24**, 367–373.
- Forrest, C. and Young, J.P. (2006) The effects of organic and inorganic nitrogen fertilizer on the morphology and anatomy of *Cannabis sativa* “Fedrina” (industrial fibre hemp) grown in Northern British Columbia, Canada. *Journal of Industrial Hemp*, **11**, 3–24.
- Greenwood, D.J., Gastal, F. and Lemaire, G. (1991) Growth rate and %N of field grown crops: theory and experiments. *Annals of Botany*, **67**, 181–190.
- Greenwood, D.J., Lemaire, G., Gosse, G. *et al.* (1990) Decline in percentage N of C₃ and C₄ crops with increasing plant mass. *Annals of Botany*, **66**, 425–436.
- Hall, J., Bhattarai, S.P. and Midmore, D.J. (2014) Effect of industrial hemp (*Cannabis sativa* L.) planting density on weed suppression, crop growth, physiological responses, and fibre yield in the subtropics. *Renewable Bioresources*, **2**, 1–7.
- Jeuffroy, M.H. and Bouchard, C. (1999) Intensity and duration of nitrogen deficiency on wheat grain number. *Crop Science*, **39**, 1385–1393.
- Justes, E., Mary, B., Meynard J.-M. *et al.* 1994. Determination of a critical nitrogen dilution curve for winter wheat crops. *Annals of Botany*, **74**, 397–407.
- Khan, M.M.R., Chen, Y. and Laguë, C. (2010) Compressive properties of Hemp (*Cannabis sativa* L.) stalks. *Biosystems Engineering*, **106**, 315–323.

- Legros, S., Picault, S. and Cerruti, N. (2013) Factors affecting the yield of industrial hemp - experimental results from France. In: *Hemp: industrial production and uses* (eds Allegret, S., Bouloc, P. and Arnaud, L.), pp. 72–97. CPi Group Ltd, Croydon, UK.
- Lemaire, G. and Meynard, J.M. (1997) Use of the nitrogen nutrition index for the analysis of agronomical data, in: *Diagnosis of the Nitrogen Status in Crops* (ed Lemaire, G.), pp. 45–55. Springer Berlin Heidelberg, Berlin, Heidelberg.
- Lemaire, G., Jeuffroy, M.H. and Gastal, F. (2008a) Diagnosis tool for plant and crop N status in vegetative stage: Theory and practices for crop N management. *European Journal of Agronomy*, **28**, 614–624.
- Lemaire, G., Van Oosterom, E., Jeuffroy, M.-H. *et al.* (2008b) Crop species present different qualitative types of response to N deficiency during their vegetative growth. *Field Crops Research*, **105**, 253–265.
- Lemaire, G. and Gastal, F. (2009) Quantifying crop responses to nitrogen deficiency and avenues to improve nitrogen use efficiency, In: *Crop Physiology: Applications for Genetic Improvement and Agronomy* (eds Sadras V.O. and Calderini D.), pp. 171–211. Academic Press, San Diego, USA.
- Lin, F., Deng, J. and Shi, Y. (2010) Investigation of SPAD meter-based indices for estimating rice nitrogen status. *Computers and Electronics in Agriculture*, **71**, S60–S65.
- Lisson, S.N., Mendham, N.J. and Carberry, P.S. (2000) Development of a hemp (*Cannabis sativa* L.) simulation model 1. General introduction and the effect of temperature on the pre-emergent development of hemp. *Australian Journal of Experimental Agriculture*, **40**, 405–411.
- London, J.G. (2005) Nitrogen study fertilises fears of pollution. *Nature*, 791–791.
- Marija, M., Māra, V. and Veneranda, S. (2011) Changes of photosynthesis-related parameters and productivity of *Cannabis sativa* under different nitrogen supply. *Environmental and Experimental Biology*, **9**, 61–69.
- Martinov, M., Markovic, D., Tesic, M. *et al.* (1996) Hemp harvesting mechanization. *Agricultural engineering*, **2**, 1–2.
- Matsunaka, T., Watanabe, Y., Miyawaki, T. *et al.* (1997) Prediction of grain protein content in winter wheat through leaf color measurements using a chlorophyll meter. *Soil Science and Plant Nutrition*, **43**, 127–134.
- Plaut, Z., Butow, B.J., Blumenthal, C.S. *et al.* (2004) Transport of dry matter into developing wheat kernels and its contribution to grain yield under post-anthesis water deficit and elevated temperature. *Field Crops Research*, **86**, 185–198.
- Plénet, D. and Cruz, P. (1997) Maize and sorghum, In: *Diagnosis of the Nitrogen Status in Crops* (ed. Lemaire, G.), pp. 93–106. Springer Berlin Heidelberg, Berlin, Germany.
- Plénet, D. and Lemaire, G. (1999) Relationships between dynamics of nitrogen uptake and dry matter accumulation in maize crops: Determination of critical N concentration. *Plant Soil* **216**, 65–82.
- Prade, T., Svensson, S.E., Andersson, A. *et al.* (2011) Biomass and energy yield of industrial hemp grown for biogas and solid fuel. *Biomass and Bioenergy*, **35**, 3040–3049.

- Sadras, V.O. and Lemaire, G. (2014) Quantifying crop nitrogen status for comparisons of agronomic practices and genotypes. *Field Crops Research*, **164**, 54–64.
- Sheehy, J.E., Dionora, M.J.A., Mitchell, P.L. *et al.* (1998) Critical nitrogen concentrations: implications for high-yielding rice (*Oryza sativa* L.) cultivars in the tropics. *Field Crops Research*, **59**, 31–41.
- Starčević, L. (1996) Production technology of fibre hemp. *Agricultural engineering*, **2**, 12–22.
- Struik, P.C., Amaducci, S., Bullard, M.J. *et al.* (2000) Agronomy of fibre hemp (*Cannabis sativa* L.) in Europe. *Industrial Crops and Products*, **11**, 107–118.
- Stulen, I., Perez-Soba, M., De Kok, L.J. *et al.* (1998) Impact of gaseous nitrogen deposition on plant functioning. *New Phytologist*, **139**, 61–70.
- Van der Werf, H.M.G. (1997) The effect of plant density on light interception in hemp (*Cannabis sativa* L.). *Journal of the International Hemp Association*, **4**, 8–13.
- Van der Werf, H.M.G., Brouwer, K., Wijlhuizen, M. *et al.* (1995a) The effect of temperature on leaf appearance and canopy establishment in fibre hemp (*Cannabis sativa* L.). *Annals of Applied Biology*, **126**, 551–561.
- Van der Werf, H.M.G., Vangeel, W.C.A. and Vangils, L.J.C. (1995b) Nitrogen fertilization and row width affect self-thinning and productivity of fibre hemp (*Cannabis sativa* L.). *Field Crops Research*, **42**, 27–37.
- Van der Werf, H.M.G., Mathijssen, E.W.J.M. and Haverkort, A.J. (1996) The potential of hemp (*Cannabis sativa* L.) for sustainable fibre production: A crop physiological appraisal. *Annals of Applied Biology*, **129**, 109–123.
- Vera, C.L., Malhi, S.S., Phelps, S.M., *et al.* (2010) N, P, and S fertilization effects on industrial hemp in Saskatchewan. *Canadian Journal of Plant Science*, **90**, 179–184.
- Vera, C.L., Malhi, S.S., Raney, J.P. *et al.* (2004). The effect of N and P fertilization on growth, seed yield and quality of industrial hemp in the Parkland region of Saskatchewan. *Canadian Journal of Plant Science*, **84**, 939–947.
- Westerhuis, W., Amaducci, S., Struik, P.C. *et al.* (2009) Sowing density and harvest time affect fibre content in hemp (*Cannabis sativa* L.) through their effects on stem weight. *Annals of Applied Biology*, **155**, 225–244.
- Willey, R.W. and Heath, S.B. (1969) The quantitative relationships between plant population and crop yield. *Advances in Agronomy*, **21**, 281–321.
- Xiaoping, X., Jianguo, W., Zhiwei, W. *et al.* (2007) Determination of a critical dilution curve for nitrogen concentration in cotton. *Journal of Plant Nutrition and Soil Science*, **170**, 811–817.
- Yin X. and Van Laar H.H. (2005) *Crop systems dynamics: an ecophysiological simulation model for genotype-by-environment interactions*, Wageningen, Wageningen Academic, the Netherlands.
- Yuan, Z., Ata-Ul-Karim, S.T., Cao, Q. *et al.* (2016) Indicators for diagnosing nitrogen status of rice based on chlorophyll meter readings. *Field Crops Research*, **185**, 12–20.
- Zhao, B., Liu, Z., Ata-Ul-Karim, S.T. *et al.* (2016) Rapid and nondestructive estimation of the

nitrogen nutrition index in winter barley using chlorophyll measurements. *Field Crops Research*, **185**, 59–68.

Ziadi, N., Bélanger, G., Claessens, A. *et al.* (2010) Plant-based diagnostic tools for evaluating wheat nitrogen status. *Crop Science*, **50**, 2580–2590.

Supplementary Materials in Chapter 3

Table S3.1 Sowing date and growth degree day at emergence, full flowering (H1) and harvesting (H2).

Year	Location ^a	Sowing date	Emergence (°Cd) ^b	Full flowering (°Cd) ^b	H1 (°Cd) ^b	H2 (°Cd) ^b
2013	Piacenza-IT	14-May	79.3	1532 (Futura 75)	1759	2608
2014	Piacenza-IT	07-Apr	96.5	1742 (Futura 75) 1150 (Bialobrzeskie)	1832	2970
	LV	02-May	75.1	1835 (Futura 75) 1632 (Bialobrzeskie)	1717	2058
2015	Piacenza-IT	16-Apr	112.5	1982 (Futura 75)	1882	2966
	Budrio-IT	14-May	NA	1582 (Futura 75)	1757	2648
	FR	22-Apr	NA	1772 (Futura 75)	2085	2805
	CZ	24-Apr	77.0	1758 (Futura 75)	1910	2396
	LV	05-May	97.4	1858 (Futura 75)	1874	NA

^a The location names are abbreviated as: Piacenza-IT (Piacenza, Italy); Budrio-IT (Budrio, Italy); FR (La Trugalle, France); CZ (Sumperk, the Czech Republic) and LV (Vilani, Latvia).

^b The growth degree day was calculated with a base temperature of 1 °C.

NA: data not available.

Table S3.2 The effect of planting density and nitrogen fertilization on the biomass yields and plant biometrics at H1 (full flowering) and H2 (seed maturity) in Piacenza, Italy, in 2013.

	Plant number (plant m ⁻²)	Plant height (cm)	Stem diameter (mm)	Biomass yield (Mg ha ⁻¹)	Stem yield (Mg ha ⁻¹)	Leaf yield (Mg ha ⁻¹)	Seed yield (Mg ha ⁻¹)
Density (D) ^a							
D30	45 a ^c	220 c	6.9 c	12.0 a	8.3 a	2.8 a	2.0 a
D60	81 b	198 bc	5.8 b	12.0 a	8.5 a	2.5 a	2.0 a
D120	131 c	170 a	4.6 a	12.6 a	9.1 a	2.6 a	1.9 a
D240	167 d	180 ab	4.8 a	12.8 a	9.1 a	2.7 a	2.0 a
Nitrogen (N) ^b							
N0	116 b	167 a	4.8 a	10.1 a	6.9 a	2.4 a	1.8 a
N50	102 ab	203 b	5.7 b	13.2 b	9.5 b	2.7 b	2.1 b
N100	100 a	206 b	6.1 b	13.8 b	9.9 b	2.9 b	2.0 ab
Harvest (H)							
H1	106	192	5.5	10.6a	7.8 a	2.8 b	2.0
H2				14.2b	9.7 b	2.5 a	
Statistics (<i>P</i> values)							
D	0.000	0.000	0.000	0.208	0.047	0.133	0.908
N	0.025	0.000	0.000	0.000	0.000	0.000	0.019
H				0.000	0.000	0.000	
D × N	0.790	0.620	0.597	0.694	0.669	0.661	0.983
D × H				0.268	0.148	0.665	
N × H				0.147	0.203	0.182	
D × N × H				0.688	0.608	0.865	

^a D30, D60, D120 and D240 stand for planting density 30 plants m⁻², 60 plants m⁻², 120 plants m⁻² and 240 plants m⁻², respectively.^b N0, N30, N60 and N120 stand for nitrogen application rate 0 kg N ha⁻¹, 30 kg N ha⁻¹, 60 kg N ha⁻¹ and 120 kg N ha⁻¹, respectively.^c Numbers followed by different letters under the same category are statistically different at *P* = 0.05 (Bonferroni test).

Table S3.3 The effect of planting density and nitrogen application associated with cultivar on the biomass yields and plant biometrics. Data presented was collected at full flowering in Piacenza-IT (Piacenza, Italy) and LV (Vilani, Latvia) in 2014.

	Plant number (plants m ⁻²)	Height (cm)	Diameter (mm)	Biomass yield (Mg ha ⁻¹)	Stem yield (Mg ha ⁻¹)	Leaf yield (Mg ha ⁻¹)
Density (D) ^a						
D60	57.4 c ^c	185.6 a	6.9 a	11.6 b	9.4 a	2.3 a
D120	102.2 b	191.4 a	6.6 a	13.2 ab	10.4 a	2.8 a
D240	179.5 a	180.4 a	5.7 b	13.8 a	11.0 a	2.1 a
Nitrogen (N) ^b						
N0	107.3 a	152.3 d	5.5 c	9.5 c	7.7 c	1.8 c
N30	117.3 a	176.1 c	6.2 b	10.9 c	8.7 c	2.2 c
N60	110.1 a	197.0 b	6.8 ab	13.8 b	11.0 b	2.9 b
N120	117.6 a	218.0 a	7.1 a	17.1 a	13.6 a	3.6 a
Cultivar (G)						
Bialobrzeskie	110.5 a	171.9 b	6.1 a	12.0 a	9.3 b	2.8 a
Futura 75	115.6 a	199.7 a	6.7 a	13.6 a	11.2 a	2.5 a
Statistics (<i>P</i> values)						
D	0.000	0.323	0.000	0.310	0.055	0.050
N	0.387	0.000	0.000	0.000	0.000	0.000
G	0.517	0.001	0.340	0.750	0.009	0.235
D × G	0.511	0.651	0.968	0.870	0.863	0.945
N × G	0.895	0.236	0.340	0.687	0.687	0.828

^a D60, D120 and D240 stand for planting density 60 plants m⁻², 120 plants m⁻² and 240 plants m⁻², respectively.

^b N0, N30, N60 and N120 stand for nitrogen application rate 0 kg N ha⁻¹, 30 kg N ha⁻¹, 60 kg N ha⁻¹ and 120 kg N ha⁻¹, respectively.

^c Numbers followed by different letters under the same category are statistically different at *P* = 0.05 (Bonferroni test).

Table S3.4 Comparison of the coefficients of hemp critical nitrogen concentration (N_{critical}) dilution curve with other crops. a denotes the N_{critical} at above ground biomass yield (W) equal to 1 Mg ha^{-1} ; b denotes the ratio between the relative decline in N_{critical} and the relative W increasing rate; $W_{\text{threshold}}$ means the minimum W for which the relationship between N_{critical} and W can be described using a negative exponential curve (i.e. Eqn 3.3). N_{constant} means the nitrogen concentration when $W \leq \text{threshold } W$. NA: data not available.

Species	a	b	$W_{\text{threshold}}$	N_{constant}	References
C3					
Hemp (<i>Cannabis sativa</i> L.)	3.3	0.38	0.80	3.57	Present studies
Linseed (<i>Linum usitatissimum</i> L.)	4.7	0.53	NA	NA	Flenet et al. 2006)
Oilseed rape (<i>Brassica napus</i> L.)	4.5	0.25	0.88	4.63	Colnenne et al. (1998)
Wheat (<i>Triticum aestivum</i> L.)	5.3	0.44	1.55	4.4	Justes et al. (1994)
Rice (<i>Oryza sativa</i> L. ssp. indica)	5.2	0.52	NA	NA	Sheehy et al. (1998)
Rice (<i>Oryza sativa</i> L. ssp. japonica)	3.5	0.28	1.55	3.05	Ata-Ul-Karim et al. (2013)
Sunflower (<i>Helianthus annuus</i> L.)	4.5	0.42	0.75	5.1	Debaeke et al. (2012)
Cotton (<i>Gossypium hirsutum</i> L.)	4.3	0.13	NA	NA	Xiaoping et al. (2007)
C4					
Maize (<i>Zea mays</i> L.)	3.4	0.37	1.0	3.4	Plénet (1999)
Sorghum [<i>Sorghum bicolor</i> (L.) Moench]	3.9	0.39	NA	NA	Plénet and Cruz (1997)

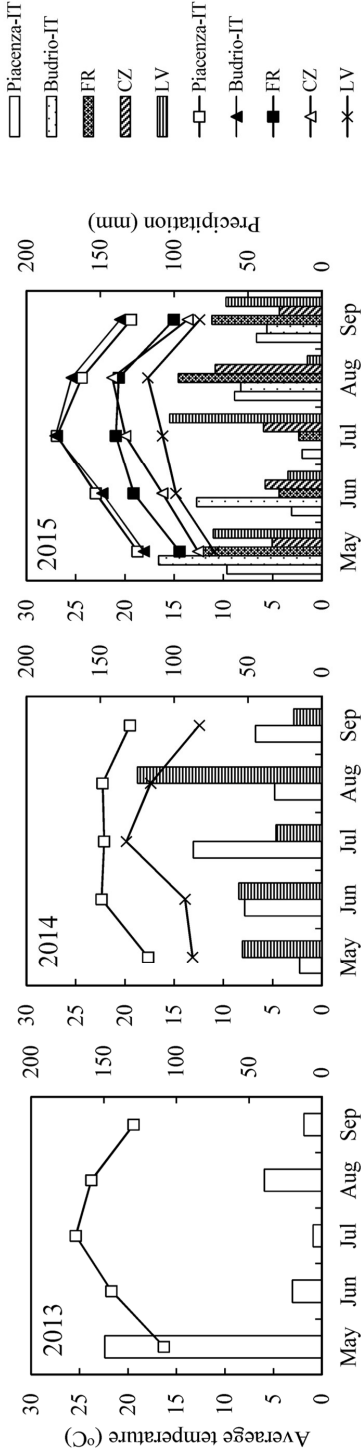


Figure S3.1 The monthly average temperature (lines) and precipitation (bars) during the growing season of hemp in 2013, 2014 and 2015. The location names are abbreviated as: Piacenza-IT (Piacenza, Italy); Budrio-IT (Budrio, Italy); FR (La Trugalle, France); CZ (Sumperk, the Czech Republic) and LV (Vilani, Latvia).

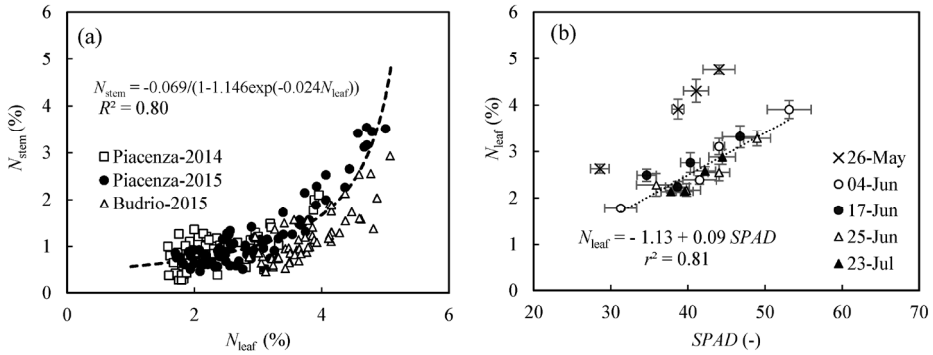


Figure S3.2 Panel a: the relationship between stem nitrogen concentration (N_{stem}) and leaf nitrogen concentration (N_{leaf}). Data was measured in Piacenza in 2014 and in 2015, and in Budrio in 2015, in Italy. Panel b: the relationship between $SPAD$ and N_{leaf} . Data was measured in Piacenza in 2015. The first measurement was excluded from the regression line. Bars indicate standard error.

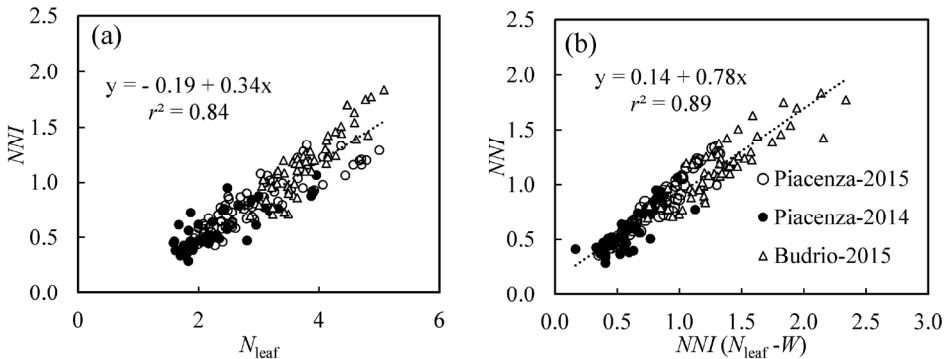


Figure S3.3 Indirect estimation of nitrogen nutrition index (NNI). Panel a: relationship between leaf nitrogen concentration (N_{leaf}) and NNI . Panel b: estimation of NNI combining N_{leaf} and above ground biomass yield (W). Note the stem nitrogen concentration (N_{stem}) is estimated using the relationship presented in Figure S3.2a.

Chapter 4

Hemp (*Cannabis sativa* L.) leaf photosynthesis in relation to nitrogen content and temperature: implications for hemp as a bio-economically sustainable crop

K. Tang^{a, b}, P.C. Struik^a, S. Amaducci^b, T.J. Stomph^a, X. Yin^a

^a *Centre for Crop Systems Analysis, Department of Plant Sciences, Wageningen University & Research, Droevendaalsesteeg 1, Wageningen, The Netherlands*

^b *Department of Sustainable Crop Production, Università Cattolica del Sacro Cuore, via Emilia Parmense, 84, Piacenza, Italy*

Abstract

Hemp (*Cannabis sativa* L.) may be a suitable crop for the bio-economy as it requires low inputs while producing a high and valuable biomass yield. With the aim of understanding the physiological basis of hemp's high resource use efficiency and yield potential, photosynthesis was analysed on leaves exposed to a range of nitrogen and temperature levels. Light-saturated net photosynthesis rate (A_{\max}) increased with an increase in leaf nitrogen up to $31.2 \pm 1.9 \mu\text{mol m}^{-2} \text{s}^{-1}$ at 25 °C. The A_{\max} initially increased with an increase in leaf temperature (T_L), levelled off at 25–35 °C and decreased when T_L became higher than 35 °C. Based on a C_3 leaf photosynthesis model, we estimated mesophyll conductance (g_m), efficiency of converting incident irradiance into linear electron transport under limiting light (κ_{2LL}), linear electron transport capacity (J_{\max}), Rubisco carboxylation capacity (V_{cmax}), triose phosphate utilization capacity (T_p) and day respiration (R_d), using data obtained from gas exchange and chlorophyll fluorescence measurements at different leaf positions and various levels of incident irradiance, CO_2 and O_2 . The effects of leaf nitrogen and temperature on photosynthesis parameters were consistent at different leaf positions and among different growth environments except for κ_{2LL} , which was higher for plants grown in the greenhouse than for those grown outdoors. Model analysis showed that compared with cotton and kenaf, hemp has higher photosynthetic capacity when leaf nitrogen is less than 2.0 g N m^{-2} . The high photosynthetic capacity measured in this study, especially at low nitrogen level, provides additional evidence that hemp can be grown as a sustainable bio-energy crop over a wide range of climatic and agronomic conditions.

Key words: hemp (*Cannabis sativa* L.), photosynthesis, model, nitrogen, temperature, sustainable crop.

4.1 Introduction

The multiple societal challenges such as climate change, natural resource scarcity and environmental pollution have fuelled interest in bio-economy (Jordan *et al.*, 2007). Previous comprehensive research programmes indicated that hemp (*Cannabis sativa* L.) fits well in the concept of bio-economy (Amaducci *et al.*, 2015; McCormick & Kautto, 2013). Hemp has the potential to produce up to 27 Mg ha⁻¹ biomass yield (Chapter 2) at relatively low inputs (Amaducci *et al.*, 2002; Struik *et al.*, 2000) and has a positive impact on the environment (Barth & Carus, 2015; Bouloc & van der Werf, 2013). Its stem contains high-quality cellulose (De Meijer & van der Werf, 1994), the seeds contain high-quality oil (Oomah *et al.*, 2002) and the inflorescence contains valuable resins (Bertoli *et al.*, 2010). From speciality pulp and paper to nutritional food, medicine and cosmetics, there are as many as 50,000 uses claimed for hemp products derived from its stem, seed and inflorescence (Carus & Sarmiento, 2016; Carus *et al.*, 2013). Recent research demonstrated that hemp is also a suitable feedstock for bioenergy production (Kreuger *et al.*, 2011; Prade *et al.*, 2011; Rice, 2008).

Although once an important crop for the production of textiles and ropes, hemp has not been subjected to the intensive research that has driven great improvements in major crops in the last 50 years (Amaducci *et al.*, 2015; Salentijn *et al.*, 2015) due to the continuous decrease in hemp acreage after the Second World War and its slow revival in the last couple of decades (Allegret, 2013; Wirtshafter, 2004). To advance research needed to consolidate and expand the market of hemp renewable materials, within the frame of the EC funded project Multihemp (www.multihemp.eu), it was proposed to develop a process based hemp growth model similar to the successful models for major staple crops (Bouman *et al.*, 2007). With the aim of understanding the physiological basis of hemp's high resource use efficiency and yield potential using a modelling approach, this study focuses on analysing leaf photosynthesis of hemp as a primary source of biomass production.

Very few studies report on leaf photosynthesis of hemp. De Meijer *et al.* (1995) reported a light-saturated rate of leaf photosynthesis for hemp of 30 kg CO₂ ha⁻¹ hr⁻¹ (equivalent to 19 μmol m⁻² s⁻¹) under field conditions. Chandra *et al.* (2015, 2011a,b, 2008) showed the response of leaf photosynthesis of hemp to irradiance intensity, CO₂ concentration and temperature by measuring gas exchange of leaves from greenhouse grown plants. Marija *et al.* (2011) found that nitrogen fertilization significantly affected different aspects of photosynthetic photochemistry, as shown by chlorophyll *a* fluorescence analysis. To the best of our knowledge,

a comprehensive analysis of the relation between leaf nitrogen status and photosynthesis rate is not yet available for hemp.

Leaf photosynthesis rate depends on both nitrogen nutrition status and environmental conditions (Sinclair & Horie, 1989). Thanks to a thorough understanding of the biochemical mechanisms of leaf photosynthesis, the response of leaf photosynthesis to irradiance intensity and CO₂ concentration can be modelled (von Caemmerer *et al.*, 2009; Yin *et al.*, 2006; Farquhar *et al.*, 1980). Such a model dissects net leaf photosynthesis into mesophyll conductance (g_m), linear electron transport capacity (J_{max}), Rubisco carboxylation capacity (V_{cmax}), triose phosphate utilization capacity (T_p) and day respiration (R_d). The effects of leaf nitrogen status and temperature on leaf photosynthesis are considered through their effects on these photosynthetic parameters (Hikosaka *et al.*, 2016). Experimental protocols for parameterizing the biochemical photosynthesis model have been well documented (Bellasio *et al.*, 2015; Yin *et al.*, 2009; Sharkey *et al.*, 2007), and the model has been successfully embedded as a sub-model in process based crop growth models for upscaling to canopy photosynthesis and crop production (Yin & Struik, 2009), such as the GECROS crop model (Yin & van Laar, 2005). Therefore, parameterizing the photosynthesis model for hemp is an excellent opportunity to understand its photosynthetic resource use efficiency, as well as to provide essential information for modelling hemp growth.

The first objective of the present study was to analyse leaf photosynthesis of hemp as affected by irradiance intensity, CO₂ concentration, temperature and nitrogen status. Secondly, this study aimed to parameterize a widely used C₃ leaf photosynthesis model (Yin *et al.*, 2006; Farquhar *et al.*, 1980) for hemp. In the final section, the photosynthetic capacity of hemp is compared with that of two other bio-economic crops, cotton (*Gossypium hirsutum* L.) and kenaf (*Hibiscus cannabinus* L.), using a modelling method. Cotton and kenaf were chosen because they are bioeconomically important crops and, in particular, kenaf is considered as an alternative for hemp in tropical and sub-tropical climates (Alexopoulou *et al.*, 2015; Lips & van Dam, 2013; Patanè & Cosentino, 2013).

4.2 Materials and methods

4.2.1 Plant growth and data collection

Three independent experiments were carried out at the research facilities of the Università Cattolica del Sacro Cuore (45.0° N, 9.8° E, 60 m asl; Piacenza, Italy). Seeds of hemp (*cv.* Futura

75) were received from the Fédération National des Producteurs de Chanvre, Le Mans, France. The plants were grown outdoors in 2013 and 2014, and in a greenhouse in 2015.

4.2.1.1 An experiment on the effect of nitrogen on leaf photosynthetic capacity (N-trial)

Seeds were sown in 18 containers ($40 \times 40 \times 30 \text{ cm}^3$) placed outdoors on 9 May 2014. Each container was filled with 23 kg of soil (dry weight) that contained 0.22% total nitrogen and had a clay-silt-sand ratio of 30:43:27. After seedling emergence, the plants were hand-thinned to 18 plants per container and three levels of urea fertilization were applied (0, 1.0 and 2.0 g N per container, respectively). There were six containers for each fertilization level. Other nutrients (e.g. phosphate and potassium) were assumed not limiting factors according to historic experience in the field from which the soil was collected. The same applies to the other two trials. During plant growth, all containers were positioned randomly and tightly in one block surrounded by a green shading net (transmitting 3% of the light). The net height was adjusted daily according to the increment of plant height. The plants were well watered during the entire experiment. The daily temperature and global radiation during the growth period are presented in Supplementary Material Figure S4.1.

Photosynthetic measurements were started on 46 days after sowing (the 6th–8th pair of leaves had appeared) in a growth chamber with the temperature set at 25 °C. The container was moved into the growth chamber 2 hrs before measurements. On one representative plant in each container, the middle leaflets of the youngest, fully expanded top leaf and of the middle leaf (i.e., two nodes below the top leaf) were measured. Simultaneous gas exchange (GE) and chlorophyll fluorescence (CF) measurements were implemented *in situ* using a portable open gas exchange system with a 1.7 cm² clamp-on leaf chamber (CIRAS-2, PP Systems International, Inc., USA) combining with FMS2 (Hansatech Instruments Ltd, UK). The system setup of the combined CIRAS-2 and FMS2 for performing simultaneous GE and CF measurements was implemented according to the instructions provided by PP Systems International, Inc., USA. Light response curve of net photosynthesis rate (A) (A - I_{inc}) and its CO₂ response curve (A - C_a) were assessed for each leaf under ambient O₂ (i.e. 21%) conditions. The A - I_{inc} curves were assessed by decreasing incident light intensity (I_{inc}) as: 2000, 1500, 1000, 500, 300, 200, 150, 100, 60 and 30 $\mu\text{mol m}^{-2} \text{ s}^{-1}$, while keeping leaf chamber CO₂ concentration (C_a) at 400 $\mu\text{mol mol}^{-1}$. At the end of assessing the A - I_{inc} curve, the light source was turned off for 15 minutes to measure leaf respiration in darkness (R_{dk}). The A - C_a curves were assessed by changing C_a as: 400, 250, 150, 80, 70, 60, 50, 400, 400, 600, 800, 1000, and 1500 $\mu\text{mol mol}^{-1}$,

while keeping I_{inc} at $1000 \mu\text{mol m}^{-2} \text{s}^{-1}$. Leaf temperature (T_L) and vapour pressure of supplying air during measurements were set constant at $25 \text{ }^\circ\text{C}$ and 2 kPa , respectively. The response curves were started when the leaf had adapted to the condition at the first I_{inc} or C_a level for 30 min. Data was recorded programmatically with 2 min interval for A - I_{inc} curves and 3 min interval for A - C_a curves. Pre-measurements indicated these time intervals were sufficiently long for A to reach a steady state. Three plants were measured for each fertilization level.

To obtain a calibration factor that can properly convert fluorescence-based PSII efficiency into linear electron transport rate, parts of A - I_{inc} and A - C_a curves were also assessed under 2% O_2 . This condition was realized by supplying the CIRAS-2 with a humidified mixture of 2% O_2 and 98% N_2 . To avoid O_2 leakage, the air-in pump in the CIRAS-2 was replaced by a sealed one according to the manufacturer's instruction. The curves for 2% O_2 were assessed in accordance with the ones for ambient O_2 but the A - I_{inc} curves were only assessed at $I_{\text{inc}} \leq 150 \mu\text{mol m}^{-2} \text{s}^{-1}$ and the A - C_a curves were only assessed at $C_a \geq 600 \mu\text{mol mol}^{-1}$. These particular I_{inc} and C_a conditions are required for obtaining the calibration factor (Yin *et al.* 2009), i.e., to ensure that A is limited by electron transport.

When the photosynthetic measurements were completed, *SPAD*, a proxy for chlorophyll concentration, was measured using a SPAD-502 (Minolta, Japan). Leaf area was determined from scans using ImageJ (version 1.49; <https://imagej.nih.gov/>). Dry weight was measured after drying at $75 \text{ }^\circ\text{C}$ until constant weight. Total leaf nitrogen concentration was analysed using a *CN* analyser (Vario Max CN Analyzer; Elementar Americas, Inc., Hanau, Germany). Specific leaf nitrogen (*SLN*; g N m^{-2}) was calculated for each measured leaf using the leaf dry weight, leaf area and nitrogen concentration. CO_2 leakage of the CIRAS-2 leaf chamber was assessed by performing A - C_a curves on three heat-killed leaves. Based on these measurements, values of A and the intercellular CO_2 concentration (C_i) of A - C_a curves were recalculated using the CIRAS-2 built-in formulae.

4.2.1.2 An experiment on the effect of temperature on leaf photosynthetic capacity (*T*-trial)

Seeds were sown in 6 pots ($10 \times 10 \times 15 \text{ cm}^3$) placed in a greenhouse on 12 February 2015. Each pot contained 1 kg of soil that had identical properties with the ones in the *N*-trial. The temperature in the greenhouse was maintained at approximately $25 \text{ }^\circ\text{C}$. A LED lamp (270 Watt, Shenzhen GTL Lighting Co. Ltd, China) mounted 50 cm above the canopy for 16 hrs each day gave the light level in greenhouse of approximately $600 \mu\text{mol m}^{-2} \text{s}^{-1}$. After emergence, the

plants were hand-thinned to 2 plants per pot and urea fertilization was applied (0.3 g N per pot). The plants were well watered during growth.

Starting on 46 days after sowing, GE measurements were conducted in a temperature controllable chamber. On one plant in each pot, the middle leaflet of the youngest, fully expanded top leaf was measured. The $A-I_{\text{inc}}$ and $A-C_a$ curves were assessed subsequently at T_L 15, 20, 25, 30, 35 and 40 °C. The levels of I_{inc} and C_a were set in accordance with the N-trial under ambient O_2 . During the measurements, the temperature in the growth chamber was controlled close to the targeting T_L and the vapour pressure of supplying air was set at 1.5 kPa for all temperature levels except for 15 °C, when it was set at 1.0 kPa to avoid water condensation. Three plants were measured. *SPAD*, *SLN* and gas leakage were analysed using the procedures described for the N-trial.

4.2.1.3 An experiment on leaf photosynthesis in response to fluctuating temperature under different leaf nitrogen levels (TN-trial).

Seeds were sown in 18 containers ($60 \times 20 \times 18 \text{ cm}^3$) placed outdoor on 5 August 2013. Each container was filled with 10 kg of soil that contained 0.11% of total nitrogen and had a clay-silt-sand ratio of 15:22:63. After seedling emergence, the plants were hand-thinned to 10 plants per container and three levels of urea fertilization were applied (0, 0.78 and 1.95 g N per container, respectively). Each fertilization level had six containers. The plants were well watered during growth. Because of very late sowing, a halogen lamp (54 Watt) that was mounted at 50 cm from the top of canopy was turned on for 16 hrs per day to prevent plants from flowering. The daily temperature and radiation during the growth period are presented in Supplementary Material Figure S4.1.

Starting on 50 days after sowing (the 8th–10th pair of leaves had appeared), GE measurements were conducted outdoors on three representative plants for each nitrogen level. $A-I_{\text{inc}}$ and $A-C_a$ curves were assessed on the middle leaflet of the youngest, fully expanded leaf. The levels of light for the $A-I_{\text{inc}}$ curves were identical to those in the N-trial under ambient O_2 , while the $A-C_a$ curves were assessed by increasing C_a as: 50, 60, 70, 80, 150, 250, 400, 650, 1000, and 1500 $\mu\text{mol mol}^{-1}$ while keeping I_{inc} at 1000 $\mu\text{mol m}^{-2} \text{ s}^{-1}$. During measurement, T_L and vapour pressure were not controlled, therefore, varied depending on ambient conditions. A response curve was started when the leaf had adapted to the leaf chamber for 15 min at the first I_{inc}/C_a level. Data were recorded manually when the real-time net photosynthesis (A) had apparently

reached steady state (~ 3 min for A - I_{inc} and ~ 5 min for A - C_a). *SPAD*, *SLN* and gas leakage were analysed using the procedures described for the N-trial.

4.2.2 Model description

The photosynthesis model of Farquhar *et al.* (1980) coupled with CO₂ diffusion model, as described in Yin & Struik (2009), was used in this study.

4.2.2.1 Modelling net leaf photosynthesis rate at the carboxylation sites of Rubisco

The net leaf photosynthesis rate (A , $\mu\text{mol m}^{-2} \text{s}^{-1}$) was modelled as the minimum of the Rubisco limited rate (A_c), the electron transport limited rate (A_j) and the triose phosphate utilization limited rate (A_p):

$$A = \min (A_c, A_j, A_p) \quad (4.1)$$

A_c is described, following the Michaelis–Menten kinetics, as:

$$A_c = \frac{(C_c - \Gamma^*)V_{cmax}}{C_c + K_{mc}(1 + O/K_{mo})} - R_d \quad (4.2)$$

where C_c ($\mu\text{mol mol}^{-1}$) and O (mmol mol^{-1}) are the CO₂ and O₂ levels at the carboxylation sites of Rubisco; V_{cmax} ($\mu\text{mol m}^{-2} \text{s}^{-1}$) is the maximum rate of carboxylation; K_{mc} ($\mu\text{mol mol}^{-1}$) and K_{mo} (mmol mol^{-1}) are Michaelis-Menten constants of Rubisco for CO₂ and O₂, respectively; R_d ($\mu\text{mol m}^{-2} \text{s}^{-1}$) is the day respiration (respiratory CO₂ release other than by photorespiration); Γ^* ($\mu\text{mol mol}^{-1}$) is the CO₂ compensation point in the absence of R_d .

A_j is described as:

$$A_j = \frac{(C_c - \Gamma^*)J}{4C_c + 8\Gamma^*} - R_d \quad (4.3)$$

where J ($\mu\text{mol m}^{-2} \text{s}^{-1}$) is the potential linear e⁻ transport rate that is used for CO₂ fixation and photorespiration, and it is described as:

$$J = \frac{\kappa_{2LL}J_{inc} + J_{max} - \sqrt{(\kappa_{2LL}J_{inc} + J_{max})^2 - 4\theta J_{max}\kappa_{2LL}J_{inc}}}{2\theta} \quad (4.4)$$

where J_{max} ($\mu\text{mol m}^{-2} \text{s}^{-1}$) is the maximum value of J under saturated light; I_{inc} is the incident light ($\mu\text{mol m}^{-2} \text{s}^{-1}$); κ_{2LL} (mol mol^{-1}) is the conversion efficiency of incident light into J at strictly limiting light; θ (dimensionless) is convexity factor for the response of J to I_{inc} .

A_p is described as:

$$A_p = 3T_p - R_d \quad (4.5)$$

where T_p ($\mu\text{mol m}^{-2} \text{s}^{-1}$) is the rate of triose phosphate export from the chloroplast.

The T_L response of R_d , T_p and kinetic properties of Rubisco (involving V_{cmax} , K_{mc} , K_{mo} and Γ^*) are described using an Arrhenius function normalized with respect to their values at 25 °C (Eqn. 4.6) while the response of J_{max} is described using a peaked Arrhenius function (Eqn. 4.7):

$$X = X_{25} \exp \left[\frac{E_x(T_L - 25)}{298R(T_L + 273)} \right] \quad (4.6)$$

$$X = X_{25} \exp \left[\frac{E_x(T_L - 25)}{298R(T_L + 273)} \right] \left[\frac{1 + \exp\left(\frac{298S_x - D_x}{298R}\right)}{1 + \exp\left(\frac{(T_L + 273)S_x - D_x}{R(T_L + 273)}\right)} \right] \quad (4.7)$$

where X_{25} is the value of each parameter at 25 °C (i.e., R_d , V_{cmax} , K_{mc} , K_{mo} , Γ^* and J_{max}). E_x and D_x are the energies of activation and deactivation (i.e., E_{R_d} , $E_{V_{\text{cmax}}}$, $E_{K_{\text{mc}}}$, $E_{K_{\text{mo}}}$, E_{T_p} , E_{Γ^*} , $E_{J_{\text{max}}}$ and $D_{J_{\text{max}}}$, all in J mol^{-1}); S_x is the entropy term ($S_{J_{\text{max}}}$ in $\text{J K}^{-1} \text{mol}^{-1}$); R is the universal gas constant ($=8.314 \text{ J K}^{-1} \text{mol}^{-1}$).

4.2.2.2 Modelling mesophyll conductance for CO_2

The CO_2 concentration at intercellular space (C_i) was taken from gas exchange measurement whereas the estimation of C_c relies on proper estimation of mesophyll conductance (g_m). g_m , calculated by the variable J method (Harley *et al.*, 1992a), appeared to vary with CO_2 and irradiance levels (see Results section). Whether or not g_m varies with CO_2 and irradiance levels is debatable (Flexas *et al.*, 2012, 2007). We used the model of Yin *et al.* (2009) that is able to deal with both constant and variable g_m models, and have a similar form as Eqn. (4.8):

$$g_m = g_{m0} + \frac{\delta(A + R_d)}{C_c - \Gamma^*} \quad (4.8)$$

where g_{m0} ($\text{mol m}^{-2} \text{s}^{-1}$) is the minimum g_m if irradiance approaches zero; parameter δ (dimensionless) in this model defines the $C_c : C_i$ ratio at saturating light as $(C_c - \Gamma^*) / (C_i - \Gamma^*) = 1 / (1 + 1/\delta)$. Any positive value of δ predicts a variable g_m pattern in response to C_i and I_{inc} , and a higher δ implies higher g_m and therefore a higher $C_c : C_i$ ratio. If $\delta = 0$, Eqn. (4.8) predicts an independence of g_m on C_i and I_{inc} (i.e., $g_m = g_{m0}$), equivalent to the constant- g_m model.

4.2.3 Model parameterization and validation

The data collected in the N-trial was used to assess the effect of leaf nitrogen on the values of model parameters at 25 °C. The data collected in the T-trial was used to assess the effect of leaf temperature on the values of (peaked) Arrhenius model parameters. The parameterized model was validated against the data collected in the TN-trial. In the model, Rubisco kinetic properties related parameters (i.e., K_{mc} , K_{mo} and Γ^*) and θ , convexity factor for the response of J to I_{inc} , are conserved amongst C₃ species (von Caemmerer *et al.*, 2009). Thus, the value of θ was set to 0.7 (Ögren & Evans, 1993); the values of K_{mc} , K_{mo} and Γ^* at 25 °C were set to 272 $\mu\text{mol mol}^{-1}$, 165 mmol mol^{-1} and 37.5 $\mu\text{mol mol}^{-1}$ (at 21% O₂), respectively (Bernacchi *et al.*, 2002). The energies of activation $E_{K_{mc}}$, $E_{K_{mo}}$ and E_{Γ^*} were adapted from the values of Bernacchi *et al.* (2002) as $E_{K_{mc}} = 80990 \text{ J mol}^{-1}$; $E_{K_{mo}} = 23720 \text{ J mol}^{-1}$; $E_{\Gamma^*} = 24460 \text{ J mol}^{-1}$.

4.2.3.1 Model parameterization with data collected in the N-trial: nitrogen effect

The step-wise parameterizing procedures described by Yin *et al.* (2009) were adapted in this study. Specifically:

Step 1: Estimating electron transport parameters (J_{max} and κ_{2LL}) and R_d

According to Yin *et al.* (2009), the observed A_j under non-photorespiratory conditions can be expressed using Eqn. (4.9):

$$A_j = \frac{sI_{inc}\Phi_2}{4} - R_d \quad (4.9)$$

$$s = \beta\rho_2\left(1 - \frac{f_{\text{pseudo(b)}}}{1-f_{\text{cyc}}}\right) \quad (4.9a)$$

where s is a lumped parameter; Φ_2 is PSII operating efficiency, usually assessed from the chlorophyll fluorescence measurements, indicating quantum efficiency of PSII e^- flow on PSII-absorbed light basis; β is leaf absorptance; ρ_2 is proportion of absorbed I_{inc} partitioned to PSII; f_{cyc} and $f_{\text{pseudo(b)}}$ are the fraction of cyclic and basal pseudocyclic electron transport, respectively. Thus, a simple linear regression can be performed for the observed A against ($I_{inc}\Phi_2/4$) using data of the e^- transport-limited range under non-photorespiratory conditions (measurements conducted at 2% O₂). The slope of the regression yields an estimate of the calibration factor s , and the intercept gives an estimate of R_d under 2% O₂ condition. The estimated s allowed the conversion of CF-based PSII operating efficiency into the actual rate of linear electron transport as:

$$J = sI_{\text{inc}}\Phi_2 \quad (4.10)$$

Thus, J_{max} and $\kappa_{2\text{LL}}$ can be estimated from fitting Eqn. (4.4) to the values of J .

The same linear regression for the observed A against $(I_{\text{inc}}\Phi_2/4)$ using data of the e^- transport-limited range may be applied as well to photorespiratory conditions (i.e., ambient O_2) for estimating R_d although the slight variation of C_i with I_{inc} can have bearing under these conditions (Yin *et al.*, 2011, 2009).

Step 2: Parameterization of the g_m model and V_{cmax} and T_p

Combining Eqn. (4.8) with Eqn. (4.2) and Eqn. (4.3), and replacing C_c with $(C_i - A/g_m)$ yields (Yin *et al.* 2009):

$$A_c \text{ or } A_j = \frac{-b - \sqrt{b^2 - 4ac}}{2a} \quad (4.11)$$

where

$$a = x_2 + \Gamma^* + \delta(C_i + x_2)$$

$$b = -\{(x_2 + \Gamma^*)(x_1 - R_d) + (C_i + x_2)[g_{m0}(x_2 + \Gamma^*) + \delta(x_1 - R_d)] + \delta[x_1(C_i - \Gamma^*) - R_d(C_i + x_2)]\}$$

$$c = [g_{m0}(x_2 + \Gamma^*) + \delta(x_1 - R_d)][x_1(C_i - \Gamma^*) - R_d(C_i + x_2)]$$

$$\text{with } x_1 = \begin{cases} V_{\text{cmax}} & \text{for } A_c \\ \frac{J}{4} & \text{for } A_j \end{cases}$$

$$\text{and } x_2 = \begin{cases} K_{\text{mc}}(1 + \frac{O}{K_{\text{mo}}}) & \text{for } A_c \\ 2\Gamma^* & \text{for } A_j \end{cases}$$

Thus, V_{cmax} , T_p , and δ (or g_{m0}) can be estimated simultaneously by fitting Eqn. (4.1), Eqn. (4.4), Eqn. (4.5) and Eqn. (4.11) to A - I_{inc} and A - C_i using pre-estimated J_{max} , $\kappa_{2\text{LL}}$ and R_d as input.

Since it is uncertain if g_m varies with CO_2 and irradiance levels, g_m was first assessed according to the variable J method (Harley *et al.*, 1992a):

$$g_m = \frac{A}{C_i - \frac{\Gamma^*[J+8(A+R_d)]}{J-4(A+R_d)}} \quad (4.12)$$

where A and C_i were taken from gas exchange measurements and J was calculated by Eqn. (4.10). If g_m does vary in response to changing C_i and I_{inc} , we could fit only δ by fixing g_{m0} to 0 (Yin *et al.* 2009). In such a case, g_m can be calculated as:

$$g_m = \frac{A + \delta(A + R_d)}{C_i - \Gamma^*} \quad (4.13)$$

4.2.3.2 Model parameterization with data collected in the T-trial: temperature effect

By assuming the value of δ is independent of leaf temperature, the values of J_{max} , κ_{2LL} , V_{cmax} and T_p at each leaf temperature were solved from Eqn. (4.1), Eqn. (4.4), Eqn. (4.5) and Eqn. (4.11) by simultaneously fitting $A-I_{inc}$ and $A-C_i$. Subsequently, the parameter values at different T_L were fitted to either Eqn. (4.6) for estimating E_{Rd} , E_{Vcmax} , E_{Tp} , or Eqn. (4.7) for estimating E_{Jmax} , D_{Jmax} and S_{Jmax} .

4.2.3.3 Model validation

The parameterized model was validated against the data obtained in the TN-trial. The model parameters R_d , J_{max} , V_{cmax} and T_p at 25 °C were derived from their linear relationships with SLN (see Results section), and the effect of T_L on the values of these parameters was quantified through Eqn. (4.6) or Eqn. (4.7) with the estimated E_{Rd} , E_{Vcmax} , E_{Tp} , E_{Jmax} , D_{Jmax} and S_{Jmax} .

4.2.4 Comparison of hemp leaf photosynthetic competence with that of cotton and kenaf

To illustrate the leaf photosynthetic competence of hemp in comparison with cotton and kenaf, $A-C_i$, $A-I_{inc}$, $A-T_L$ and $A-SLN$ curves were constructed for hemp using the validated model while those of cotton and kenaf were constructed using the FvCB models and corresponding parameters reported in Harley *et al.* (1992b) for cotton (*cv.* Coker 315) and in Archontoulis *et al.* (2011) for kenaf (*cv.* Everglades 41).

4.2.5 Statistics

Simple linear regression was performed using Microsoft Excel. Non-linear fitting was carried out using the GAUSS method in PROC NLIN of SAS (SAS Institute Inc., Cary, NC, USA). If parameters were proven independent from leaf nitrogen or temperature, the dummy variables method was used to estimate one common value (Yin *et al.*, 2009). The goodness of fit was assessed by calculating the coefficient of determination (r^2) and the relative mean root square ($rRMSE$). The effect of leaf position on parameter values was tested by performing ANOVA test considering leaf nitrogen as covariate.

4.3 Results

4.3.1 Results of model parameterization and validation

4.3.1.1 Results of the N-trial: nitrogen dependent photosynthetic capacity

Measurements to assess the effect of leaf nitrogen on leaf photosynthetic capacity of hemp (N-trial) were conducted on leaves having an average SLN of 0.87 g N m^{-2} , 1.25 g N m^{-2} and 1.75 g N m^{-2} at the top of the canopy, or 0.65 g N m^{-2} , 0.78 g N m^{-2} and 1.22 g N m^{-2} at the middle of the canopy, for the three N treatments, respectively. Examples of A - I_{inc} and A - C_i curves at different SLN levels are shown in Figure 4.1. The R_{dk} ($\mu\text{mol m}^{-2} \text{ s}^{-1}$; leaf respiration in the dark) and light-saturated net photosynthesis rate (A_{max} ; measured at $2000 \mu\text{mol m}^{-2} \text{ s}^{-1}$) increased linearly with increasing SLN , and these linear relationships did not differ between the top and middle leaves (Figure 4.2).

Using the data of electron transport limited range under non-photorespiratory conditions (i.e., at 2% O_2 , $C_a \geq 600 \mu\text{mol mol}^{-1}$ in the A - C_a curve and $I_{\text{inc}} \leq 150 \mu\text{mol m}^{-2} \text{ s}^{-1}$ in the A - I_{inc} curve), parameter s was estimated as the slope of a linear regression of A against $(I_{\text{inc}}\Phi_2/4)$. The value of s was independent of SLN and canopy position ($P > 0.05$; see Supplementary Material Figure S4.2a). Thus, a common s (0.33 ± 0.01) was estimated from pooled data. κ_{2LL} and J_{max} were estimated from fitting Eqn. (4.4) to the data on calculated J from Eqn. (4.10). A preliminary estimation indicated that κ_{2LL} was unlikely to change with SLN and canopy position

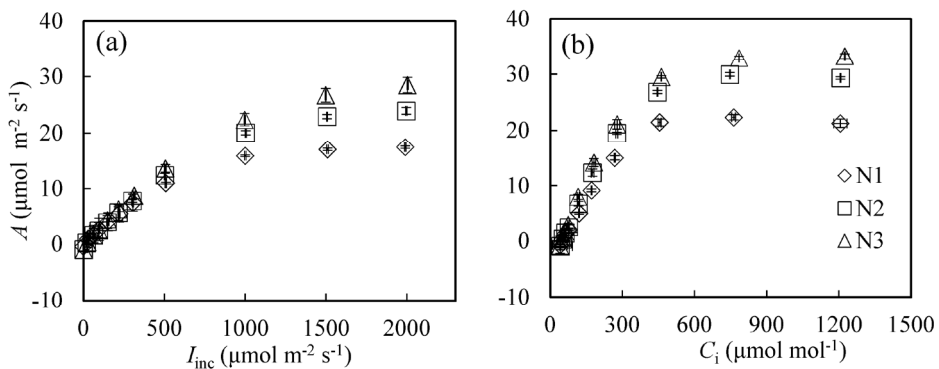


Figure 4.1 The net leaf photosynthesis (A) in response to incident irradiance (I_{inc} ; panel a) and intercellular CO_2 concentration (C_i ; panel b) under different leaf nitrogen levels. Data presented were measured at 21% O_2 on the top leaves in the N-trial. N1, N2 and N3 correspond to nitrogen treatments, resulting in average specific leaf nitrogen values of 0.87 g N m^{-2} , 1.25 g N m^{-2} and 1.75 g N m^{-2} , respectively. The bars indicate standard errors of the mean ($n = 3$).

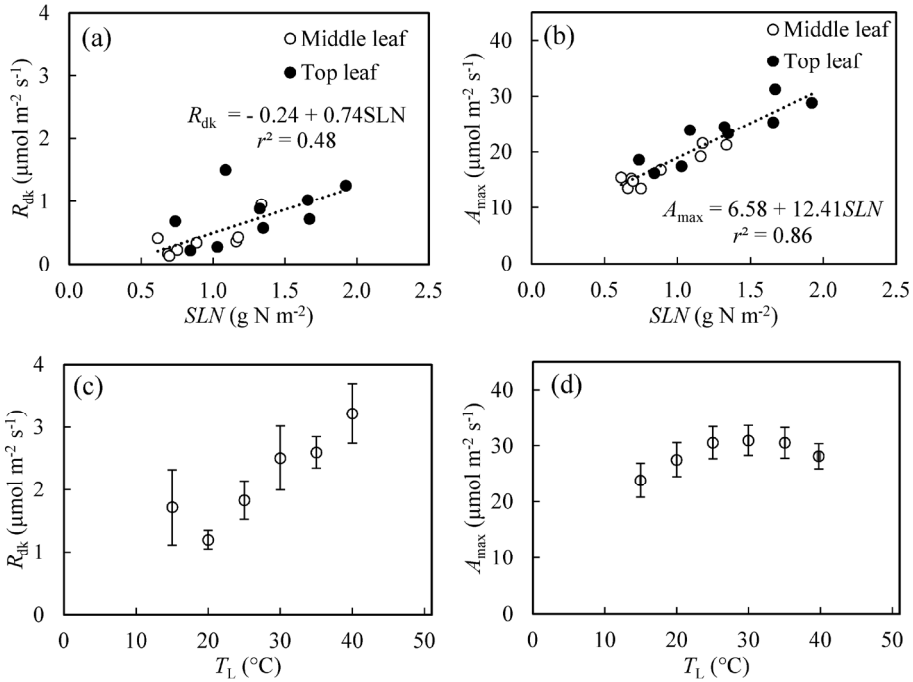


Figure 4.2 The response of leaf respiration in dark (R_{dk} , panels a and c) and maximum light-saturated net photosynthesis rate (A_{max} ; panels b and d) to specific leaf nitrogen (SLN ; panels a and b) and leaf temperature (T_L ; panels c and d). R_{dk} was measured after adapting leaves in dark for 15 minutes after measuring the $A - I_{inc}$ curve. A_{max} was measured at $2000 \mu\text{mol m}^{-2} \text{s}^{-1}$ for incident light intensity and $400 \mu\text{mol mol}^{-1}$ for ambient CO_2 concentration. The data presented in panel a and panel b were obtained in the N-trial while those in panel c and panel d indicate standard errors of the mean ($n = 3$).

($P > 0.01$; Supplementary Material Figure S4.2b). Thus, a common κ_{2LL} ($0.21 \pm 0.004 \text{ mol mol}^{-1}$) was estimated together with J_{max} using the dummy variable method. The J_{max} ranged from $116.1 \mu\text{mol m}^{-2} \text{s}^{-1}$ to $316.4 \mu\text{mol m}^{-2} \text{s}^{-1}$ and increased linearly with an increase in SLN at the rate of $132.9 \mu\text{mol s}^{-1} (\text{g N})^{-1}$ (Figure 4.3a). The relationship between J_{max} and SLN was independent of canopy position ($P > 0.05$).

The estimated R_d values at 21% O_2 were roughly in line with the ones at 2% O_2 (Supplementary Material Figure S4.3). Although the latter were on average 25% lower, a test of covariance indicated that R_d did not differ significantly between the different O_2 levels ($P = 0.17$). At 21% O_2 , R_d ranged from $0.29 \mu\text{mol m}^{-2} \text{s}^{-1}$ to $1.61 \mu\text{mol m}^{-2} \text{s}^{-1}$, increasing linearly with SLN at a rate of $0.85 \mu\text{mol s}^{-1} (\text{g N})^{-1}$ (Figure 4.3b). The R_d - SLN relationship did not differ much between the middle and top leaves ($P > 0.05$).

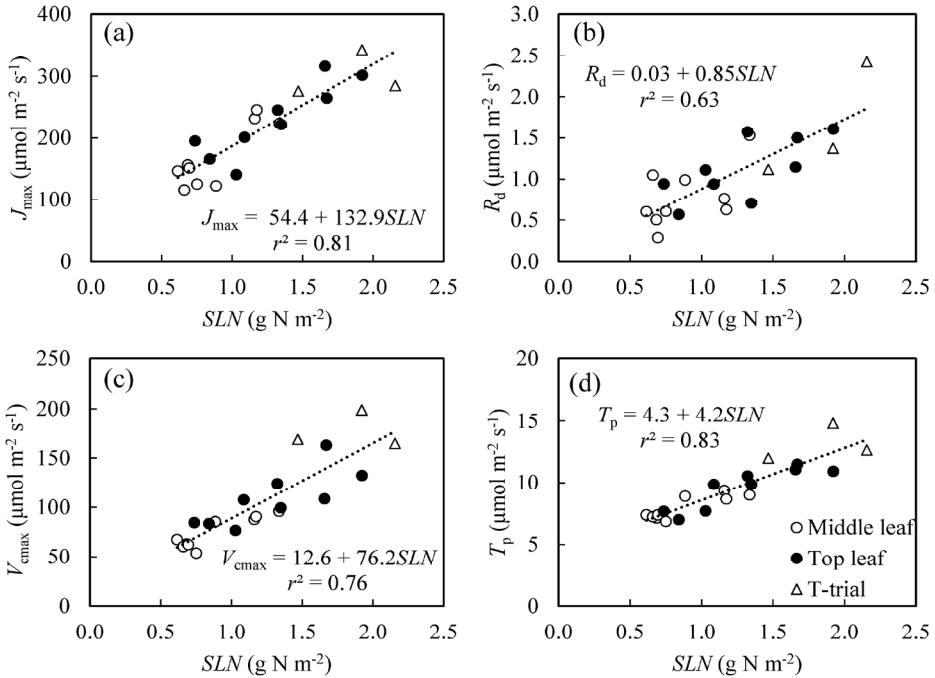


Figure 4.3 Dependence of maximum potential linear e^- transport rate (J_{\max} ; panel a), day respiration (R_d ; panel b), maximum rate of carboxylation (V_{cmax} ; panel c) and the rate of triose phosphate export from the chloroplast (T_p ; panel d) on specific leaf nitrogen (SLN). Values indicated as circles (\circ and \bullet denote leaves at the middle and top of canopy, respectively) were derived from the data collected in the N-trial; values indicated as triangles (Δ) were derived from the data collected in the T-trial at a leaf temperature of 25 °C.

The g_m calculated using the variable J method, Eqn. (4.12), indicated that it varied with changing I_{inc} and C_i (Figure 4.4a, b). A preliminary analysis indicated that the value of g_{m0} in Eqn. (4.8) was close to zero. By fixing g_{m0} to zero, a common value of δ (2.12 ± 0.09) was estimated together with V_{cmax} and T_p using the dummy variable method. With the estimated δ , Eqn. (4.13) estimates that g_m changes with I_{inc} and C_i in a similar trend as observed for the g_m calculated using Eqn. (4.12); the latter, however, was 38% lower (Figure 4.4a, b), probably as a result that the variable J method assumes the limitation on photosynthesis by electron transport over the full range of A - I_{inc} and A - C_i curves (Yin *et al.* 2009). The estimated g_m with Eqn. (4.13) increases with an increase in SLN (Figure 4.4c).

The estimated V_{cmax} ranged from $53.7 \mu\text{mol m}^{-2} \text{s}^{-1}$ to $163.2 \mu\text{mol m}^{-2} \text{s}^{-1}$ and increased linearly with an increase in SLN at the rate of $76.2 \mu\text{mol s}^{-1} (\text{g N})^{-1}$ (Figure 4.3c). The estimated

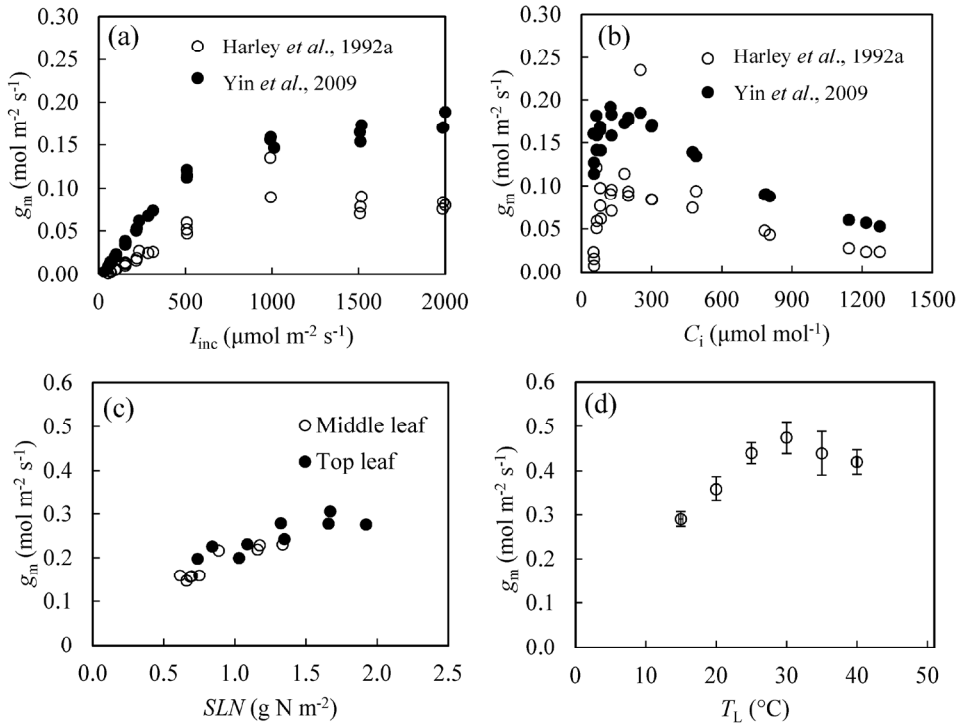


Figure 4.4 Illustration of mesophyll conductance (g_m) in relation to changing incident irradiance (I_{inc} : panel a), intercellular CO₂ concentration (C_i : panel b), specific leaf nitrogen (SLN ; panel c) and leaf temperature (T_L ; panel d). In panels a and b, the data presented were obtained from the leaves at the middle of the canopy in the treatment without nitrogen fertilization in the N-trial; the open (\circ) and closed (\bullet) circles were calculated using the variable J method of Harley *et al.* (1992a) (see Eqn. 4.12 in the text) and the method of Yin *et al.* (2009) (see Eqn. 4.13 in the text), respectively. In panel c, the data presented were obtained at $I_{inc} = 1000 \mu\text{mol m}^{-2} \text{s}^{-1}$ and $C_a = 400 \mu\text{mol mol}^{-1}$ in the N-trial; the open (\circ) and closed (\bullet) circles represent data obtained from leaves from the middle and the top of the canopy, respectively. In panel d, the data presented were obtained at $I_{inc} = 1000 \mu\text{mol m}^{-2} \text{s}^{-1}$ and $C_a = 400 \mu\text{mol mol}^{-1}$ in the T-trial; the bars indicate standard errors of the mean ($n = 3$). Note the differences in scale along the y-axes.

T_p ranged from $6.9 \mu\text{mol m}^{-2} \text{s}^{-1}$ to $11.5 \mu\text{mol m}^{-2} \text{s}^{-1}$ and increased linearly with an increase in SLN at the rate of $4.2 \mu\text{mol s}^{-1} (\text{g N})^{-1}$ (Figure 4.3d). The effects of SLN on V_{cmax} and T_p were independent of leaf position ($P > 0.05$). With the estimated R_d , κ_{2LL} , J_{max} , δ , V_{cmax} and T_p , the r^2 and $rRMSE$ of the model description of the measured A in the N-trial were 0.99 and 18.5%, respectively.

4.3.1.2 Results of T-trial: temperature dependent photosynthetic capacity

The R_{dk} increased continuously from $0.9 \mu\text{mol m}^{-2} \text{s}^{-1}$ to $4.1 \mu\text{mol m}^{-2} \text{s}^{-1}$ at increasing T_L from $15 ^{\circ}\text{C}$ to $40 ^{\circ}\text{C}$ while the A_{max} initially increased with increasing T_L , levelled off at $25\text{--}35 ^{\circ}\text{C}$ and decreased when T_L became higher than $35 ^{\circ}\text{C}$ (Figure 4.2c, d).

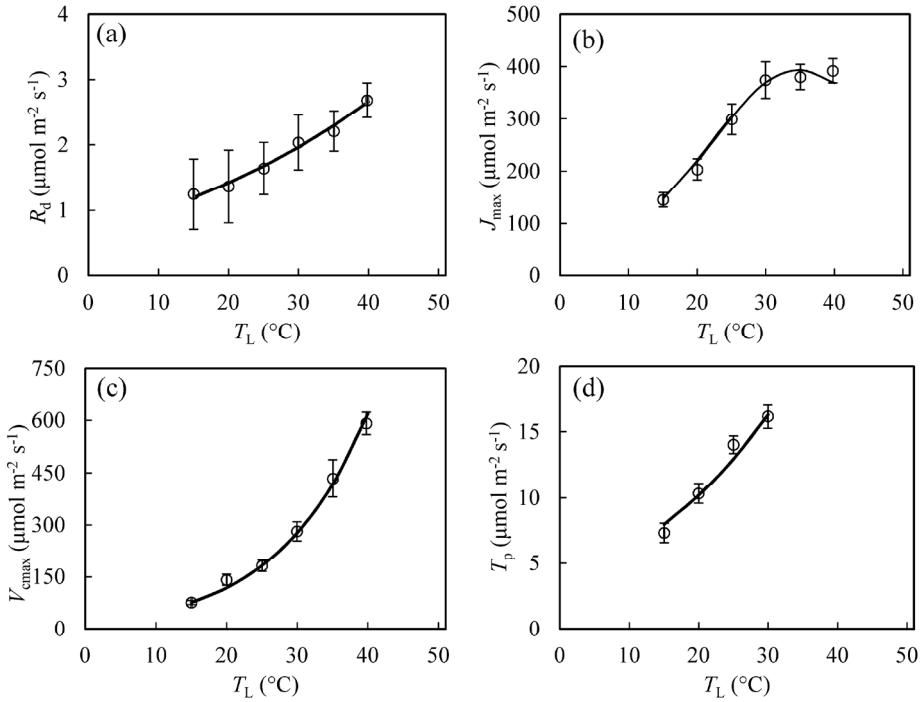


Figure 4.5 Response of day respiration (R_d ; panel a), maximum potential linear e^- transport rate (J_{\max} ; panel b), maximum rate of carboxylation ($V_{c\max}$; panel c) and the rate of triose phosphate export from the chloroplast (T_p ; panel d) to leaf temperature (T_L). The solid lines denote the predicted relations according to Eqn. (4.6) or Eqn. (4.7) with values presented in Table 4.1. The bars indicate standard errors of the mean ($n = 3$).

The estimated R_d increased continuously with an increase in T_L , ranging from $0.3 \mu\text{mol m}^{-2} \text{s}^{-1}$ until $3.2 \mu\text{mol m}^{-2} \text{s}^{-1}$ (Figure 4.5a). The κ_{2LL} , J_{\max} , $V_{c\max}$ and T_p were estimated simultaneously by assuming $\delta = 2.12$ (estimated in N-trial) at each T_L . With the constant δ , the model predicted that g_m changed with an increase in T_L following a similar trend as A_{\max} (cf. Figures 4.2d, 4.4d). A preliminary analysis indicated that κ_{2LL} was conserved at different levels of T_L ($P > 0.05$; see Supplementary Material Figure S4.2c) but significantly higher than the value estimated in the N-trial (i.e., $\kappa_{2LL} = 0.21 \pm 0.004 \text{ mol mol}^{-1}$). Thus, a common κ_{2LL} ($0.37 \pm 0.01 \text{ mol mol}^{-1}$) was estimated together with J_{\max} , $V_{c\max}$ and T_p using the dummy variable method. The J_{\max} , $V_{c\max}$ and T_p at 25°C were comparable with those derived from the N-trial (Figure 4.3). The value of T_p increased consistently with an increase in T_L from 15°C to 30°C (Figure 4.5d). When T_L was higher than 30°C , the curve fitting failed to assess T_p properly because the triose phosphate utilization is not limited at such high temperatures (Busch & Sage, 2016; Sage & Kubien, 2007). Therefore, T_p limitation was excluded to estimate J_{\max} and $V_{c\max}$

at 35 °C and 40 °C. The V_{cmax} increased continuously at increasing T_L from 15 °C to 40 °C while the value of J_{max} peaked at 30-35 °C (Figure 4.5b, c).

By fitting the R_d - T_L , V_{cmax} - T_L and T_p - T_L to Eqn. (4.6), the activation energies E_{R_d} , $E_{V_{\text{cmax}}}$ and E_{T_p} were estimated at $21634.8 \pm 4085.5 \text{ J mol}^{-1}$, $63042.7 \pm 1562.2 \text{ J mol}^{-1}$ and $34417.8 \pm 5297.7 \text{ J mol}^{-1}$, respectively. By fitting J_{max} - T_L to Eqn. (4.7), the values of $E_{J_{\text{max}}}$, $D_{J_{\text{max}}}$ and $S_{J_{\text{max}}}$ were estimated at $67292.1 \pm 35985.5 \text{ J mol}^{-1}$, $114701.0 \pm 28709.6 \text{ J mol}^{-1}$ and $375.6 \pm 82.3 \text{ J K}^{-1} \text{ mol}^{-1}$, respectively. With the estimated parameters, the model described well the response of A to changing I_{inc} and C_i at different T_L ($r^2=0.94$ and $rRMSE=24.1\%$).

4.3.1.3 Model validation

The measurements in the TN-trial were conducted on leaves with SLN ranging from 0.63 g N m^{-2} to 1.44 g N m^{-2} . During the measurement, the T_L ranged from 21 °C to 33 °C, and VPD ranged from 0.61 kPa to 2.61 kPa.

The parameterized model was validated against the data obtained in the TN-trial. The measured A was overestimated with either the κ_{2LL} derived in the N-trial ($\kappa_{2LL} = 0.21 \text{ mol mol}^{-1}$) or in the T-trial ($\kappa_{2LL} = 0.37 \text{ mol mol}^{-1}$) (Figure 4.6a, b). The $rRMSE$ reduced significantly with decreasing value of κ_{2LL} until $0.13 \text{ mol mol}^{-1}$ (Figure 4.6c). Assuming $\kappa_{2LL} = 0.13 \text{ mol mol}^{-1}$ for the TN-trial, the r^2 and $rRMSE$ were 0.94 and 26%, respectively; the error of model prediction distributed evenly across measured SLN and T_L (see Supplementary Material Figure S4.4).

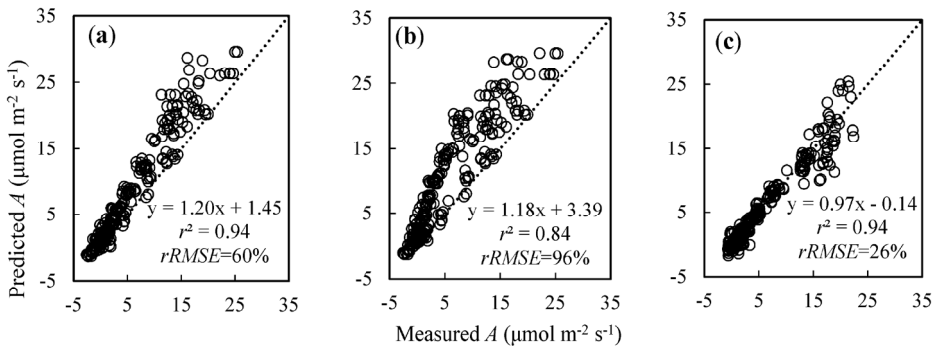


Figure 4.6 Results of model validation against the data measured net photosynthesis rate (A) in the TN-trial. The dotted lines represent the 1:1 line. The predicted A values in panels a, b and c were with a value of $\kappa_{2LL} = 0.21 \text{ mol mol}^{-1}$ (derived from the N-trial), $\kappa_{2LL} = 0.37 \text{ mol mol}^{-1}$ (derived from the T-trial) and $\kappa_{2LL} = 0.13 \text{ mol mol}^{-1}$ (obtained by minimizing prediction error of A), respectively.

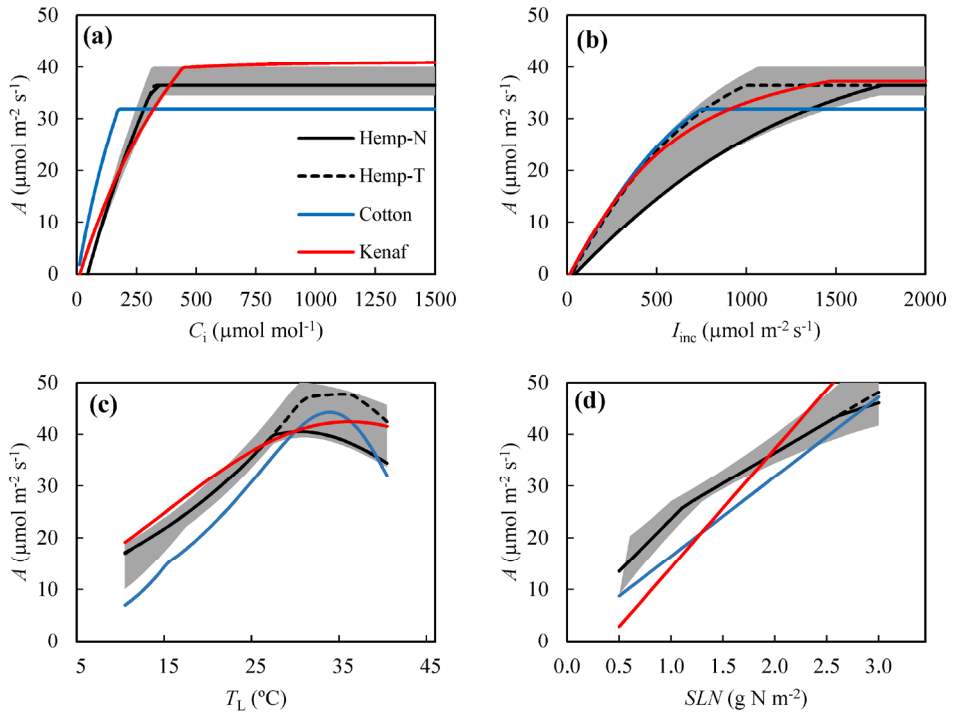


Figure 4.7 Simulation of leaf photosynthetic capacity (A) of hemp (black lines), kenaf (red line) and cotton (blue line) in response to intercellular CO_2 concentration (C_i ; panel a), incident light intensity (I_{inc} ; panel b), leaf temperature (T_L ; panel c) and leaf nitrogen (SLN ; panel d). The hemp leaf photosynthesis presented by a continuous line was simulated with $\kappa_{2LL} = 0.21 \text{ mol mol}^{-1}$ (derived from the N-trial) while the dashed line was simulated with $\kappa_{2LL} = 0.37 \text{ mol mol}^{-1}$ (derived from the T-trial). The shaded area presents 95% confidence interval of hemp leaf photosynthesis. The photosynthesis rates of cotton were simulated using the model and values described in Harley *et al.* (1992b) while for kenaf the model and values came from Archontoulis *et al.* (2011). Except when used as the independent variable, the variables were set constant as: $C_i = 400 \mu\text{mol mol}^{-1}$; $I_{\text{inc}} = 2000 \mu\text{mol m}^{-2} \text{s}^{-1}$; $SLN = 2.0 \text{ g N m}^{-2}$; $T_L = 25 \text{ }^\circ\text{C}$.

4.3.2 Leaf photosynthetic competence of hemp in comparison with kenaf and cotton

Comparison of leaf photosynthetic competence of hemp with kenaf and cotton is presented in Figure 4.7. The values of the main parameters are summarised in Table 4.1. In this illustration, we considered the uncertainty in estimated values of parameters (i.e., R_d , J_{max} , V_{cmax} and T_p) for their linear relationships with SLN and non-linear relationships with T_L (presented as the shaded area). The modelled values of A for hemp are shown using lower and upper bounds of 95% confidence interval of these parameter values. Given that there was a large variation in the value of κ_{2LL} among different growth environments and each estimate of κ_{2LL} had a very small standard error (Table 4.1), the lower bounds were combined with κ_{2LL} of $0.21 \text{ mol mol}^{-1}$

Table 4.1 List of model parameters (\pm standard errors if available) of hemp, cotton and kenaf.

Parameter	Unit	Hemp	Cotton ^b	Kenaf ^d	
<i>Respiration</i>					
R_d - SLN	Slope	$\mu\text{mol s}^{-1} (\text{g N})^{-1}$	0.85 ± 0.15	0 ^c	0.80
	Intercept	$\mu\text{mol m}^{-2} \text{s}^{-1}$	0.03 ± 0.19	0.82 ^c	-0.37
E_{Rd}		J mol^{-1}	21634 ± 4085	84450	83440
<i>e⁻ transport parameters</i>					
J_{max} - SLN	Slope	$\mu\text{mol s}^{-1} (\text{g N})^{-1}$	132.9 ± 14.6	98.1	122.1
	Intercept	$\mu\text{mol m}^{-2} \text{s}^{-1}$	54.4 ± 18.8	-4.6	-47.6
$E_{J\text{max}}$		J mol^{-1}	67292 ± 35986	79500	28149
$D_{J\text{max}}$		J mol^{-1}	114701 ± 28710	201000	474614 ^f
$S_{J\text{max}}$		$\text{J K}^{-1} \text{mol}^{-1}$	375 ± 82	650	1482 ^f
κ_{2LL}		mol mol^{-1}	0.21 ± 0.004 (N-trial)	0.24 ^a	0.28
θ		-	0.70 ^a	0.83 ^a	0.63
<i>Rubisco parameters</i>					
V_{cmax} - SLN	Slope	$\mu\text{mol s}^{-1} (\text{g N})^{-1}$	76.2 ± 9.8	60.0 ^e	66.7 ^e
	Intercept	$\mu\text{mol m}^{-2} \text{s}^{-1}$	12.6 ± 12.5	-9.6 ^e	26.0 ^e
$E_{v\text{cmax}}$		J mol^{-1}	63024 ± 1562	116300	61812
<i>TPU parameters</i>					
T_p - SLN	Slope	$\mu\text{mol s}^{-1} (\text{g N})^{-1}$	4.2 ± 0.4	5.1	NA
	Intercept	$\mu\text{mol m}^{-2} \text{s}^{-1}$	4.3 ± 0.6	0.6 ^e	
E_{Tp}		J mol^{-1}	34417 ± 5298	53100	NA
<i>g_m parameters</i>					
δ		-	2.12 ± 0.09	NA	NA
g_{m0}		$\text{mol m}^{-2} \text{s}^{-1}$	0 ^a	NA	NA

NA: not estimated or not available

^a: parameter values are fixed beforehand.

^b: parameter values are derived from Harley *et al.* (1992b) with plants grown at an ambient $[\text{CO}_2]$ of 35 Pa; the parameter values of temperature response are converted to fit Eqn. (4.6) or Eqn. (4.7) in the text; the value of θ is converted to fit Eqn. (4.4) in the text.

^c: R_d was held constant at different nitrogen levels and equal to $0.82 \mu\text{mol m}^{-2} \text{s}^{-1}$.

^d: parameter values are derived from Archontoulis *et al.* (2011). In his paper, the value of E_{Rd} is a function of SLN . The value presented here is derived at $SLN = 2.0 \text{ g N m}^{-2}$. Slopes of R_d - SLN are calculated from simulation of R_d against SLN using original model.

^e: note that the absolute value of these parameters may be lower than the presented one when g_m is considered;

^f: the optimum temperature J_{max} was not observed, so its J_{max} was fitted to the Arrhenius Eqn. (4.6), thereby $D_{J\text{max}}$ and $S_{J\text{max}}$ were not estimated. The presented value gave equal temperature sensitivities but it was rejected by the authors due to a high standard error of the estimate.

(derived from N-trial) while the upper bounds were combined with κ_{2LL} of $0.37 \text{ mol mol}^{-1}$ (derived from T-trial).

For the response to C_i , these three crops had similar A at the current atmosphere CO_2 level (Figure 4.7a). In case of a further increase in CO_2 level in the future, kenaf may become more productive than hemp. For both crops, there was a large uncertainty in the responses of A to I_{inc} and T_L (Figure 4.7b, c) because these curves are affected by the value of κ_{2LL} . When using κ_{2LL}

of $0.37 \text{ mol mol}^{-1}$, a value close to that of healthy C_3 leaves (presented as dashed black lines), the calculated A for hemp was similar to that for kenaf across different I_{inc} levels, but was slightly higher than for cotton at intermediate I_{inc} . Reducing κ_{2LL} to $0.21 \text{ mol mol}^{-1}$ (presented as solid black lines) resulted in a reduction of A under light limiting condition and in a reduction of the optimal temperature. For the response to leaf nitrogen, the leaf photosynthetic competence of hemp, including its 95% confidence interval, was consistently higher than that of cotton and kenaf at $SLN < 2.0 \text{ g N m}^{-2}$, which is close to the maximum SLN measured in this study (Figure 4.7d).

4.4 Discussion

Hemp is considered an ideal annual crop for the bio-economy as it has the potential to produce a high multipurpose biomass yield while requiring little inputs (Chapters 2, 3; Finnan & Burke, 2013). However, very limited information is available on the physiological basis of hemp resource use efficiency. With the aim of understanding the response of leaf photosynthesis capacity of hemp to leaf nitrogen status and environmental factors and setting the basis for a hemp growth model, this study presents the results of extensive hemp leaf photosynthetic measurements and parameterization of a widely-used photosynthesis model.

4.4.1 Parameterization of the leaf photosynthesis model for hemp

Theoretically, the method to estimate R_d (day respiration) works best for the NPR (non-photorespiratory) condition (Yin *et al.*, 2011). The estimated R_d in this study did not differ significantly between PR (photorespiratory) and NPR conditions ($P > 0.05$). This result suggests that estimating R_d from Eqn. (4.9) is practicable even under PR condition (Yin *et al.*, 2009, 2011). Note that assessing the true R_d is somewhat difficult and the estimated R_d differs according to methodologies. A comparison of the method used in this study with other ones to estimate R_d is discussed in Yin *et al.* (2011). The estimated R_d values were on average 20% lower than R_{dk} values (respiration in the dark) in line with other reports (Yin *et al.*, 2011, 2009, Brooks & Farquhar, 1985). An *in vivo* metabolic study (Tcherkez *et al.*, 2005) indicated that the main inhibited steps were the entrance of hexose molecules into the glycolytic pathway and the Krebs cycle. Nevertheless, detailed mechanism of this difference still needs further research (Tcherkez *et al.*, 2012).

Both R_d and R_{dk} increased monotonically with an increase in SLN and T_L (Figures 4.2, 4.3, 4.5) within the tested ranges. The result agrees with those of Yin *et al.* (2011, 2009), but does

not support those in Harley *et al.* (1992b) for cotton, where a constant R_a was considered at changing nitrogen and temperature. For hemp, Chandra *et al.* (2011a, 2008) reported that R_{dk} levelled off or slightly decreased with an increase in temperature from 30 °C to 40 °C. This was not confirmed in the present study, although the highest R_{dk} measured at 25 °C in our study is comparable with the value observed in Chandra *et al.* (2011a, 2008). The reason for such discrepancy of R_{dk} in response to T_L is not clear. It is probably due to an artefact of different protocols or due to changes of thermal sensitivity of respiration at different growth environments and plant status (e.g., drought, nutrient availability and sugar concentration) (Katja *et al.*, 2012; Atkin *et al.*, 2005). If an increase of respiration with increasing SLN and T_L is proven for hemp, it could counteract, at least partly, the positive effects of SLN and T_L on A (net photosynthesis rate) when considering at daily basis.

Based on the findings that the maximum quantum yields (the initial slopes of the response of CO_2 uptake to photon absorption) were conserved across age classes within species or across the mature photosynthetic organs of different species (Long *et al.*, 1993), κ_{2LL} was often fixed as a constant across different growth environments and species in studies of plant photosynthesis (Medlyn *et al.*, 2002; Harley *et al.*, 1992b). However, very different values have been assumed in different studies without clear explanation, ranging from 0.18 mol mol⁻¹ until 0.39 mol mol⁻¹ (Yamori *et al.*, 2010; Medlyn *et al.*, 2002; Wullschlegel, 1993; Harley *et al.*, 1992b). The estimated κ_{2LL} in the present study did not change with SLN and with T_L but it was not constant across growth environments (0.21 mol mol⁻¹ for the N-trial; 0.37 mol mol⁻¹ for the T-trial and 0.13 mol mol⁻¹ resulted in the best prediction of measurements in the TN-trial), in line with Archontoulis *et al.* (2011) who observed that cardoon (*Cynara cardunculus*) had a higher κ_{2LL} in the cold season than in the warm season. The reason for the variation in κ_{2LL} in different environments is still not fully understood. We speculate that the low κ_{2LL} in the N-trial and the TN-trial in comparison with the κ_{2LL} in the T-trial is a consequence of photoinhibition that occurs naturally in field plants grown in West-Europe when the temperature is low and the sky is clear (Long *et al.*, 1994). The plants of the N-trial and the TN-trial were grown outdoors, with fluctuations in temperature and irradiance, particularly the plants in the TN-trial experienced a sudden drop of temperature five days before measuring (Supplementary Material Figure S4.1). These conditions could have resulted in severe photoinhibition (Long *et al.*, 1983; Powles *et al.*, 1983) causing a reduction in Φ_{2LL} (PSII quantum use efficiency under strictly limiting light) and an increase in the fraction of alternative electronic transport (i.e., $\frac{f_{pseudo(b)}}{1-f_{cyc}}$;

cf. Eqn. 4.9a) (Murata *et al.*, 2012; Curwiel & van Rensen, 1993), hence a low κ_{2LL} . In contrast, the plants of the T-trial were grown in the greenhouse where both light intensity and temperature were controlled at a condition free of photoinhibition. Thus, the value of κ_{2LL} (0.37 mol mol⁻¹) was high and close to the range for healthy C₃ leaves (between 0.32 mol mol⁻¹ and 0.35 mol mol⁻¹) (Hikosaka *et al.*, 2016 and their references). Moreover, the variation in κ_{2LL} could be partly attributed to the change in β (leaf absorbance; cf. Eqn. 4.9a) as a result of environmental acclimation (Archontoulis *et al.*, 2011). A higher β in the T-trial than in the N-trial and the NT-trial is reflected by the higher *SPAD* values when considered at the same *SLN* (Supplementary Material Figure S4.5). Given that the value of κ_{2LL} varied significantly across different environments and that it affected significantly the prediction of photosynthesis when electron transport was limited (i.e., A_j) (Figure 4.7), caution is needed when modelling photosynthesis rate using a value of κ_{2LL} derived from different environments, particularly if these include both greenhouse and open field conditions. To improve modelling of crop growth in field conditions, further study should be conducted to investigate the mechanisms underlying variation in κ_{2LL} during the whole growth season.

The relationships J_{\max} -*SLN*, V_{\max} -*SLN* and T_p -*SLN* were consistent across canopy positions and growth environments whereas linear regression of these relationships resulted in negative intersections at the x -axis (Figure 4.3), in line with Akita *et al.* (2012) but different from Archontoulis *et al.* (2011) and Braune *et al.* (2009) where the intersection of linear extrapolating resulted in a minimum *SLN* required for photosynthesis (SLN_b). Given that it is not physiologically possible to have a negative SLN_b , the results in this study indicate that the relationships J_{\max} -*SLN*, V_{\max} -*SLN* and T_p -*SLN* for hemp may not be perfectly linear. Further study would be needed to elucidate the relationship between these parameters and *SLN* at *SLN* levels approaching zero.

It is well recognized that g_m is not infinite (Bernacchi *et al.*, 2002). Using both the variable J method and the modelling method, our analysis for hemp (Figure 4.4) supports that g_m varies with changing C_i and I_{inc} (Flexas *et al.*, 2012, 2007; Yin *et al.*, 2009), which is in contrast with the assumption that g_m is independent of C_i and I_{inc} (Bernacchi *et al.*, 2002). This highlights an important uncertainty in the present understanding of CO₂ diffusion processes in leaves. The g_m obtained from Eqn. (4.13) with a constant δ changed in line with A (cf. Figures 4.2, 4.4), confirming the assumption of Piel *et al.* (2002) and Ethier *et al.* (2006) that g_m is correlated with A . The value of δ (2.12) is lower than that of wheat (2.54) (Yin *et al.*, 2009) but higher than that of rice (0.45~1.57) (Gu *et al.*, 2012).

4.4.2 Does hemp have high photosynthetic competence?

The observed A_{\max} was levelled off at 25–35 °C (Figure 2d) that is comparable with the 27 °C reported in Cosentino *et al.* (2012) and the 30 °C reported in Chandra *et al.* (2011a) for hemp leaf photosynthesis. The wide range of optimal temperature for leaf photosynthesis confirms the fact that hemp has been cultivated from the tropic (Tang *et al.*, 2012) to the polar circle (Pahkala *et al.*, 2008).

The highest A_{\max} (light-saturated net photosynthesis rate) at 25 °C was measured at $31.2 \pm 1.9 \mu\text{mol m}^{-2} \text{s}^{-1}$ (Figure 4.2b). This value is higher than the highest value reported for hemp in De Meijer *et al.* (1995) and (Chandra *et al.*, 2011a, 2008), which were $19.0 \mu\text{mol m}^{-2} \text{s}^{-1}$ and $24.0 \mu\text{mol m}^{-2} \text{s}^{-1}$, respectively. The highest A_{\max} in this study is comparable with that of other C_3 bioenergy crops. Archontoulis *et al.* (2011) reported that the highest A_{\max} of kenaf, sunflower (*Helianthus annuus* L.) and cardoon ranged between $30 \mu\text{mol m}^{-2} \text{s}^{-1}$ and $35 \mu\text{mol m}^{-2} \text{s}^{-1}$ under optimum temperature.

As direct comparison of A_{\max} among crops is difficult due to the variation of experimental protocols and plant status, we constructed $A-C_i$, $A-I_{\text{inc}}$, $A-T_L$ and $A-SLN$ curves for hemp, cotton and kenaf with the same values of variables (i.e. C_i , I_{inc} , T_L and SLN) (Figure 4.7). The comparison highlighted that hemp has higher leaf photosynthesis rate than cotton and kenaf at a low nitrogen condition (i.e., $SLN < 2.0 \text{ g N m}^{-2}$). This was presumably because hemp has a relatively low SLN_b . Analysis of newly senesced hemp leaves resulted in a nitrogen content of $0.25 \pm 0.01 \text{ g N m}^{-2}$. This value is at the low range of SLN_b among C_3 crops and weeds (average value = $0.31 \pm 0.03 \text{ g N m}^{-2}$) and is considerably lower than the estimation for kenaf ($0.39 \pm 0.13 \text{ g N m}^{-2}$) (Archontoulis *et al.*, 2011).

The high photosynthesis rate of hemp at low nitrogen condition is in line with its observed high productivity at low nitrogen input (Finnan & Burke, 2013, Struik *et al.*, 2000) and puts hemp ahead of cotton and kenaf from a perspective of bio-economy. However, our model approach has limitations. Firstly, the comparison was based on parameters derived from different studies conducted in different environments. Secondly, even though the FvCB model is biochemically based and the relationships $J_{\max}\text{-}SLN$, $V_{\text{cmax}}\text{-}SLN$ and $T_p\text{-}SLN$ were consistent in this study across canopy positions and growth environments (Figure 4.3), increasing evidences show that the model parameters may change when plant acclimates to growing environments. For example, Harley *et al.*, (1992b) reported that the slope of $V_{\text{cmax}}\text{-}SLN$ decreased with an increase in CO_2 concentration in the growth environment. The present study

also indicated that the value of κ_{2LL} may differ among growth environments. Thirdly, variation of photosynthetic competence among cultivars has been reported for hemp (Chandra *et al.*, 2011b). As only one cultivar was studied, it is not clear if the advantage of photosynthetic competence of hemp is persistent across cultivars. Therefore, to consolidate the potential of hemp as a bio-economic sustainable crop, further study is needed to compare hemp leaf photosynthetic competence with those of cotton, kenaf and other bioenergy crops in the same growing environment with multiple cultivars.

Acknowledgements

The research leading to these results has received funding from the European Union's Seventh Framework Programme for research, technological development and demonstration under grant agreement n° 311849.

References

- Akita, R., Kamiyama, C. and Hikosaka, K. (2012) Polygonum sachalinense alters the balance between capacities of regeneration and carboxylation of ribulose-1,5-bisphosphate in response to growth CO₂ increment but not the nitrogen allocation within the photosynthetic apparatus. *Physiologia Plantarum*, **146**, 404–412.
- Alexopoulou, E., Li, D., Papatheohari, Y. *et al.* (2015) How kenaf (*Hibiscus cannabinus* L.) can achieve high yields in Europe and China. *Industrial Crops and Products*, **68**, 131–140.
- Allegret, S. (2013) The history of hemp. In: *Hemp: industrial production and uses*. (eds Allegret, S., Bouloc, P. and Arnaud, L.), pp. 4–26. CPi Group Ltd, Croydon, UK.
- Amaducci, S., Errani, M. and Venturi, G. (2002) Response of hemp to plant population and nitrogen fertilisation. *Italian Journal of Agronomy*, **6**, 103–111.
- Amaducci, S., Scordia, D., Liu F. *et al.* (2015) Key cultivation techniques for hemp in Europe and China. *Industrial Crops and Products*, **68**, 2–16.
- Archontoulis, S.V., Yin, X., Vos, J. *et al.* (2011) Leaf photosynthesis and respiration of three bioenergy crops in relation to temperature and leaf nitrogen: how conserved are biochemical model parameters among crop species? *Journal of Experimental Botany*, **63**, 895–911.
- Atkin, O.K., Bruhn, D., Hurry, V.M. *et al.* (2005) The hot and the cold: unravelling the variable response of plant respiration to temperature. *Functional Plant Biology*, **32**, 87–105.
- Barth, M. and Carus, M. (2015) *Carbon footprint and sustainability of different natural fibres for biocomposites and insulation material*, Hürth, Germany, nova-Institute. Available at (2017, November 29): <http://bio-based.eu/ecology/>.
- Bellasio, C., Beerling, D.J. and Griffiths, H. (2015) An Excel tool for deriving key photosynthetic parameters from combined gas exchange and chlorophyll fluorescence: theory and practice. *Plant, Cell & Environment*, **69**, 80–97.

- Bernacchi, C.J., Portis, A.R., Nakano, H. *et al.* (2002) Temperature response of mesophyll conductance. Implications for the determination of Rubisco enzyme kinetics and for limitations to photosynthesis in vivo. *Plant Physiology*, **130**, 1992–1998.
- Bertoli, A., Tozzi, S., Pistelli, L. *et al.* (2010) Fibre hemp inflorescences: From crop-residues to essential oil production. *Industrial Crops and Products*, **32**, 329–337.
- Bouloc, P. and Van der Werf, H.M.G. (2013) The role of hemp in sustainable development. In: *Hemp: industrial production and uses* (eds Bouloc, P., Allegret, S. and Arnaud, L.), pp. 278–289. CPI Group Ltd, Croydon, UK.
- Bouman, B.M., Feng, L., Tuong, T.P. *et al.* (2007) Exploring options to grow rice using less water in northern China using a modelling approach: II. Quantifying yield, water balance components, and water productivity. *Agricultural Water Management*, **88**, 23–33.
- Braune, H., Müller, J. and Diepenbrock, W. (2009) Integrating effects of leaf nitrogen, age, rank, and growth temperature into the photosynthesis-stomatal conductance model LEAFC3-N parameterised for barley (*Hordeum vulgare* L.). *Ecological Modelling*, **220**, 1599–1612.
- Brooks, A. and Farquhar, G.D. (1985) Effect of temperature on the CO₂/O₂ specificity of ribulose-1,5-bisphosphate carboxylase/oxygenase and the rate of respiration in the light. *Planta*, **165**, 397–406.
- Busch, F.A. and Sage, R.F. (2016) The sensitivity of photosynthesis to O₂ and CO₂ concentration identifies strong Rubisco control above the thermal optimum. *New Phytologist*, **213**, 1036–1051.
- Carus, M., Karst, S., Kauffmann, A. *et al.* (2013) *The European Hemp Industry: Cultivation, processing and applications for fibres, shivs and seeds*. European Industrial Hemp Association (EIHA), Hürth, Germany. Available at (2017, November 29): <http://eiha.org/media/2014/10/13-06-European-Hemp-Industry.pdf>
- Carus, M. and Sarmento, L. (2016) *The European Hemp Industry: Cultivation, processing and applications for fibres, shivs and seeds*. European Industrial Hemp Association (EIHA), Hürth, Germany. Available at (2017, November 29): <http://eiha.org/media/2016/05/16-05-17-European-Hemp-Industry-2013.pdf>
- Chandra, S., Lata, H., Khan, I.A. *et al.* (2008) Photosynthetic response of *Cannabis sativa* L. to variations in photosynthetic photon flux densities, temperature and CO₂ conditions. *Physiology and Molecular Biology of Plants*, **14**, 299–306.
- Chandra, S., Lata, H., Khan, I.A. *et al.* (2011a) Temperature response of photosynthesis in different drug and fiber varieties of *Cannabis sativa* L. *Physiology and Molecular Biology of Plants*, **17**, 297–303.
- Chandra, S., Lata, H., Khan, I.A. *et al.* (2011b) Photosynthetic response of *Cannabis sativa* L., an important medicinal plant, to elevated levels of CO₂. *Physiology and Molecular Biology of Plants*, **17**, 291–295.
- Chandra, S., Lata, H., Mehmedic, Z. *et al.* (2015) Light dependence of photosynthesis and water vapor exchange characteristics in different high Δ⁹-THC yielding varieties of *Cannabis sativa* L. *Journal of Applied Research on Medicinal and Aromatic Plants*, **2**, 39–47.
- Cosentino, S.L., Testa, G., Scordia, D. *et al.* (2012) Sowing time and prediction of flowering of

- different hemp (*Cannabis sativa* L.) genotypes in southern Europe. *Industrial Crops and Products*, **37**, 20–33.
- Curwiel, V.B. and Van Rensen, J.J.S. (1993) Influence of photoinhibition on electron transport and photophosphorylation of isolated chloroplasts. *Physiologia Plantarum*, **89**, 97–102.
- De Meijer, E.P.M. and Van der Werf, H.M.G. (1994) Evaluation of current methods to estimate pulp yield of hemp. *Industrial Crops and Products*, **2**, 111–120.
- De Meijer, W.J.M., Van der Werf, H.M.G., Mathijssen E.W.J.M *et al.* (1995) Constraints to dry matter production in fibre hemp (*Cannabis sativa* L.). *European Journal of Agronomy*, **4**, 109–117.
- Ethier, G., Livingston, N., Harrison, D. *et al.* (2006) Low stomatal and internal conductance to CO₂ versus Rubisco deactivation as determinants of the photosynthetic decline of ageing evergreen leaves. *Plant, Cell & Environment*, **29**, 2168–2184.
- Farquhar, G.D., Von Caemmerer, S. and Berry, J.A. (1980) A biochemical model of photosynthetic CO₂ assimilation in leaves of C₃ species. *Planta*, **149**, 78–90.
- Finnan, J. and Burke, B. (2013) Nitrogen fertilization to optimize the greenhouse gas balance of hemp crops grown for biomass. *GCB Bioenergy*, **5**, 701–712.
- Flexas, J., Barbour, M.M. and Brendel, O. *et al.* (2012) Mesophyll diffusion conductance to CO₂: an unappreciated central player in photosynthesis. *Plant Science*, **193**, 70–84.
- Flexas, J., Diaz-Espejo, A., Galmes, J. *et al.* (2007) Rapid variations of mesophyll conductance in response to changes in CO₂ concentration around leaves. *Plant, Cell & Environment*, **30**, 1284–1298.
- Gu, J, Yin, X, Stomph, T.J. *et al.* (2012) Physiological basis of genetic variation in leaf photosynthesis among rice (*Oryza sativa* L.) introgression lines under drought and well-watered conditions. *Journal of Experimental Botany*, **63**, 5137–5153.
- Harley, P.C., Loreto, F., Di Marco, G. *et al.* (1992a) Theoretical considerations when estimating the mesophyll conductance to CO₂ flux by analysis of the response of photosynthesis to CO₂. *Plant Physiology*, **98**, 1429–1436.
- Harley, P.C., Thomas, R.B., Reynolds, J.F. *et al.* (1992b) Modelling photosynthesis of cotton grown in elevated CO₂. *Plant, Cell & Environment*, **15**, 271–282.
- Hikosaka, K., Noguchi, K. and Terashima, I. (2016) Modeling leaf gas exchange. In: *Canopy Photosynthesis: From Basics to Applications* (eds Hikosaka, K., Niinemets, Ü. and Anten N.P.R.), pp 61–100. Springer, London, UK.
- Jordan, N., Boody, G., Broussard, W. *et al.* (2007) Sustainable development of the agricultural bio-economy. *Science*, **316**, 1570–1571.
- Katja, H., Irina, B., Hiie, I. *et al.* (2012) Temperature responses of dark respiration in relation to leaf sugar concentration. *Physiologia Plantarum*, **144**, 320–334.
- Kreuger, E., Prade, T., Escobar, F. *et al.* (2011) Anaerobic digestion of industrial hemp — Effect of harvest time on methane energy yield per hectare. *Biomass and Bioenergy*, **35**, 893–900.
- Lips, S.J.J. and van Dam, J.E.G. (2013) Kenaf fibre crop for bioeconomic industrial

- development. In: *Kenaf: a multi-purpose crop for several industrial applications*. (eds Monti, A. and Alexopoulou, E.), pp. 105–143. Springer, London, UK.
- Long, S., East, T. and Baker, N. (1983) Chilling damage to photosynthesis in young *Zea mays* L. Effects of light and temperature variation on photosynthetic CO₂ assimilation. *Journal of Experimental Botany*, **34**, 177–188.
- Long, S., Humphries, S. and Falkowski, P.G. (1994) Photoinhibition of photosynthesis in nature. *Annual review of plant biology*, **45**, 633–662.
- Long, S., Postl, W.F. and Bolhár-Nordenkampf, H.R. (1993) Quantum yields for uptake of carbon dioxide in C₃ vascular plants of contrasting habitats and taxonomic groupings. *Planta*, **189**, 226–234.
- Marija, M., Māra, V. and Veneranda, S. (2011) Changes of photosynthesis-related parameters and productivity of *Cannabis sativa* under different nitrogen supply. *Environmental and Experimental Biology*, **9**, 61–69.
- Mccormick, K. and Kautto, N. (2013) The bioeconomy in Europe: An overview. *Sustainability*, **5**, 2589–2608.
- Medlyn, B.E., Dreyer, E., Ellsworth, D. *et al.* (2002) Temperature response of parameters of a biochemically based model of photosynthesis. II. A review of experimental data. *Plant, Cell & Environment*, **25**, 1167–1179.
- Murata, N., Allakhverdiev, S.I. and Nishiyama, Y. (2012) The mechanism of photoinhibition in vivo: Re-evaluation of the roles of catalase, α -tocopherol, non-photochemical quenching, and electron transport. *Biochimica et Biophysica Acta (BBA) - Bioenergetics*, **1817**, 1127–1133.
- Ögren, E. and Evans, J. (1993) Photosynthetic light-response curves. *Planta*, **189**, 182–190.
- Oomah, B.D., Busson, M., Godfrey, D.V. *et al.* (2002) Characteristics of hemp (*Cannabis sativa* L.) seed oil. *Food Chemistry*, **76**, 33–43.
- Patanè, C. and Cosentino, S.L. (2013) Yield, water use and radiation use efficiencies of kenaf (*Hibiscus cannabinus* L.) under reduced water and nitrogen soil availability in a semi-arid Mediterranean area. *European Journal of Agronomy*, **46**, 53–62.
- Piel, C., Frak, E., Le Roux, X. *et al.* (2002) Effect of local irradiance on CO₂ transfer conductance of mesophyll in walnut. *Journal of Experimental Botany*, **53**, 2423–2430.
- Powles, S.B., Berry, J.A. and Bjorkman, O. (1983) Interaction between light and chilling temperature on the inhibition of photosynthesis in chilling-sensitive plants. *Plant, Cell & Environment*, **6**, 117–123.
- Prade, T., Svensson, S-E, Andersson, A. *et al.* (2011) Biomass and energy yield of industrial hemp grown for biogas and solid fuel. *Biomass and Bioenergy*, **35**, 3040–3049.
- Rice, B. (2008) Hemp as a feedstock for biomass-to-energy conversion. *Journal of Industrial Hemp*, **13**, 145–156.
- Sage, R.F. and Kubien, D.S. (2007) The temperature response of C₃ and C₄ photosynthesis. *Plant, Cell & Environment*, **30**, 1086–1106.
- Salentijn, E.M.J., Zhang, Q., Amaducci, S. *et al.* (2015) New developments in fiber hemp

- (*Cannabis sativa* L.) breeding. *Industrial Crops and Products*, **68**, 32–41.
- Sharkey, T.D., Bernacchi, C.J., Farquhar, G.D. *et al.* (2007) Fitting photosynthetic carbon dioxide response curves for C₃ leaves. *Plant, Cell & Environment*, **30**, 1035–1040.
- Sinclair, T.R. and Horie, T. (1989) Leaf nitrogen, photosynthesis, and crop radiation use efficiency: a review. *Crop Science*, **29**, 90–98.
- Struik, P.C., Amaducci, S., Bullard, M.J. *et al.* (2000) Agronomy of fibre hemp (*Cannabis sativa* L.) in Europe. *Industrial Crops and Products*, **11**, 107–118.
- Tang, Z., Hu, X., Sun, T. *et al.* (2012) Adaptability of different hemp varieties (lines) in Xishuangbanna prefecture. *Journal of southern agriculture*, **43**, 160–163. (Chinese with English abstract)
- Tcherkez, G., Boex-Fontvieille, E., Mahé, A. *et al.* (2012) Respiratory carbon fluxes in leaves. *Current Opinion in Plant Biology*, **15**, 308–314.
- Tcherkez, G., Cornic, G., Bligny, R. *et al.* (2005) In vivo respiratory metabolism of illuminated leaves. *Plant Physiology*, **138**, 1596–1606.
- Von Caemmerer, S., Farquhar, G. and Berry, J. (2009) Biochemical model of C₃ photosynthesis. In: *Photosynthesis in silico* (eds Laisk, A., Nedbal, L. and Govindjee), pp 209–230, Springer, London, UK.
- Wirtshafter, D.E. (2004) Ten years of a modern hemp industry. *Journal of Industrial Hemp*, **9**, 9–14.
- Wullschleger, S.D. (1993) Biochemical Limitations to Carbon Assimilation in C₃ Plants: A Retrospective Analysis of the A/C_i Curves from 109 Species. *Journal of Experimental Botany*, **44**, 907–920.
- Yamori, W., Evans, J.R. and Von Caemmerer, S. (2010) Effects of growth and measurement light intensities on temperature dependence of CO₂ assimilation rate in tobacco leaves. *Plant, Cell & Environment*, **33**, 332–343.
- Yin, X., Harbinson, J. and Struik, P.C. (2006) Mathematical review of literature to assess alternative electron transports and interphotosystem excitation partitioning of steady-state C-3 photosynthesis under limiting light. *Plant Cell & Environment*, **29**, 1771–1782.
- Yin, X., Struik, P.C., Romero, P. *et al.* (2009) Using combined measurements of gas exchange and chlorophyll fluorescence to estimate parameters of a biochemical C₃ photosynthesis model: a critical appraisal and a new integrated approach applied to leaves in a wheat (*Triticum aestivum* L.) canopy. *Plant, Cell & Environment*, **32**, 448–464.
- Yin, X. and Struik, P.C. (2009) C₃ and C₄ photosynthesis models: An overview from the perspective of crop modelling. *NJAS-Wageningen Journal of Life Sciences*, **57**, 27–38.
- Yin, X. and Van Laar, H.H. (2005) *Crop systems dynamics : an ecophysiological simulation model for genotype-by-environment interactions*, Wageningen Academic, Wageningen, the Netherlands.
- Yin, X., Sun, Z.P., Struik, P.C. *et al.* (2011) Evaluating a new method to estimate the rate of leaf respiration in the light by analysis of combined gas exchange and chlorophyll fluorescence measurements. *Journal of Experimental Botany*, **62**, 3489–3499.

Supplementary Materials in Chapter 4

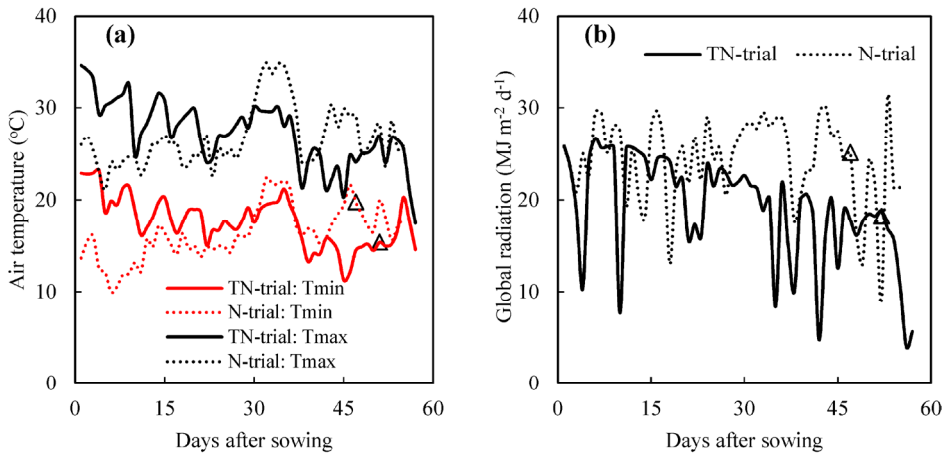


Figure S4.1 The daily temperature and global radiation during the period from sowing to the end of the experiment for plants grown in the open field (i.e., TN-trial in 2013 and N-trial in 2014).

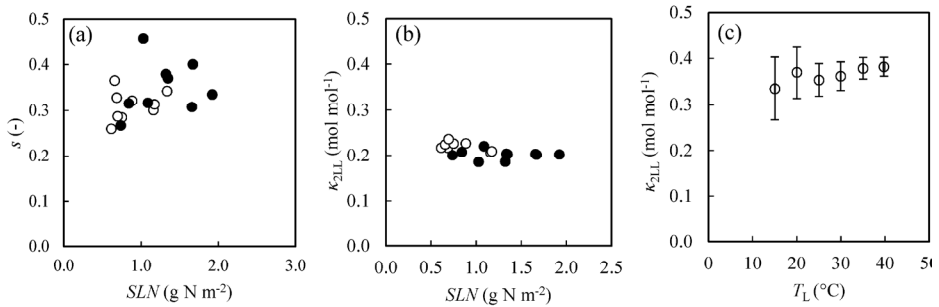


Figure S4.2 Dependence of lumped parameter (s) in Eqn. (4.9) on leaf nitrogen (SLN) and dependence of the efficiency of converting incident irradiance into linear electron transport under limiting light (κ_{2LL}) on SLN and leaf temperature (T_L).

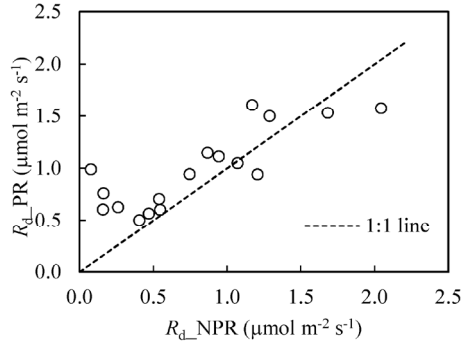


Figure S4.3 The estimated day respiration under photorespiratory condition, i.e. at 21% O_2 , (R_{d_PR}) against that under non-photorespiratory condition, i.e. at 2% O_2 (R_{d_NPR}).

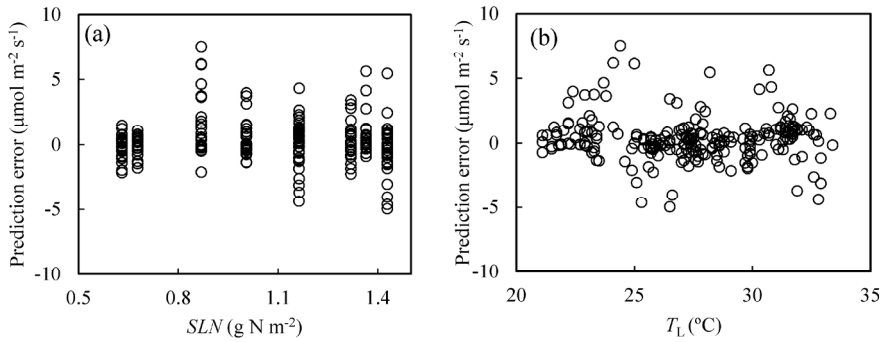


Figure S4.4 The error of model validation against leaf nitrogen (SLN , panel a) and temperature (T_L , panel b).

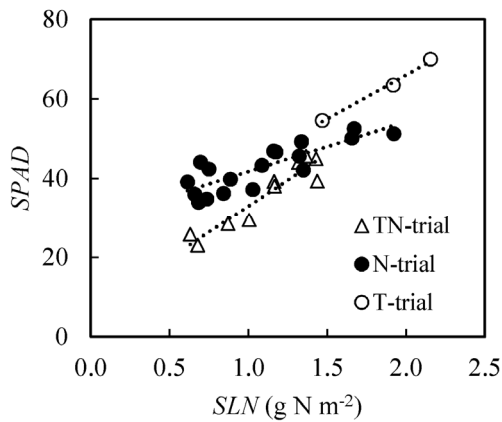


Figure S4.5 The effect of growth environment on the relationship between $SPAD$ values and leaf nitrogen (SLN).

Chapter 5

Water- and nitrogen-use efficiencies of hemp (*Cannabis sativa* L.) based on whole-canopy measurements and modelling

K. Tang^{a,b}, A. Fracasso^b, P.C. Struik^a, X. Yin^a, S. Amaducci^b

^a *Centre for Crop Systems Analysis, Department of Plant Sciences, Wageningen University & Research, Droevendaalsesteeg 1, Wageningen, The Netherlands*

^b *Department of Sustainable Crop Production, Università Cattolica del Sacro Cuore, via Emilia Parmense, 84, Piacenza, Italy*

Abstract

Interest in hemp (*Cannabis sativa* L.) as a bio-economical crop is growing worldwide because hemp produces a high and valuable biomass while requiring low inputs. To understand the physiological basis of hemp's resource-use efficiency, canopy gas exchange was assessed using a chamber technique on canopies exposed to a range of nitrogen (N) and water levels. Since canopy transpiration and carbon assimilation were very sensitive to variations in microclimate among canopy chambers, observations were adjusted for microclimatic differences using a physiological canopy model, with leaf-level parameters estimated for hemp from our previous study. Canopy water-use efficiency (WUE_c), defined as the ratio of gross canopy photosynthesis to canopy transpiration, ranged from 4.0 mmol CO₂ (mol H₂O)⁻¹ to 7.5 mmol CO₂ (mol H₂O)⁻¹. Canopy nitrogen-use efficiency (NUE_c), the ratio of the gross canopy photosynthesis to canopy leaf-N content, ranged from 0.3 mol CO₂ d⁻¹ (g N)⁻¹ to 0.7 mol CO₂ d⁻¹ (g N)⁻¹. The effect of N-input levels on WUE_c and NUE_c was largely determined by the N effect on canopy size or leaf area index (LAI), whereas the effect of water-input levels differed between short- and long-term stresses. The effect of short-term water stress was reflected by stomatal regulation. The long-term stress increased leaf senescence, decreased LAI but retained total canopy N content; however, the increased average leaf-N could not compensate for the lost LAI , leading to a decreased NUE_c . Although hemp is known as a resource-use efficient crop, its final biomass yield and nitrogen use efficiency may be restricted by water limitation during growth. Our results also suggest that crop models should take stress-induced senescence into account in addition to stomatal effects if crops experience a prolonged water stress during growth.

Key words: canopy gas exchange, hemp (*Cannabis sativa* L.), nitrogen use efficiency, water use efficiency.

5.1 Introduction

The pressures of climate change, natural resource scarcity and environmental pollution have fuelled interest in bio-economically sustainable agronomy that requires effective use of scarcely available resources. A range of focused studies have indicated that hemp (*Cannabis sativa* L.) may be a suitable crop for the bio-economy (Amaducci & Gusovius, 2010). Hemp is a high-yielding multi-purpose crop that requires low inputs (Chapters 2, 3; Struik *et al.*, 2000) and has a positive impact on the environment (Barth & Carus, 2015; Bouloc & Werf, 2013). Its stems contain high-quality cellulose (De Meijer & van der Werf, 1994); high added-value compounds can be recovered from the female inflorescence and from threshing residues (Calzolari *et al.*, 2017; Bertoli *et al.*, 2010) after harvesting the seeds, that contain healthy oil (Leizer *et al.*, 2000). Although once an important crop to produce raw materials for textiles and ropes, hemp acreage declined in the last century and was displaced largely by cotton and synthetic fibres. Consequently, little attention has been paid to understanding the physiological basis of the high resource-use efficiency of hemp.

Crop water-use efficiency (WUE) and nitrogen-use efficiency (NUE) can be measured at different organizational levels from leaf to canopy. A range of focused studies provided key insights at leaf level (Cabrera-Bosquet *et al.*, 2007; Van den Boogaard *et al.*, 1995). However, canopy water-use efficiency (WUE_c , defined as the ratio of gross canopy photosynthesis to canopy transpiration) and nitrogen-use efficiency (NUE_c , the ratio of the gross canopy photosynthesis to canopy leaf-N content) reflect the actual balance between photosynthate gain and its water and nitrogen costs (Linderson *et al.*, 2012). While lack of significant correlations between leaf and canopy WUE or NUE has been reported (Tomás *et al.*, 2012), there is a need for focused quantitative studies on the scaling up of WUE and NUE from leaf to canopy.

One challenge in studying WUE_c and NUE_c is to properly assess canopy CO_2 and H_2O exchange rates under varying nitrogen and water regimes. To date, the canopy gas exchange rate is mainly assessed by micro-meteorological methods or by means of canopy-enclosure chamber systems. The micro-meteorological techniques such as the eddy covariance or Bowen ratio methods enable gas flux measurements without disturbing canopy micro-environment, and they are often applied to large homogeneous areas but are unsuitable in plot/pot-sized experiments (Jones, 2013). In contrast, the canopy chamber technique enables to determine precisely canopy gas exchange at a relatively small scale (Müller *et al.*, 2009, 2005). However, enclosing a crop canopy with a chamber might result in significant changes in micro-

environmental variables (e.g., CO₂ concentration, air temperature and vapour pressure) as a consequence of photosynthetic CO₂ uptake, the greenhouse effect and transpiration (Müller *et al.*, 2009; Takahashi *et al.*, 2008). The effect of micro-environmental changes within a canopy chamber on photosynthesis rates should be assessed when the chamber is used to analyse the responses of canopy photosynthesis to water shortage and nitrogen deficiency.

On the basis of a thorough understanding of the underlying mechanisms of leaf and canopy photosynthesis, models have been developed to quantify the response of canopy photosynthesis to varying micro-environments under different physiological conditions (Hikosaka *et al.*, 2016). Such canopy models are capable of simulating instantaneous canopy gas exchange measurements by micro-meteorological techniques (Wright *et al.*, 2013; Leuning *et al.*, 1998) and in canopy chambers (Müller *et al.*, 2005). In that context, a well-defined canopy model is a useful tool to normalize the changes in micro-environmental variables within a canopy chamber and to quantitatively assess the responses of canopy photosynthesis to nitrogen and water deficiencies.

The objective of this study was to experimentally assess hemp WUE_c and NUE_c in relation to nitrogen and water availabilities. To that end, we parameterized a canopy photosynthesis model (Yin & Struik, 2017; Yin & van Laar, 2005), with leaf-level parameters estimated from our previous study for hemp (Chapter 4). This model was used to correct gas exchange measurements within different canopy chambers and to assess the main components of hemp WUE_c and NUE_c , providing supporting information for effective use of water and nitrogen resources.

5.2 Materials and methods

5.2.1 Experimental design and data collection

Field and container experiments were carried out at the research facilities of the Università Cattolica del Sacro Cuore (45.0° N, 9.8° E, 60 m asl; Piacenza, Italy). Field experiments were carried out in 2014 and 2015 to assess light and nitrogen distribution profiles of hemp canopies in response to nitrogen deficiency. A container experiment was carried out in 2014 to assess instantaneous and daily canopy gas exchange of hemp in response to nitrogen and water limitations. Between May and October (during the hemp season), the study site had monthly average temperatures ranging from 17.7 °C to 26.9 °C; the monthly sum of precipitation ranged from 13.5 mm to 87 mm.

5.2.1.1 Field experiments to assess light and nitrogen distribution profiles of hemp canopies

The experimental fields had silty clay loam soil (the clay:silt:sand ratio was 39:46:15) that contained 0.14% of total nitrogen and 2.2–2.6% of organic matter. Seeds of hemp *cv.* Futura 75 (obtained from Fédération National des Producteurs de Chanvre, Le Mans, France) were drilled, with a target density of 120 plants m^{-2} , at 3–4 cm depth using an experimental plot machine on 7 April in 2014 and on 16 April in 2015. Single plot size was 60 m^2 . Nutrients other than nitrogen were assumed to be abundantly available in the experimental fields based on past experience. During the growth season, plants were irrigated when signs of water deficiency emerged. A total of 60 mm and 155 mm water was provided with a travelling sprinkler in 2014 and 2015, respectively.

Nitrogen fertilization effect was investigated in a randomized complete block design with four replicates. In both years, four levels of calcium nitrate were top-dressed after seedling emergence as: N0 (no fertilizer applied); N30 (30 kg N ha^{-1}); N60 (60 kg N ha^{-1}), and N120 (120 kg N ha^{-1}). In the field experiment in 2014, the plants suffered from severe weed competition. Therefore, only the data collected in the plots of N60 that were not affected by weeds were reported in this chapter.

Two destructive samplings were conducted in each plot at the onset of the linear growth phase and at full flowering. At each sampling, light interception by the canopy (the ratio of light intensity at depth i to that at the top of canopy: I_i/I_0) was first assessed at 90%, 75%, 50% and 0% of canopy height using a ceptometer (AccuPAR LP-80, Decagon Devices, Inc., Pullman, Washington, USA). Subsequently, all plants in an area of 1 m^2 were cut at ground surface to assess leaf area index (*LAI*) and specific leaf nitrogen (*SLN*) on four layers according to canopy height: 0–50 %, 50–75 %, 75–90 %, and 90–100 %. The *LAI* was calculated as the product of leaf weight and specific leaf area (*SLA*) that was obtained by measuring the weight and area of all leaves of two representative plants. Leaf nitrogen concentration (N_{leaf}) was assessed using a CN analyser (Vario Max CN Analyzer; Elementar Americas, Inc., Hanau, Germany). The *SLN* was calculated as N_{leaf} divided by *SLA*.

5.2.1.2 Container experiment to assess canopy gas exchange rate

Seeds of *cv.* Futura 75 were sown on 9 May 2014 in 18 containers (length \times width \times height: 40 \times 40 \times 30 cm^3). Each container was filled with 23 kg of soil (dry weight) that contained 0.22% total nitrogen and had a clay:silt:sand ratio of 30:43:27. Seeds were sown in excess in two rows

and seedlings were hand-thinned to 18 uniform plants per container (*ca.* 113 plants m⁻²). Other nutrients than nitrogen were assumed to be abundantly available based on past experience in the field from which the soil was collected. During the growth period, sufficient water was supplied daily to each container. The containers were placed outdoor and positioned tightly in a 1.2 × 2.4 m² block. To avoid any border effect, the block perimeter was surrounded with a green shading net (transmitting 3% of the light); the height of the shading net was adjusted daily to account for the increment in plant height. The containers were rearranged weekly.

Three levels of dissolved urea fertilizer were applied to the soil after seedling emergence as: N1, no fertilizer applied; N2, 1.0 g N per container; N3, 2.0 g N per container, equivalent to *ca.* 0, 60, and 120 kg N (ha ground)⁻¹, respectively. There were six containers per N level, subject to different levels of water supply during measurement (see later).

Whole canopy gas exchange was assessed twice during the course of the experiment by enclosing the canopy of each container in a flow-through gas exchange system. The first cycle of measurements (CAN1 hereafter) aimed to assess the response of diurnal canopy gas exchange to nitrogen and short-term water shortage. Canopy gas exchange in this cycle was assessed on 12 containers for three days, four containers per N treatment. Two of the containers per N treatment were supplied with sufficient water (measured as the amount of transpired water in the previous day) during the measurement while the water supply for the other two was halved. This cycle of measurements started 49 days after sowing when the 6th–8th pair of leaves appeared, the same leaf stages at which gas exchange at leaf level was assessed (Chapter 4). The second cycle of canopy gas exchange assessment (CAN2 hereafter) aimed to assess the response of canopy gas exchange to prolonged water shortage. In this cycle canopy gas exchange was assessed on six containers for 13 days, two containers per N treatment. Measurement in this cycle started 79 days after sowing at the beginning of flowering. During the measurement, one container received sufficient water while the other one received half the amount. At the 8th day from the start of measurement, plants under stress showed signs of severe wilting, and were re-watered briefly to avoid their possible death before the end of the experimental period.

Configuration of the flow-through gas exchange system was described by Poni *et al.* (2014) and refined by Fracasso *et al.* (2017). It consists of 12 cylindrical canopy chambers (diameter 50 cm) that are sealed with flexible plastic polyethylene on the side wall (transmitting 87% of the light) and a plastic polymethylmethacrylate disc on the top (transmitting 93% of the light).

The air flowing through the canopy chamber (from the bottom to the top) was drawn from 3 m above ground using two centrifugal blowers (Vorticent C25/2M, Vortice, Milan, Italy). The system records instantaneous information for each chamber every 12 minutes using a CR1000 datalogger wired to an AM16/32B Multiplexer (Campbell Scientific, Logan, USA) as follows: CO₂ concentration, vapour pressure and air temperature at the entrance of the chamber ($CO_{2,in}$, VP_{in} and T_{in} , respectively) and the differences at the exit ($CO_{2,dif}$, VP_{dif} and T_{dif} , respectively; calculated as the value at exit minus that at entrance), container weight ($W_{container}$) and incident solar radiation intensity outside the chamber. The $CO_{2,in}$, $CO_{2,dif}$, VP_{in} and VP_{dif} were assessed using a CIRAS-DC dual-channel absolute CO₂/H₂O infrared gas analyser (PP-Systems, Amesbury, USA). The T_{in} and T_{dif} were assessed using PFA-Teflon insulated type-T thermocouples (Omega Engineering, Stamford, USA). The $W_{container}$ was monitored using a single cell platform scale placed under each container (ABC Bilance, Campogalliano, Italy).

In this study, the volume of each canopy chamber was 0.3 m³ (cross cutting area was 0.2 m² and height was 1.5 m). Air flux entering each chamber was regulated at $4.3 \times 10^{-3} \text{ m}^3 \text{ s}^{-1}$. Thus, a complete volume air change required *ca.* 70 s. The flow rate was maintained constant during the whole measurement period. To prevent gas exchange between soil and plant chamber, the surface of each container was sealed with a plastic polyethylene film in which little slits were cut to allow hemp plants growing through. A small hole was made on the side wall of the container to supply water and allow gas exchange between soil and open air.

At the end of the canopy gas exchange assessment of each cycle, each container was assessed for the following parameters: the biomass weight of stems (W_{stem}), green leaves ($W_{leaf,g}$), senesced leaves ($W_{leaf,s}$; if present), inflorescences (W_{inflo} ; if present) and roots (W_{root}), I_i/I_o , LAI and SLN . For the containers receiving sufficient water in CAN1 the I_i/I_o , LAI and SLN were assessed for four layers according to canopy height: 0–50 %, 50–75 %, 75–90 %, and 90–100 %, while for the remaining containers the same parameters were assessed on the entire canopy. To estimate any system error introduced by gas leakage or soil respiration, gas exchange measurements were performed for 1–2 days on each container after the plants had been cut.

5.2.2 Data analysis

5.2.2.1 Estimation of light and nitrogen extinction coefficients

PAR was assumed to attenuate through the canopy following the Beer's law, based on LAI :

$$\frac{I_i}{I_o} = e^{-k_L LAI_i} \quad (5.1)$$

where LAI_i is the LAI at depth i measured from the top; k_L is the light extinction coefficient. k_L was estimated by fitting the measured I/I_0 and LAI_i to Eqn. (5.1). To avoid any effect of measuring hour on the value of k_L , all measured I/I_0 were normalized to a value at zenith angle 0° , according to the manufacturer manual of AccuPAR LP-80.

The vertical gradient of SLN can be similarly described (Archontoulis *et al.*, 2011; Yin *et al.*, 2003):

$$SLN_i = SLN_0 e^{-k_n LAI_i} \quad (5.2)$$

where k_n is the SLN extinction coefficient, SLN_0 and SLN_i are the SLN at the top of the canopy (i.e. at $LAI_i = 0$) and at depth i , respectively. Thus, from canopy top to bottom, the cumulative nitrogen at depth i (N_i) can be solved from Eqn. (5.2) as:

$$N_i = \int_0^{LAI_i} SLN_i dLAI_i = SLN_0 (1 - e^{-k_n LAI_i}) / k_n \quad (5.3)$$

By fitting the measured data for N_i - LAI_i relationships to Eqn. (5.3), k_n and SLN_0 were estimated.

5.2.2.2 Calculation of canopy photosynthesis and transpiration rates

Data recorded from the multi-chamber gas exchange system was filtered to eliminate measurements impaired by short time fluctuations of air CO_2 concentration and vapour pressure, and system mishaps. Subsequently, the values of $CO_{2,dif}$ and VP_{dif} were corrected for potential system error due to gas leakage or soil respiration using data recorded in the chamber after the plants had been cut. Instantaneous canopy transpiration rate (E_c ; $mmol H_2O m^{-2} s^{-1}$) and net photosynthesis rate ($A_{c,net}$; $\mu mol CO_2 m^{-2} s^{-1}$) were calculated using Eqn. (5.4) and Eqn. (5.5), respectively. These formulae were based on the study of Von Caemmerer and Farquhar (1981) for leaf gas exchange measurements. Different forms of these formulae were commonly used for calculating E_c and $A_{c,net}$ in the studies of canopy gas exchange using the chamber system (Poni *et al.*, 2014; Baker *et al.*, 2009; Müller *et al.*, 2005).

$$E_c = \frac{1000 u_e VP_{dif}}{a [P - (VP_{in} + VP_{dif})]} \quad (5.4)$$

$$A_{c,net} = - \left(\frac{u_e CO_{2,dif}}{a} + 10^{-3} E_c CO_{2,out} \right) \quad (5.5)$$

where u_e ($mol s^{-1}$) is air flux entering the plant chamber; a (m^2) is the ground area of the canopy chamber; P (kPa) is the air pressure inside the plant chamber. The standard air pressure (101.3 kPa) was used as a proxy of P in the present study although a slight overpressure was maintained

inside the plant chamber (less than 10 Pa) to avoid any flux of ambient air through possible leaks. The effect of overpressure on E_c and $A_{c,net}$ was considered negligible (Burkart *et al.*, 2007).

Canopy gross photosynthesis ($A_{c,gross}$) is the sum of $A_{c,net}$ and canopy respiration (R_c). R_c during the night was estimated directly from Eqn. (5.5) as $CO_{2,dif}$ during the night was mainly a result of canopy respiration. During daytime, R_c was estimated considering the variation of temperature as:

$$R_c = R_{c,25} \exp \left[\frac{E_{Rc}(T_{air}-25)}{298R(T_{air}+273)} \right] \quad (5.6)$$

where $R_{c,25}$ is the value of R_c at 25 °C; E_{Rc} is the energy of activation; R is the universal gas constant (= 8.314 J K⁻¹ mol⁻¹). The values of $R_{c,25}$ and E_{Rc} were estimated from the measurements of R_c during night (Reichstein *et al.*, 2005).

5.2.2.3 Validation of a canopy photosynthetic model

The sun/shade model of de Pury & Farquhar (1997), as implemented in the crop model GECROS (Yin & Struik, 2017; Yin & Laar, 2005), was validated against measured $A_{c,gross}$. In this model, canopy leaves are divided into sunlit and shaded fractions and each fraction is modelled separately using a leaf photosynthesis model. When there is no water stress, potential leaf photosynthesis rate (A_p) is calculated using analytical solution of combined stomatal conductance, CO₂ diffusion and biochemical leaf-photosynthesis models (Yin & Struik, 2017, 2009). In the presence of water limitation, actual canopy photosynthesis is calculated considering the change of actual stomatal resistance to water vapour ($r_{sw,a}$) due to stomatal closure. The $r_{sw,a}$ is modelled as (Yin & Struik 2017):

$$r_{sw,a} = (E_p - E_a)(sr_{bh} + \gamma r_{bw})/(\gamma E_a) + r_{sw,p}E_p/E_a \quad (5.7)$$

where E_p and E_a are potential leaf transpiration rate and actual available water for leaf transpiration, respectively; s is the slope of the saturated vapour pressure curve; r_{bh} , r_{bw} and $r_{sw,p}$ are boundary layer resistances to heat, boundary resistance to water, and stomatal resistance to water transfer in absence of water stress, respectively; γ is the psychrometric constant (= 0.067 kPa °C⁻¹). For calculation of s , r_{bh} and r_{bw} , see Yin & van Laar (2005) and Yin & Struik (2017). $r_{sw,p}$ is assumed equal to 1/(1.6 g_s), where g_s is calculated according to A_p . The E_p is calculated using Penman-Monteith equation while E_a depends on the actual plant water uptake. Relevant model algorithms are summarised in the Supplementary Material Text S5.1.

The values of model input parameters required for leaf photosynthesis were presented in Chapter 4 for the same hemp cultivar and are summarized in Supplementary Material Table S5.1. The canopy related parameters LAI , SLN , k_L (for diffuse light) and k_a were derived in this study. The leaf angle that was used to calculate the direct light extinction coefficient was fixed at 15° , an average value assessed using a goniometer. Instantaneous environmental parameters, i.e. CO_2 , VP , T_{air} and irradiation intensity, were recorded by the canopy chamber system. E_a is obtained from the measured E_c (see Results).

5.2.2.4 Normalization of gas exchange measurements within canopy chambers

The micro-environment differed between canopy chamber and ambient open air, and among treatments (see Results). Thus, the measured E_c and $A_{c,gross}$ in the canopy chamber were normalized to that in the open air using the validated canopy model. Firstly, a correction factor f_{Ec} was obtained, based on simulated potential canopy transpiration E_{cp} as:

$$f_{Ec} = \frac{E_{cp,air(s)}}{E_{cp,chamber(s)}} \quad (5.8)$$

where $E_{cp,air(s)}$ and $E_{cp,chamber(s)}$ are simulated potential canopy transpiration using weather data in open air and in the canopy chamber, respectively. The value of E_c corresponding to the open-air condition was then obtained by multiplying the measured E_c in the chamber with the correction factor f_{Ec} . Subsequently, the corrected value of E_c for the open air and the measured E_c in the canopy chamber were used as inputs to obtain simulated canopy photosynthesis, $A_{c,gross,air(s)}$ and $A_{c,gross,chamber(s)}$, using weather data in the open air and in the canopy chamber, respectively. This gave a correction factor for $A_{c,gross}$ (f_{Ac}) as:

$$f_{Ac} = \frac{A_{c,gross,air(s)}}{A_{c,gross,chamber(s)}} \quad (5.9)$$

Finally, the value of $A_{c,gross}$ corresponding to the open-air condition was calculated by multiplying the measured $A_{c,gross}$ in the chamber with the factor f_{Ac} .

5.2.3 Statistical analysis

Nonlinear fitting was carried out using the GAUSS method in PROC NLIN of SAS (SAS Institute Inc., Cary, NC, USA). Analysis of variance was conducted to assess the effects of nitrogen fertilization and water shortage on canopy structure and gas exchange related parameters using SPSS statistics 22.0 (SPSS, Chicago, Illinois, USA).

5.3 Results

5.3.1 The effects of nitrogen and water levels on canopy physiological parameters

Nitrogen fertilization resulted in an increase in canopy size and leaf nitrogen content. In the N60 plots where weed competition was negligible in the field experiment in 2014, *LAI* (leaf area index) was on average $3.2 \text{ m}^2 \text{ m}^{-2}$ and $4.8 \text{ m}^2 \text{ m}^{-2}$ at linear growth stage and full flowering, respectively; *SLN* (specific leaf nitrogen) was on average $0.97 \text{ g N (m}^2 \text{ leaf)}^{-1}$ and $0.67 \text{ g N (m}^2 \text{ leaf)}^{-1}$, respectively. In the field experiment in 2015, *LAI* of the N120 plots was $4.0 \text{ m}^2 \text{ m}^{-2}$ and $6.4 \text{ m}^2 \text{ m}^{-2}$ at the onset of the linear growth stage and at full flowering, respectively, while *SLN* was $1.27 \text{ g N (m}^2 \text{ leaf)}^{-1}$ and $1.17 \text{ g N (m}^2 \text{ leaf)}^{-1}$, respectively (Figure 5.1). The *LAI* and *SLN* were on average 2.8 times and 1.2 times higher than those of non-fertilized canopies. In CAN1, *LAI* ranged from $1.8 \text{ m}^2 \text{ m}^{-2}$ to $2.6 \text{ m}^2 \text{ m}^{-2}$; *SLN* ranged from $0.84 \text{ g N (m}^2 \text{ leaf)}^{-1}$ to $1.02 \text{ g N (m}^2 \text{ leaf)}^{-1}$. Nitrogen fertilization in CAN1 resulted in increases in *LAI* and *SLN* by 40% and 19%, respectively (Table 5.1). For the well-watered containers in CAN2, the average values of *LAI* and *SLN* were $2.0 \text{ m}^2 \text{ m}^{-2}$ and $0.68 \text{ g N (m}^2 \text{ leaf)}^{-1}$, respectively (Table 5.2). Withholding water for 13 days in CAN2 resulted in an increase in the weight of senesced leaves while the weight of green leaves was reduced (Table 5.3). Consequently, water-stressed canopies had a 36% lower *LAI* than well-watered canopies (Table 5.2). While water stress resulted in a reduction in canopy size, the *SLN* of water-stressed canopies was 51% higher than that of well-watered canopies.

Light intensity and *SLN* decreased progressively with increasing depth from top to bottom (Supplementary Material Figure S5.1). The value of k_L (the light extinction coefficient) was

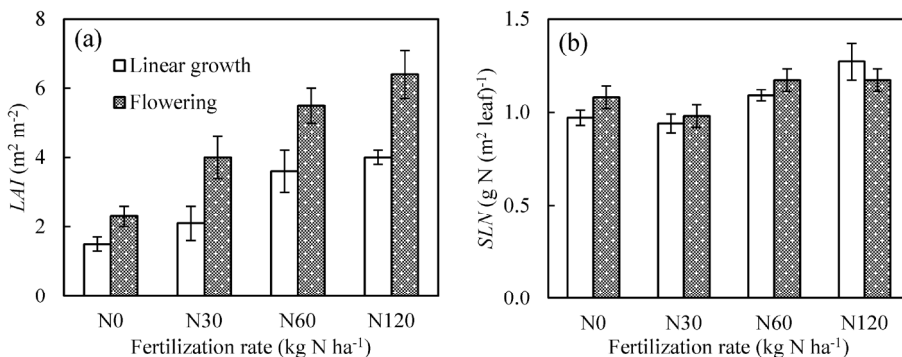


Figure 5.1 The effects of nitrogen fertilization on leaf area index (*LAI*; panel a) and specific leaf nitrogen (*SLN*; panel b) at the onset of linear growth and at full flowering in the field experiment in 2015.

Table 5.1 The effects of nitrogen deficiency and water shortage on canopy transpiration and carbon assimilation. Data presented was collected in CAN1. The data of the last four columns is presented as the average of 3 days after being normalized to the open-air conditions.

	N_c	LAI	SLN	E_c	$A_{c, gross}$	WUE_c	NUE_c
Nitrogen							
N1	1.53 b	1.84 b	0.84 b	162 b	0.70 b	4.49	0.46
N2	2.11 a	2.26 ab	0.94 ab	236 ab	0.94 ab	4.09	0.44
N3	2.58 a	2.59 a	1.02 a	268 a	1.14 b	4.41	0.44
<i>P-value</i>	0.00	0.00	0.03	0.03	0.02	0.32	0.78
Water							
WS	2.08	2.36	0.88	187 b	0.84	4.65 a	0.40 b
WW	2.07	2.01	0.97	256 a	1.01	4.00 b	0.49 a
<i>P-value</i>	0.95	0.07	0.06	0.03	0.11	0.03	0.02

Acronyms: canopy nitrogen content (N_c ; g N (m² ground)⁻¹), leaf area index (LAI ; m² m⁻²), specific leaf nitrogen (SLN ; g N (m² leaf)⁻¹), actual transpiration (E_c ; mol H₂O m⁻² d⁻¹), canopy gross photosynthesis ($A_{c, gross}$; mol CO₂ m⁻² d⁻¹), canopy water-use efficiency (WUE_c ; mmol CO₂ (mol H₂O)⁻¹) and canopy nitrogen-use efficiency (NUE_c ; mol CO₂ d⁻¹ (g N)⁻¹). N1, N2 and N3 denote nitrogen fertilization rate at 0, 1.0, and 2.0 g N container⁻¹, respectively. WW denotes well-watered containers while WS denotes the containers where water supply was half of WW.

ANOVA analysis was conducted considering nitrogen and water levels as main factors and measuring day as repeated factor. Interaction between nitrogen and water was excluded because it was not significant for all parameters in a preliminary test. Numbers followed by different letters under the same category are statistically different for $P = 0.05$ (Tukey HSD).

Table 5.2 The effects of nitrogen deficiency and long-term water shortage on canopy transpiration and carbon assimilation. The data of the last four columns was collected in the last consecutive 3 days in CAN2 and is presented after being normalized to the open-air conditions.

	N_c	LAI	SLN	E_c	$A_{c, gross}$	WUE_c	NUE_c
Nitrogen							
N1	0.79 b	1.15	0.71	69	0.36	6.28	0.44
N2	1.19 b	1.69	0.73	164	0.67	5.74	0.58
N3	2.08 a	1.99	1.12	182	0.87	5.58	0.42
<i>P-value</i>	0.024	0.06	0.19	0.39	0.36	0.72	0.61
Water							
WS	1.35	1.26 b	1.03	43	0.31	7.53 a	0.26
WW	1.35	1.97 a	0.68	234	0.96	4.20 b	0.70
<i>P-value</i>	0.95	0.03	0.11	0.08	0.10	0.04	0.62

Acronyms: canopy nitrogen content (N_c ; g N (m² ground)⁻¹), leaf area index (LAI ; m² m⁻²), specific leaf nitrogen (SLN ; g N (m² leaf)⁻¹), actual transpiration (E_c ; mol H₂O m⁻² d⁻¹), canopy gross photosynthesis ($A_{c, gross}$; mol CO₂ m⁻² d⁻¹), canopy water-use efficiency (WUE_c ; mmol CO₂ (mol H₂O)⁻¹) and canopy nitrogen-use efficiency (NUE_c ; mol CO₂ d⁻¹ (g N)⁻¹). N1, N2 and N3 denote nitrogen fertilization rate at 0, 1.0, and 2.0 g N container⁻¹, respectively. WW denotes well-watered containers while WS denotes the containers where water supply was half of WW.

ANOVA analysis was conducted considering nitrogen and water levels as main factors and measuring day as repeated factor. Interaction between nitrogen and water was excluded because it was not significant for all parameters in a preliminary test. Numbers followed by different letters under the same category are statistically different for $P = 0.05$ (Tukey HSD).

$0.96 \pm 0.04 \text{ m}^2 \text{ m}^{-2}$ and was similar for nitrogen fertilization levels and growth environments (Figure 5.2a). The SLN_0 (SLN at the top of the canopy) ranged from $1.43 \text{ g N (m}^2 \text{ leaf)}^{-1}$ to $2.72 \text{ g N (m}^2 \text{ leaf)}^{-1}$ and the k_n (nitrogen extinction coefficient) ranged from $0.09 \text{ m}^2 \text{ m}^{-2}$ to $0.89 \text{ m}^2 \text{ m}^{-2}$. The values of k_n decreased exponentially with an increase in LAI (Figure 5.2b). This relationship between k_n and LAI was consistent among nitrogen fertilization levels and growth environments. Thus, this relationship was applied to calculate k_n in subsequent model analyses.

5.3.2 The effects of chamber system on canopy transpiration and photosynthesis

The night-time chamber air temperature T_{air} ranged from $14.7 \text{ }^\circ\text{C}$ to $25.7 \text{ }^\circ\text{C}$ and from $17.1 \text{ }^\circ\text{C}$ to $27.0 \text{ }^\circ\text{C}$ during the measurements in CAN1 and CAN2, respectively. There was little difference in micro-environmental variables (i.e., T_{air} , CO_2 and VP) during the night-time between chamber and ambient open air, and among treatments within chambers (Figure 5.3). During daytime, incident PAR reached up to $2100 \text{ } \mu\text{mol m}^{-2} \text{ s}^{-1}$ while T_{air} , CO_2 and VP in the

Table 5.3 The effects of long-term water shortage on the partitioning of biomass. Data presented was collected in CAN2.

	Biomass (g m^{-2})	Stem (g m^{-2})	Green leaf (g m^{-2})	Senesced leaf (g m^{-2})	Inflorescence (g m^{-2})	Root (g m^{-2})
WS ^a	480	245	62.0	43.6	30.7	99
WW ^a	590	278	96.9	37.3	49.0	128
<i>P</i> -value ^b	0.10	0.23	0.04	0.05	0.08	0.22

Acronyms: WW denotes well-watered containers while WS denotes the containers where water supply was half of WW.

Analysis of variance was performed considering canopy nitrogen content as covariate.

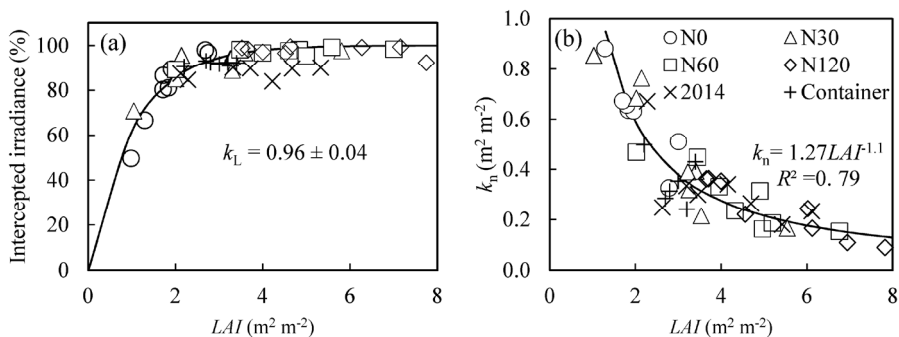


Figure 5.2 Canopy light interception (panel a) and nitrogen extinction coefficient (k_n ; panel b) against leaf area index (LAI) at different growth conditions. N0, N30, N60, N120 denote nitrogen fertilization rate in 2015 at 0, 30, 60, and 120 kg N ha^{-1} , respectively. “2014” denotes data collected in 2014 in the plots that received a nitrogen fertilization of 60 kg N ha^{-1} . Data collected in the other plots is not shown because there was severe weed competition. “Container” denotes data collected in the container experiment.

open air ranged from 17.6 °C to 35.9 °C, from 359.7 $\mu\text{mol mol}^{-1}$ to 439.4 $\mu\text{mol mol}^{-1}$, and from 1.7 kPa to 2.5 kPa, respectively. The daytime T_{air} and VP within chambers were higher than those in the open air while the CO_2 was lower (Figure 5.3). Increasing nitrogen fertilization rate increased the differences in T_{air} , VP and CO_2 between chamber and ambient open air while

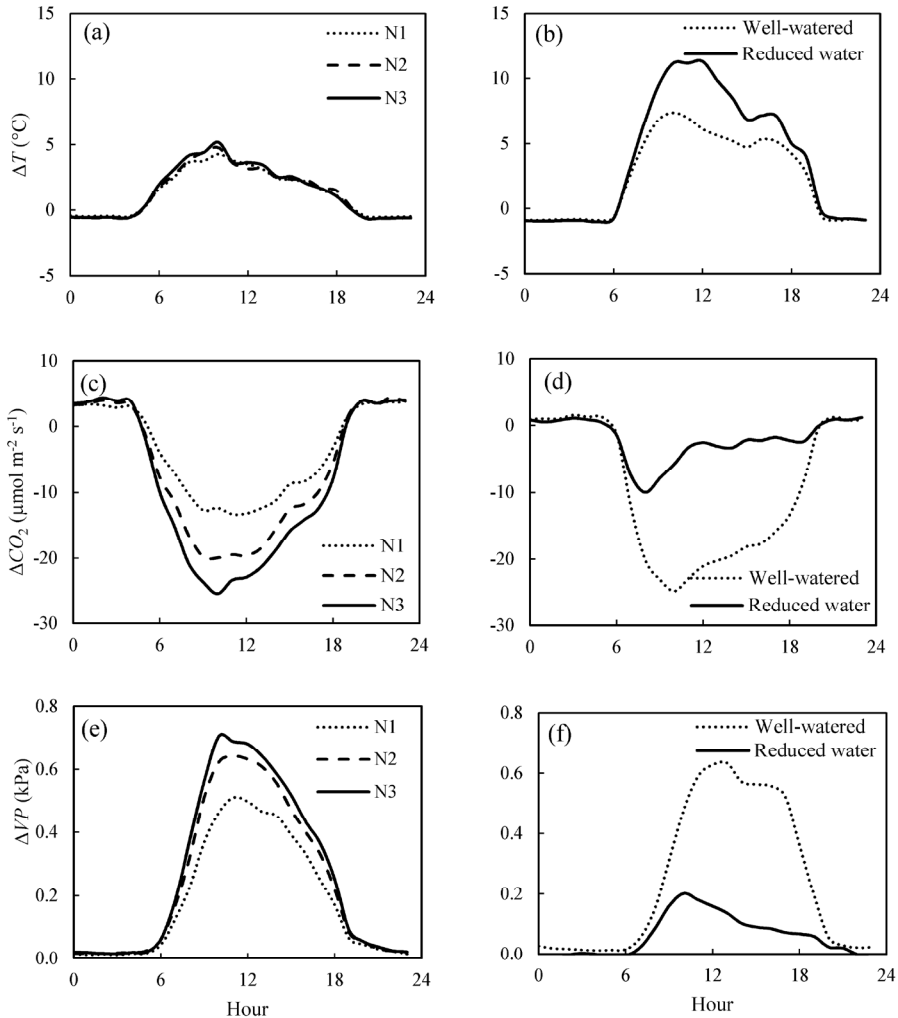


Figure 5.3 Diurnal courses of canopy chamber effects on air temperature (ΔT), CO_2 concentration (ΔCO_2) and vapour pressure (ΔVP) under different nitrogen (panels a, c, e) and water (panels b, d, f) regimes. Data presented in Panels a, c, e is the average of 3 days in CAN1. N1, N2 and N3 denote the level of received nitrogen, see text for details. Data presented in panels b, d, f is the average of the last consecutive 3 days in CAN2.

reducing water supply increased the difference in T_{air} but decreased the differences in VP and CO_2 .

The night-time canopy respiration R_c varied largely from minute to minute, presumably due to a relatively low R_c and high flow rate. Nevertheless, R_c increased slightly with increasing chamber T_{air} (Supplementary Material Figure S5.2). By fitting these data to Eqn. (5.6), E_{Rc} (activation energy for R_c) was estimated as $9559 \pm 2779 \text{ J mol}^{-1}$. The estimate of R_{c25} (R_c at 25 °C) ranged from $3.9 \mu\text{mol CO}_2 \text{ m}^{-2} \text{ s}^{-1}$ to $4.9 \mu\text{mol CO}_2 \text{ m}^{-2} \text{ s}^{-1}$ in CAN1, and from $0.50 \mu\text{mol CO}_2 \text{ m}^{-2} \text{ s}^{-1}$ to $2.09 \mu\text{mol CO}_2 \text{ m}^{-2} \text{ s}^{-1}$ in CAN2 (Figure 5.4a). With the estimated E_{Rc} and R_{c25} , instantaneous gross canopy photosynthesis rate $A_{c,\text{gross}}$ in CAN1 and CAN2 was estimated. The daily R_c (canopy respiration) increased with increasing $A_{c,\text{gross}}$ in both CAN1 and CAN2 but with different relationships (Figure 5.4b), and accounted for on average 40% and 15% of $A_{c,\text{gross}}$ in CAN1 and CAN2, respectively.

Examples of diurnal courses of measured canopy transpiration E_c and $A_{c,\text{gross}}$ within canopy chambers are presented in Figure 5.5. The E_c and $A_{c,\text{gross}}$ were close to nil during night-time while during the daytime their values rose up to $11.1 \text{ mmol H}_2\text{O m}^{-2} \text{ s}^{-1}$ and $38.1 \mu\text{mol CO}_2 \text{ m}^{-2} \text{ s}^{-1}$, respectively. For the containers that received sufficient water, the values of E_c and $A_{c,\text{gross}}$ throughout the day followed closely their simulated potential transpiration E_{cp} and simulated potential photosynthesis $A_{cp,\text{gross}}$ (Figure 5.5). As expected, the values of E_c and $A_{c,\text{gross}}$ of the

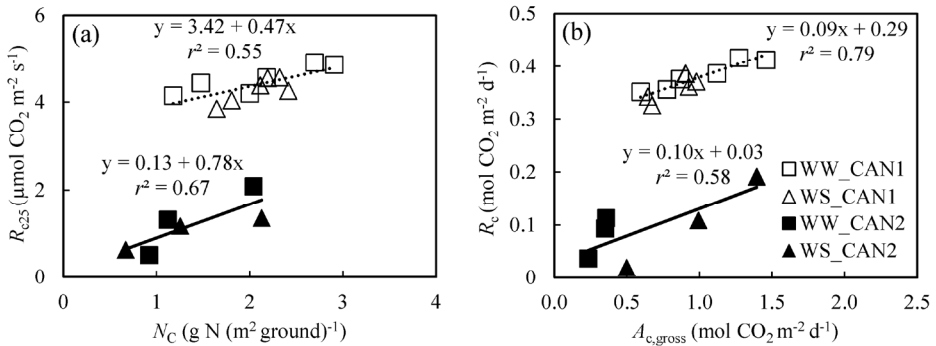


Figure 5.4 Panel a: responses of canopy respiration at 25 °C (R_{c25}) to canopy leaf nitrogen content (N_c). Panel b: relationship between daily integrated canopy respiration (R_c) and gross photosynthesis ($A_{c,\text{gross}}$). WW and WS denote well-watered and water-limited conditions, respectively. CAN1 and CAN2 are experimental codes, see text for details.

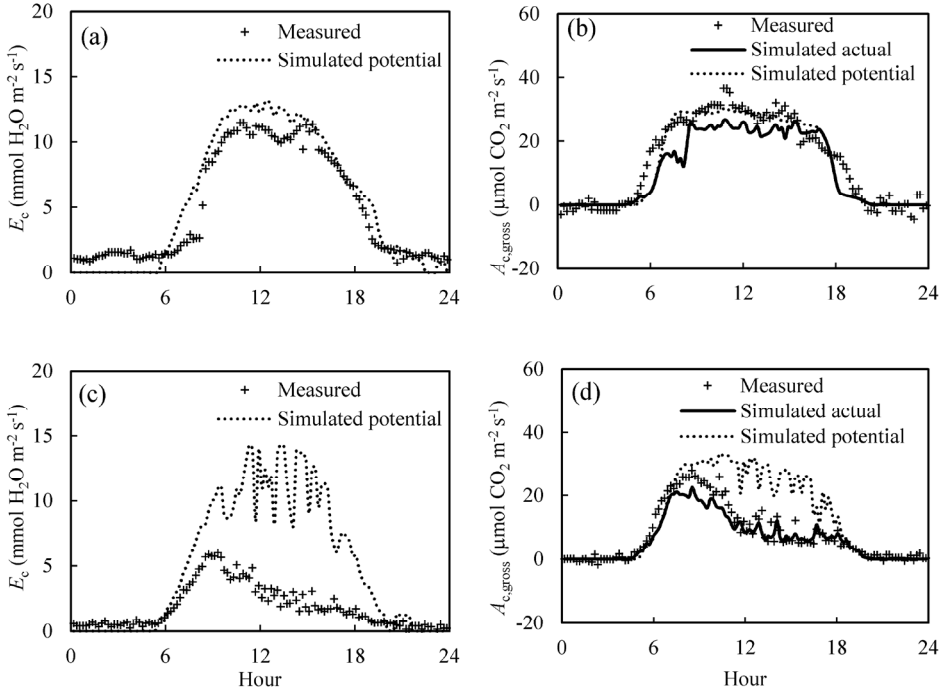


Figure 5.5 Diurnal courses of measured and simulated canopy transpiration (E_c ; panels a, c) and gross photosynthesis rates ($A_{c, gross}$; panels b, d). Data presented was collected in the first day of N2 in CAN1. The canopy in panels a, b received sufficient water while water supply in panels c, d was halved.

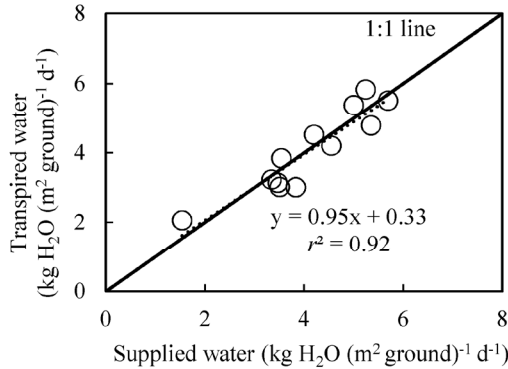


Figure 5.6 Integrated water loss through transpiration as measured by canopy gas exchange in comparison with the amount of supplied water. Each point represents the daily average of water loss versus water gain over the measuring period for each container in CAN1. The amount of supplied water was calculated as the difference of container weight at before and after watering.

containers that received half amount of water were lower than their E_{cp} and $A_{cp, gross}$ from the late morning to the end of daytime. Integration of the instantaneous E_c to daily values matched well with the amount of supplied water per day (Figure 5.6). Thus, the $A_{c, gross}$ was simulated considering E_c as available water for transpiration at canopy level. The E_c was partitioned between sunlit and shaded leaves according to the relative share of their E_{cp} to obtain their actual transpiration (E_a) in Eqn. (5.7). There was a good agreement between the measured and simulated $A_{c, gross}$ under different nitrogen and water regimes (Figure 5.5). The values of r^2 and $rRMSE$ for the comparison between simulated and measured values of all data points in CAN1 were 0.80 and 32%, respectively (part of the data points can be seen in Supplementary Material Figure S5.3). For the measurements in CAN2, they were 0.78 and 66%, respectively.

The effects of micro-environmental differences between chamber and open air, and among treatments within chambers on canopy gas exchange were assessed using the validated model (Table 5.4). The presence of the plant chamber increased E_{cp} by 6.9–11.2% in CAN1 and by 19.6–34.2% in CAN2 while it decreased $A_{cp, gross}$ by 0.3–1.4% in CAN1 and by 3.5–4.2% in CAN2. The chamber effect on E_{cp} varied little among nitrogen treatments while the effect on $A_{cp, gross}$ increased with an increase in nitrogen rate. Water shortage increased the effects of the chamber on both E_{cp} and $A_{cp, gross}$. Therefore, to account for any effect of varying micro-environmental variables due to the presence of the canopy chamber, the measured E_c and $A_{c, gross}$ within each chamber were normalized to the conditions in the open air.

Table 5.4 The effects of plant chamber on canopy transpiration and photosynthesis under different nitrogen and water regimes. Potential canopy transpiration (E_{cp}) and photosynthesis ($A_{cp, gross}$) were simulated using weather data in the open air and in the chambers for each treatment while the other parameters were kept at the average value of well-watered N3 containers. The differences of simulated E_{cp} and $A_{cp, gross}$ between open air and plant chamber are presented as percentage of the value in the open air. The presence of the plant chamber resulted in an increase in E_{cp} while it resulted in a decrease in $A_{cp, gross}$.

	CAN1		CAN2	
	ΔE_{cp} (%)	$\Delta A_{cp, gross}$ (%)	ΔE_{cp} (%)	$\Delta A_{cp, gross}$ (%)
N1	9.0	-1.0	28.5	-3.5
N2	8.9	-1.0	25.5	-3.7
N3	9.1	-1.4	26.8	-4.2
WS	11.2	-1.2	34.2	-4.0
WW	6.9	-0.3	19.6	-3.6

Acronyms: N1, N2 and N3 denote nitrogen fertilization rate at 0, 1.0, and 2.0 g N container⁻¹, respectively; WW denotes well-watered containers while WS denotes the containers where water supply was half of WW; CAN1 and CAN2 are experimental codes, see text for details.

5.3.3 The effects of nitrogen fertilization and short-term water shortage on canopy water- and nitrogen-use efficiencies

Examples of the diurnal courses of normalised E_c and $A_{c, gross}$ in CAN1 are presented in Figure 5.7. Despite minute-to-minute fluctuation due to environmental variability, the E_c and $A_{c, gross}$ were consistently higher in the fertilized canopies than those of non-fertilized and water shortage resulted in reductions in E_c and $A_{c, gross}$ that emerged from the late morning to the end of the day. Consequently, daily integrated E_c and $A_{c, gross}$ increased with an increase in nitrogen fertilization rate while they decreased under water limiting conditions (Table 5.1). The daily integrated E_c and $A_{c, gross}$ ranged from 162 mol H₂O m⁻² d⁻¹ to 268 mol H₂O m⁻² d⁻¹ and from 0.70 mol CO₂ m⁻² d⁻¹ to 1.14 mol CO₂ m⁻² d⁻¹, respectively. Calculated as $A_{c, gross}/E_c$, the canopy water-use efficiency (WUE_c) ranged from 4.00 mmol CO₂ (mol H₂O)⁻¹ to 4.65 mmol CO₂ (mol H₂O)⁻¹. The WUE_c did not vary significantly among nitrogen treatments while it increased by 16% under water limiting conditions because the WUE_c increased with decreasing ratio of E_c/E_{cp} (Figure 5.8), an indicator of the degree of water shortage. Calculated as $A_{c, gross}/N_c$, canopy

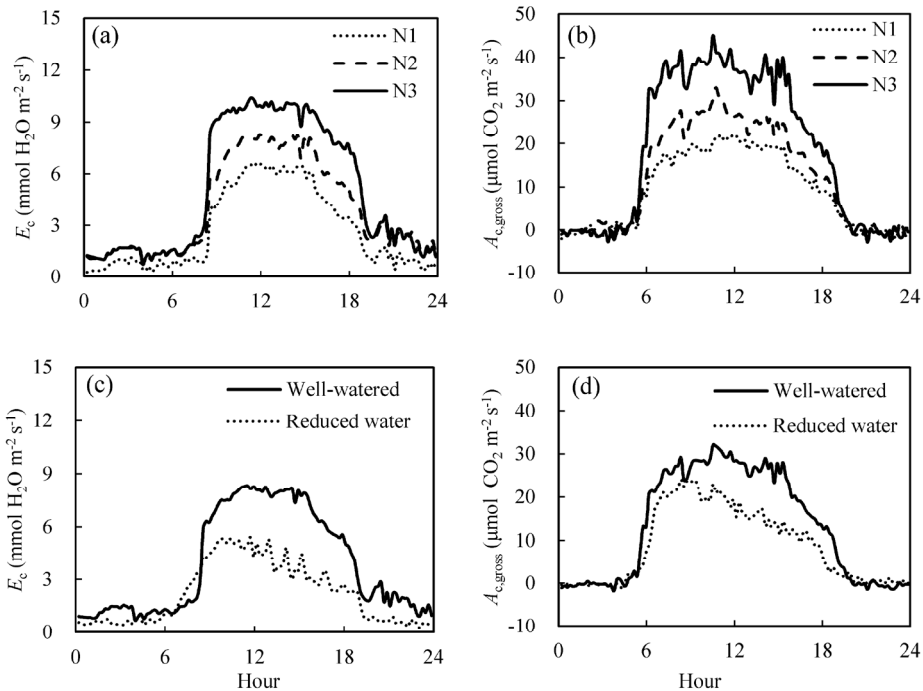


Figure 5.7 The effect of nitrogen (panels a, b) and short-term water stress (panels c, d) on instantaneous canopy transpiration (panels a, c) and photosynthesis rate (panels b, d). Data presented was collected in the first day in CAN1. The data has been normalized to the open-air conditions. N1, N2 and N3 denote the level of received nitrogen, see text for details.

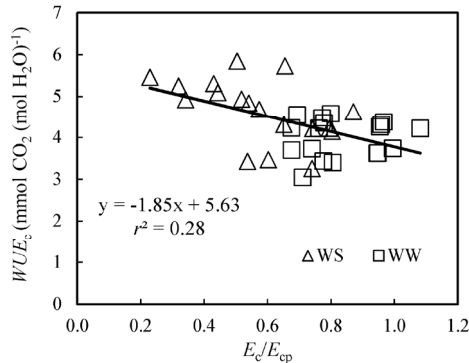


Figure 5.8 Relationship between gross canopy water-use efficiency (WUE_c) and the degree of water shortage (E_c/E_{cp}). Data presented were collected in CAN1. Each point represents the daily value of each container. WW denotes well-watered containers while WS denotes the containers where water supply was half of WW.

nitrogen-use efficiency (NUE_c) ranged from $0.40 \text{ mol CO}_2 \text{ d}^{-1} (\text{g N})^{-1}$ to $0.49 \text{ mol CO}_2 \text{ d}^{-1} (\text{g N})^{-1}$. No significant effect of nitrogen fertilization on NUE_c was observed ($P > 0.05$), while NUE_c decreased significantly (by 18%; $P < 0.05$) under water limiting conditions (Table 5.1).

5.3.4 The effects of long-term water shortage on canopy water- and nitrogen-use efficiencies

As water shortage was prolonged in CAN2, the progressive responses of E_c , $A_{c,\text{gross}}$, WUE_c and NUE_c are presented in Figure 5.9. Reductions of E_c and $A_{c,\text{gross}}$ emerged 4 days after withholding water and lasted until the end of the gas exchange measurement (except for the 8th day) when all plants were cut for analysis. A short recovery was observed during the 8th day due to a brief re-watering of wilting plants in the water-stressed canopies (see the Materials and Methods section). During the last three days, the average daily E_c , $A_{c,\text{gross}}$, WUE_c and NUE_c in the well-watered canopies were $234 \text{ mol H}_2\text{O m}^{-2} \text{ d}^{-1}$, $0.96 \text{ mol CO}_2 \text{ m}^{-2} \text{ d}^{-1}$, $4.20 \text{ mmol CO}_2 (\text{mol H}_2\text{O})^{-1}$ and $0.70 \text{ mol CO}_2 \text{ d}^{-1} (\text{g N})^{-1}$, respectively (Table 5.2). The values of E_c , $A_{c,\text{gross}}$ and NUE_c were higher than those of water-stressed canopies by 82%, 68% and 63%, respectively, while the WUE_c was lower than that of water-stressed canopies by 79%.

5.3.5 The importance of canopy physiological parameters in determining canopy water- and nitrogen-use efficiencies

Model analyses were performed to assess the relative importance of LAI and SLN , the two important canopy physiological parameters, in determining potential WUE_c (WUE_{cp}) and NUE_c (NUE_{cp}) in both the field experiment and the chamber experiment. This was done by first using

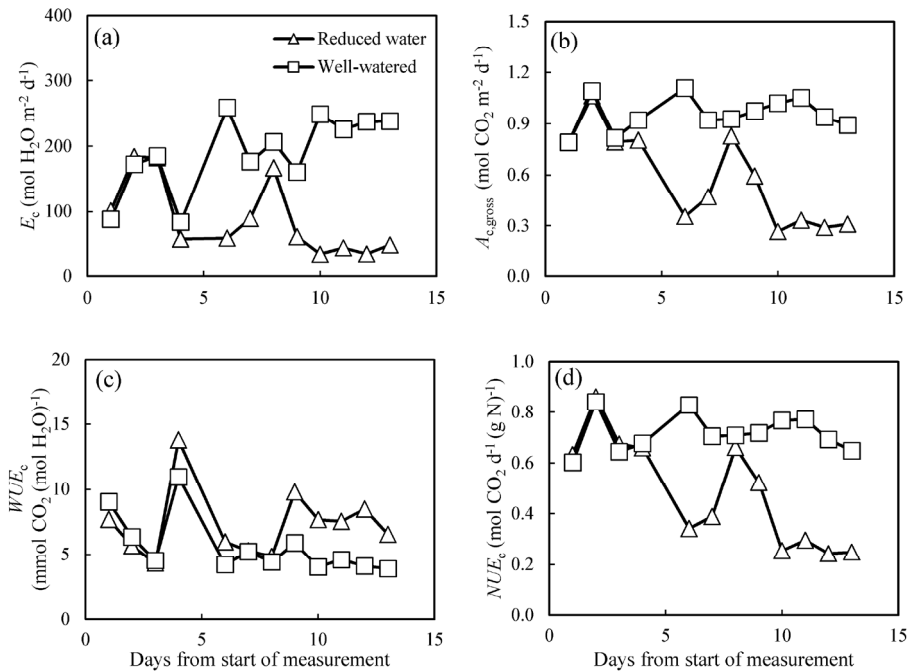


Figure 5.9 The evolution of prolonged water limitation effects on daily canopy transpiration (E_c), gross photosynthesis ($A_{c,gross}$), canopy water-use efficiency (WUE_c) and canopy nitrogen-use efficiency (NUE_c). Data presented was collected in CAN2. The data has been normalized to the open-air conditions.

the measured SLN and LAI of each nitrogen level as the default simulation and then forcing LAI or SLN of all treatments to their respective values at the non-fertilized or water stressed treatment (Figure 5.10). For both linear-growth and flowering stages of the field experiment, when forcing SLN to the value at non-fertilized treatment the values of E_{cp} , $A_{cp,gross}$, WUE_{cp} and NUE_{cp} changed little in comparison with those of the default simulation, whereas when forcing LAI to the value at non-fertilized treatment their values deviated significantly from the default simulation. In the chamber experiment in CAN1, the variations of E_{cp} , $A_{cp,gross}$ and WUE_{cp} with increasing nitrogen rate were mainly due to a change in LAI whereas the variation of NUE_{cp} was due to combined changes in LAI and SLN . In the chamber experiment in CAN2, the decrease in E_{cp} under long-term stress was mainly due to a change in LAI while the variations of $A_{c,gross}$, WUE_{cp} and NUE_{cp} were due to combined changes in LAI and SLN .

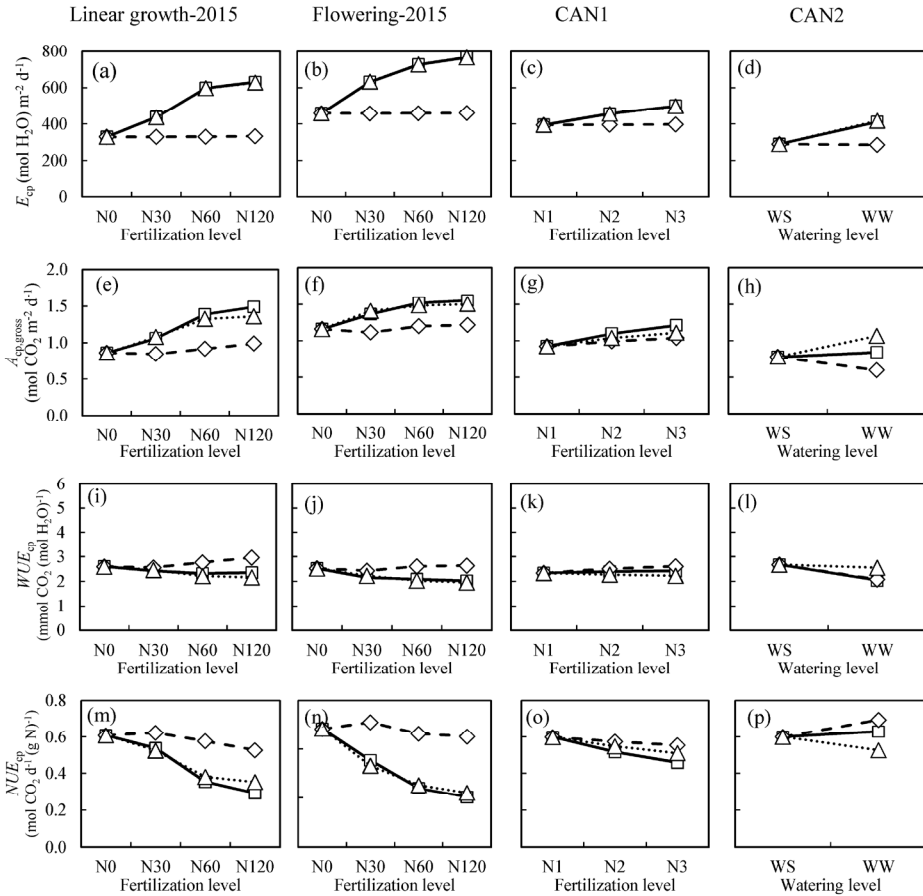


Figure 5.10 The simulated effects of nitrogen fertilization and water shortage on daily potential canopy transpiration (E_{cp} ; panels a–d), gross photosynthesis ($A_{cp,gross}$; panels e–h), and canopy water-use efficiency (WUE_{cp} ; panels i–l), and nitrogen-use efficiency (NUE_{cp} ; panels m–p). Continuous line with squares: the default simulations performed using the measured leaf area index (LAI) and specific leaf nitrogen (SLN) at each nitrogen level or each water level. Dashed line with diamonds: simulations performed with measured SLN at each nitrogen level (or each water level) while keeping LAI fixed at the values of non-fertilization (or water-stressed) treatment. Dot line with triangles: simulations performed with measured LAI at each nitrogen level (or each water level) while keeping SLN fixed at the values of non-fertilization (or water-stressed) treatment. Linear growth-2015 (panels a, e, i and m) denotes the case where the values of LAI and SLN were collected at the linear growth stage in the field experiment in 2015; Flowering-2015 (panels b, f, j and n) denotes the case where the values of LAI and SLN were collected at full flowering in the field experiment in 2015; CAN1 (panels c, g, k and o) denotes the case where the values of LAI and SLN were collected in the CAN1; CAN2 (panels d, h, l and p) denotes the case where values of LAI and SLN were collected in the CAN2. N0, N30, N60, N120 denote nitrogen fertilization rate in 2015 at 0, 30, 60, and 120 kg N ha⁻¹, respectively; N1, N2 and N3 denote nitrogen fertilization rate in CAN1 at 0, 1.0, and 2.0 g N container⁻¹, respectively; WW denotes well-watered containers in CAN2 while WS denotes the containers where water supply was half of WW.

5.4 Discussion

Bio-economically sustainable agronomy requires effective use of scarce nitrogen and water resources. While hemp is considered as a bio-economically sustainable crop (Amaducci *et al.*, 2015; Finnan & Styles, 2013), its canopy water- and nitrogen-use efficiencies have not been studied. In this study, experimental and modelling analyses were conducted to assess hemp canopy water- and nitrogen-use efficiencies in relation to leaf and canopy physiological parameters under different nitrogen and water regimes.

5.4.1 Determination of canopy transpiration and photosynthesis

The canopy chamber technique is a useful tool to assess crop responses to nitrogen deficiency and water shortage at canopy scale. However, the presence of the chamber wall had a significant effect on the micro-environment within the chambers (Figure 5.3), in line with the results of previous studies (Müller *et al.*, 2009; Takahashi *et al.*, 2008; Poni *et al.*, 1997). In the present study, the micro-environment conditions within the chamber resulted in a lower $A_{cp, gross}$ and a higher E_{cp} than those in the open air, and this effect was larger in the chambers with higher fertilization rate and lower water supply (Table 5.4). As responses of E_c and $A_{c, gross}$ to environmental variables are probably not linear (Hikosaka *et al.*, 2016), it is necessary to normalize measurements within different chambers to avoid any confounding effect due to the differences in chamber micro-environmental factors.

In line with previous studies (Müller *et al.*, 2005; Leuning *et al.*, 1998), the variation of E_c and $A_{c, gross}$ in response to fluctuating environmental condition under different nitrogen and water regimes can be precisely described using a process-based physiological model (Figure 5.5). Thus, discrepancies in E_c and $A_{c, gross}$ among chambers due to differences in micro-environment at measuring time could be properly accounted for through correction factors f_{E_c} and f_{A_c} , respectively (see Eqns 5.8 and 5.9), in our study.

5.4.2 Hemp canopy water- and nitrogen-use efficiencies in relation to nitrogen availability

The reason for the lack of significant responses of WUE_c and NUE_c to the decrease nitrogen rate in the container experiments is not clear (Table 5.1). It is probably a consequence of small variations in LAI and SLN among nitrogen treatments. This is confirmed in the model analysis for the field experiment in 2015, where the variation in LAI among N treatments was much more significant than that in our container experiment. This model analysis suggested that both WUE_c and NUE_c increased with decreasing nitrogen fertilization rate, and that the increases in

WUE_c and NUE_c were mainly a result of a reduction in LAI (Figure 5.10). The reduced LAI resulted in increases in WUE_c and NUE_c , i.e. the reduction in $A_{c, gross}$ with a decrease in LAI is less than the reductions in E_c and in N_c . This could be explained by an optimum SLN gradient relative to the light gradient in the canopy. It has been reported that the profile of SLN in a canopy is a whole-plant process that depends on canopy size (Moreau *et al.*, 2012). Our data showed that the value of k_n increased with decreasing LAI (Figure 5.2b), up to a value of *ca.* 0.9 close to the LAI -independent value of k_L ($0.96 \text{ m}^2 \text{ m}^{-2}$, Figure 5.2a). So, the value of k_n in a large hemp canopy was generally lower than its theoretical value for a maximized canopy photosynthesis, which could be achieved only when $k_n = k_L$ (Hikosaka *et al.*, 2016; Hirose & Werger, 1987). When LAI is low, canopy photosynthesis is close to a maximum value as a result of k_n being close to k_L ; in such a case, the average leaf photosynthesis rate could be increased for a given amount of N_c , while E_c stayed largely unchanged.

The variation in WUE_c and NUE_c with decreasing nitrogen fertilization rate may also be attributed to the variation in the absolute amount of SLN . It has been widely reported that SLN positively correlates with water-use efficiency while it negatively correlates with nitrogen-use efficiency at leaf level (Shangguan *et al.*, 2000; Van den Boogaard *et al.*, 1995). However, in response to nitrogen stress, hemp tends to maintain SLN at the expense of LAI (Figure 5.1). This response is in line with that of sunflower (*Helianthus annuus* L.), canola (*Brassica napus* L.) and wheat (*Triticum aestivum* L.) whereas it contrasts with that of maize (*Zea mays* L.), which tends to maintain LAI under nitrogen stress at the expense of SLN (Lemaire *et al.*, 2008). As a result of the relative small variation in SLN among nitrogen treatments, little effect of SLN was detected on the hemp WUE_c and NUE_c (Figure 5.10).

The effects of nitrogen fertilization on crop water-use efficiency and nitrogen-use efficiency are whole plant process that depends on leaf photosynthetic capacity and canopy size, and our analysis showed that relative to leaf photosynthetic capacity (determined by SLN), canopy size (LAI) plays a predominant role on this.

5.4.3 Hemp canopy water- and nitrogen-use efficiencies in relation to water availability

Field observations generally show that water stress results in an increase in hemp water-use efficiency (Cosentino *et al.*, 2013). This is confirmed by our results showing both short-term and long-term water shortages that resulted in an increase in WUE_c (Tables 5.1, 5.2). However, our study further showed that the effect differed between short- and long-term stresses.

In response to short-term water stress, the increase in WUE_c is mainly a consequence of stomatal closure as the variations in E_c and $A_{c, gross}$ with decreasing water supply were precisely captured by considering the response of stomatal conductance (Figure 5.5). In fact, stomatal closure is one of the earliest responses to water deficit, protecting the plants from extensive water loss (Chaves *et al.*, 2003). Stomatal closure restricts both H_2O and CO_2 exchange between leaf intercellular and ambient air that leads to great decreases in E_c and $A_{c, gross}$ (Table 5.1, Figure 5.5). However, the reductions in E_c and $A_{c, gross}$ are not parallel and the WUE_c gradually increases with decreasing E_c/E_{cp} (Figure 5.8), probably because of the non-linear relationship between carbon assimilation rate and CO_2 concentration in the intercellular space (Chapter 4) that results in an increase in WUE_c . The increase in WUE_c with decreasing E_c/E_{cp} indicates that the estimation of canopy photosynthesis under water limiting condition by assuming a consistent WUE_c in the crop models, such as SUCROS (van Laar *et al.* 1997), is only approximate. Instead, the present study considered the response of stomatal conductance using Eqn. (5.7) that results in an increase in WUE_c with decreasing E_c/E_{cp} . This approach is therefore preferable in the simulation of canopy photosynthesis under short-term water stress conditions. Nevertheless, we could not exclude the possibility that non-stomatal limitations were involved in our experiment. Further researches are needed to understand the effect of non-stomatal change under water stress condition on canopy photosynthesis, such as change of leaf angle (Archontoulis *et al.*, 2011).

As water stress continued, hemp responded through reducing LAI and increasing SLN , while N_c stayed unchanged (Table 5.2). The reduced LAI was largely caused by increased senescence (Table 5.3). Because of this additional response, model analysis for the sensitivity in response to changing LAI or SLN was contrasting between CAN1 and CAN2 (Figure 5.10). This type of response to a long-term water stress was also observed in studies on other species such as kenaf (*Hibiscus cannabinus*) and sunflower (Archontoulis *et al.*, 2011; Danalatos & Archontoulis, 2010). The response could result in more significant increases in WUE_c as a result of both the stomatal response discussed above and the reduced evaporative surfaces. However, an increase in SLN could not compensate for the loss in LAI ; so, the long-term stress resulted in large reductions in the $A_{cp, gross}$, E_{cp} and NUE_c (Table 5.2). This result indicates that crop models for predicting the effect of long-term water stress should introduce mechanisms on the responses of canopy-level traits (like LAI) in addition to stomatal regulation. It also suggests that although hemp is tolerant to long-term water stress through improving water-use efficiency (Cosentino

et al., 2013), its final biomass yield and nitrogen-use efficiency may be restricted largely by water limitation during growth.

Acknowledgements

The research leading to these results has received funding from the European Union's Seventh Framework Programme for research, technological development and demonstration under grant agreement n° 311849. Drs Steven Driever and Tjeerd-Jan Stomph are thanked for their early discussions.

References

- Amaducci, S. and Gusovius, H.J., (2010) Hemp — cultivation, extraction and processing, In: *Industrial applications of natural fibres: Structure, properties and technical applications* (ed, Müssig, J.), pp. 109–134. John Wiley & Sons Ltd, West Sussex, UK.
- Amaducci, S., Scordia, D., Liu, F. *et al.* (2015) Key cultivation techniques for hemp in Europe and China. *Industrial Crops and Products*, **68**, 2–16.
- Archontoulis, S.V., Vos, J., Yin, X. *et al.* (2011) Temporal dynamics of light and nitrogen vertical distributions in canopies of sunflower, kenaf and cynara. *Field Crops Research*, **122**, 186–198.
- Baker, J.T., Van Pelt, S., Gitz, D.C. *et al.* (2009) Canopy gas exchange measurements of cotton in an open system. *Agronomy Journal*, **101**, 52–59.
- Barth, M. and Carus, M. (2015) *Carbon footprint and sustainability of different natural fibres for biocomposites and insulation material*, Hürth, Germany, nova-Institute. Available at (2017, November 29): <http://bio-based.eu/ecology/>.
- Bertoli, A., Tozzi, S., Pistelli, L. *et al.* (2010) Fibre hemp inflorescences: From crop-residues to essential oil production. *Industrial Crops and Products*, **32**, 329–337.
- Bouloc, P. and Van der Werf, H.M.G. (2013) The role of hemp in sustainable development. In: *Hemp: industrial production and uses*. (eds Bouloc P, Allegret S and Arnaud L), pp. 278–289. CPi Group Ltd, Croydon, UK.
- Burkart, S., Manderscheid, R. and Weigel, H.J. (2007) Design and performance of a portable gas exchange chamber system for CO₂-and H₂O-flux measurements in crop canopies. *Environmental and Experimental Botany*, **61**, 25–34.
- Cabrera-Bosquet, L., Molero, G. and Bort, J. (2007) The combined effect of constant water deficit and nitrogen supply on WUE, NUE and $\Delta^{13}\text{C}$ in durum wheat potted plants. *Annals of Applied Biology*, **151**, 277–289.
- Calzolari, D., Magagnini, G., Lucini, L. *et al.* (2017) High added-value compounds from Cannabis threshing residues. *Industrial Crops and Products*, **108**, 558–563.
- Chaves, M.M., Maroco, J.P. and Pereira, J.S. (2003) Understanding plant responses to drought — from genes to the whole plant. *Functional plant biology*, **30**, 239–264.
- Cosentino, S.L., Riggi, E., Testa, G. *et al.* (2013) Evaluation of European developed fibre hemp

- genotypes (*Cannabis sativa* L.) in semi-arid Mediterranean environment. *Industrial Crops and Products*, **50**, 312–324.
- Danalatos, N.G. and Archontoulis, S.V. (2010) Growth and biomass productivity of kenaf (*Hibiscus cannabinus*, L.) under different agricultural inputs and management practices in central Greece. *Industrial Crops and Products*, **32**, 231–240.
- De Meijer, E.P.M. and van der Werf, H.M.G. (1994) Evaluation of current methods to estimate pulp yield of hemp. *Industrial Crops and Products*, **2**, 111–120.
- De Pury, D. and Farquhar, G. (1997) Simple scaling of photosynthesis from leaves to canopies without the errors of big-leaf models. *Plant, Cell & Environment*, **20**, 537–557.
- Finnan, J. and Styles, D. (2013) Hemp: A more sustainable annual energy crop for climate and energy policy. *Energy Policy*, **58**, 152–162.
- Fracasso, A., Magnanini, E., Marocco, A. *et al.* (2017) Real-time determination of photosynthesis, transpiration, water-use efficiency and gene expression of two sorghum bicolor (Moench) genotypes subjected to dry-down. *Frontiers in Plant Science*, **8**, 1–12.
- Hikosaka, K., Noguchi, K. and Terashima, I. (2016) Modeling leaf gas exchange. In: *Canopy Photosynthesis: From Basics to Applications* (eds eds Hikosaka, K., Niinemets, Ü. and Anten N.P.R.), pp 61–100. Springer, London, UK.
- Jones, H.G., (2013) Heat, mass and momentum transfer. In: *Plants and microclimate: a quantitative approach to environmental plant physiology* (ed, Jones, H.G.), pp. 47–67. Cambridge university press, UK.
- Leizer, C., Ribnicky, D., Poulev, A. *et al.* (2000). The Composition of Hemp Seed Oil and Its Potential as an Important Source of Nutrition. *Journal of Nutraceuticals, Functional & Medical Foods*, **2**, 35–53.
- Lemaire, G., Van Oosterom, E., Jeuffroy, M.H. *et al.* (2008) Crop species present different qualitative types of response to N deficiency during their vegetative growth. *Field Crops Research*, **105**, 253–265.
- Leuning, R., Dunin, F. and Wang, Y.P. (1998) A two-leaf model for canopy conductance, photosynthesis and partitioning of available energy. II. Comparison with measurements. *Agricultural and Forest Meteorology*, **91**, 113–125.
- Linderson, M.L., Mikkelsen, T.N., Ibrom, A. *et al.* (2012) Up-scaling of water use efficiency from leaf to canopy as based on leaf gas exchange relationships and the modeled in-canopy light distribution. *Agricultural and Forest Meteorology*, **152**, 201–211.
- Moreau, D., Allard, V. and Gaju, O. (2012) Acclimation of leaf nitrogen to vertical light gradient at anthesis in wheat is a whole-plant process that scales with the size of the canopy. *Plant physiology*, **160**, 1479–1490.
- Müller, J., Behrens, T. and Diepenbrock, W. (2005) Measurement and modelling of canopy gas exchange of oilseed rape. *Agricultural and Forest Meteorology*, **132**, 181–200.
- Müller, J., Eschenröder, A. and Diepenbrock, W. (2009) Through-flow chamber CO₂/H₂O canopy gas exchange system — Construction, microclimate, errors, and measurements in a barley (*Hordeum vulgare* L.) field. *Agricultural and Forest Meteorology*, **149**, 214–229.

- Poni, S., Magnanini, E. and Rebutti, B. (1997) An automated chamber system for measurements of whole-vine gas exchange. *HortScience*, **32**, 64–67.
- Poni, S., Merli, M.C., Magnanini, E. *et al.* (2014) An improved multichamber gas exchange system for determining whole canopy water use efficiency in the grapevine. *American Journal of Enology and Viticulture*, **65**, 268–276.
- Reichstein, M., Falge, E., Baldocchi, D. *et al.* (2005) On the separation of net ecosystem exchange into assimilation and ecosystem respiration: review and improved algorithm. *Global Change Biology*, **11**, 1424–1439.
- Shangguan, Z., Shao, M. and Dyckmans, J. (2000) Nitrogen nutrition and water stress effects on leaf photosynthetic gas exchange and water use efficiency in winter wheat. *Environmental and Experimental Botany*, **44**, 141–149.
- Struik, P.C., Amaducci, S., Bullard, M.J. *et al.* (2000) Agronomy of fibre hemp (*Cannabis sativa* L.) in Europe. *Industrial Crops and Products*, **11**, 107–118.
- Takahashi, N., Ling, P.P. and Frantz, J.M. (2008) Considerations for accurate whole plant photosynthesis measurement. *Environmental Control in Biology*, **46**, 91–101.
- Tomás, M., Medrano, H., Pou, A. *et al.* (2012) Water-use efficiency in grapevine cultivars grown under controlled conditions: effects of water stress at the leaf and whole-plant level. *Australian Journal of Grape and Wine Research*, **18**, 164–172.
- Van den Boogaard, R., Kostadinova, S., Veneklaas, E. *et al.* (1995) Association of water use efficiency and nitrogen use efficiency with photosynthetic characteristics of two wheat cultivars. *Journal of Experimental Botany*, **46**, 1429–1438.
- Van Laar, H.H., Goudriaan, J. and van Keulen, H. (1997) *SUCROS97: Simulation of crop growth for potential and water-limited production situations, as applied to spring wheat*. Wageningen, The Netherlands.
- Von Caemmerer, S. and Farquhar, G.D. (1981) Some relationships between the biochemistry of photosynthesis and the gas exchange of leaves. *Planta*, **153**, 376–387.
- Wright, J., Williams, M., Starr, G. *et al.* (2013) Measured and modelled leaf and stand-scale productivity across a soil moisture gradient and a severe drought. *Plant, Cell & Environment*, **36**, 467–483.
- Yin, X. and Struik, P.C. (2009) C₃ and C₄ photosynthesis models: An overview from the perspective of crop modelling. *NJAS - Wageningen Journal of Life Sciences*, **57**, 27–38.
- Yin, X. and Struik, P.C. (2017) Can increased leaf photosynthesis be converted into higher crop mass production? A simulation study for rice using the crop model GECROS. *Journal of Experimental Botany*, **68**, 2345–2360.
- Yin, X. and Van Laar, H.H. (2005) *Crop systems dynamics: an ecophysiological simulation model for genotype-by-environment interactions*, Wageningen Academic, Wageningen, the Netherlands.
- Yin, X., Lantinga, E.A. and Schapendonk, A.H.C.M. *et al.* (2003) Some quantitative relationships between leaf area index and canopy nitrogen content and distribution. *Annals of Botany*, **91**, 893–903.

Supplementary Materials in Chapter 5

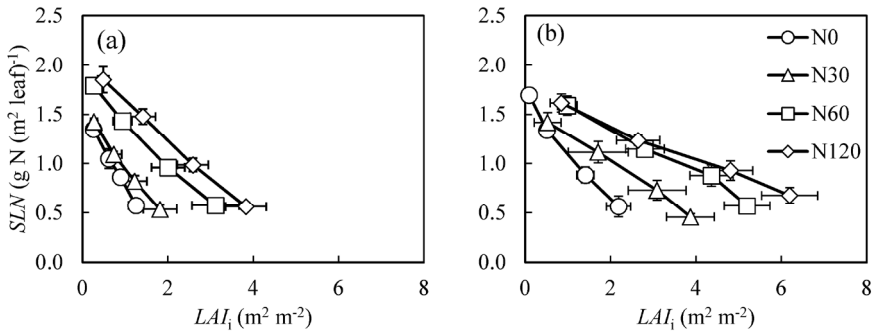


Figure S5.1 Specific leaf nitrogen (SLN) against the leaf area index at depth i measured from the top (LAI_i). Data presented was obtained at linear growth (on 17 June in panel a) and at full flowering (on 23 July in panel b) in 2015. N0, N30, N60, N120 denote nitrogen fertilization rate in 2015 at 0, 30, 60 and 120 kg N ha⁻¹, respectively.

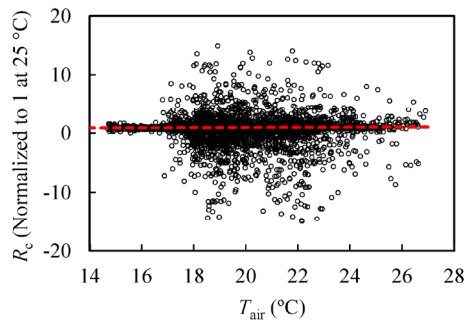


Figure S5.2 Normalized canopy respiration (R_c) in relation to air temperature T_{air} .

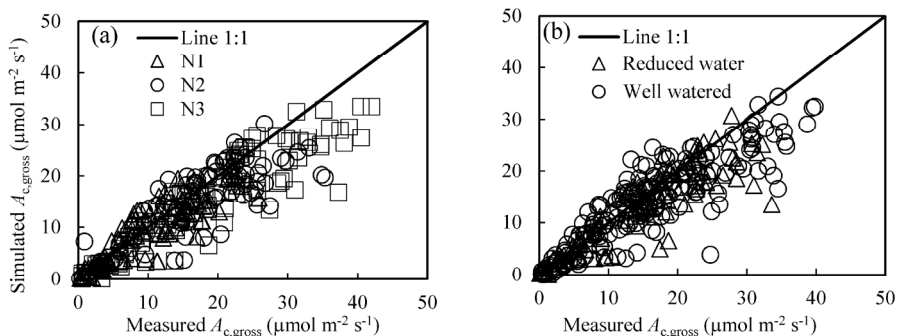


Figure S5.3 Plots of simulated $A_{c, gross}$ against measured $A_{c, gross}$ under different nitrogen and water regimes. Data presented were collected in CAN1. To avoid overcrowding of data points, only one tenth of the data is presented. N1, N2 and N3 denote the level of received nitrogen, see text for details.

Table S5.1 List of parameters (\pm standard error, if applicable) of leaf photosynthesis model.

Category	Symbol	Definition	Unit	Value	Reference
Leaf respiration	χ_{Rd}	Slope of linear relationship between R_{d25} and $(SLN-n_b)^a$	$\mu\text{mol s}^{-1} (\text{g N})^{-1}$	1.06 ± 0.08	Chapter 4
	E_{Rd}	Activation energy for R_d	J mol^{-1}	21634 ± 4085	Chapter 4
e- transport	$\chi_{J_{\max}}$	Slope of linear relationship between $J_{\max25}$ and $(SLN-n_b)^a$	$\mu\text{mol s}^{-1} (\text{g N})^{-1}$	220.7 ± 11.2	Chapter 4
	$E_{J_{\max}}$	Activation energy for J_{\max}	J mol^{-1}	67292 ± 35986	Chapter 4
	$D_{J_{\max}}$	Deactivation energy for J_{\max}	J mol^{-1}	114701 ± 28710	Chapter 4
	$S_{J_{\max}}$	Entropy term for J_{\max}	$\text{J K}^{-1} \text{mol}^{-1}$	375 ± 82	Chapter 4
	κ_{2LL}	Efficiency of converting incident irradiance into linear electron transport (J) under limiting light		0.21 ± 0.004	Chapter 4
Enzyme kinetics and activity	θ	Convexity factor for the response of J to J_{inc}	-	0.70	Ögren & Evans, 1993
	$\chi_{V_{\text{emax}}}$	Slope of linear relationship between $V_{\text{emax}25}$ and $(SLN-n_b)^a$	$\mu\text{mol s}^{-1} (\text{g N})^{-1}$	101.3 ± 5.7	Chapter 4
	$E_{V_{\text{emax}}}$	Activation energy for V_{emax}	J mol^{-1}	63024 ± 1562	Chapter 4
	Γ^* at 25 °C		$\mu\text{mol mol}^{-1}$	37.5	Bernacchi et al., 2002
	E_{Γ^*}	Activation energy for Γ^*	J mol^{-1}	24460	Bernacchi et al., 2002
	$K_{\text{mC}25}$	K_{mC} at 25 °C	$\mu\text{mol mol}^{-1}$	272	Bernacchi et al., 2002
	$E_{K_{\text{mC}}}$	Activation energy for K_{mC}	J mol^{-1}	80990	Bernacchi et al., 2002
	$K_{\text{mO}25}$	K_{mO} at 25 °C	mmol mol^{-1}	165	Bernacchi et al., 2002
	$E_{K_{\text{mO}}}$	Activation energy for K_{mO}	J mol^{-1}	23720	Bernacchi et al., 2002
	χ_{T_p}	Slope of linear relationship between T_{p25} and $(SLN-n_b)^a$	$\mu\text{mol s}^{-1} (\text{g N})^{-1}$	9.3 ± 0.7	Chapter 4
	E_{T_p}	Activation energy for T_p	J mol^{-1}	34417 ± 5298	Chapter 4
CO ₂ diffusion	g_{s0}	Minimum stomatal conductance	$\text{mol m}^{-2} \text{s}^{-1}$	0.11 ± 0.04^b	
	a_1	Empirical constant for g_s response to I/PPD	-	1.13 ± 0.10^b	
	b_1	Empirical constant for g_s response to I/PPD	kPa^{-1}	0.42 ± 0.03^b	
	E_{b1}	Activation energy for b_1	J mol^{-1}	-51755 ± 6389.4^b	
	r_{m-T_s}	Ratio of mesophyll: stomatal resistances	-	1.05^b	

^a: SLN denotes specific leaf nitrogen, with which photosynthetically active leaf nitrogen is defined as $SLN-n_b$, n_b was assumed to be the SLN of senesced leaves, measured at 0.25 g N m⁻² in this study.

^b: the value was derived using the data collected in Chapter 4 for the purpose of the present study.

Text S5.1 Summary information for the models used in Chapter 5

Leaf photosynthesis model The model of Farquhar, von Caemmerer & Berry (1980; the FvCB model hereafter) calculates net CO₂-assimilation rate (A) as the minimum of the Rubisco-limited (A_c), electron (e^-) transport-limited (A_j), and triose phosphate utilisation-limited (A_p) rates. The three limiting rates can be expressed collectively as:

$$A = \frac{(C_c - \Gamma^*)x_1}{C_c + x_2} - R_d \quad (\text{S5.1})$$

where for A_c : $x_1 = V_{\text{cmax}}$ and $x_2 = K_{\text{mC}}(1+O/K_{\text{mO}})$; for A_j : $x_1 = J/4$ and $x_2 = 2\Gamma^*$; and for A_p : $x_1 = 3T_p$ and $x_2 = -\Gamma^*$. In the model, C_c and O are the CO₂ and O₂ level, respectively, at the carboxylation sites of Rubisco, Γ^* is the CO₂ compensation point in the absence of day respiration (R_d), and J is the linear e^- transport rate and is described as a function of incident irradiance I_{inc} as:

$$J = \left(\kappa_{2\text{LL}} I_{\text{inc}} + J_{\text{max}} - \sqrt{(\kappa_{2\text{LL}} I_{\text{inc}} + J_{\text{max}})^2 - 4\theta J_{\text{max}} \kappa_{2\text{LL}} I_{\text{inc}}} \right) / (2\theta) \quad (\text{S5.2})$$

The sub-model for stomatal conductance for CO₂ transfer (g_s) is:

$$g_s = g_0 + \frac{A + R_d}{C_i - C_{i^*}} f_{\text{vpd}} \quad (\text{S5.3})$$

where g_0 is the residual value of g_s when irradiance approaches to zero, C_{i^*} is the intercellular CO₂ level (C_i) at which $A+R_d = 0$, and f_{vpd} is the relative effect of the leaf-to-air vapour difference (VPD) on g_s (see later).

CO₂ transfer from C_a (the ambient CO₂ level) to C_c can be written as (Flexas *et al.* 2013):

$$C_i = C_a - A(1/g_b + 1/g_s) \quad (\text{S5.4})$$

$$C_c = C_i - A/g_m \quad (\text{S5.5})$$

Combining Eqns (S5.1, S5.3–S5.5) gives a standard cubic equation for solution to A . The solution is complicated and not shown here but see Yin & Struik (2009, 2017).

In the g_s model, Eqn (S5.3), f_{vpd} is the function for the effect of VPD, which may be described phenomenologically as (Yin & Struik 2009):

$$f_{\text{vpd}} = \frac{1}{1/(a_1 - b_1 \cdot \text{VPD}) - 1} \quad (\text{S5.6})$$

where a_1 and b_1 represent the $C_i:C_a$ ratio in water vapour saturated air and the slope of the decrease of this ratio with increasing VPD, respectively, if g_0 approaches nil.

A number of parameters are related to leaf temperature (T_L), and some of these can be described by the Arrhenius equation normalised with respect to 25°C:

$$\text{Parameter} = \text{Parameter}_{25} \cdot e^{\left(\frac{1}{298} - \frac{1}{273+T_L}\right) \frac{E}{R}} \quad (\text{S5.7})$$

where R is the universal gas constant (8.314 J K⁻¹ mol⁻¹). Eqn (S5.7) applies to R_d , F^* , V_{cmax} , K_{mC} , K_{mO} , T_p , and b_1 . The temperature response of J_{max} is described by the modified Arrhenius equation:

$$\text{Parameter} = \text{Parameter}_{25} \cdot e^{\left(\frac{1}{298} - \frac{1}{273+T_L}\right) \frac{E}{R}} \cdot \frac{1 + e^{(S-D/298)/R}}{1 + e^{[S-D/(273+T_L)]/R}} \quad (\text{S5.8})$$

The values at 25°C of parameters R_d , V_{cmax} , J_{max} , and T_p can be further quantified as a linear function of specific leaf nitrogen (SLN) above a certain base value (n_b), at or below which leaf photosynthesis is zero:

$$\text{Parameter}_{25} = \chi(SLN - n_b) \quad (\text{S5.9})$$

where χ have different values for different parameters.

All these parameter values were based on our previous estimate for hemp (Chapter 4) or based on the literature for those conservative parameter values in C₃ species (see Supplementary Material Table S5.1).

Leaf transpiration model When there is no water stress, photosynthesis rate largely determines the transpiration rate. The basic equation to estimate potential leaf transpiration, E_p , is the Penman-Monteith equation (Monteith 1973):

$$E_p = \frac{sR_n + \rho c_p D_a / r_{\text{bh}}}{\lambda \{s + \gamma [(r_{\text{bw}} + r_{\text{sw,p}}) / r_{\text{bh}}]\}} \quad (\text{S5.10})$$

where R_n is net absorbed radiation, r_{bh} and r_{bw} are the boundary layer resistance to heat and water transfer, respectively, $r_{\text{sw,p}}$ is the stomatal resistance to water transfer if there is no water stress, D_a is saturation vapour pressure deficit of the external air, ρc_p is volumetric heat capacity of air, λ is the latent heat of vapourisation of water, γ is the psychrometric constant. Calculation of r_{bw} , r_{bh} , and R_n was the same as used in the GECROS model (Yin & Struik 2017).

In the presence of water limitation, actual transpiration is assumed to be the amount of actual available water. Then, the change of actual stomatal resistance to water vapour ($r_{\text{sw,a}}$) due to stomatal closure was obtained (see Eqn 5.7 in the main text), and this actual $r_{\text{sw,a}}$ was then used to calculate actual photosynthesis using an analytical, quadratic solution as presented by Yin & Struik 2017).

Scaling up to canopy The sun/shade model (de Pury & Farquhar 1997) is adopted, in which the canopy is divided into sunlit and shaded fractions and each fraction is modelled separately with a single-layer leaf model (described above).

Radiation absorbed by a canopy, I_c , was determined as:

$$I_c = (1 - \rho_{cb})I_{b0}(1 - e^{-k'_b L}) + (1 - \rho_{cd})I_{d0}(1 - e^{-k'_d L}) \quad (S5.11)$$

where I_{b0} and I_{d0} are incident direct-beam and diffuse radiation above the canopy, ρ_{cb} and ρ_{cd} are canopy reflection coefficient for direct-beam and diffuse light, respectively, k'_b and k'_d are extinction coefficients for beam and scattered beam, diffuse and scattered diffuse lights, respectively.

Radiation absorbed by the sunlit fraction of the canopy, $I_{c,su}$, is given as the sum of direct-beam, diffuse, and scattered beam components (de Pury & Farquhar 1997):

$$I_{c,su} = (1 - \sigma)I_{b0}(1 - e^{-k'_b L}) + (1 - \rho_{cd})I_{d0} \frac{k'_d [1 - e^{-(k'_d + k'_b)L}]}{k'_d + k'_b} + I_{b0} \left\{ (1 - \rho_{cb}) \frac{k'_b [1 - e^{-(k'_b + k'_b)L}]}{k'_b + k'_b} - (1 - \sigma) \frac{1 - e^{-2k'_b L}}{2} \right\} \quad (S5.12)$$

where σ is leaf scattering coefficient.

Radiation absorbed by the shaded fraction of the canopy, $I_{c,sh}$, is calculated as the difference between the total radiation absorbed by the canopy, I_c , and the radiation absorbed by the sunlit fraction, $I_{c,su}$ (de Pury & Farquhar 1997):

$$I_{c,sh} = I_c - I_{c,su} \quad (S5.13)$$

Eqns (S5.11-S5.13) were applied separately to visible or photosynthetically active radiation (PAR) and near-infrared radiation (NIR), because they have different values for σ , ρ_{cb} , ρ_{cd} , k'_b , k'_b and k'_d . The model assumes that half of the incident solar radiation is in the visible and other half is in the NIR waveband. All these coefficients are described as in GECROS (Yin & Struik 2017).

Many photosynthetic parameters are related to SLN , and r_{bh} and r_{bw} are related to wind speed u . Both SLN and u change with the depth of the canopy. To estimate these parameters for the entire canopy, and for the sunlit and shaded fractions of the canopy, photosynthetically active leaf nitrogen has to be scaled up. Assuming an exponential profile for the vertical decline of SLN in the canopy (Supplementary Material Figure S5.1), photosynthetically active nitrogen for the entire canopy (N_{cp}), for the sunlit

fraction of the canopy ($N_{cp,su}$) and for the shaded fraction of the canopy ($N_{cp,sh}$), can be estimated by (Yin & van Laar 2005):

$$N_{cp} = SLN_0(1 - e^{-k_n L}) / k_n - n_b L \quad (S5.14)$$

$$N_{cp,su} = SLN_0[1 - e^{-(k_n + k_b)L}] / (k_n + k_b) - n_b(1 - e^{-k_b L}) / k_b \quad (S5.15)$$

$$N_{cp,sh} = N_{cp} - N_{cp,su} \quad (S5.16)$$

where SLN_0 is the SLN for uppermost leaves, k_n is the leaf nitrogen extinction coefficient in the canopy (see the main text). With a similar logic, boundary-layer conductance can be scaled up to the canopy level.

References used in Text S5.1 and Table S1 not already cited in main text

- Bernacchi, C.J., Portis, A.R., Nakano, H. *et al.* (2002) Temperature response of mesophyll conductance. Implications for the determination of Rubisco enzyme kinetics and for limitations to photosynthesis in vivo. *Plant Physiology*, **130**, 1992–1998.
- de Pury, D. and Farquhar, G. (1997) Simple scaling of photosynthesis from leaves to canopies without the errors of big-leaf models. *Plant, Cell & Environment*, **20**, 537–557.
- Farquhar, G.D., von Caemmerer, S. and Berry, J.A. (1980) A biochemical model of photosynthetic CO₂ assimilation in leaves of C₃ species. *Planta*, **149**, 78–90.
- Flexas, J., Niinemets, Ü., Gallé, A. *et al.* (2013) Diffusional conductances to CO₂ as a target for increasing photosynthesis and photosynthetic water-use efficiency. *Photosynthesis research*, **117**, 45–59.
- Monteith, J.L. (1973) *Principles of environmental physics*. Edward Arnold, London, UK.
- Ögren, E. and Evans, J. (1993) Photosynthetic light-response curves. *Planta*, **189**, 182–190.

Chapter 6

General discussion

Abstract

This chapter first provides a brief summary of the main findings presented in the previous chapters. Subsequently, in view of these findings and information from the literature, the potential of hemp for the sustainable development of the agricultural bio-economy is discussed. In the final section, implications for future research are discussed, focusing on the need for crop modelling to develop strategies to optimise cultivation and breeding in hemp.

6.1 Introduction

The multiple societal challenges such as climate change, natural resource scarcity and environmental pollution have fuelled interests in sustainable development of the agricultural bio-economy. In Chapter 1 of this thesis I argued that hemp may be a multi-purpose crop that fits well in the context of sustainable bio-economy. However, hemp remains poorly developed because hemp production declined in the last century and was displaced largely by cotton and synthetic fibres. Therefore, the EC funded project Multihemp (www.multihemp.eu) was launched in 2012 with the aim to have significant impacts from both scientific and economic aspects, by building on fundamental scientific understanding from the development of hemp raw materials through to providing the basis for innovations in the areas of crop breeding, agronomy and harvesting, and biorefinery. Within the framework of Multihemp, this thesis reports key research findings on the agronomy of hemp production and the photosynthesis physiology of hemp's resource-use efficiencies (RUE). This chapter broadens the discussion of preceding chapters to the overall achievements and to critical issues for bio-economically sustainable hemp production. Specifically, the following sections are presented: (1) advances made in agronomic aspects; (2) insights into photosynthesis physiology of hemp; (3) hemp production for the development of a sustainable bio-economy; and (4) implications for future research: crop modelling to develop strategies for optimisation of cultivation and breeding in hemp.

6.2 Advances made in agronomic aspects

Driven by the shift of a rapidly expanding market for hemp seeds coupled with lower-quality fibre requirements for innovative biomaterials, harvesting hemp for both stems and seeds is now a common practice in Europe while crop management strategies for the dual-purpose hemp cultivation have not been properly addressed so far. To support the dual-purpose cultivation of hemp, this thesis brought new information on the agronomy of hemp production, paying attention to cultivar choice (Chapter 2) and management of planting density and nitrogen fertilization (Chapter 3).

The number of available hemp cultivars has risen rapidly since the 1990s, when hemp cultivation was progressively authorized throughout the EU. Currently, there are more than 60 hemp cultivars registered in the common catalogue of varieties of agricultural plant species (<https://ec.europa.eu/>). Given that these cultivars differ in many traits related either to quantity or to quality of their products, and that large environmental effects on the yields of stems and

seeds have been widely reported (Cosentino *et al.*, 2013; Faux *et al.*, 2013; Höppner & Menge-Hartmann, 2007; Struik *et al.*, 2000), to choose a cultivar that is suitable for a particular environment is of paramount importance to the success of hemp cultivation. In Chapter 2, productivity of 14 commercial cultivars was investigated under contrasting European environments. The results showed that hemp stem yield was strictly related to the duration of the vegetative phase while seed yield was low in the late flowering cultivars (Figures 2.4, 2.6). Thus, for dual-purpose hemp production, a cultivar that gives a long vegetative phase while leaves enough time for seed growth is preferable. In addition, the results also suggested that genotype-specific characteristics, such as sex type and stem fibre content, are important to maximize economic return of hemp cultivation. A monoecious cultivar with a high bark fibre content is preferable because bark fibre is considered more valuable than wood core and the male plants of dioecious cultivar senesce soon after flowering that causes biomass loss and heterogeneous quality.

The duration of the vegetative phase of a hemp crop is mainly affected by genotype and environment (Figure 2.2). Hemp development rate increases with increasing temperature between a base and a cut-off temperature, and as a short-day plant, hemp development rate also increases with decreasing day-length during the photoperiod-sensitive phase (Amaducci *et al.*, 2008a). Thus, a few studies have aimed at predicting hemp flowering time using genotype-specific parameters, temperature and photoperiod (Cosentino *et al.*, 2012; Amaducci *et al.*, 2008a; Lisson *et al.*, 2000d). Results of this thesis showed that the phenological model proposed by Amaducci *et al.* (2008a) renders a good estimation of hemp flowering time under contrasting environments (Figure 2.3). Such a model could, therefore, facilitate cultivar choice basing on historical meteorological information and genotype-specific parameter values.

Planting density is an important factor for growing hemp as it relates to the quantity of seed input and may affect the quantity and quality of stem and seed yields (see review by Amaducci *et al.*, 2015). In Chapter 3, a series of planting densities ranging from 30 plants m⁻² to 240 plants m⁻² were tested for their effects on stem and seed yields under contrasting environments. The results showed that increasing planting density resulted in thin and short stems (Figure 3.5) while it had limited effect on the yields of stem and seed (Figures 3.1, 3.2). Slender stems contain a higher percentage of long fibre (Westerhuis *et al.*, 2009) and require less energy for their mechanical processing (Khan *et al.*, 2010) that is desirable for fibre targeted production (Westerhuis *et al.*, 2009). But the pursuit of stem slenderness through a very dense crop is not encouraged because it not only increases the risk of lodging but also results in high fibre loss

during processing (Amaducci *et al.*, 2008b; Amaducci *et al.*, 2005). On the other hand, planting at extremely low density could result in reduction in biomass yield due to delayed canopy closure and weed competition (authors' experience). The optimum planting density for dual-purpose hemp cultivation could be set at 90–150 plants m⁻².

Optimization of crop nitrogen fertilization is a key issue for sustainable development of the agricultural bio-economy. The responses of hemp crops to nitrogen fertilization under contrasting environments were tested in Chapter 3. While the yields of stem and seed were limited by insufficient nitrogen supply (Figures 3.1, 3.2), this effect varied considerably, depending on soil fertility. In line with previous studies (Amaducci *et al.*, 2002; Struik *et al.*, 2000), the effect of nitrogen fertilization on hemp stem and seed yields did not interact with planting density.

There were a number of studies that addressed the effect of nitrogen fertilization on hemp productivity (Campiglia *et al.*, 2017; Finnan & Burke, 2013). However, none of them has quantified the nitrogen demand of this crop. Chapter 3 filled this knowledge gap up by analysing the dynamics of hemp nitrogen uptake and then determining a critical nitrogen (N_{critical}) dilution curve for hemp crop (Figure 3.7). The N_{critical} of hemp is comparable with that of linseed but indicates a lower nitrogen requirement than found for other C₃ crops for producing the same biomass, such as rice (*ssp. japonica*; Ata-UI-Karim *et al.*, 2013) and cotton (Xiaoping *et al.*, 2007). This result confirms the widely reported low fertilization requirement of the hemp crop (Finnan & Burke, 2013; Struik *et al.*, 2000). Moreover, the presented N_{critical} dilution curve is a useful tool to quantify crop nitrogen status (Lemaire *et al.*, 2008). Based on this curve a nitrogen nutrition index (NNI) can be calculated as the ratio of $N: N_{\text{critical}}$, where N is actual nitrogen concentration in aboveground biomass. $NNI < 1$ indicates nitrogen is limiting while $NNI > 1$ indicates nitrogen is sufficient (Lemaire *et al.*, 2008).

6.3 Insights into photosynthesis physiology of hemp

This section focuses on hemp's RUE at leaf and canopy levels, basing on the assessments of its photosynthetic capacity conducted in Chapters 4 and 5. It is argued that photosynthesis is central for interpreting biomass production in response to genotype, environment, management interactions and hemp's high RUE.

While the mechanisms of leaf photosynthesis have been studied in detail for major crops, those of hemp have rarely been investigated. In Chapter 4, based on the C₃ leaf photosynthesis

model of Farquhar *et al.* (1980), the responses of hemp photosynthesis to leaf nitrogen status and environmental factors were analysed following the procedures described in Yin *et al.* (2009), and a complete set of photosynthetic parameters were made available for hemp (Figure 4.6). These parameters provide fundamental information for the understandings of hemp's RUE at leaf level (Figure 4.7), and for the modelling of hemp growth. However, caution is needed when modelling photosynthesis rate using the value of parameters derived from different environments. In this thesis, it was found that the effects of leaf nitrogen and temperature on almost all photosynthesis parameters were consistent at different leaf positions and among different growth environments. The exception is the effect on the efficiency of converting incident irradiance into linear electron transport under limiting light (κ_{2LL}), and the value of κ_{2LL} was higher for plants grown in the glasshouse than for those grown outdoors (Figure 4.6).

Based on the results obtained in Chapter 4, the leaf photosynthesis of hemp was scaled up to canopy level in Chapter 5 with the aim to assess water-use efficiency (WUE) and nitrogen-use efficiency (NUE) in relation to levels of water and nitrogen supply. The results showed that the WUE_c (defined as the ratio of gross canopy photosynthesis to canopy transpiration) and the NUE_c (the ratio of the gross canopy photosynthesis to canopy leaf-N content) decreased with an increase in nitrogen-input levels; these effects were largely determined by the nitrogen effect on LAI (Figure 5.10). Water stress resulted in an increase in WUE_c but a decrease in NUE_c . The effect of short-term water stress was reflected by stomatal regulation, whereas the long-term stress increased leaf senescence, decreased LAI but retained total canopy nitrogen content. The lost LAI coupled with the increased average leaf-nitrogen content resulted in a further increase in WUE_c (Figure 5.10). These results not only imply that hemp's final biomass yield and nitrogen use efficiency may be restricted by water limitation during growth (Cosentino *et al.*, 2013), but also suggest that crop models should take stress-induced senescence into account in addition to stomatal effects if crops experience a prolonged water stress during growth.

An innovative aspect in Chapter 5 of this thesis is that a multi-chamber system (Poni *et al.*, 2014) was used to determine hemp canopy gas exchange. To date, the canopy gas exchange rate is mainly assessed by micro-meteorological methods or by means of canopy-enclosure chamber systems. The micro-meteorological techniques such as the eddy covariance or Bowen ratio methods enable gas flux measurements without disturbing canopy micro-environment, and they are often applied to large homogeneous areas but do not suit for plot/pot-sized experiments (Jones, 2013). In contrast, the canopy chamber technique enables to determine precisely canopy gas exchange at a relatively small scale (Müller *et al.*, 2009; Müller *et al.*, 2005) that is a useful

tool to assess crop responses to nitrogen deficiency and water shortage at canopy scale. However, in line with previous studies (Müller *et al.*, 2009; Poni *et al.*, 1997), the presence of the chamber wall had a significant effect on the micro-environment within the chambers (Figure 5.3) due to photosynthetic CO₂ uptake, the greenhouse effect and transpiration. Results of model analysis showed that the micro-environment conditions within the chamber had large effects on canopy gas exchange and this effect were larger in the chambers with higher fertilization rate and lower water supply (Table 5.4). Therefore, a model based approach was applied to normalize measurements within different chambers to avoid any confounding effect due to the differences in chamber in micro-environmental factors (Chapter 5).

6.4 Hemp production for the development of a sustainable bio-economy

Hemp can be considered an exemplary crop to develop and promote the concept of bio-economy (Fike, 2016; Amaducci *et al.*, 2015; Finnan & Styles, 2013) as it produces a high and valuable biomass yield while requiring low inputs. This section assesses the productivity of hemp crops and its environmental effects.

6.4.1 The productivity of hemp

The high productivity of hemp is confirmed in this thesis (Table 2.8). The maximum stem yield measured in this study was 22.7 Mg ha⁻¹. This yield was slightly higher than the maximum stem yield reported in a previous work that compared hemp yield potential across Europe (Struik *et al.*, 2000). Results of the comprehensive field experiments conducted in the present study and that in the literature suggested that typical hemp stem yield were in the broad range of about 5–15 Mg ha⁻¹ (Aubin *et al.*, 2016; Finnan & Burke, 2013; Höppner & Menge-Hartmann, 2007; Struik *et al.*, 2000). The observed hemp stem yields were likely limited, to some extent, by the production of seeds in many studies. Mostly cultivated for harvesting stem and seeds simultaneously, Carus *et al.* (2013) and Carus & Sarmiento (2016) reported that the industrial yield of hemp stem across Europe is on average 7 Mg ha⁻¹. In Canada, where cultivation of hemp is mainly for harvesting seeds, Vera *et al.* (2010) and Aubin *et al.* (2016) reported the stem yields of 4–7 Mg ha⁻¹.

Earlier studies had revealed that light-use efficiency (LUE) of hemp was low after flowering (De Meijer *et al.*, 1995). Struik *et al.* (2000) reported that hemp crop had LUE at 2.2–2.3 g MJ⁻¹ (on the basis of intercepted photosynthetically active radiation) during vegetative phase while this value decreased to 1.0–1.1 g MJ⁻¹ after flowering. Van der Werf *et al.* (1994) analysed the

effect of flowering on hemp LUE and pointed out that a minor part of the post-flowering decline in the LUE of hemp can be accounted for by larger losses of shed leaves and increased growth respiration due to the synthesis of fat and protein in the seed. The results of this thesis suggested that a major part of the decline of LUE after flowering is likely caused by reduction of crop gross photosynthesis due to senescence of the leaves (Figure 4.2).

The yields of hemp seed ranged from none up to 2.3 Mg ha⁻¹ in this thesis. Cherney & Small (2016) pointed out that the present productivity of hemp seeds, about 1.0 Mg ha⁻¹ under good conditions, occasionally 1.5–2.0 Mg ha⁻¹, is not yet sufficient for the crop to be competitive with major oilseeds. However, the reported yields of hemp seed were, to some extent, underestimated due to shattering prior to and during harvesting as a result of heterogeneity in inflorescence maturity (Figure 6.1), particularly if harvested outside the optimal harvest time windows, ranging between 50% and 70% maturity. Another important reason for the underestimation of the hemp seed yield was bird predation. Bird predation can cause a significant loss of seed but measures of prevention such as using nets or bird scarers are hardly economically successful. At present, losses up to 30% of the hemp seed yields are not uncommon (Cherney & Small, 2016). Therefore, great improvement of hemp seed yield may be achieved through reducing loss due to shattering. To this end, breeder could select for shattering resistant cultivars while technical engineering could improve harvesting machines.

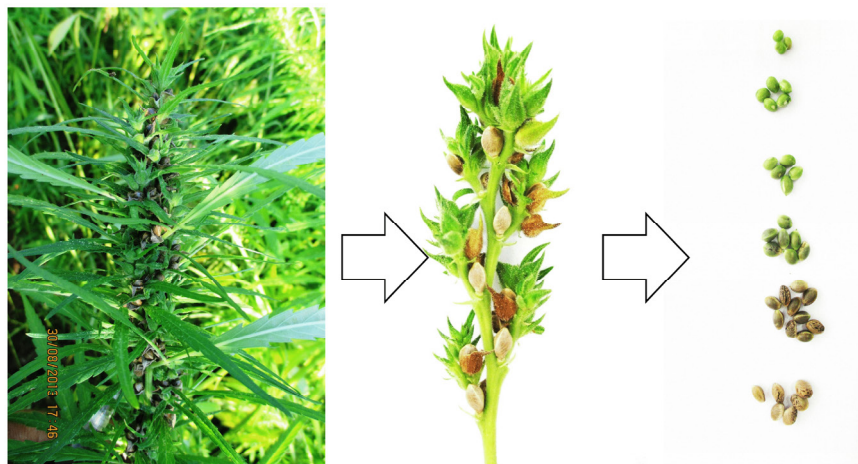


Figure 6.1 Heterogeneity in inflorescence maturity of hemp. From left to right: inflorescence of individual plant, a branch on the inflorescence (small leaves have been removed), seeds in the same branch.

6.4.2 The environmental effects of hemp cultivation

Hemp is advantageous over other annual crops in terms of their impact on environment. Firstly, as discussed previously, hemp has a high nitrogen-use efficiency and requires low nitrogen inputs (Chapters 3, 4). In addition, hemp was generously fertilized with manure in the past, and is naturally adapted to employing mammalian manure as fertilizer. It, therefore, has the potential of efficiently employing stocks of livestock manure. A study carried out within the framework of Multihemp to compare the carbon footprint of flax, hemp, jute and kenaf for the natural fibres consumed in Europe (Barth & Carus, 2015) suggested that use of organic fertilizer for hemp cultivation could minimize greenhouse gas emissions that puts hemp ahead of the other crops.

Secondly, hemp cultivation is virtually free of herbicides and pesticides, which may reduce biodiversity. Hemp generally has few problems of weed due to its ability to outcompete most weed species under favourable conditions. However, several weeds may occur in hemp field when canopy closure is limited by insufficient nutrition supply, low planting density, pre-flowering, drought, *etc.* The species of weeds differ among environments. Legros *et al.* (2013) identified six main weed species in a French field, including weeds from the *Sinapis* and *Chenopodium* genera. In Northern Italy, *Echinochloa crus-galli* occurred dominantly and it caused significant yield loss in our study in the field trials carried out in 2014 (Chapter 3). Hemp can also be affected by parasitic and climbing weeds. Parasitic plants, such as broomrape (*Orobancha* L.) and dodder (*Cuscuta* L.), can cause hemp plants to die before maturity and reduce productivity. Although some form of weed control may be needed to prevent economic losses, no herbicide is currently registered for use on hemp. Different trials carried out in France (Legros *et al.*, 2013) showed that hemp crops are sensitive to herbicides, especially when they are applied before sowing or immediately after emergence. It is common to see several bugs on the inflorescence of hemp plants and some diseases have been identified (Van der Werf *et al.*, 1995). A list of management practices and biological control agents for hemp pests and diseases have been made available (McPartland *et al.*, 2000) while some do not consider the pests and diseases a problem of economic consequence (Desanlis *et al.*, 2013).

Thirdly, hemp has potential to improve soil quality. Hemp has a deep root system (Amaducci *et al.*, 2008c) that decays rapidly to provide both soil aeration and fertilization for the subsequent crops. Gorchs *et al.* (2017) reported that, after growing hemp, the yield of subsequent wheat increased by 1368 kg ha⁻¹ and 155 kg ha⁻¹ in the subsequent first and second years, respectively, to the wheat monoculture. Moreover, several studies suggested that hemp

has the capability to decontaminate soils that are polluted with heavy metals (Angelova *et al.*, 2004; Linger *et al.*, 2002).

6.5 Implication on future research: crop modelling to develop strategies for optimisation of cultivation and breeding in hemp

In order to favour the need of high-quality hemp raw materials, field trials have undoubtedly been considered the most direct ways in understanding the effects of genotype-by-environment-by-management interactions ($G \times E \times M$) on hemp production. However, except being costly and labour intensive, field trials are easily affected by many undesirable factors due to the complicated field conditions (Amaducci *et al.*, 2000). Since the pioneering work on crop modelling by De Wit (1959), crop growth models have been applied extensively in support of the theoretical research, yield prediction, and decision making in agriculture (Yin & Struik, 2010) and examples have been reported widely (Keating *et al.*, 2003). As exemplified by the successful applications for staple crops (Bouman *et al.*, 2007; Aggarwal *et al.*, 1997), crop growth models that are based on physiological mechanisms, capture crop growth and development processes in response to management, genotypic, soil and climate factors, have a potential to design strategies for improving hemp production. Furthermore, recent studies successfully integrated the genetic information into advanced crop models (Gu *et al.*, 2014; Prudent *et al.*, 2011), showing the possibility of using crop growth models to assist breeding. For these reasons, developing a heuristic hemp growth model that is based on fundamental understanding of the effects of $G \times E \times M$ on hemp biomass production is necessary to develop strategies for optimization of cultivation and breeding in hemp.

Several attempts have been made for modelling hemp production. For estimating the potential of hemp as a crop for sustainable farming systems in temperate regions, based on experimental results, Van der Werf *et al.* (1996) described the first hemp growth model (LINTUL-hemp) on the basis of “light interception and utilization” concept. The LINTUL-hemp focused on the assessment of hemp potential production, ignored the larger variation of hemp growth due to the changing environmental variables and different genotypes, and therefore has a limited value for analysing hemp production in response to $G \times E \times M$ under field conditions. Inspired by the criteria of Carberry *et al.* (1992) for kenaf (*Hybiscus cannabinus* L.), a short-day plant similar to hemp, Lisson *et al.* (2000a–d) quantified hemp phenology and LAI in response to environmental variables and plant density and developed a model called APSIM-Hemp for simulating the growth, development and yield of hemp in response to

climatic, soil and management. These studies, to some extent, explored the hemp model development. However, they were developed on the basis of limited, largely agronomic perspectives and observations. Many summary concepts (e.g. LUE) were used in the description of complicated physiological mechanisms. Important yield relevant factors were ignored (e.g., nitrogen application). Therefore, these models may not play a heuristic role or correctly predict each process or crop growth over a wide range of conditions. A common view (e.g., Boote *et al.*, 2013) is that accurate modelling of G×E×M would require more mechanistic approaches.

In this thesis, advances have been made in understanding the physiology of growth and development processes of hemp. Some of the processes were quantified at the biochemical level, e.g., leaf photosynthesis (Chapter 4). Corresponding simulation models were used to integrate physiological information from leaf to canopy scales (Chapter 5). These results provide an excellent opportunity to parameterise a generic crop growth model (i.e., Genotype-by-Environment interaction on CROp growth Simulator, GECROS) (Yin & van Laar, 2005; Yin & Struik 2017) for hemp, as analyses described in Chapters 4 and 5 followed exactly the model methodology as used in the GECROS model. In addition, GECROS simulates the growth and development of the crop, and generates phenotypes for a multitude of traits, based on concepts of the interaction and feedback mechanisms among various contrasting components of crop growth, carbon-nitrogen interaction in particular (Yin & Struik, 2010). If successful, such a growth modelling could facilitate the development strategies for optimisation of cultivation and breeding in hemp, as exemplified by the successful applications in major crops (Gu *et al.*, 2014, Khan *et al.*, 2014; Biernath *et al.*, 2011).

6.6 Concluding remarks

With the aim of providing novel information to support cultivation of hemp, particularly dual-purpose (stems + seeds) cultivation in Europe, in this thesis, comprehensive studies have been conducted on the agronomy of hemp production and photosynthesis physiology of hemp's RUE. Hemp has a great potential for dual-purpose production. The cultivation of dual-purpose hemp is not difficult. A monoecious cultivar that has high content of bark fibre in stem and gives a long vegetative phase while leaves enough time for seed growth should be chosen. The planting density should be set at 90–150 plants m⁻². Nitrogen fertilization depends on soil fertility but generally 60 N ha⁻¹ is sufficient across most European conditions.

Hemp is one of the very few crops that have the capacity to be cultivated on non-organic farms with few or no agrochemicals and have positive effects on soil conditions. Therefore, it

can be concluded that hemp has the right profile to fit in the concept of sustainable development of the agricultural bio-economy. Advances have been made in understanding the physiology of hemp growth and development processes. These understandings provide essential knowledge for developing a generic hemp growth model that can facilitate to develop strategies for optimisation of cultivation and breeding in hemp.

References

- Aggarwal, P., Kropff, M., Cassman, K. *et al.* (1997) Simulating genotypic strategies for increasing rice yield potential in irrigated, tropical environments. *Field Crops Research*, **51**, 5–17.
- Amaducci, S., Amaducci, M.T., Benati, R. *et al.* (2000) Crop yield and quality parameters of four annual fibre crops (hemp, kenaf, maize and sorghum) in the North of Italy. *Industrial Crops and Products*, **11**, 179–186.
- Amaducci, S., Colauzzi, M. and Bellocchi G. (2008a) Modelling post-emergent hemp phenology (*Cannabis sativa* L.): Theory and evaluation. *European Journal of Agronomy*, **28**, 90–102.
- Amaducci, S., Errani, M. and Venturi, G. (2002) Response of hemp to plant population and nitrogen fertilisation. *Italian Journal of Agronomy*, **6**, 103–111.
- Amaducci, S., Pelatti, F. and Bonatti, P.M. (2005) Fibre development in hemp, (*Cannabis sativa* L.) as affected by agrotechnique: preliminary results of a microscopic study. *Journal of Industrial Hemp*, **10**, 31–48.
- Amaducci, S., Scordia, D., Liu, F. *et al.* (2015) Key cultivation techniques for hemp in Europe and China. *Industrial Crops and Products*, **68**, 2–16
- Amaducci, S., Zatta, A., Pelatti, F. *et al.* (2008b) Influence of agronomic factors on yield and quality of hemp (*Cannabis sativa* L.) fibre and implication for an innovative production system. *Field Crops Research*, **107**, 161–169.
- Amaducci, S., Zatta, A., Raffanini, M. *et al.* (2008c) Characterisation of hemp (*Cannabis sativa* L.) roots under different growing conditions. *Plant and Soil*, **313**, 227–235.
- Angelova, V., Ivanova, R., Delibaltova, V. *et al.* (2004) Bio-accumulation and distribution of heavy metals in fibre crops (flax, cotton and hemp). *Industrial Crops and Products*, **19**, 197–205.
- Ata-Ul-Karim, S.T., Yao, X., Liu, X. *et al.* (2013) Development of critical nitrogen dilution curve of Japonica rice in Yangtze River Reaches. *Field Crops Research*, **149**, 149–158.
- Aubin, M.P., Seguin, P., Vanasse, A. *et al.* (2016) Evaluation of eleven industrial hemp cultivars grown in eastern Canada. *Agronomy Journal*, **108**, 1972–1980.
- Barth, M. and Carus, M. (2015) *Carbon Footprint and Sustainability of Different Natural Fibres for Biocomposites and Insulation Material*. Nova-Institute, Hürth, Germany. Available at (2017, November 6): <http://eiha.org/media/2017/01/15-04-Carbon-Footprint-of-Natural-Fibres-nova1.pdf>

- Biernath, C., Gayler, S., Bittner, S. *et al.* (2011) Evaluating the ability of four crop models to predict different environmental impacts on spring wheat grown in open-top chambers. *European Journal of Agronomy*, **35**, 71–82.
- Boote, K.J., Jones, J.W., White, J.W. *et al.* (2013) Putting mechanisms into crop production models. *Plant, Cell & Environment*, **36**, 1658–1672.
- Bouman, B.M., Feng, L., Tuong, T.P. *et al.* (2007) Exploring options to grow rice using less water in northern China using a modelling approach: II. Quantifying yield, water balance components, and water productivity. *Agricultural Water Management*, **88**, 23–33.
- Campiglia, E., Radicetti, E. and Mancinelli, R. (2017) Plant density and nitrogen fertilization affect agronomic performance of industrial hemp (*Cannabis sativa* L.) in Mediterranean environment. *Industrial Crops and Products*, **100**, 246–254.
- Carberry, P., Muchow, R., Williams, R. *et al.* (1992) A simulation model of kenaf for assisting fibre industry planning in northern Australia. I. General introduction and phenological model. *Australian Journal of Agricultural Research*, **43**, 1501–1513.
- Carus, M., Karst, S., Kauffmann, A. *et al.* (2013) *The European hemp industry: Cultivation, processing and applications for fibres, shivs and seeds*. European hemp Industry Association. Available at (2017, November 29): <http://eiha.org/media/2014/10/13-06-European-Hemp-Industry.pdf>
- Carus, M. and Sarmiento, L. (2016) *The European hemp industry: cultivation, processing and applications for fibres, shivs and seeds*. Industrial Hemp Association (EIHA), Hürth, Germany, European. Available at (2017, November 29): <http://eiha.org/media/2016/05/16-05-17-European-Hemp-Industry-2013.pdf>
- Cherney, J. and Small, E. (2016) Industrial hemp in North America: production, politics and potential. *Agronomy*, **6**, 58–82.
- Cosentino, S.L., Riggi, E., Testa, G. *et al.* (2013) Evaluation of European developed fibre hemp genotypes (*Cannabis sativa* L.) in semi-arid Mediterranean environment. *Industrial Crops and Products*, **50**, 312–324.
- Cosentino, S.L., Testa, G. and Scordia, D. (2012) Sowing time and prediction of flowering of different hemp (*Cannabis sativa* L.) genotypes in southern Europe. *Industrial Crops and Products*, **37**, 20–33.
- De Meijer, W.J.M., Van der Werf, H.M.G., Mathijssen E.W.J.M. *et al.* (1995) Constraints to dry matter production in fibre hemp (*Cannabis sativa* L.). *European Journal of Agronomy*, **4**, 109–117.
- De Wit, C.T. (1959) Potential photosynthesis of crop surfaces. *Netherlands Journal of Agricultural Science*, **7**, 141–149.
- Desanlis, F., Cerruti, N., Warner, P. *et al.* (2013) Hemp agronomics and cultivation. In *Hemp: industrial production and uses* (eds Allegret, S., Bouloc, P. and Arnaud, L.), pp. 98–124. CPi Group Ltd, Croydon, UK.
- Farquhar, G.D., Von Caemmerer, S. and Berry, J.A. (1980) A biochemical model of photosynthetic CO₂ assimilation in leaves of C₃ species. *Planta*, **149**, 78–90.

- Faux, A.M., Draye, X. and Lambert, R. (2013) The relationship of stem and seed yields to flowering phenology and sex expression in monoecious hemp (*Cannabis sativa* L.). *European Journal of Agronomy*, **47**, 11–22.
- Fike, J (2016) Industrial hemp: renewed opportunities for an ancient crop. *Critical Reviews in Plant Sciences*, **35**, 406–424.
- Finnan, J. and Burke, B. (2013) Nitrogen fertilization to optimize the greenhouse gas balance of hemp crops grown for biomass. *GCB Bioenergy*, **5**, 701–712.
- Finnan, J. and Styles, D. (2013) Hemp: A more sustainable annual energy crop for climate and energy policy. *Energy Policy*, **58**, 152–162.
- Gorchs, G., Lloveras, J., Serrano, L. *et al.* (2017) Hemp yields and its rotation effects on wheat under rainfed mediterranean conditions. *Agronomy Journal*, **109**, 1551–1560.
- Gu, J., Yin, X., Stomph, T.J. *et al.* (2014) Can exploiting natural genetic variation in leaf photosynthesis contribute to increasing rice productivity? A simulation analysis. *Plant Cell & Environment*, **37**, 22–34.
- Hikosaka, K., Kumagai, T.O. and Ito, A. (2016) Modeling canopy photosynthesis. In: *Canopy Photosynthesis: From Basics to Applications*. (eds Hikosaka, K., Niinemets, Ü. and Anten, N.P.R.), pp. 239–268. Springer, Dordrecht, Netherlands.
- Höppner, F. and Menge-Hartmann, U. (2007) Yield and quality of fibre and oil of fourteen hemp cultivars in Northern Germany at two harvest dates. *Landbauforschung Volkenrode*, **57**, 219–232.
- Jones, H.G., 2013. Heat, mass and momentum transfer. In: *Plants and microclimate: a quantitative approach to environmental plant physiology* (ed, Jones, H.G.), pp. 47–67. Cambridge university press, UK.
- Keating, B.A., Carberry, P.S., Hammer, G.L. *et al.* (2003) An overview of APSIM, a model designed for farming systems simulation. *European Journal of Agronomy*, **18**, 267–288.
- Khan, M.M.R., Chen, Y., Laguë, C. *et al.* (2010) Compressive properties of hemp (*Cannabis sativa* L.) stalks. *Biosystems Engineering*, **106**, 315–323.
- Khan, M.S., Yin, X., Van der Putten, P.E.L. *et al.* (2014) An ecophysiological model analysis of yield differences within a set of contrasting cultivars and an F1 segregating population of potato (*Solanum tuberosum* L.) grown under diverse environments. *Ecological Modelling*, **290**, 146–154.
- Legros, S., Picault, S. and Cerruti, N. (2013) Factors affecting the yield of industrial hemp - experimental results from France. In: *Hemp: industrial production and uses* (eds Allegret, S., Bouloc, P. and Arnaud, L.), pp. 72–97. CPi Group Ltd, Croydon, UK.
- Lemaire, G., Jeuffroy, M.H. and Gastal, F. (2008) Diagnosis tool for plant and crop N status in vegetative stage: Theory and practices for crop N management. *European Journal of Agronomy*, **28**, 614–624.
- Linger, P., Müssig, J., Fischer, H. *et al.* (2002) Industrial hemp (*Cannabis sativa* L.) growing on heavy metal contaminated soil: fibre quality and phytoremediation potential. *Industrial Crops and Products*, **16**, 33–42.

- Lisson, S.N., Mendham, N.J. and Carberry, P.S. (2000a) Development of a hemp (*Cannabis sativa* L.) simulation model 1. General introduction and the effect of temperature on the pre-emergent development of hemp. *Australian Journal of Experimental Agriculture*, **40**, 405–411.
- Lisson, S.N., Mendham, N.J. and Carberry, P.S. (2000b) Development of a hemp (*Cannabis sativa* L.) simulation model 2. The flowering response of two hemp cultivars to photoperiod. *Australian Journal of Experimental Agriculture*, **40**, 413–417.
- Lisson, S.N., Mendham, N.J. and Carberry, P.S. (2000c) Development of a hemp (*Cannabis sativa* L.) simulation model 3. The effect of plant density on leaf appearance, expansion and senescence. *Australian Journal of Experimental Agriculture*, **40**, 419–423.
- Lisson, S.N., Mendham, N.J. and Carberry, P.S. (2000d) Development of a hemp, (*Cannabis sativa* L.) simulation model 4. Model description and validation. *Australian Journal of Experimental Agriculture*, **40**, 425–432.
- Mcpartland, J.M., Clarke, R.C. and Watson, D.P. (2000) *Hemp diseases and pests: management and biological control: an advanced treatise*, CABI Publishing, Wallingford, UK.
- Müller, J., Behrens, T. and Diepenbrock, W. (2005) Measurement and modelling of canopy gas exchange of oilseed rape. *Agricultural and Forest Meteorology*, **132**, 181–200.
- Müller, J., Eschenröder, A. and Diepenbrock W. (2009) Through-flow chamber CO₂/H₂O canopy gas exchange system — Construction, microclimate, errors, and measurements in a barley (*Hordeum vulgare* L.) field. *Agricultural and Forest Meteorology*, **149**, 214–229.
- Poni, S., Magnanini, E. and Rebutti B. (1997) An automated chamber system for measurements of whole-vine gas exchange. *HortScience*, **32**, 64–67.
- Poni, S., Merli, M.C., Magnanini, E. *et al.* (2014) An improved multichamber gas exchange system for determining whole canopy water use efficiency in the grapevine. *American Journal of Enology and Viticulture*, **65**, 268–276.
- Prudent, M., Lecomte, A., Bouchet, J.P. *et al.* (2010) Combining ecophysiological modelling and quantitative trait locus analysis to identify key elementary processes underlying tomato fruit sugar concentration, *Journal of Experimental Botany*, **62**, 907–919.
- Struik, P.C., Amaducci, S., Bullard, M.J. *et al.* (2000) Agronomy of fibre hemp (*Cannabis sativa* L.) in Europe. *Industrial Crops and Products*, **11**, 107–118.
- Van der Werf, H.M.G., Van Geel and W., Wijnhuizen, M. (1995) Agronomic research on hemp (*Cannabis sativa* L.) in the Netherlands, 1987–1993. *Journal of the International Hemp Association*, **2**, 14–17.
- Van der Werf, H.M.G., Haasken, H.J. and Wijnhuizen, M. (1994) The effect of daylength on yield and quality of fibre hemp (*Cannabis sativa* L.). *European Journal of Agronomy*, **3**, 117–123.
- Van der Werf, H.M.G., Mathijssen, E.W.J.M. and Haverkort, A.J. (1996) The potential of hemp (*Cannabis sativa* L.) for sustainable fibre production: A crop physiological appraisal. *Annals of Applied Biology*, **129**, 109–123.
- Vera, C.L., Malhi, S.S., Phelps, S.M. *et al.* (2010) N, P, and S fertilization effects on industrial

- hemp in Saskatchewan. *Canadian Journal of Plant Science*, **90**, 179–184.
- Westerhuis, W., Amaducci, S., Struik, P.C. *et al.* (2009) Sowing density and harvest time affect fibre content in hemp (*Cannabis sativa* L.) through their effects on stem weight. *Annals of Applied Biology*, **155**, 225–244.
- Xiaoping, X., Jianguo, W., Zhiwei, W *et al.* (2007) Determination of a critical dilution curve for nitrogen concentration in cotton. *Journal of Plant Nutrition and Soil Science*, **170**, 811–817.
- Yin, X. and Van Laar, H.H. (2005) *Crop systems dynamics: an ecophysiological simulation model for genotype-by-environment interactions*, Wageningen, Wageningen Academic, the Netherlands.
- Yin, X. and Struik, P.C. (2010) Modelling the crop: From system dynamics to systems biology. *Journal of Experimental Botany*, **61**, 2171–2183.
- Yin, X. and Struik, P.C., 2017. Can increased leaf photosynthesis be converted into higher crop mass production? A simulation study for rice using the crop model GECROS. *Journal of Experimental Botany*, **68**, 2345–2360.
- Yin X., Struik P.C., Romero P. *et al.* (2009) Using combined measurements of gas exchange and chlorophyll fluorescence to estimate parameters of a biochemical C₃ photosynthesis model: a critical appraisal and a new integrated approach applied to leaves in a wheat (*Triticum aestivum*) canopy. *Plant Cell & Environment*, **32**, 448–464.

Summary

Hemp (*Cannabis sativa* L.) is a sustainable high-yielding crop that delivers valuable fibres, seeds and psychoactive substances. Traditionally cultivated mainly for the production of textiles and ropes, hemp is now considered as an ideal crop to produce innovative biomaterials. In recent years, the innovative uses of hemp materials and the increasing concern on sustainable development of the agricultural bio-economy have encouraged and sustained the development of the hemp industry that supports the cultivation, processing and use of hemp and its products, particularly in Europe. However, there is a lack of novel information to support this industry as hemp production declined in the last century and was displaced largely by cotton and synthetic fibres; consequently, hemp has not been subject to the intensive research that has driven great improvements in major crops in the last 50 years. With the aim to support the resurging hemp production, in this thesis, comprehensive studies were defined to assess the effects of genotype, environment and management on the performance of hemp crops, and to elucidate the physiological basis of hemp's high resource-use efficiencies (RUE).

Chapter 1 provides a brief introduction to the hemp plant and the state of knowledge on hemp agronomy and photosynthesis physiology. Knowledge gaps on the effects of genotype, environment, and management on hemp production and on hemp's RUE are identified thereof.

In the following four chapters (Chapters 2–5) research results gained in the experimental studies are presented. Chapters 2 and 3 present investigations to improve our understanding of hemp agronomy for dual-purpose cultivation (fibre + seeds) that is a common practice in Europe, driven by the shift of a rapidly expanding market for hemp seeds coupled with lower quality fibre requirements for innovative biomaterials. Chapters 4 and 5 present experimental research, combined with modelling analyses, to improve our understanding of hemp photosynthesis physiology. In the final chapter (Chapter 6) the overall achievement of this study is discussed.

Chapter 2 presents the production of stems and seeds of hemp in relation to genotype and environment. The variation of stem and seed yield among cultivars was mainly determined by the difference in flowering time. In the later flowering cultivars stem yield was high but seed yield was constrained. Thus, a cultivar that gives a long vegetative phase while leaving enough time for seed growth is preferable for dual-purpose hemp production. The flowering time of hemp is under control of the genotype \times environment interactions that can be accurately simulated using mathematical models, with genotype-specific parameters, temperature and

Summary

photoperiod as inputs. Such a model could, therefore, facilitate cultivar choice based on historical meteorological information and genotype-specific parameter values. In addition to the time of flowering, considerable variation among cultivars in sex morphology and stem fibre content were observed. A monoecious cultivar with a high bark fibre content is preferable for dual-purpose production because bark fibre is considered more valuable than wood core and the male plants of dioecious cultivar senesce soon after flowering resulting in biomass loss and heterogeneous quality.

Chapter 3 presents the stem and seed productivities of hemp in response to two important management practices: planting density and nitrogen fertilization. The effects of these two factors on hemp stem and seed yields neither interacted with each other nor with the cultivar effect. Changing planting density over a wide range had limited effect on both stem and seed yields while plant height and stem diameter decreased with increasing population density. The optimum planting density for dual-purpose hemp cultivation could be set at 90-150 plants m^{-2} . Nitrogen demand of hemp crop during growth was analysed and a critical nitrogen (N_{critical}) dilution curve was determined thereof. The N_{critical} of hemp is comparable with that of linseed but indicates a lower nitrogen requirement than found for other C_3 crops, such as rice and cotton, for producing the same amount of biomass. Nitrogen fertilization rate at 60 kg N ha^{-1} is generally sufficient in the European conditions whereas further optimization of nitrogen fertilization requires accurate assessment of the crop nitrogen status.

The responses of hemp leaf photosynthesis to nitrogen content and environmental factors were quantified in Chapter 4. Based on such data, a biochemical model for C_3 leaf photosynthesis was parameterized and validated for hemp. It was shown that the effect of leaf nitrogen and temperature on all the photosynthetic parameters of hemp were consistent at different development stages and growth environments, except for the effect on the efficiency of converting incident irradiance into linear electron transport under limiting light (κ_{2LL}). The value of κ_{2LL} was higher for plants grown in the glasshouse than for those grown outdoors. Model analysis with the photosynthetic parameters obtained in this study and those in literature showed that hemp has higher leaf photosynthesis rate than cotton and kenaf at a low nitrogen (i.e. at a specific nitrogen content of less than 2.0 g N m^{-2}).

Chapter 5 investigates the effect of nitrogen and water supply on the use efficiencies of these resources at canopy level. Canopy photosynthesis and transpiration were assessed using a multi-chamber canopy gas exchange system. Canopy chambers differed significantly in microclimate

and therefore observations were corrected for such differences using a validated physiological canopy model. After correcting for the differences in microclimate, the WUE_c (defined as the ratio of gross canopy photosynthesis to canopy transpiration) and the NUE_c (the ratio of the gross canopy photosynthesis to canopy leaf-N content) depended on the levels of water and nitrogen supply. Water stress resulted in an increase in WUE_c but a decrease in NUE_c . The WUE_c and the NUE_c were lower at higher nitrogen level; this effect was strictly related to the effect of nitrogen supply on canopy size or leaf area index (LAI). The effect of short-term water stress was reflected in the stomatal regulation, whereas the effect of long-term water stress was complicated. In addition to the stomatal effect, long-term water stress enhanced leaf senescence, reduced LAI but retained total canopy nitrogen content, and therefore, resulted in a further increase in WUE_c .

Chapter 6 broadens the discussion of the preceding chapters to the overall achievements of this thesis. I highlight the advances made in hemp agronomy and in photosynthesis physiology, and critically assess the environmental effects of hemp cultivation. Hemp has a high-yielding potential while its cultivation is environmentally friendly. Therefore, it can be concluded that hemp can be grown as a sustainable crop over a wide range of climatic and agronomic conditions.

Acknowledgements

I would like to thank all the people who inspired, encouraged and helped me during this memorable PhD journey. Without them, I would never have finished this thesis.

I would like to express my deepest gratitude to the excellent multidisciplinary supervisory team consisting of Prof. Paul C. Struik [Centre for Crop Systems Analysis, Wageningen University & Research, Wageningen, the Netherlands (CSA)], Dr Xinyou Yin (CSA) and Dr Stefano Amaducci [(Università Cattolica del Sacro Cuore, Piacenza, Italy (UCSC)]. The team supported me in all the aspects allowing me to complete this challenging work. Paul, thank you for your excellence guidance during my PhD study and your energetic and efficient support of my work. Working with you, I learned that I must look after every single detail; to be precise and concrete. Xinyou, thank you for your unconditional help throughout the whole academic training process: literature review – hypothesis formulation – experimental design – data collection – data analysis and interpreting – writing and publishing. You are very patient, and your office was always open to me for discussion. I could not have wished for a better daily supervisor. Stefano, thank you for bringing me to the unforgettable PhD journey. I am very grateful for your patience in spending many hours in guiding me to articulate clear definitions and questions.

I would like to express my gratitude to Prof. Weihong Luo [Nanjing Agricultural University, Nanjing, China (NAU)], Dr Tjeerd Jan Stomph (CSA) and Dr Francesca O’Kane although they were not directly included in my supervisory team. Weihong, my supervisor during my master study at NAU, thank you for encouraging and supporting me to pursue a PhD abroad. Tjeerd Jan, thank you for your constructive contributions to the proposal development, and for your valuable comments on my manuscripts. Francesca, thank you for your kind help whenever I needed it. Without you, I would never have passed my English exam and would not have had a smooth stay in Italy and in the Netherlands.

I am very grateful to those people whom provided me great help in arranging the experimental equipment, field management and data collection. Prof. Adriano Marocco (UCSC), Prof. Vincenzo Tabaglio (UCSC) and Mr. Remigio Calligaro (UCSC), your kind help made it possible for me to run the field experiments smoothly. Dr Gianpaolo Grassi, Mr. Gianmaria Magagnini, Ms. Claire Thouminot, Ms. Marie Bjelková, Mr. Tālis Laizāns and Mr. Eibert Tigchelaar, thanks for your excellent co-operation within the framework of Multihemp.

Acknowledgements

Mr. Andrea Maffini, Mr. Leonardo Poni, Mr. Stefano Pinna, Ms. Rebecca Sudati, Mr. Francesco Saraconi and Ms. Raffaella Santagata, thanks for doing your master studies associated with my project. Working with you, I learnt to change my position from a student to a supervisor and to change the way of behaviour and thinking. Most importantly, I learnt from you so much on Italian language and culture.

I would like to thank all the people whom made me have an enjoyable time in Italy. Alessandra Fracasso, Andrea Ferrarini, Paolo Serra, Salvatore Musio, Davide Calzolari, Carlo Chimento, Murjal Chiazzese, Andrea Fiorini, Alessia Perego, Maria Almagro, Luca Poletti, thanks for making me feel at home in Italy. It's great to have you around. I wish you a lot of success.

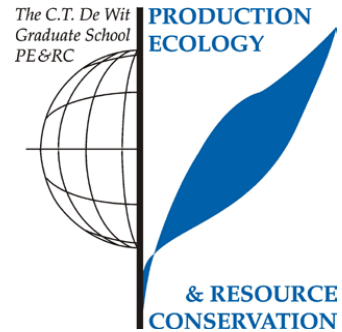
I will not forget to thank all my friends and colleagues in Wageningen. My special thanks to the excellent secretaries and financial officer in CSA: Ms. Sjanie van Wetten, Ms. Nicole Wolffensperger and Mr. Alex-Jan de Leeuw. You are very professional and efficient. Thank for your assistance whenever I asked for it. I would also like to express my appreciation to all other CSA colleagues, especially to Prof. Niels Anten, Dr Steven Driever, Dr Alejandro Morales Sierra, Dr Jochem Evers, Dr Lammert Bastiaans, Dr Bob Douma, and Dr Wopke van der Werf. Thank you all for your nice tips during coffee time and great comments and suggestions during lunch seminars. I would also like to thank many friends and PhD fellows in Wageningen: Li Huayi, Zhang Ningyi, Wang Zhaojun, Li Guohua, Wang Jingmeng, Zhang Peiyu, Wu Liansun, Zhang Hao, Zou Yi, Cong Wenfeng, Chen Bin, Zhu Junqi, Yu Yang, Gou Fang, Herman Berghuijs, Ouyang Wenjing, Luuk van Dijk, Gu Shenghao, Marcelo Labra Fernandez, Martin Sikma, Giovanni Theisen, Dennis Tippe, Ioannis Baltzakis, Niteen Kadam, Shi Wanju, Ali Elhakeem, Uta Priegnitz, Jorad de Vries, Franca Bongers, Ambra Tosto, Cai Chuang, Tan Meixiu, Wei Huanghe, Meng Tianyao, Wang Yuyun, Yan Zenzen and everyone that I shamefully forgot to mention. I enjoyed a lot the time with you during the scientific seminars, PhD meetings, lunch/dinner discussions, Thursday drinks, outdoor activities, etc. Wenjing and Luuk, thank you very much for your willingness to be my paranymphs and your great help in preparing my public defence.

Last but by no means least, I would like to express my deepest gratitude to my family. Thank you for encouraging and supporting me to pursue my career abroad. My special thanks to my wife, Wang Ting, whom gave me lots of mental support to get me out of hardship.

PE&RC Training and Education

Statement

With the training and education activities listed below the PhD candidate has complied with the requirements set by the C.T. de Wit Graduate School for Production Ecology and Resource Conservation (PE&RC) which comprises of a minimum total of 32 ECTS (= 22 weeks of activities)



Review of literature (6 ECTS)

- Modelling the effect of agronomic practices on hemp production

Writing of project proposal (4.5 ECTS)

- Experimentation and crop modelling to develop strategies for optimisation of cultivation and breeding in hemp

Post-graduate courses (3 ECTS)

- Measuring the photosynthetic phenome; PE&RC (2014)
- Lignocellulosic crops as feedstock for value added bioproducts and bioenergy; IBFC, China (2015)
- Fibre quality workshop for young researchers; Université de Lille, France (2016)
- Long fibre technical meeting; Linificio, Italy (2017)

Laboratory training and working visits (3.1 ECTS)

- Assessment of hemp biomass yields; CREA, Italy (2013)
- Hemp breeding; YAAS, China (2015)

Deficiency, refresh, brush-up courses (1.5 ECTS)

- Basic statistics; PE&RC (2014)

Competence strengthening / skills courses (2.1 ECTS)

- Information literacy including EndNote introduction (ILP); WGS (2013)

- Data management; WGS (2014)
- The essentials of writing and presenting a scientific paper (WPRP); WGS (2016)

PE&RC Annual meetings, seminars and the PE&RC weekend (1.5 ECTS)

- First year's weekend; PE&RC (2013)
- Last year's weekend; PE&RC (2017)

Discussion groups / local seminars / other scientific meetings (5.9 ECTS)

- Twinning event of Fibra project; Wageningen (2013)
- First annual meeting of multipurpose crops for industrial bio-products and biomass; Wageningen (2013)
- CSA Photosynthesis meetings (2013-2017)
- Second annual meeting of multipurpose crops for industrial bio-products and biomass; oral presentation; UK (2015)
- Third annual meeting of multipurpose crops for industrial bio-products and biomass; oral presentation; France (2016)

International symposia, workshops and conferences (3.5 ECTS)

- Final annual meeting of multipurpose crops for industrial bio-products and biomass; oral presentation; Italy (2017)
- 2nd Agriculture and climate change conference; oral presentation; Spain (2017)

Supervision of MSc students (12 ECTS)

- Comparing hemp cultivars for dual-purpose production
- The effect of planting density and nitrogen fertilisation on hemp yield and yield components
- The effect of planting density and nitrogen fertilisation on hemp canopy development
- Analysis of hemp nitrogen demand

Curriculum vitae

Kailei Tang was born in Yunnan province, China, on 18 August 1987. From 2006 to 2010, he studied Agronomy at Nanjing Agricultural University, China (NAU), for a BSc degree. After his Bachelor studies, he continued his study on Agronomy at NAU and obtained a MSc degree in 2013. In the same year, he was granted a four-year scholarship from Università Cattolica del Sacro Cuore, Italy, and enrolled to the PhD programme of Wageningen University in the Centre for Crop Systems Analysis. During his PhD study, he worked on “Experimentation and crop modelling to develop strategies for optimisation of cultivation and breeding in hemp”.

Funding

The research described in this thesis was funded by MultiHemp (<http://multihemp.eu>), a programme within the European Union's Seventh Framework Programme for research, technological development and demonstration under Grant agreement n° 311849.

